Chem.

SECTION A

APR 12 '71

A UNITED STATES DEPARTMENT OF COMMERCE PUBLICATION

JOURNAL OF RESEARCH

of the NATIONAL BUREAU OF STANDARDS

Volume 75A, Number 1 Jan.-Feb. 1971

Physics and Chemistry

APR 6 - 197

MIAMI

U.S. DEPARTMENT OF COMMERCE National Bureau of Standards

Journal of Research

of the

National Bureau of Standards

A. Physics and Chemistry

Jan.–Feb. • 1971

VOLUME • 75A

NUMBER • 1

Editor: C. W. Beckett

Associate Editor: D. D. Wagman

Publication dates:
Feb. 1, Apr. 1, June 1, Aug. 1, Oct. 1, Dec. 1, 1971

J. Res. Nat. Bur. Stand. (U.S.), A
CODEN: JNBAA 75A (1) 1–95 (1971)

JOURNAL OF RESEARCH

The National Bureau of Standards Journal of Research reports research and development in the fields of activity shown at right. Also included from time to time are survey articles on topics closely related to the Bureau's scientific and technical program.

The Journal is published in three separate sections as follows:

A. Physics and Chemistry

Contains papers of interest primarily to scientists working in these fields. Issued six times a year. Annual subscription: domestic, $9.50; foreign, $11.75. Single copy, varies.

B. Mathematical Sciences

Presents studies and compilations designed mainly for the mathematician and the theoretical physicist. Issued quarterly. Annual subscription: domestic, $5.00; foreign, $6.25. Single copy, $1.25.

C. Engineering and Instrumentation

Reports research and development results of interest chiefly to the engineer and the applied scientist. Issued quarterly. Annual subscription: domestic, $5.00; foreign, $6.25. Single copy, $1.25.

U.S. DEPARTMENT OF COMMERCE
Maurice H. Stans, Secretary
NATIONAL BUREAU OF STANDARDS
Lewis M. Branscomb, Director

Order all publications from the Superintendent of Documents
U.S. Government Printing Office, Washington, D.C. 20402
Use of funds for printing this publication approved by the Director of the Bureau of the Budget (June 22, 1966).

JOURNAL OF RESEARCH of the National Bureau of Standards—A. Physics and Chemistry
Vol. 75A, No. 1, January–February 1971

High-Speed (Subsecond) Measurement of Heat Capacity, Electrical Resistivity, and Thermal Radiation Properties of Tantalum in the Range 1900 to 3200 K*

A. Cezairliyan, J. L. McClure, and C. W. Beckett

Institute for Materials Research, National Bureau of Standards, Washington, D.C. 20234

(September 11, 1970)

Measurements of heat capacity, electrical resistivity, hemispherical total and normal spectral emittances of tantalum above 1900 K by a pulse heating technique are described. Duration of an individual experiment, in which the specimen is heated from room temperature to near its melting point, is less than one second. Temperature measurements are made with a photoelectric pyrometer. Experimental quantities are recorded with a digital data acquisition system. Time resolution of the entire system is 0.4 ms. Results on the above properties of tantalum in the range 1900 to 3200 K are reported and are compared with those in the literature. Estimated inaccuracy of measured properties in the above temperature range is 2 to 3 percent for heat capacity, 0.5 percent for electrical resistivity, 3 percent for hemispherical total emittance, and 2 percent for normal spectral emittance.

Key words: Electrical resistivity; emittance; heat capacity; high-speed measurements; high temperature; tantalum; thermal radiation properties; thermodynamics.

1. Introduction

Conventional methods of measuring heat capacity, electrical resistivity, and other thermophysical properties at high temperatures employ "drop", steady-state, and quasi steady-state techniques in which the specimen is exposed to high temperatures for long periods of time, ranging from minutes to hours. Extension of these techniques to temperatures above 2000 K creates problems resulting from increased heat transfer, chemical reactions, evaporation, diffusion, loss of mechanical strength, etc. To overcome these limitations, this laboratory has recently developed a high-speed measurement technique in which the specimen is heated and pertinent quantities required for the determination of properties are measured in short times. The duration of an individual experiment, in which the specimen is heated from room temperature to near its melting point, is less than 1 s. A millisecond resolution photoelectric pyrometer is used to measure the specimen temperature. The recordings of experimental quantities are made with a high-speed digital data acquisition system, which has a time resolution of 0.4 ms. The application of this technique to measurements on molybdenum has been published [1].[1] General reviews on high-speed methods for the measurement of thermophysical properties of electrical conductors have been presented recently [2, 17].

In the present study the technique was used to determine the heat capacity and electrical resistivity of tantalum in the temperature range 1900 to 3200 K, and the hemispherical total and normal spectral emittances up to 3000 K.

2. Method

The method employed in this study is based upon rapid resistive heating of the specimen by the passage of high currents and measuring the pertinent quantities with appropriate time resolution. The required quantities are the power imparted to the specimen and the temperature of the specimen, both as functions of time. Imparted power is obtained from measurements of current flowing through the specimen and the potential difference across the "effective" [2] specimen as a function of time.

The relationship for heat capacity is obtained from power balances for the specimen during the pulse heating and the following free cooling periods. The expression for heat capacity, which was derived in an earlier publication [1], is

$$C_p = \frac{ei - \epsilon\sigma A_s(T^4 - T_0^4)}{n(dT/d\imath)_h} \qquad (1)$$

*This work was supported in part by the Propulsion Division of the U.S. Air Force Office of Scientific Research under contract ISSA-69-0001.

[1] Figures in brackets indicate the literature references at the end of this paper.

[2] "Effective" refers to the portion of the specimen between the knife-edge voltage probes.

where

c_p = heat capacity in J mol^{-1} K^{-1}

e = potential difference across the effective specimen in V

i = current through the specimen in A

ϵ = hemispherical total emittance

σ = Stephan-Boltzmann constant ($5.6697 \times 10^{-8} W m^{-2} K^{-4}$)

A_s = effective specimen surface area in m^2

T = specimen temperature in K

T_0 = room temperature in K

n = amount of effective specimen in mol

$(dT/dt)_h$ = heating rate in K s^{-1}

The hemispherical total emittance, ϵ, which appears in the radiation loss term of the heat capacity relation, is determined from data collected during the free cooling period. Derived from the power balance relationship during the cooling period and eq (1), the expression for ϵ is

$$\epsilon = \frac{ei}{\sigma A_s (T^4 - T_0^4)(1+M)} \tag{2}$$

where

$$M = -\frac{(dT/dt)_h}{(dT/dt)_c} \tag{3}$$

$(dT/dt)_c$ = cooling rate in K s^{-1}

Equation (2) is used to compute values for ϵ at selected temperatures, which are used to obtain a function for ϵ in terms of temperature. Then, ϵ values from this function are substituted in eq (1) to obtain heat capacity over the entire temperature range.

Data from the heating period is also used to calculate the electrical resistivity with the aid of the equation

$$\rho = \frac{RA_c}{l} \tag{4}$$

where

ρ = electrical resistivity in Ω m

R = resistance of effective specimen in Ω

A_c = specimen cross-sectional area in m^2

l = effective specimen length in m.

The normal spectral emittance, $\epsilon_{n,\lambda}$, is obtained from separate pulse experiments in which radiance from the surface of the specimen is measured. The relation for $\epsilon_{n,\lambda}$ is

$$\epsilon_{n,\lambda} = \frac{L_s}{L_b} \tag{5}$$

where

L_s = radiance from surface of specimen as observed by the pyrometer.

L_b = blackbody radiance from sighting hole in specimen as observed by the pyrometer.

In all the above equations, geometrical quantities are corrected for the presence of the sighting hole, and the quantities related to radiation from the sighting hole are corrected for scattered light and departure from blackbody conditions.

3. Apparatus

A functional diagram of the measurement system used in this study is shown in figure 1. The details of the system were described in an earlier publication [1].

The specimen was a tube approximately 100 mm long with a small rectangular hole fabricated in the wall at the middle of its length to approximate blackbody conditions. The knife-edge probes, which were used for potential measurements, were made of tantalum and were placed 50 mm apart on the middle portion of the specimen. The portion between the probes, defined as "effective" specimen, was free from significant temperature gradients for the duration of an experiment. The specimen and the associated components were contained in a vacuum chamber.

The specimen temperature was measured with a high-speed photoelectric pyrometer [12], which permits 1200 evaluations of the specimen temperature per second. The pyrometer alternately compares the radiance from the blackbody hole in the specimen to that of a reference lamp.

Electrical signals corresponding to voltage, current, and temperature were recorded with a high-speed digital data acquisition system, which consists of a multiplexer, analog-to-digital converter, and a core memory together with various control and interfacing equipment. At the end of each experiment, the data were retrieved and recorded in printed numeric form and on punched paper tape via a teletypewriter. During this retrieval period, data were also sent to a time-sharing computer for immediate processing.

Electrical signals corresponding to voltage, current, and temperature were also monitored simultaneously with oscilloscopes.

4. Measurements

Measurements were made on four tantalum specimens. The first two specimens were used for experiments in the temperature interval 1900 to 3000 K. To optimize the operation of the pyrometer, this temperature interval was divided into three ranges with three experiments per range. These nine experiments are referred to as a series. The temperature ranges were: low, 1900 to 2250 K; medium, 2100 to 2600 K; and high, 2350 to 3000 K.

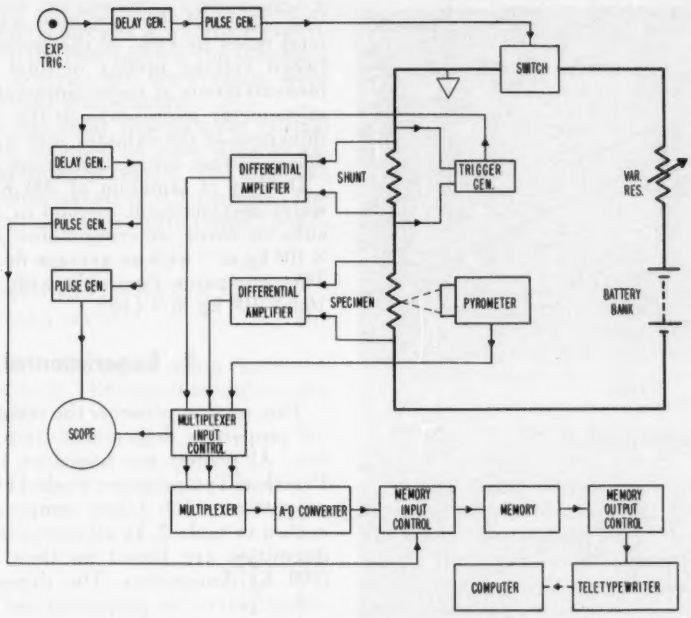

FIGURE 1. *Functional diagram of the complete high-speed measurement system.*

Two complete series of experiments were conducted on the first specimen (Ta–1). During the second series, two additional experiments were conducted, one in the low range and one in the high range, to measure the surface radiance of the specimen. Before the start of the first series of experiments, the specimen (Ta–1) was subjected to approximately 30 heating pulses (in the range 2200 to 3000 K) to anneal the specimen and to determine the optimum heating rate for each temperature range. At the end of the first series of experiments and before the start of the second series, the specimen was pulse heated 15 times to 3000 K. One experiment per temperature range was conducted on the second specimen (Ta–2) without any prior heating pulses.

To obtain heat capacity and electrical resistivity in the temperature range 2950 to 3200 K, two other specimens, (Ta–3) and (Ta–4), were used.

The duration of the current pulses ranged from 280 to 520 ms depending on the temperature. The average heating rate of the specimen was 5700 and 3700 K s^{-1} at 2000 and 3200 K, respectively. At these temperatures, radiative heat losses from the specimen amounted to approximately 3 and 22 percent of the input power, respectively. All of the experiments were conducted with the specimen in a vacuum environment of approximately 10^{-4} torr.

The data on voltage, current, and temperature were used to obtain third degree polynomial functions for each quantity in terms of time, which then provided the input information for the equations of section 2.

During the entire set of experiments, the pyrometer was calibrated five times against a tungsten filament standard lamp, which in turn was calibrated against the NBS Temperature Standard. The digital recording system including the differential amplifiers was calibrated three times during the experiments. The details of the calibration procedures are given in an earlier publication [1].

Prior to the start of the experiments, the optical system of the pyrometer was modified to reduce the effect of light scattered from the area around the sighting hole in the specimen. In the present system this effect is approximately one percent. The blackbody quality of the specimen sighting hole was estimated to be 0.99 using DeVos' [13] method. The temperature data from the pyrometer were corrected for both scattered light and departure from blackbody conditions. The details of the methods employed for these corrections are given in an earlier publication [1].

The nominal dimensions of the tubular tantalum specimens were: length = 4 in (101 mm), outside diameter = 0.25 in (6.3 mm), and wall thickness = 0.02 in (0.5 mm). The outer surface of each specimen was polished to reduce heat loss due to thermal radiation.

Specimen characterization was made on one specimen (Ta–1) by the following methods: photomicrography, chemical analysis, and residual resistivity ratio.

Photomicrographs of the specimen before and after the entire set of experiments are shown in figure 2. It may be seen that considerable grain growth has taken place as the result of pulse heating the specimen to high temperatures.

Chemical analyses were made of the specimen before and after the entire set of experiments. Comparison of results does not indicate any detectable change in impurity content. A list of the nature and composition of impurities in the specimen is given in table 1.

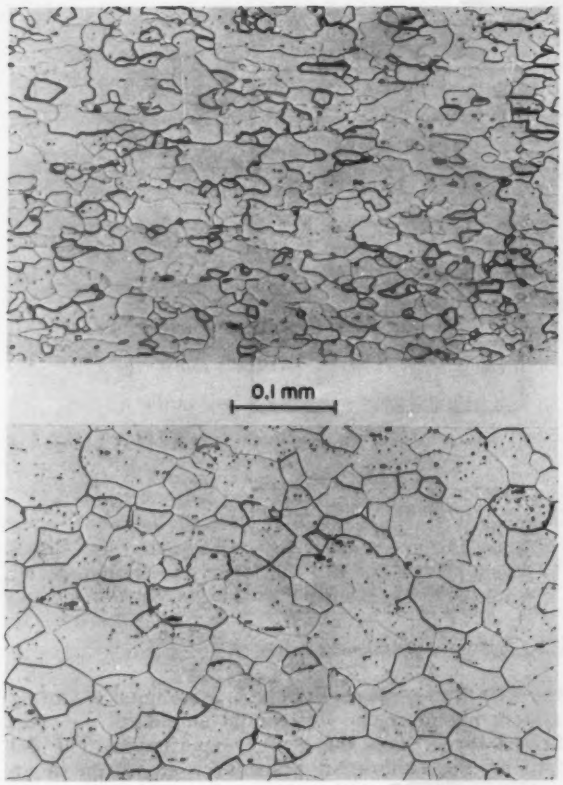

FIGURE 2. *Photomicrographs of the tantalum specimen before (upper photograph) and after (lower photograph) the entire set of experiments.*

TABLE 1. *Impurities in tantalum specimen*

Impurity	Composition ppm (by weight)
Al	< 5
C	60
Ca	< 5
Cr	< 10
Cu	< 5
Fe	70
Mg	< 5
Mo	10
N	20
Nb	500
O	50
W	< 200

710 < Total < 940

The residual resistivity ratio of the specimen (ratio of electrical resistivity at 273 K to that at 4 K) before and after the entire set of experiments was 22 ± 1. The fact that the value of this ratio remained unchanged indicates that the specimen did not undergo any major chemical or physical changes.

The total mass of the specimen was determined before and after each series of experiments. The "effective" mass of the specimen was calculated from the total mass by ratio of the geometric surface area between voltage probes to total surface area. Length measurements at room temperature were made with a micrometer microscope to the nearest 0.03 mm. The thickness of the cylinder wall was calculated from the mass, surface areas, and density.

Density of tantalum at 298 K was obtained by the water displacement method in a pycnometer. The results of three determinations gave a value of 16.65 $\times 10^3$ kg m^{-3} with an average deviation of 0.03 percent. This compares favorably with the reported value of 16.6×10^3 kg m^{-3} [16].

5. Experimental Results

This section presents the results on the thermophysical properties determined from the measured quantities. All values are based on the 1968 International Practical Temperature Scale [14]. The final results on properties at 100 degree temperature intervals are presented in table 2. In all computations, the geometrical quantities are based on their ambient temperature (298 K) dimensions. The experimental results (individual points) on properties are given in the appendix (tables A–1 to A–5).

TABLE 2. *Heat capacity, electrical resistivity, hemispherical total and normal spectral emittances of tantalum*

Temperature, K	c_p J mol^{-1}K^{-1}	ρ^a $10^{-8}\Omega$m	ϵ^a	$\epsilon_{N,\lambda}$
1900	30.66	75.56	[b] 0.288	[b] 0.413
2000	31.19	78.80	[b] .293	.411
2100	31.71	82.00	[b] .298	.409
2200	32.25	85.14	[b] .302	.407
2300	32.83	88.23	.307	.406
2400	33.46	91.26	.312	.404
2500	34.17	94.24	.316	.403
2600	34.97	97.17	.321	.401
2700	35.89	100.04	.326	.400
2800	36.95	102.86	.330	.400
2900	38.16	105.63	.335	.399
3000	39.55	108.34	.340	.398
3100	41.39	111.00		
3200	44.48	113.60		

[a] Based on ambient temperature (298 K) dimensions.
[b] Extrapolated from higher temperature results.

5.1. Normal Spectral Emittance

To calculate the normal spectral emittance, two experiments were performed to measure the surface radiance of the Ta–1 specimen during the second heating series. The measurements were made at the effective wavelength of the pyrometer interference filter (650 nm; bandwidth 10 nm). The normal spectral emittance was calculated using the radiance data from each surface experiment together with the data from a previous or later regular blackbody experiment

according to eq (5). Since the specimen's true temperature could not be measured directly in a surface experiment, the times at which the resistance of the specimen in the two adjacent experiments were equal were taken as the times of equal temperature.

A second degree polynomial function for normal spectral emittance was obtained by least squares approximation of the experimental results. The standard deviation (of an individual point) is 0.3 percent. The function that is valid in the temperature range 2000 to 3000 K is:

$$\epsilon_{n,\lambda} = 0.4892 - 5.644 \times 10^{-5} T + 8.734 \times 10^{-9} T^2 \quad \text{(second series)} \qquad (6)$$

Normal spectral emittance computed using the above equation is given in table 2. The experimental results are presented in figure 3.

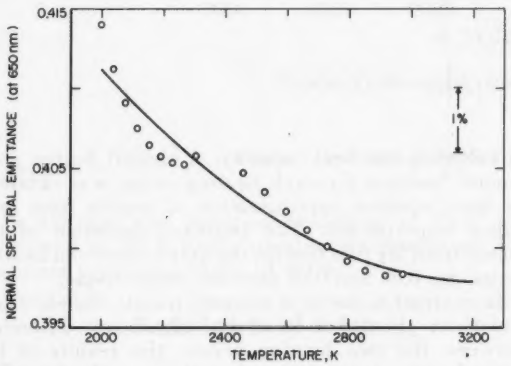

FIGURE 3. *Normal spectral emittance of tantalum at* $\lambda = 650$ *nm.*

5.2. Hemispherical Total Emittance

The hemispherical total emittance of the Ta–1 specimen was computed with the aid of eq (2) using temperature data taken during both heating and initial free cooling periods in an experiment.

A linear function for hemispherical total emittance for each heating series was obtained by least squares approximation of the individual values. The standard deviation of the points from the function for the first and second heating series were 0.7 and 0.5 percent, respectively. The functions that are valid in the temperature range 2300 to 3000 K are:

$$\epsilon = 0.2197 + 4.146 \times 10^{-5} T \quad \text{(first series)} \qquad (7)$$

$$\epsilon = 0.1991 + 4.687 \times 10^{-5} T \quad \text{(second series)} \qquad (8)$$

Hemispherical total emittance computed using eq (8) is given in table 2. The experimental results are presented in figure 4.

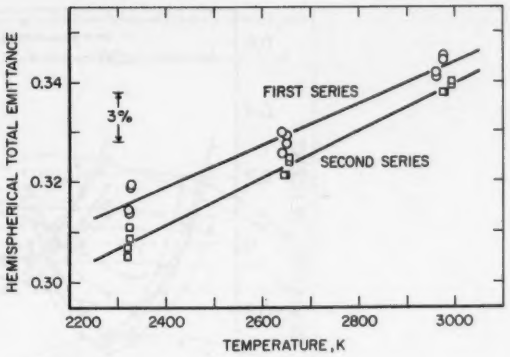

FIGURE 4. *Hemispherical total emittance of tantalum.*

5.3. Heat Capacity

A third degree polynomial function for heat capacity in terms of temperature for each heating series on Ta–1 was obtained by least squares approximation of results from individual experiments. The standard deviation of the points from the function for the first and second heating series were 0.19 and 0.17 percent, respectively. A similar function was also obtained for the combined results of experiments in the first and second series with a standard deviation of 0.18 percent.

Figure 5 shows the deviations of the experimental results from the smooth function for the combined heating series. The figure also shows the deviation of the function for each individual heating series from the heat capacity function for the combined series. Compared to the function for the combined series, the average difference between the functions for the first and second heating series is about 0.1 percent, which is smaller than the measurement resolution. Therefore, it may be concluded that the measured heat capacity shows no significant difference between the two heating series. The function for the combined series that is valid in the temperature range 1900 to 3000 K is:

$$c_p = -6.549 + 4.583 \times 10^{-2} T - 2.013 \times 10^{-5} T^2 + 3.325 \times 10^{-9} T^3 \qquad (9)$$

where T is in K and c_p in J mol^{-1} K^{-1}. Heat capacity up to 3000 K computed using the above equation is given in table 2. In the computations of heat capacity, the atomic weight of tantalum was taken as 180.95 [15].

Without any prior heating pulses, three experiments were conducted on a second tantalum specimen (Ta–2). Figure 6 shows the difference in measured heat capacity between Ta–1 and Ta–2. The base line in figure 6 represents the smooth function for heat capacity of Ta–1 given by eq (9). The maximum deviation between the heat capacity results of the two specimens occurs at the lowest temperature and is less than 1 percent. The tendency for the heat capacity of Ta–2 to approach that of Ta–1 as the temperature increases may be due to annealing effects as the temperature range for the Ta–2 specimen was increased.

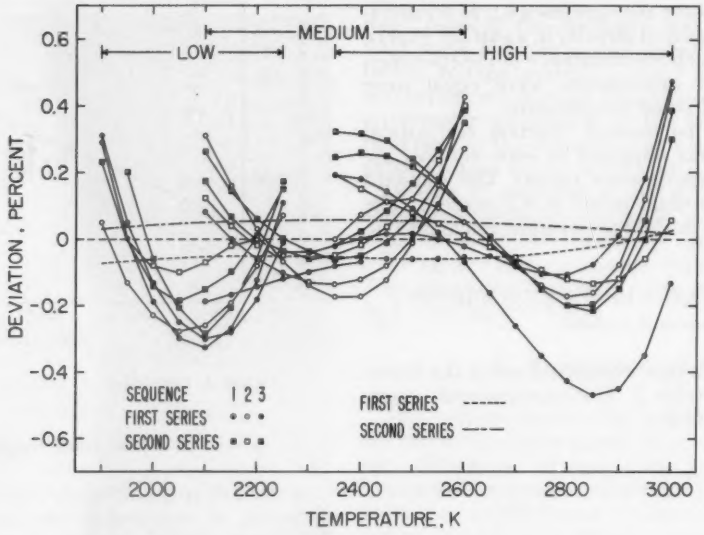

FIGURE 5. *Deviation of heat capacity results for tantalum from eq (9).*

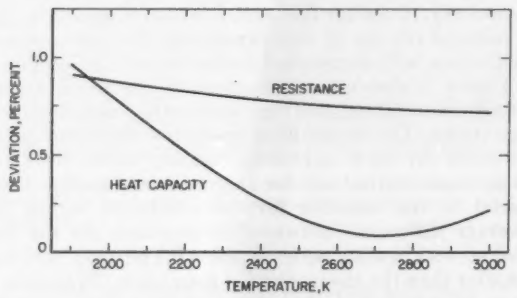

FIGURE 6. *Difference in heat capacity and electrical resistivity between two tantalum specimens.*

Base line represents results for Ta–1 given by eqs (9) and (10).

The preliminary results on heat capacity of tantalum up to 3000 K were reported in an earlier publication [3]. In this study the measurements were extended to 3200 K by performing one experiment each on Ta–3 and Ta–4, and averaging the results. Hemispherical total emittance needed to correct heat capacity above 3000 K was obtained from the extrapolation of the experimental results at lower temperatures. The results of measurements above 3000 K are given in table 2. At 3000 K the heat capacity for this extended temperature range is approximately 0.1 percent lower than the value given by eq (9).

5.4. Electrical Resistivity

The electrical resistivity of the Ta–1 specimen was determined from the same experiments that were used to calculate the heat capacity. A second degree polynomial function for each heating series was obtained by least squares approximation of results from individual experiments. The standard deviation of the points from the function for the first and second heating series are 0.03 and 0.02 percent, respectively.

In contrast to the heat capacity results, the electrical resistivity showed a small but significant difference between the two heating series; the results of the second series being lower than those of the first. The combined data from both heating series were fitted to a second degree polynomial function. Figure 7 shows the deviations of the experimental results from the smooth function for the combined series. The figure also shows the deviation of the function for each individual heating series from the electrical resistivity function for the combined series. The average difference between the functions for the first and second heating series is approximately 0.15 percent. The function for the combined series that is valid for the temperature range 1900 to 3000 K is:

$$\rho = 3.671 + 4.292 \times 10^{-2} T - 2.677 \times 10^{-6} T^2 \quad (10)$$

where T is in K and ρ in $10^{-8}\,\Omega\,\mathrm{m}$. Electrical resistivity up to 3000 K computed using the above equation is given in table 2.

The difference between the results on Ta–1 and Ta–2 is presented graphically in figure 6. In contrast to heat capacity, electrical resistivity did not converge as Ta–2 was exposed to high temperatures.

The results of experiments on Ta–3 and Ta–4 were used to compute electrical resistivity above 3000 K. These are included in table 2. At 3000 K electrical resistivity obtained from Ta–3 and Ta–4 was approximately 0.3 percent lower than the value given by eq (10).

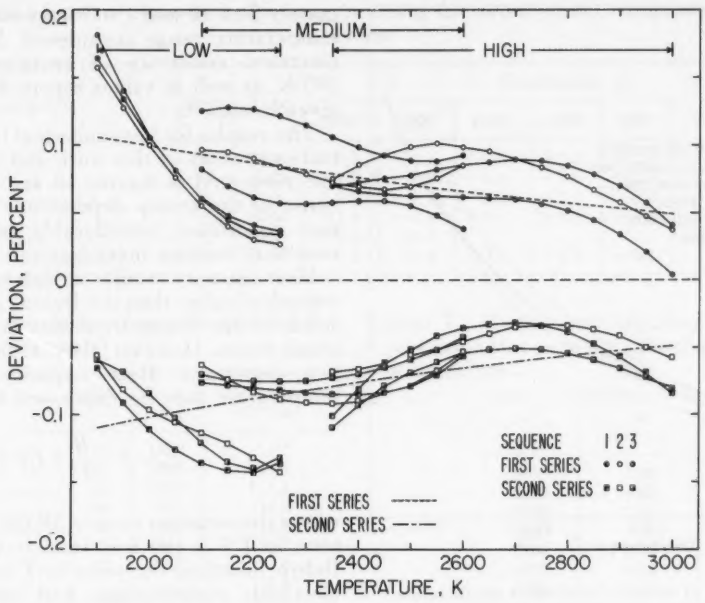

FIGURE 7. *Deviation of electrical resistivity results for tantalum from eq (10).*

In addition, the electrical resistivity of Ta–1 was measured at 293 K under steady-state conditions. The resultant value was $14.0 \times 10^{-8} \Omega$m.

6. Estimate of Errors

Results on imprecision[3] and inaccuracy[4] of measured and computed quantities are given in table 3.

TABLE 3. *Imprecision and inaccuracy of measured and computed quantities*

Quantity	Imprecision (percent)	Inaccuracy (percent)
Temperature	0.02 (0.5 K)	0.2 (4 K) at 2000 K 0.3 (10 K) at 3200 K
Voltage	0.02	0.05
Current	.03	.06
Power	.04	.08
Resistance	.04	.08
Length	.04	.08
Weight	.01	.1
Density	.03	.1
Heat Capacity	.5	2 at 2000 K 3 at 3200 K
Resistivity	.04	0.5
Hem. Total Emittance	.7	3
Norm. Spectral Emittance	.3	2

[3] Imprecision refers to the standard deviation of an individual point as computed from the difference between measured and calculated values.

[4] Inaccuracy refers to the estimated maximum error (random and systematic) approximately equivalent to two standard deviations.

Numbers listed under imprecision were obtained from a least squares analysis of experimental results. Numbers listed under inaccuracy were estimated considering the contribution of various items that introduce random and systematic errors in the pertinent quantities. These items are listed below:

(a) In temperature measurements: pyrometer reproducibility, scattered light correction, light source alinement, radiation standard lamp, blackbody quality, specimen temperature uniformity, magnetic fields.

(b) In electrical measurements: skin effect, inductive effects, thermoelectric effects.

(c) In interpretation of results: specimen evaporation, thermionic emission, time synchronization, measurements of length and weight.

Details regarding the estimates of errors and their combination are given in another publication [1]. Specific items in the error analysis were recomputed whenever the present conditions differed from those in the earlier publication.

7. Discussion

The heat capacity and electrical resistivity results of this work are compared graphically with those in the literature in figures 8 and 9, respectively. Numerical comparisons are given in tables 4 and 5. It may be seen that present results agree favorably with all others at 2000 K and also at higher temperatures, with the exception of heat capacity results of Hoch and Johnston [8]. Estimates of errors in papers cited lead to an estimate of inaccuracies in previously reported heat capacity and electrical resistivity of approxi-

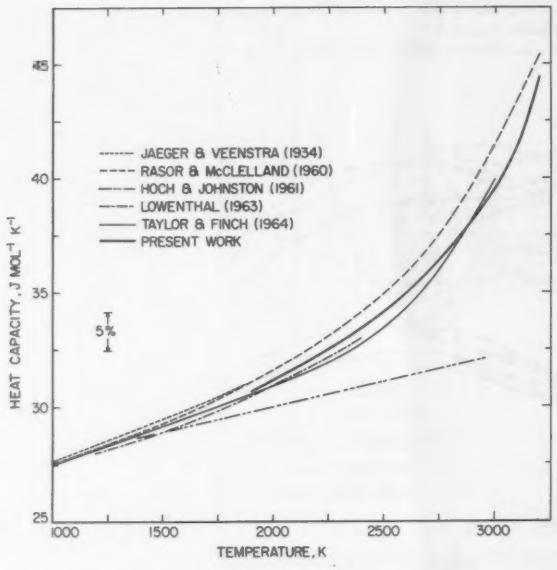

FIGURE 8. *Heat capacity of tantalum reported in the literature.*

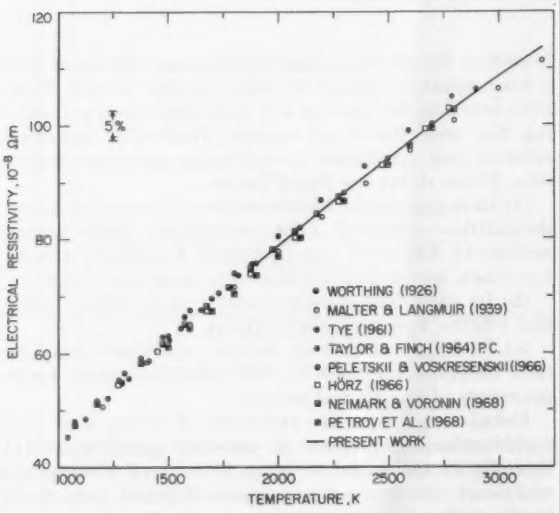

FIGURE 9. *Electrical resistivity of tantalum reported in the literature.*

mately 5 to 10 and 1 to 3 percent, respectively, in the temperature range considered. Measurements of the electrical resistivity of tantalum corresponding to 293 K, as well as values reported in the literature, are given in table 6.

The results for hemispherical total and normal spectral emittances of this work and those in the literature are presented in figures 10 and 11, respectively. Because of the strong dependence of emittance on surface conditions, considerable deviations exist in the results of various investigators.

Heat capacity results at high temperatures are considerably higher than the Dulong and Petit value of $3R$. Some of this departure is due to $c_p - c_v$ and the electronic terms. However, they do not account for the entire departure. Heat capacity above the Debye temperature may be expressed by

$$c_p = A - \frac{B}{T^2} + CT + \Delta c \qquad (11)$$

where the constant term is $3R$ (24.943 J mol^{-1} K^{-1}), the term in T^{-2} is the first term in the expansion of the Debye function, the term in T represents $c_p - c_v$ and electronic contributions, and the quantity Δc represents excess in measured heat capacity at high temperatures, which is not accounted for by the first three terms. The coefficients $B(4.88 \times 10^4)$ and $C(2.59$

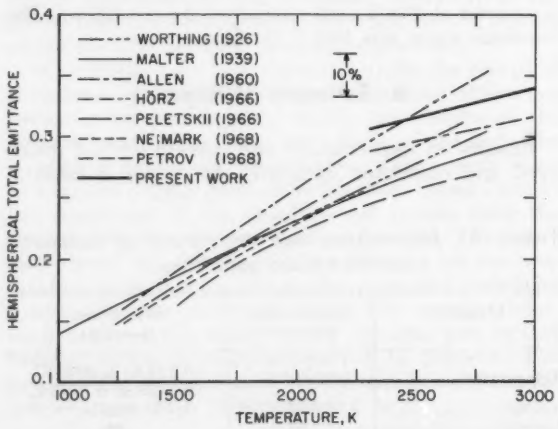

FIGURE 10. *Hemispherical total emittance of tantalum reported in the literature.*

TABLE 4. *Tantalum heat capacity difference (previous literature values minus present work values) in percent*

Investigator	Ref.	Year	Method	Temperature, K						
				2000	2200	2400	2600	2800	3000	3200
Jaeger and Veenstra.....	7	1934	drop	[a]+1.2						
Rasor and McClelland.....	5	1960	pulse	+1.3	+1.4	+1.9	+2.4	+3.4	+5.0	+2.0
Hoch and Johnston.....	8	1961	drop	−3.8	−5.6	−7.6	−10.4	−14.0		
Lowenthal.....	4	1963	modul.	−0.8	−1.0	−1.3				
Taylor and Finch.....	6	1964	pulse	−0.9	−1.6	−2.2	−1.9	−0.8	+0.9	

[a] Extrapolated from 1873 K.

TABLE 5. *Tantalum electrical resistivity difference (previous literature values minus present work values) in percent*

Investigator	Ref.	Year	Temperature, K						
			2000	2200	2400	2600	2800	3000	3200
Worthing	18	1926	+2.3	+2.1	+2.1	+2.2	+2.4		
Malter and Langmuir	19	1939	−1.2	−1.3	−1.5	−1.6	−1.8	−1.9	−2.0
Peletskii and Voskresenskii	21	1966	+0.2	−0.1	−0.1	+0.1	+0.4		
Hörz	20	1966	−1.0	−0.8	−0.4	+0.1	+0.9		
Neimark and Voronin	22	1968	+0.4	+0.2					
Petrov et al	23	1968	−2.1	−1.8	−1.4	−0.8	−0.1		

TABLE 6. *Electrical resistivity of tantalum at 293 K (literature)*

Investigator	Ref.	Year	Resistivity $10^{-8}\Omega m$
Worthing	18	1926	14.2
Malter and Langmuir	19	1939	13.5
White and Woods	25	1959	[a] 13.1
Tye	26	1961	14.5
Hörz	20	1966	13.4
Peletskii and Voskresenskii	21	1968	13.7
Neimark and Voronin	22	1938	15.0
Present work			14.0

[a] Ideal resistivity.

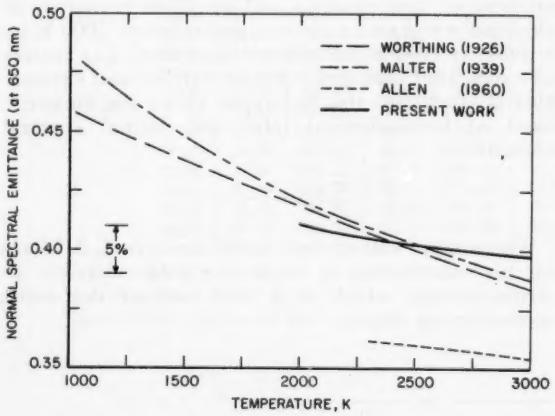

FIGURE 11. *Normal spectral emittance of tantalum at $\lambda' = 650$ nm reported in the literature.*

$\times 10^{-3}$) were obtained from data on heat capacity at low and moderate temperatures (at 250 and 1000 K) given by Hultgren et al. [11].

Using eq (11) and the heat capacity results of this work, the quantity Δc was computed for temperatures above 1900 K. The results are tabulated in table 7. The estimated uncertainty in the computed Δc may be as high as 1 J mol^{-1}K^{-1}. This was obtained from the combined uncertainties in the coefficients in eq (11) and the measured heat capacities.

TABLE 7. *Excess heat capacity Δc in equation (11) and estimated vacancy contribution to heat capacity of tantalum*

T K	Δc J mol^{-1}K^{-1}	c_{vac} J mol^{-1}K^{-1}
2000	1.08	0.003
2200	1.62	.01
2400	2.31	.04
2600	3.30	.10
2800	4.76	.21
3000	6.84	.41
3200	9.70	.73

Although the mechanisms of vacancy generation become important at high temperatures, it was not possible to attribute the high values entirely to vacancies. To demonstrate this, a crude estimate of the contribution of vacancies to heat capacity was made using the following equation [1]:

$$c_{vac} = \frac{N_A A E_f^2}{kT^2} e^{-E_f/kT} \qquad (12)$$

where

N_A = Avogadro's number

k = Boltzmann constant

E_f = vacancy formation energy

A = constant which is obtained from vacancy concentration at the melting point.

If one assumes that vacancy formation energy is approximately proportional to the melting point and considers the value of 3.3 eV reported by Schultz [9] for tungsten, one obtains 2.9 ± 0.5 eV for the vacancy formation energy for tantalum. There are no accurate measurements on tantalum related to vacancy concentrations. Results of quenching experiments on various refractory elements [9, 10] have indicated that vacancy concentrations are probably in the range 0.01 to 0.1 percent at their melting points. Estimates corresponding to a vacancy concentration of 0.1 percent at the melting point and a vacancy formation energy of 2.9 eV are given in table 7. The results indicate that vacancy contribution is small, less than 0.7 J mol^{-1}K^{-1} (upper limit) at 3200 K, and does not account for high heat capacity values. A

possible contribution of higher order terms in the electronic heat capacity may partially account for high values of heat capacity at high temperatures.

If the entire deviation of measured heat capacity from the sum of $3R$ and the linear term at high temperatures is represented by an expression similar to eq (12), one could obtain after rearrangement

$$\ln (T^2 \Delta c) = \ln I - \frac{S}{T}. \tag{13}$$

This equation indicates that a plot of the left side versus $1/T$ should yield a straight line with slope equal to $-S$. From the data on tantalum in the range 1900 to 3200 K, a straight line with a standard deviation of 0.8 percent was obtained. However, the parameters obtained through this fit do not seem to have any physical significance. As a crude analogy to vacancy concentration, the computations yielded a value of 1.4 eV for energy and 4.2 percent for concentration at the melting point. Both of these values seem to be unrealistic for tantalum.

In order to give a simple expression for the heat capacity of tantalum over a wide temperature range, an empirical term in T^5 for the quantity Δc in eq (11) was substituted. The coefficient of this term was obtained from the results of the present work in conjunction with the values given by Hultgren et al. [11] at temperatures below 1000 K. Then, eq (11) for the range 300 to 3100 K becomes

$$c_p = 24.943 - \frac{4.88 \times 10^4}{T^2} + 2.59 \times 10^{-3} T + 2.85 \times 10^{-17} T^5 \tag{14}$$

where T is in K and c_p in J mol^{-1} K^{-1}. Average deviation of the individual points from the function over the temperature range considered is 0.4 percent. Equation (14) is presented graphically in figure 12.

The T^{-2} term in eq (14) corresponds to a Debye θ of approximately 200 K for tantalum. This value is somewhat lower than the generally accepted value of 247 K [28]. Such a deviation may be expected since in the above analysis only data above 250 K were considered while determinations reported in the literature were based on more elaborate treatment of lower temperature data.

It was interesting to note that the difference in heat capacity between Ta–1 and Ta–2 was reduced from approximately 1 percent at 1900 K to 0.2 percent at 3000 K. The convergence of the results as Ta–2 was exposed to high temperatures indicates the difference in the initial states of the two specimens; Ta–1 was preheated while Ta–2 was used as received from the manufacturer prior to the start of the measurements.

There was a small, but significant difference in electrical resistivity between the two heating series of Ta–1. The second series results, which were lower than those of the first by approximately 0.15 percent, indicate that the specimen had undergone additional annealing during its exposure to high temperatures.

Unlike most metallic elements, the electrical resistivity of tantalum, in the range of present measurements, showed a negative departure from linearity in the curve of electrical resistivity against temperature. A small Fermi energy is believed to be responsible for some of this negative departure [27].

The experimental results reported in this paper have further substantiated the feasibility of accurate measurement of heat capacity and electrical resistivity of electrical conductors above approximately 2000 K by a pulse method of millisecond resolution. The results also indicated that under proper surface and environmental conditions the technique allows the measurement of hemispherical total and normal spectral emittances.

The authors extend their appreciation to M. S. Morse for his contribution in connection with electronic instrumentation, which is a vital part of the entire measurement system.

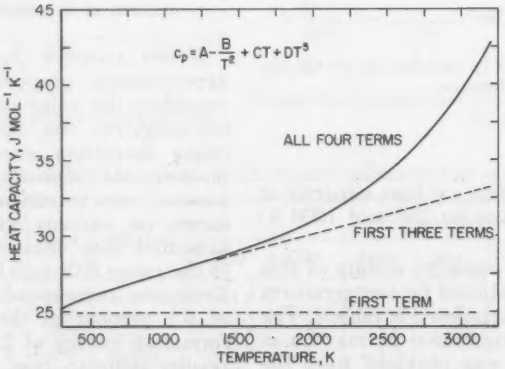

FIGURE 12. *Heat capacity of tantalum according to eq (14).*

8. Appendix

TABLE A–1. *Experimental results on heat capacity and electrical resistivity of tantalum–1* [a]

Range	Series	First series						Second series					
	Run	1		2		3		1		2		3	
	T	c_p	ρ	c_p	ρ	c_p	ρ	c_p	ρ	c_p	ρ	c_p	ρ
	1900	30.75	75.68	30.67	75.68	30.75	75.70	30.73	75.51	30.73	75.52	30.83	75.51
	1950	30.92	77.29	30.88	77.29	30.94	77.30	30.92	77.12	30.92	77.13	30.98	77.14
	2000	31.12	78.89	31.11	78.89	31.14	78.89	31.14	78.72	31.16	78.73	31.16	78.74
Low	2050	31.35	80.48	31.36	80.47	31.36	80.47	31.39	80.31	31.41	80.33	31.38	80.33
	2100	31.60	82.05	31.62	82.05	31.61	82.05	31.65	81.89	31.68	81.91	31.63	81.90
	2150	31.88	83.62	31.91	83.61	31.88	83.62	31.94	83.46	31.96	83.48	31.91	83.46
	2200	32.20	85.17	32.22	85.17	32.18	85.18	32.25	85.02	32.24	85.03	32.22	85.02
	2250	32.56	86.72	32.55	86.72	32.52	86.72	32.57	86.57	32.51	86.57	32.58	86.58
	2100	31.73	82.10	31.80	82.08	31.65	82.07	31.76	81.94	31.74	81.95	31.79	81.94
	2150	31.97	83.69	32.02	83.66	31.92	83.64	31.99	83.51	31.98	83.52	32.02	83.52
	2200	32.22	85.25	32.25	85.22	32.20	85.19	32.24	85.07	32.24	85.07	32.26	85.08
	2250	32.49	86.80	32.50	86.77	32.49	86.74	32.51	86.62	32.51	86.62	32.52	86.63
	2300	32.77	88.33	32.77	88.30	32.78	88.28	32.80	88.16	32.80	88.15	32.80	88.16
Med.	2350	33.08	89.85	33.07	89.82	33.10	89.80	33.12	89.68	33.11	89.67	33.10	89.69
	2400	33.41	91.35	33.39	91.33	33.42	91.32	33.46	91.19	33.44	91.18	33.43	91.20
	2450	33.76	92.85	33.75	92.82	33.77	92.81	33.82	92.68	33.80	92.68	33.79	92.70
	2500	34.15	94.33	34.15	94.31	34.13	94.30	34.21	94.17	34.20	94.17	34.18	94.19
	2550	34.58	95.80	34.60	95.79	34.52	95.76	34.63	95.65	34.63	95.65	34.60	95.66
	2600	35.05	97.26	35.11	97.25	34.92	97.23	35.09	97.12	35.10	97.12	35.08	97.13
	2350	33.12	89.82	33.12	89.82	33.19	89.82	33.21	89.66	33.19	89.69	33.23	89.65
	2400	33.45	91.33	33.47	91.34	33.51	91.32	33.53	91.19	33.50	91.20	33.55	91.18
	2450	33.80	92.83	33.83	92.85	33.84	92.82	33.87	92.70	33.83	92.70	33.89	92.69
	2500	34.16	94.32	34.20	94.34	34.18	94.30	34.23	94.19	34.18	94.19	34.24	94.18
	2550	34.54	95.79	34.58	95.81	34.55	95.77	34.60	95.67	34.56	95.66	34.60	95.66
	2600	34.95	97.25	34.98	97.27	34.93	97.23	34.99	97.14	34.96	97.13	34.99	97.12
	2650	35.38	98.70	35.40	98.71	35.34	98.67	35.40	98.58	35.39	98.57	35.40	98.56
High	2700	35.85	100.13	35.85	100.13	35.78	100.10	35.85	100.01	35.85	100.01	35.85	99.99
	2750	36.35	101.55	36.34	101.54	36.26	101.52	36.33	101.42	36.35	101.43	36.33	101.41
	2800	36.89	102.95	36.87	102.94	36.77	102.92	36.86	102.82	36.89	102.83	36.86	102.81
	2850	37.49	104.33	37.46	104.32	37.34	104.30	37.44	104.20	37.47	104.21	37.44	104.19
	2900	38.15	105.70	38.11	105.69	37.97	105.67	38.08	105.57	38.10	105.58	38.09	105.56
	2950	38.88	107.05	38.86	107.04	38.68	107.02	38.81	106.92	38.79	106.94	38.83	106.91
	3000	39.72	108.39	39.72	108.38	39.48	108.35	39.65	108.25	39.55	108.28	39.69	108.25

[a] Temperature in K.
Heat capacity in J mol^{-1} K^{-1}.
Electrical resistivity in $10^{-8}\Omega m$.

TABLE A–2. *Experimental results on heat capacity and electrical resistivity of tantalum–2*

Range	T K	c_p J mol^{-1}K^{-1}	ρ $10^{-8}\Omega$m
Low	1900	31.02	76.29
	1950	31.20	77.90
	2000	31.40	79.50
	2050	31.64	81.09
	2100	31.90	82.66
	2150	32.20	84.22
	2200	32.52	85.78
Med.	2100	31.88	82.72
	2150	32.11	84.29
	2200	32.36	85.85
	2250	32.62	87.40
	2300	32.90	88.94
	2350	33.21	90.47
	2400	33.54	91.98
	2450	33.90	93.48
	2500	34.30	94.98
	2550	34.74	96.46
High	2350	33.21	90.43
	2400	33.54	91.96
	2450	33.88	93.47
	2500	34.23	94.97
	2550	34.61	96.45
	2600	35.00	97.92
	2650	35.42	99.37
	2700	35.88	100.81
	2750	36.37	102.23
	2800	36.90	103.63
	2850	37.49	105.02
	2900	38.15	106.39
	2950	38.89	107.75
	3000	39.73	109.08

TABLE A–3. *Experimental results on heat capacity and electrical resistivity of tantalum–3 and tantalum–4*

Temperature	Tantalum–3		Tantalum–4	
K	c_p J mol^{-1}K^{-1}	ρ $10^{-8}\Omega$m	c_p J mol^{-1}K^{-1}	ρ $10^{-8}\Omega$m
2950	38.88	106.82	38.67	106.64
3000	39.42	108.14	39.48	107.96
3050	40.15	109.45	40.42	109.28
3100	41.12	110.75	41.50	110.58
3150	42.43	112.04	42.77	111.87
3200	44.22	113.32	44.31	113.15

TABLE A–4. *Experimental results on normal spectral emittance of tantalum at* $\lambda = 650$ nm

T K	$\epsilon_{N,\lambda}$
1999	0.414
2038	.411
2076	.409
2115	.408
2154	.406
2192	.406
2231	.405
2269	.405
2307	.406
2458	.405
2528	.404
2597	.402
2664	.401
2730	.400
2794	.399
2857	.399
2917	.398
2975	.398

TABLE A–5. *Experimental results on hemispherical total emittance of tantalum*

T K	ϵ
First Series	
2324	0.315
2324	.314
2328	.319
2328	.319
2640	.326
2640	.330
2650	.329
2650	.328
2961	.342
2961	.341
2975	.345
2975	.344
Second Series	
2319	0.307
2319	.305
2325	.311
2325	.309
2646	.321
2646	.321
2655	.325
2655	.324
2980	.338
2980	.338
2994	.340
2994	.340

9. References

[1] Cezairliyan, A., Morse, M. S., Berman, H. A., and Beckett, C. W., High-speed (subsecond) measurement of heat capacity, electrical resistivity, and thermal radiation properties of molybdenum in the range 1900 to 2800 K. J. Res. Nat. Bur. Stand. (U.S.), **74A** (Phys. and Chem.), No. 1, 65–92 (Jan.–Feb. 1970).

[2] Cezairliyan, A., High-speed methods of measuring specific heat of electrical conductors at high temperatures, High Temp.-High Pres., **1**, 517 (1969).

[3] Cezairliyan, A., McClure, J. L., Morse, M. S., and Beckett, C. W., Measurement of Heat Capacity of Tantalum in the Range 1900 to 3000 K by a Pulse Heating Method. Fifth Symposium on Thermophysical Properties (Boston), ASME, New York (1970).

[4] Lowenthal, G. C., The specific heat of metals between 1200 K and 2400 K, Australian J. Phys. **16**, 47 (1963).

[5] Rasor, N. S., and McClelland, J. D., Thermal properties of graphite, molybdenum, and tantalum to their destruction temperatures, J. Phys. Chem. Solids **15**, 17 (1960).

[6] Taylor, R. E., and Finch, R. A., The specific heats and resistivities of molybdenum, tantalum, and rhenium, J. Less-Common Metals **6**, 283 (1964).

[7] Jaeger, F. M., and Veenstra, W. A., The exact measurement of the specific heats of solid substances at high temperatures (vanadium, niobium, tantalum, and molybdenum), Rec. Trav. Chim. **53**, 677 (1934).

[8] Hoch, M., and Johnston, H. L., A high-temperature drop calorimeter, The heat capacities of tantalum and tungsten between 1000 and 3000 K, J. Chem. Phys. **65**, 855 (1961).

[9] Schultz, H., "Quenching of Vacancies in Tungsten," in Lattice Defects in Quenched Metals, R. M. J. Cotterill, M. Doyama, J. J. Jackson and M. Meshi, Eds. (Academic Press, New York, 1965), p. 761.

[10] Meakin, J. D., Lawley, A., and Koo, R. C., "Vacancy Loops in Quenched Molybdenum," in Lattice Defects in Quenched Metals, R. M. J. Cotterill, M. Doyama, J. J. Jackson, and M. Meshi, Eds. (Academic Press, New York, 1965), p.767.

[11] Hultgren, R., Orr, R. L., Anderson, P. D., and Kelley, K. K., Selected Values of Thermodynamic Properties of Metals and Alloys (John Wiley, New York, 1963).

[12] Foley, G. M., High-speed optical pyrometer, Rev. Sci. Instr. **41**, 827 (1970).

[13] DeVos, J. C., Evaluation of the quality of a blackbody, Physica **20**, 669 (1954).

[14] International Practical Temperature Scale of 1968, Metrologia **5**, 35 (1969).

[15] Compt. Rend. of the 21st Conference of the International Union of Pure and Applied Chemistry, Montreal (1961), Report of the Committee on Atomic Weights, p. 284.

[16] Tietz, T. E., and Wilson, J. W., Behavior and Properties of Refractory Metals (Stanford University Press, California, 1965), p. 28.

[17] Cezairliyan, A., High-speed methods of measuring thermophysical properties at high temperatures, Rev. Int. Hautes Tempér. et Réfract. **7**, 215 (1970).

[18] Worthing, A. G., Physical properties of well seasoned molybdenum and tantalum as a function of temperature, Phys. Rev. **28**, 190 (1926).

[19] Malter, L., and Langmuir, D. B., Resistance, emissivities and melting point of tantalum, Phys. Rev. **55**, 743 (1939).

[20] Hörz, G., Emissionsvermögen und elektrischer Widerstand von Tantal bei hohen Temperaturen. Z. Metallk. **57**, 871 (1966).

[21] Peletskii, V. E., and Voskresenskii, V. Ya., Thermophysical properties of tantalum at temperatures above 1000 °C. High Temperature **4**, 329 (1966).

[22] Neimark, B. E., and Voronin, L. K., Thermal conductivity, specific electrical resistivity, and total emissivity of refractory metals at high temperatures, High Temperature **6**, 999 (1968).

[23] Petrov, V. A., Chekhovskoi, V. Ya., and Sheindlin, A. E., Integral hemispherical radiating power and specific electrical resistance of tantalum in the temperature interval 1200–2800 K. High Temperature **6**, 525 (1968).

[24] Allen, R. D., Glasier, L. F., and Jordan, P. L., Spectral emissivity, total emissivity, and thermal conductivity of molybdenum, tantalum, and tungsten above 2300 K, J. Appl. Phys. **31**, 1382 (1960).

[25] White, G. K., and Woods, S. B., Electrical and thermal resistivity of the transition elements at low temperatures, Phil. Trans. Royal Soc. (London) **251**, 273 (1959).

[26] Tye, R. P., Preliminary measurements on the thermal and electrical conductivities of molybdenum, niobium, tantalum, and tungsten, J. Less-Common Metals **3**, 13 (1961).

[27] Powell, R. W., Thermal conductivity: A review of some important developments, Contemp. Phys. **10**, 579 (1969).

[28] Gshneidner, K. A., "Physical Properties and Interrelationships of Metallic and Semimetallic Elements," in Solid State Physics, Vol. **16**, F. Seitz and D. Turnbull, Eds. (Academic Press, New York, 1965), p. 275.

(Paper 75A1–644)

JOURNAL OF RESEARCH of the National Bureau of Standards—A. Physics and Chemistry
Vol. 75A No. 1, January–February 1971

Thermophysical Properties of Methane: Orthobaric Densities and Some Thermal Properties*

Robert D. Goodwin**

Institute for Basic Standards, National Bureau of Standards, Boulder, Colorado 80302

(June 30, 1970)

For use in the computation of thermodynamic functions, analytical descriptions are given for the following properties: the orthobaric densities and saturation temperatures; the heats of vaporization; the specific heats of saturated liquid; and the thermodynamic functions for ideal gas states.

Key words: Heats of vaporization; methane; orthobaric densities; specific heats of the saturated liquid; thermofunctions for ideal gas states; thermophysical properties.

List of Symbols

Subscripts c and t refer to critical and liquid triple points.

Subscripts g and l refer to vapor and liquid in equilibrium.

$a, b, c,$ constant coefficients
A_i constant coefficients
$\beta,$ an exponent, 0.36
$C_v,$ molal heat capacity at constant volume
$C_p,$ molal heat capacity at constant pressure
$C_\sigma,$ molal heat capacity of saturated liquid
$d,$ molal density
$\Delta,$ any relative deviation, $(y/y_{\text{calc}}-1)$
$E,$ the internal energy
$\epsilon,$ exponent in various expressions
$H,$ the enthalpy
$J,$ the joule
$k,$ conversion factor, 101.325 J/l-atm)
$l,$ the liter, 1000 cm^3
mol, 16.042 grams of methane
$P,$ pressure, 1 atm = 101325N/m^2
$\Phi(T),$ $(E^0-E_0^0)/RT$, internal energy function
$Q_r,$ heat absorbed in a reversible change of state
$R,$ the gas constant, 8.3143 J/(mol-K), [26]
$\rho,$ d/d_t, density reduced at d_t
$S,$ the entropy
$\sigma,$ d/d_c, density reduced at d_c
$T,$ temperature, K, IPTS (1968)
$T_s(\rho),$ liquid-vapor coexistence temperature
$\tau,$ T/T_c, temperature reduced at T_c
$u,$ $(T_c-T)/(T_c-T_t)$, normalized temperature, origin at T_c
$v,$ $1/d$, molal volume
$w,$ $(T_c/T-1)/(T_c/T_t-1)$, inverse normal temp., origin at T_c
$\omega,$ ϵ/x, an argument in eq (8)
$x,$ $T/400$, reduced temperature for eq (8)
$Y,$ function of C_σ, defined on figure 5
$z,$ $(1-\tau)$, reduced temperature with origin at T_c.

The number of digits, given for coefficients in the empirical functions of this report, is chosen to yield calculated results having at least the same number of figures as exist in the data to be described.

1. Introduction

The current need for thermodynamic properties of methane was described in our preceding report [1].[1] The present report concludes our selection of published properties data for coexisting vapor and liquid, and includes also a description of the ideal gas thermofunctions. All of these properties are placed in analytical form directly useful for thermal computations.

Temperatures are on the IPTS (1968), as in [1], and we use the same fixed-point constants: $T_t = 90.66$ K, $P_t = 0.1151$ atm, (0.01166MN/m^2), $d_t = 28.0536$ mol/l (liquid); and $T_c = 190.53$ K, $P_c = 45.346$ atm, (4.5947 MN/m^2), $d_c = 10.15$ mol/l.

2. The Orthobaric Densities

For the densities of coexisting vapor and liquid methane the preponderance of published data is on the liquid phase [2, 3, 4, 5, 6, 7, 8]. For the vapor phase, therefore, we have estimated data at densities

*This work was conducted at NBS under sponsorship of The American Gas Association.
**Cryogenics Division, Properties of Cryogenic Fluids Section, National Bureau of Standards Laboratories, Boulder, Colorado 80302.

[1] Figures in brackets indicate the literature references at the end of this paper.

up to 1/3 of d_c by use of the vapor pressure equation and the virial equation of state. We used the representation of second virial coefficients based on data of Sengers, Klein, and Gallagher, as well as the third virial coefficient, both as described in [1].

Analytical description of the vapor densities is given by our new form, constrained to qualitatively acceptable behavior near the critical point [9]. To facilitate selection of significant figures in the coefficients, we use variables u and w normalized to a maximum value of unity (at the triple point: see list of symbols). Vapor densities now are described by use of exponent $\beta = 0.36$,

$$\ln(\rho_g/\rho_c) = A_1 \cdot w + A_2 \cdot u^\beta + \sum_{i=3}^{8} A_i \cdot u^{i-2}, \qquad (1)$$

$A_1 = -27.42\ 792$ $\quad A_5 = -10.44\ 279$

$A_2 = -1.56\ 983$ $\quad A_6 = 23.44\ 911$

$A_3 = 10.16\ 428$ $\quad A_7 = -18.38\ 419$

$A_4 = 10.16\ 575$ $\quad A_8 = 7.56\ 705$

The value for exponent β was selected by considering the published values, $\beta = 0.367$ [10], and $\beta = 0.3566$ [11]. The number of terms in (1) was selected to bring deviations down to the level of estimated uncertainty in data derived from the vapor pressure and virial equations. Individual relative deviations of vapor densities from eq (1) are plotted on figure 1. The rms deviation for 55 points is 0.21 percent.

Saturated liquid densities are described by our simple form [9] using argument $z \equiv (1-\tau)$,

$$\rho_l/\rho_c - 1 = a \cdot z + b \cdot z^\beta + c \cdot \exp(-\epsilon \cdot \tau^2/z), \qquad (2)$$

$a = 0.62\ 253$ $\quad c = -0.08\ 367$

$b = 1.89\ 542$ $\quad \epsilon = 0.6$

Inconsistent data were eliminated successively, leaving 60 points with an rms relative deviation of 0.24 percent. Figure 2 gives individual relative deviations from eq (2), and identifies the sources. At the triple point 90.66 K, eq (2) gives a liquid density $d_l = 28.0536$ mol/l resting primarily on the data of [8], as seen on the figure.

Figure 3 gives the coexisting densities of vapor and liquid methane along the abcissa, calculated by eqs (1, 2). The ordinate gives the saturation temperature, $T_s(\rho)$. This plot provides a quick, rough estimate of the data. Conspicuously absent is the line for densities of freezing liquid. Some values recently have been estimated to 94.5 K (150 atm), including the volume change and heats of melting [12].

The rectilinear diameter may be derived by use of eqs (1, 2) for interpolation of d_g and d_l to the same temperatures. For 39 points at $112 \leq T \leq 188$ K, our representation in mol/l,

$$(d_g + d_l)/2 = a + b \cdot z + c \cdot \exp(-\epsilon/z), \qquad (3)$$

$a = 10.156, \quad b = 7.209, \quad c = 0.183, \quad \epsilon = 3/4,$

yields an rms deviation of 0.05 percent and a critical density $d_c = 10.156 + 0.02$ mol/l, as compared with $d_c = 10.15$ adopted for present work.

The relation, $T_s(\rho)$, is important in the nonanalytic equation of state [13]. For the combined data of figures 1 and 2 we obtain coefficients for the expression,

$$T_c/T_s = 1 + |\sigma - 1|^3 \cdot F(\rho), \qquad (4)$$

$$F(\rho) \equiv A_1 \cdot \ln(1/\rho) + \sum_{i=2}^{9} A_i \cdot \rho^{i-2},$$

$A_1 = 0.19\ 3073$ $\quad A_6 = -112.50\ 780$

$A_2 = -0.34\ 282$ $\quad A_7 = 141.02\ 284$

$A_3 = 2.44\ 483$ $\quad A_8 = -89.60\ 804$

$A_4 = -12.24\ 696$ $\quad A_9 = 22.74\ 904$

$A_5 = 48.68\ 975$ $\quad \text{rms} = 0.20\ \%$

The signs and magnitudes of these coefficients are comparable with values found for other substances [9].

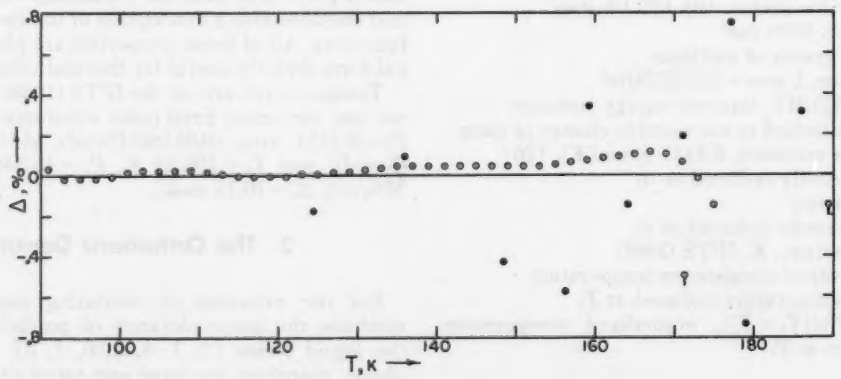

FIGURE 1. *Relative deviations of the densities of saturated methane vapor from eq (1).*

Open circles from the virial surface and vapor pressures; filled circles from [4]; circles with tails from [5].

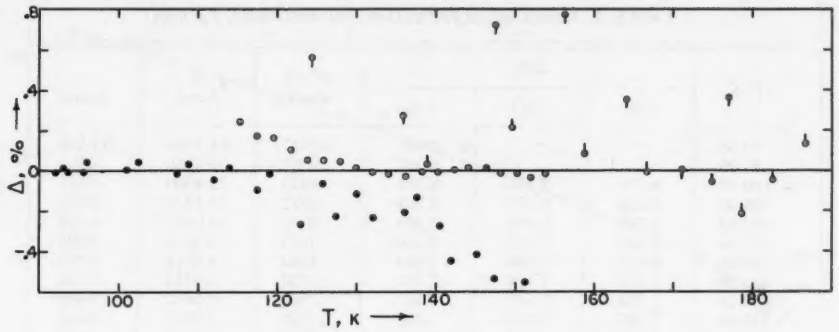

FIGURE 2. *Relative deviations of the densities of saturated liquid methane from eq (2).*

Filled circles from [8]; open circles from [7]; tails up from [5]; tails down from [4].

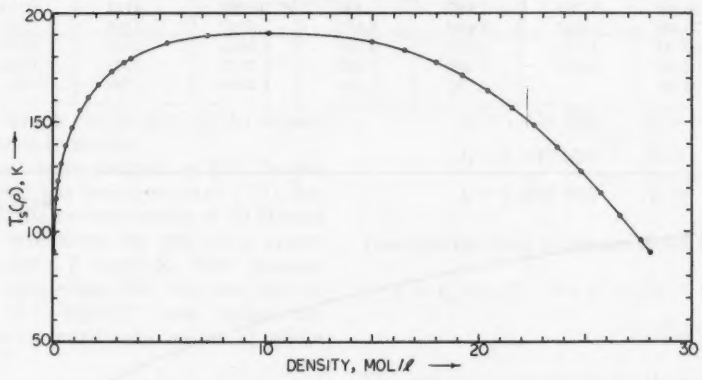

FIGURE 3. *Methane saturation temperatures as a function of vapor and liquid densities up to the triple point.*

3. The Heats of Vaporization

Some data for the heats of vaporization, ΔH_v, have been reported [14, 15]. We now use the Clapeyron equation to calculate these heats by use of our vapor pressure equation [1] and eqs (1 and 2) of the present report,

$$\Delta H_v = k \cdot T \cdot (dP/dT) \cdot (v_g - v_l). \qquad (5)$$

Column 1 of table 1 gives the same rounded temperatures used in [14, 15]. (Experimental uncertainties do not demand conversion to the IPTS–1968.) Second and third columns of table 1 give the published data in kilo-Joules/mole. The fourth column gives our results via (5). The remaining three columns are the derived data used on the right of (5). Figure 4 gives the outline for our calculated results.

For some computations it would be convenient to use a more direct description of ΔH_v than given by (5). For the 21 points in the fourth column of table 1 the following representation gives a maximum relative deviation $\Delta = -0.04$ percent at 120 K; deviations of 0.00 percent at $T = 185$ and $T = 190$ K; and an rms deviation of 0.02 percent,

$$\Delta H_v = \sum_{i=1}^{6} A_i \cdot u^{i/3}, \text{ kJ/mol}, \qquad (6)$$

$A_1 =$ 7.88 860 $\quad A_4 = -152.63\ 520$

$A_2 = -12.94\ 022 \quad A_5 =$ 136.57 252

$A_3 =$ 76.33 098 $\quad A_6 = -46.55\ 421$

4. Specific Heats of Saturated Liquid

Specific heats of the liquid phase, along the coexistence path, are useful for computing thermodynamic properties into compressed liquid states. Data for C_σ are derived from observations on the two phase, liquid-vapor system at constant volume by use of accurate PVT data for the two phases [17]. Published data for methane are quite uncertain because the authors failed to give either their experimental observations or a quantitative description of their derivations [14, 15]. The data are shown by figure 5 in

408-434 O - 71 - 2

TABLE 1. *Heats of vaporization for methane, kJ/mol*

T, K	ΔH_v			dP/dT atm/K	v_g l/mol	v_l l/mol
	[14]	[15]	Calc			
90.66			8.661	0.0147	64.1399	0.0356
95.00			8.597	.0227	39.4535	.0361
100.00	8.571	8.494	8.506	.0353	23.8300	.0367
105.00	8.433	8.355	8.394	.0522	15.1377	.0373
110.00	8.300	8.213	8.260	.0741	10.0373	.0379
115.00	8.162	8.063	8.110	.1014	6.9043	.0385
120.00	8.025	7.899	7.943	.1344	4.9011	.0392
125.00	7.878	7.724	7.761	.1734	3.5743	.0400
130.00	7.731	7.531	7.563	.2186	2.6672	.0408
135.00	7.565	7.326	7.347	.2702	2.0295	.0416
140.00	7.394	7.104	7.112	.3283	1.5698	.0425
145.00	7.203	6.862	6.856	.3930	1.2310	.0436
150.00	6.987	6.598	6.578	.4645	0.9763	.0447
155.00	6.740	6.305	6.273	.5431	.7814	.0460
160.00	6.468	5.987	5.937	.6292	.6296	.0475
165.00	6.153	5.619	5.563	.7232	.5093	.0493
170.00	5.784	5.197	5.134	.8262	.4121	.0514
175.00	5.339	4.699	4.623	.9397	.3316	.0542
180.00	4.776	4.021	3.980	1.0664	.2625	.0579
185.00	3.933	3.109	3.088	1.2122	.1995	.0636
190.00		0.782	1.267	1.4059	.1269	.0801

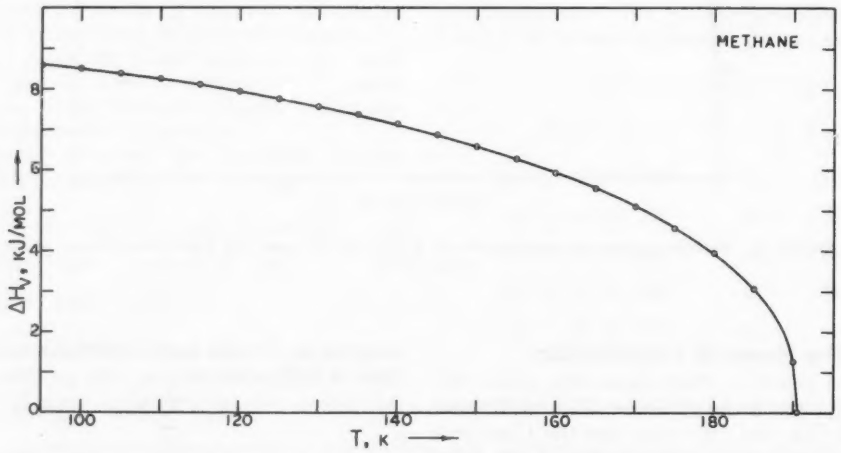

FIGURE 4. *Outline for the heats of vaporization of methane, kilo-Joules/mol, derived via the Clapeyron equation with analytical descriptions of the physical properties.*

coordinates $C_\sigma \cdot u^\epsilon$ versus T, the weighted form used for least squares determination of coefficients in

$$C_\sigma = a + b \cdot u + c/u^\epsilon, \text{ J/(mol K)}, \qquad (7)$$

$$a = 29.250 \qquad c = 18.924$$

$$b = 5.560 \qquad \epsilon = 0.55$$

The value for exponent ϵ was selected by analogy: our oxygen data yield $\epsilon = 0.54$ by trial, and our fluorine data give $\epsilon = 0.59$ [18]. Present methane data yield $\epsilon = 1.0 \pm 0.1$. The line on figure 5 is calculated from (7). The rms relative deviation is 2.6 percent for 33 values of C_σ.

5. The Ideal Gas States

Thermodynamic functions for hypothetical ideal gas states at one atmosphere pressure may be derived for simple molecules as a function of temperature from spectroscopic data by statistical methods [19, 20]. For our thermodynamic computations with PVT data, these ideal gas functions are invaluable because their

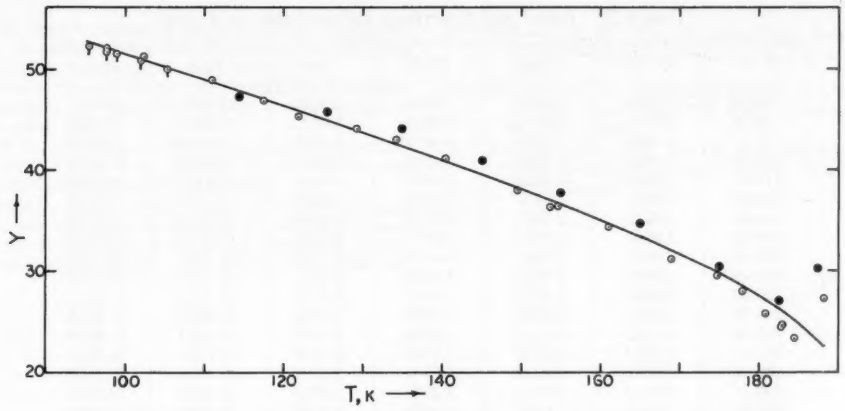

FIGURE 5. *The function* $Y \equiv C_v \cdot u^{0.55}$ *(J/mol deg) for specific heat of liquid methane along the saturation path, using* $u \equiv (T_c - T)/(T_c - T_t)$.

Filled circles are from [15]; open circles from [14]; circles with tails from [16]. The line is calculated with eq (7).

accuracy exceeds that which can be attained by experimental specific heat measurements.

Data for methane first were derived in API Project 44 [21], and work to 1961 has been reviewed [22]. For present work we select the recent results of McDowell and Kruse [23], and give them an analytical representation in the range $60 \leq T \leq 400$ K. With conventional notation [19], abbreviate the internal energy function by $\Phi(T) \equiv (E^0 - E_0^0)/RT$, and define the argument $x \equiv T/400$ with maximum value of about unity for our range of T.

A formulation with six constants was used for nitrogen [24]. For methane [23] and for oxygen [25] it does not give a highly precise representation of the specific heats. A more precise description is obtained with the power series,

$$\Phi(T) = \sum_{i=1}^{10} A_i \cdot x^{i-1}.$$

On the other hand, a modification of the form given in [24] diminishes specific heat rms deviations by a factor of about 1/2. Maximum deviations in C_v^0/R (given below) become 0.02 percent in our present range of interest for methane, $80 \leq T \leq 360$ K. This accuracy is at least an order of magnitude better than can be obtained from PVT data when using the thermodynamic computation,

$$C_v(\rho, T) = C_v^0(T) - T \cdot \int_0^\rho (\partial^2 P/\partial T^2) \cdot d\rho/\rho^2.$$

The modified form (8) uses an argument, $\omega \equiv \epsilon/x$. Constant ϵ is found by trial,

$$\Phi(T) = A_1 + A_2 \cdot x^{1/3} + A_3 \cdot x^{2/3} + A_4 \cdot x + A_5 \cdot \omega/(e^\omega - 1), \tag{8}$$

$$\epsilon = 5.022\ 880 \qquad A_3 = -1.847\ 272$$
$$A_1 = 2.599\ 898 \qquad A_4 = 0.821\ 122$$
$$A_2 = 1.444\ 942 \qquad A_5 = 4.720\ 791.$$

The specific heat is obtained via $C_v^0 = dE^0/dT$,

$$C_v^0/R = A_1 + \tfrac{1}{3} \cdot A_2 \cdot x^{1/3} + \tfrac{5}{3} \cdot A_3 \cdot x^{2/3} + 2 \cdot A_4 \cdot x + A_5 \cdot [\omega/(e^\omega - 1)]^2 \cdot e^\omega. \tag{9}$$

The entropy is obtained via its definition,

$$\Delta S \equiv Q_r/T = \int_{T_1}^{T} [C_v \cdot dT/T + P \cdot dv/T].$$

Introducing the published value of S^0/R at $T_1 = 60$ K yields,

$$S^0/R = A_0 + \ln(T/60) + A_1 \cdot \ln(x) + 4 \cdot A_2 \cdot x^{1/3} + \tfrac{5}{2} \cdot A_3 \cdot x^{2/3} + 2 \cdot A_4 \cdot x + A_5 \cdot [\omega/(e^\omega - 1) - \ln(1 - e^{-\omega})] \tag{10}$$

with constant $A_0 = 18.852\ 484$.

Specific heat at constant pressure, and the enthalpy function now are simply

$$C_p^0/R = 1 + C_v^0/R, \tag{11}$$

$$(H^0 - E_0^0)/RT = 1 + \Phi(T). \tag{12}$$

Table 2 gives temperatures in the first column. The next three pairs of columns give data and calculated values for $\Phi(T)$, for C_v^0/R, and for S^0/R.

Independent computations of above data by Harrison et al. [27] give almost identical results at $90 \leq T < 800$ K, further increasing confidence in their accuracy.

TABLE 2. *Ideal gas functions for methane at 1 atm*

T, K	$\Phi(T)$	Calc	C_p^o/R	Calc	S^o/R	Calc
60.00	2.9693	2.9693	3.0014	3.0007	15.9337	15.9337
80.00	2.9774	2.9774	3.0019	3.0021	17.0849	17.0849
90.67	2.9803	2.9803	3.0021	3.0023	17.5859	17.5859
100.00	2.9823	2.9823	3.0024	3.0023	17.9779	17.9779
111.67	2.9844	2.9844	3.0027	3.0024	18.4197	18.4197
120.00	2.9857	2.9857	3.0029	3.0026	18.7077	18.7077
140.00	2.9882	2.9882	3.0042	3.0039	19.3248	19.3248
160.00	2.9904	2.9903	3.0075	3.0075	19.8597	19.8596
180.00	2.9927	2.9927	3.0153	3.0157	20.3321	20.3320
200.00	2.9956	2.9957	3.0309	3.0313	20.7559	20.7559
220.00	3.0000	3.0000	3.0571	3.0574	21.1412	21.1412
240.00	3.0063	3.0063	3.0966	3.0966	21.4958	21.4958
260.00	3.0152	3.0152	3.1506	3.1503	21.8257	21.8258
273.15	3.0227	3.0228	3.1943	3.1939	22.0316	22.0316
280.00	3.0272	3.0272	3.2196	3.2191	22.1357	22.1358
298.15	3.0412	3.0412	3.2947	3.2942	22.4030	22.4030
300.00	3.0428	3.0427	3.3030	3.3025	22.4296	22.4296
320.00	3.0620	3.0619	3.3996	3.3994	22.7104	22.7103
340.00	3.0850	3.0849	3.5077	3.5080	22.9803	22.9802
360.00	3.1117	3.1117	3.6257	3.6264	23.2412	23.2412
380.00	3.1420	3.1421	3.7516	3.7527	23.4947	23.4947
400.00	3.1758	3.1759	3.8839	3.8847	23.7417	23.7418
450.00	3.2737	3.2737	4.2328	4.2291	24.3369	24.3369

6. Discussion

This report gives analytical descriptions of some methane properties, using existing and estimated data, as a base for preliminary computations of thermodynamic functions over the wide range from gaseous to compressed liquid states at low temperatures. It reveals deficiencies in the quantity of data available for densities of saturated vapor; in the precision of data available for saturated liquid densities; and hence uncertainty, difficult to assess, in the derived heats of vaporization. Data available for specific heats of liquid at coexistence cannot be assessed, due to a lack of published information. For thermofunctions in ideal gas states, the high quality of results derived by McDowell and Kruse suggests that they will stand for a long time.

This laboratory is undertaking an experimental program to obtain reliable and self-consistent measurements over a wide range of conditions and to compute thermodynamic properties based on their formulations.

7. References

[1] Goodwin, R. D., Thermophysical properties of methane: virial coefficients, vapor- and melting pressures, J. Res. Nat. Bur. Stand. (U.S.), **74A** (Phys. and Chem.), No. 5, (Sept.–Oct. 1970).

[2] Keyes, F. G., Taylor, R. S., and Smith, L. B., The thermodynamic properties of methane, J. Math. & Phys. **1**, 211 (1922).

[3] Matthews, C. S., and Hurd, C. O., Thermodynamic properties of methane, Trans. Am. Inst. Chem. Engrs. **42**, 55 (1946).

[4] Bloomer, O. T., and Parent, J. D., Liquid-vapor phase behavior of the methane-nitrogen system, Chem. Eng. Prog. Symposium Ser. 6, **49**, 11 (1952).

[5] Vennix, Alan J., Low temperature volumetric properties and the development of an equation of state for methane, Thesis, Dept. of Chem. Engrn'g., Rice University, Houston, Texas, April, 1965.

[6] Grigor, Anthony F., The measurement and correlation of some physical properties of methane and per-deuteromethane, Thesis, Dept. of Chem., Pennsylvania State University, December, 1966.

[7] Davenport, A. J., Rowlinson, J. S., and Saville, G., Solutions of three hydrocarbons in liquid methane, Trans. Faraday Soc. **62**, 322 (1966).

[8] Terry, M. J., Lynch, J. T., Bunclark, M., Mansell, K. R., and Staveley, L. A. K., The densities of liquid argon, krypton, xenon, oxygen, nitrogen, carbon monoxide, methane, and carbon tetrafluoride along the orthobaric liquid curve, J. Chem. Thermodynamics **1**, No. 4, 413 (1969).

[9] Goodwin, R. D., Estimation of critical constants T_c, ρ_c from the $\rho(T)$ and $T(\rho)$ relations at coexistence, J. Res. Nat. Bur. Stand. (U.S.), **74A** (Phys. and Chem.), No. 2, 221–227 (Mar.–Apr. 1970).

[10] Ricci, F. P., and Scafè, E., Orthobaric density of CH_4 in the critical region, Physics Letters **29A**, No. 11, 650 (1969).

[11] Jansoone, V., Gielen, H., DeBoelpaep, J., and Verbeke, O. B., The pressure-temperature-volume relationship of methane near the critical point, Physica **46**, 213 (1970).

[12] Sindt, C. F., Ludtke, P. R., and Roder, H. M., Slush and boiling methane characterization, private communication 9758, this laboratory, July 1, 1970.

[13] Goodwin, R. D., Formulation of a nonanalytic equation of state for parahydrogen, J. Res. Nat. Bur. Stand. (U.S.), **73A** (Phys. and Chem.), No. 6, 585–591 (Nov.–Dec. 1969).

[14] Wiebe, R., and Brevoort, M. J., The heat capacity of saturated liquid nitrogen and methane from the boiling point to the critical temperature, J. Am., Chem. Soc. **52**, 622 (1930).

[15] Hestermans, P., and White, David, The vapor pressure, heat of vaporization and heat capacity of methane from the boiling point to the critical temperature, J. Phys. Chem. **65**, No. 2, 362 (1961).

[16] Clusius, Klaus, Uber die specifische Warme einiger kondensierter Gase zwischen 10 Grad abs. und ihrem triple Punkt, Z. Physik. Chem. (Leipzig) **B3**, 41–79 (1929).

[17] Goodwin, R. D., and Weber, L. A., Specific heats of oxygen at coexistence, J. Res. Nat. Bur. Stand. (U.S.), **73A** (Phys. and Chem.), No. 1, 1–13 (Jan.–Feb. 1969).

[18] Goodwin, R. D., and Prydz, Rolf, Specific heats of fluorine at coexistence, J. Res. Nat. Bur. Stand. (U.S.), **74A** (Phys. and Chem.), No. 4, 499–505 (July–Aug. 1970).

[19] Rossini, Frederick D., Chemical Thermodynamics (John Wiley & Sons, Inc., New York, 1950).

[20] Mayer, J. E., and Mayer, M. G., Statistical Mechanics, (John Wiley & Sons, Inc., New York, 1940).

[21] Rossini, F. D., Selected values of physical and thermodynamic properties of hydrocarbons, Am. Petroleum Inst. Proj. 44, (Carnegie Press, Pittsburgh, Penna., 1953).
[22] See for example, Tester, H. E., METHANE, in Thermodynamic Functions of Gases, Vol. 3, Din, F., Editor (Butterworths, London, 1961).
[23] McDowell, R. S., and Kruse, F. H., Thermodynamic functions of methane, J. Chem. Eng. Data **8,** 547 (1963). This was kindly pointed out by Lester Haar of NBS.
[24] Barieau, Robert E., Analytical expressions for the zero pressure thermodynamic properties of nitrogen gas including corrections for the latest values of the atomic constants and the new carbon-12 atomic weight scale, J. Phys. Chem. **69,** 495 (1965).
[25] Stewart, R. B., The thermodynamic properties of oxygen, (Dissertation, Dept. of Mech. Engrn'g., Univ. of Iowa, June, 1966.)
[26] Mechtly, E. A., The international system of units (NASA SP–7012, Sept. 1966, U.S. Gov't. Printing Office, Washington, D.C. 20402.)
[27] Harrison, Roland H., private communication (U.S. Bureau of Mines Petroleum Research Center, Bartlesville, Oklahoma 74003, August, 1970.)

(Paper 75A1–645)

JOURNAL OF RESEARCH of the National Bureau of Standards—A. Physics and Chemistry
Vol. 75A, No. 1, January–February 1971

The Infrared Spectrum of Matrix Isolated BaO_2*

S. Abramowitz and N. Acquista

Institute for Materials Research, National Bureau of Standards, Washington, D.C. 20234

(September 21, 1970)

The infrared spectra of matrix isolated BaO_2 have been observed and assigned. Ba atoms were allowed to react with an argon oxygen mixture and condensed on a liquid hydrogen cooled surface. Spectra observed using $^{18}O_2$ and $^{16}O^{18}O$ confirm this assignment.

Key words: Barium; barium oxides; high temperature; infrared; matrix isolations.

1. Introduction

The reaction of O_2 with barium in the gas phase has been studied by several workers [1, 2].[1] This reaction is thought to go through an intermediate BaO_2 (1), even though mass spectrometric evidence for this species is not available. Because of the importance of such an intermediate species, particularly in connection with the recent use of barium releases in the atmosphere to form BaO and Ba clouds, it was decided to study the products of this reaction using matrix isolation techniques.

2. Experimental Procedure

A beam of barium atoms was evaporated from either a stainless steel Knudsen cell or a heated stainless steel small-diameter tube and allowed to codeposit with O_2/Ar onto a liquid hydrogen cooled CsI window. The electron beam furnace used for heating the Knudsen cell, the Air Products Cryotip and the Perkin Elmer 301 spectrophotometer[2] have been described previously [3]. In other experiments a Beckmann IR–7 spectrophotometer with a CsI interchange and a conventional cryostat were used. Higher resolution spectra were obtained using a Perkin-Elmer 99G monochromator equipped with interference filters and suitable diffraction gratings. A chromel-alumel thermocouple inserted into a 0.030″ diameter hole drilled halfway up the wall of the Knudsen cell, was used to measure the temperature of the effusing gas. The recent vapor pressure data of Hinnov and Ohlendorf for barium were utilized [4]. A vapor pressure of barium of about 10^{-3} torr was allowed to effuse through a 2 mm orifice in the Knudsen cell. This atomic beam was then reacted with an O_2/Ar mixture and the products of this reaction were condensed on the liquid hydrogen cooled CsI window. Deposition times varied from 3 to 37 h. Essentially identical experiments were also done with the barium beam from the resistively heated steel tube.

3. Results and Discussion

Initial results obtained by codepositing barium at a vapor pressure of about 10^{-3} torr with an argon oxygen mixture indicated a prominent absorption band in the region of 570 cm^{-1}. The multiplet structure of this band as shown in figure 1 varies with concentration of

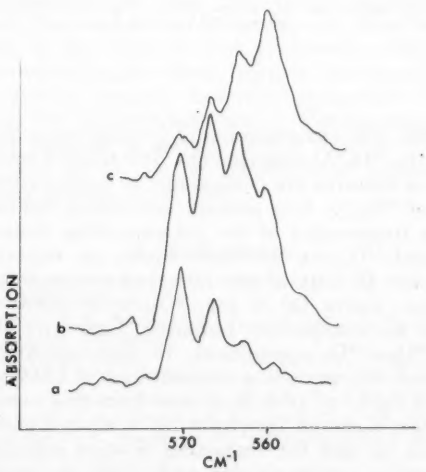

FIGURE 1. *The infrared spectra of* Ba + O_2/Ar.

(a), O_2/Ar = 1/300 (b), O_2/Ar = 1/100 (c), O_2/Ar = 1/50.

*This research was sponsored by the Air Force Office of Scientific Research, Office of Aerospace Research, United States Air Force under AFOSR–ISSA–69–001.

[1] Figures in brackets indicate the literature references at the end of this paper.

[2] Certain commercial instruments are identified in this paper to specify completely the experimental procedure. In no case does such identification imply a recommendation or endorsement by the National Bureau of Standards.

oxygen to argon. (Scan (a) is for a 1/300 O_2/Ar concentration while scan (b) and (c) are for concentrations of 1/100 and 1/50 respectively.) This indicates that these multiplet structures are not due to isotopic effects (barium has five naturally occurring isotopes with abundances greater than 2%). They could possibly be due to molecular complexes with oxygen neighbors, since the oxygen concentration is about 10 times that of the barium in the matrix. Alternatively they could be ascribed to a matrix effect which is concentration dependent. In any event the feature at 570 cm^{-1} certainly becomes more prominent as the concentration of Ar/O_2 and Ba/O_2 increases.

The reaction of Ba + $^{18}O_2$ was then studied. The spectrum shown in figure 2(b) is for about an $^{18}O_2$/Ar

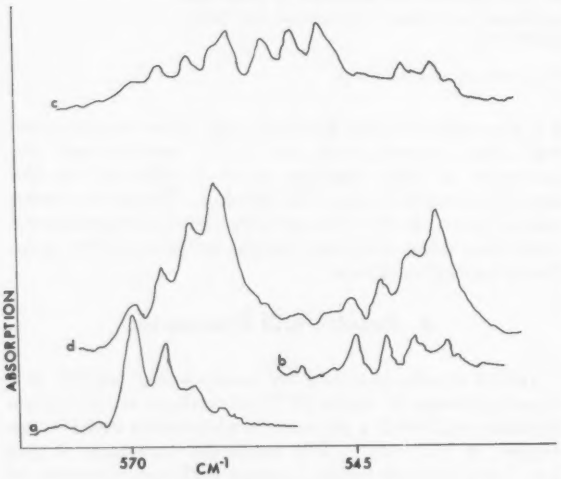

FIGURE 2. *The infrared spectra of* Ba + O_2/Ar.

(a), $^{16}O_2$/Ar = 1/300 (b), $^{18}O_2$/Ar = 1/200 (c), ($^{16}O_2$ + $^{18}O_2$ + $^{16}O^{18}O$)/Ar (d), ($^{16}O_2$ + $^{18}O_2$)/Ar = 1/50.

of 1/200. The same number of features were observed as in the $^{16}O_2$/Ar experiments. The relative intensities of these features are comparable to similar concentrations of $^{16}O_2$/Ar. It is perhaps interesting that the ratio of the frequencies of the corresponding features for $^{16}O_2$ and $^{18}O_2$ are the same within the experimental error for all four of the observed features for each species. Curve (a) is for $^{16}O_2$/Ar of 1/300 and is shown for comparison purposes. Curve (c) shows a Ba + $^{16}O_2$ + $^{18}O_2$ experiment. In this experiment the $^{16}O_2$ and $^{18}O_2$ were at a concentration of 1/100 yielding a total O_2/Ar of 1/50. It is seen from this experiment that the observed spectrum (d) is a superposition of spectra (a) and (b) neglecting relative intensities of the various features within each of the two multiplets. There is no absorption between or midway between corresponding pairs of bands indicating all these features are due to one oxygen molecule per species. In spectrum (c) Ba has been codeposited with $^{16}O_2$ + $^{16}O^{18}O$ + $^{18}O_2$. The ratio of the $^{16}O_2$/$^{18}O_2$ in the sample, which was then discharged electrically with a Tesla coil to scramble the oxygen sample, was about 2/1. The observed spectra contains all the features which are found in spectrum (d). In addition to these features there are lines in between which correspond on a one to one basis with those due to $^{16}O_2$ and $^{18}O_2$. These lines are about midway between the oxygen 16 and 18 lines.

It was then decided to try to obtain spectra of Ba + O_2 with about equal concentrations of both in the matrix. Figure 3 shows such spectra. The barium was heated resistively in a stainless steel tube with about a 5 mm orifice yielding roughly 6 times the barium (at the same pressure) as the Knudsen cell. Also the orifice was closer to the CsI low temperature surface. In these experiments only one prominent feature is found for Ba + $^{16}O_2$ and Ba + $^{18}O_2$ at 570 and 545 cm^{-1} respectively (an $^{16}O^{18}O$ impurity is present in the $^{18}O_2$). An experiment with the scrambled isotopic constitution shows features at 570 and 545 cm^{-1} and another at 559 cm^{-1} due to $Ba^{16}O^{18}O$. This result verifies our initial results indicating that the species responsible for this absorption has two oxygen atoms or one O_2 unit per barium atom. While definitive spectroscopic proof of one barium atom per molecule has not been obtained in this study, any other conclusion doesn't seem warranted. Mass spectral, Knudsen, and optical data indicate that barium evaporates as an atom. Also the only group II diatomic molecule spectroscopically found to date is Mg_2 [5] which has a dissociation energy of about 400 cm^{-1}. Reports in the Russian literature [6] purporting to show the existence of Ca_2 are most probably misinterpreted. More likely emitters for the species are thought to be either CaC or CaN because of the ω_e, B_e and extrapolated D_e values reported.

Rather long extensive runs of 36–40 h duration were necessary to produce the spectra shown in figure 4. This is the region of O—O stretching mode for a proposed BaO_2 molecule. This mode is found at 1066 cm^{-1} for the $Ba^{16}O_2$ and at 1004 cm^{-1} for $Ba^{18}O_2$. These spectra as those shown in figure 3 were obtained with the Perkin-Elmer 99G monochromator. Unfortunately it was not possible to obtain spectra of the mixed isotope in this region (because of the large amount of sample needed). Attempts at longer runs were unsuccessful because of loss of thermal contact between the liquid hydrogen surface and the cryostat's low temperature window, or increased scattering of the argon/O_2/Ba film. The results and assignment for the BaO_2 species are summarized in table 1.

TABLE 1. *Observed fundamental modes for* BaO_2 (cm^{-1})

Assignment	$Ba^{16}O_2$	$Ba^{18}O_2$	$Ba^{16}O^{18}O$
Ba—O Stretch	570	545	559
O—O Stretch	1066	1004	

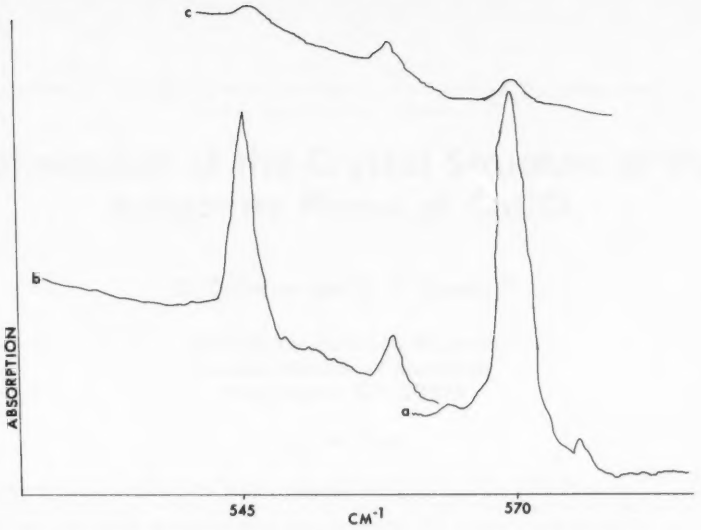

FIGURE 3. *The infrared spectra of* $Ba + O_2/Ar$ *with* Ba/O_2 *about 1:1.*
(a), $^{16}O_2/Ar = 1/100$ (b), $^{18}O_2/Ar = 1/100$ (c), $(^{16}O_2 + {}^{16}O^{18}O + {}^{18}O_2)/Ar = 1/100$.

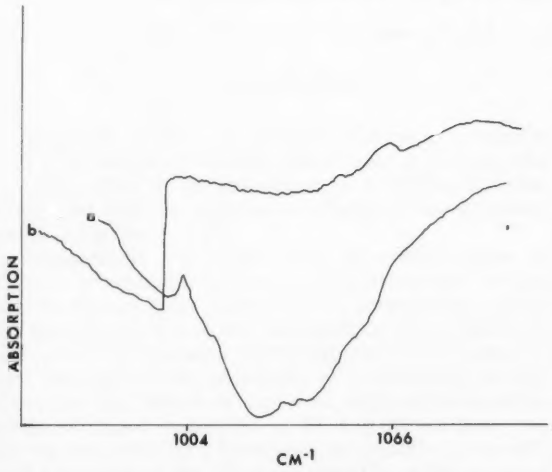

FIGURE 4. *The infrared spectra of* $Ba + O_2/Ar$ *with* Ba/O_2 *about 1:1.*
(The break in curve b is due to a slit change).
(a), $^{16}O_2/Ar = 1/100$ (b), $^{18}O_2/Ar = 1/100$.

4. Conclusions

The product of the reaction of barium atoms and oxygen can be trapped out in an argon matrix at liquid hydrogen temperatures. Isotopic results using $^{18}O_2$ and $^{16}O^{18}O$ in addition to $^{16}O_2$ confirm the existence of such a species, namely BaO_2. Despite the fact that the reaction

$$Ba(^1S) + O_2(X^3\Sigma) \longrightarrow BaO(X^1\Sigma) + O(^3P)$$

is exothermic to the extent of about 0.6 eV, no BaO was observed in these experiments. The $Ba^{16}O$ fundamental was recently found at 632 cm^{-1} in an argon matrix by Linevsky [7].

The intensity of the O—O stretching mode (at 1066 cm^{-1}) is very weak compared to the Ba—O stretching mode found at 570 cm^{-1} for $Ba^{16}O_2$. This low intensity coupled with a frequency which is similar to the O_2^- fundamental frequency reported on by several workers found in solids such as O_2^- doped alkali halide single crystals [8, 9] tends to support a charge transfer type structure consisting of $Ba^+ + O_2^-$. A completely ionic model would yield an O—O bond which would indeed not be infrared active. Crude attempts by us to observe fluorescence spectra of the O_2^- by using Hg 2537 A line were not successful possibly because of the low fluorescence yield or scattering matrix.

Unfortunately the other BaO stretching mode has not been observed as yet. It is not at all clear why the intensity of this mode is weak compared to the other BaO stretching mode. Weak features have been found in the $Ba^{16}O_2$ spectra; however, comparable bands in the $Ba^{18}O_2$ have not been found. Without these data it is not possible to assign the 570 and 545 cm^{-1} in $Ba^{16}O_2$ and $Ba^{18}O_2$ to the symmetric or asymmetric stretching frequencies of BaO_2.

5. References

[1] Sakurai, K., Johnson, S. E., and Broida, H. P., J. Chem. Phys. **52,** 1625 (1970).
[2] Newbury, R. S., Balton, G. W., Jr., and Searcy, A. W., J. Chem. Phys. **48,** 793 (1968).
[3] Mann, D. E., Calder, G. V., Seshadri, K. S., White, D., and Linevsky, M. J., J. Chem. Phys. **46,** 1138 (1967).
[4] Hinnov, E., and Ohlendorf, W., J. Chem. Phys. **50,** 3005 (1969).
[5] Balfour, W. J., and Douglas, A. E., Can. J. Phys. **48,** 901 (1970).
[6] Kovalenok, G. V., Sokolov, V. A., Izvestia Vysshikh, Uchebnykh, Zavedenii Fizika, **3,** 27 (1968).
[7] Linevsky, M. J., private communication.
[8] Holzer, W., Murphy, W. F., and Bernstein, A. J., J. Mol. Spectroscopy **32,** 13 (1969).
[9] Rolfe, J., Holzer, W., Murphy, W. F., and Bernstein, H. T., J. Chem. Phys. **49,** 963 (1968).

(Paper 75A1–646)

JOURNAL OF RESEARCH of the National Bureau of Standards—A. Physics and Chemistry
Vol. 75A No. 1, January–February 1971

Refinement of the Crystal Structure of the Aragonite Phase of $CaCO_3$

B. Dickens and J. S. Bowen*

**Institute for Materials Research
National Bureau of Standards
Washington, D.C. 20234**

(July 31, 1970)

Aragonite ($CaCO_3$) crystallizes in the unit cell $a=4.9598(5)$ Å, $b=7.9641(9)$ Å, and $c=5.7379(6)$ Å at 25 °C with four formula weights in space-group *Pmcn*. The structure has been refined to $R_w=0.024$, $R=0.040$ using 765 x-ray reflections from a single crystal. The Ca ion is coordinated to nine oxygens with Ca . . . O distances in the range 2.414(2) Å to 2.653(1) Å. The two unique C—O distances in the CO_3 group are 1.288(2) Å (on the mirror plane) and 1.283(1) Å. The two unique O—C—O angles are 119.6(2)° (across the mirror plane) and 120.13(8)°. The distances and angles in the CO_3 group are not significantly different at the 95 percent confidence level.

Key words; Calcium carbonates; carbonates; crystal structure; single crystal x-ray diffraction.

1. Introduction

Aragonite ($CaCO_3$) is found in nature as a mineral and is an important biomineral because of its presence in coral, clam shells, gallstones, and otoliths. It is isostructural with the carbonates of large divalent cations such as Ba, Sr, and Pb.

Aragonite is less stable than the calcite phase of $CaCO_3$ at room temperature, transforms into calcite, and is denser than calcite. Thus aragonite is a high pressure form of $CaCO_3$. More details are available in reference [1].[1] Because of the importance of aragonite, and because of the possibility of performing calculations on the lattice energies of selected carbonates along the lines suggested by Busing [2], we have collected new x-ray data from a single crystal of aragonite and have refined the structure from the positions given in 1924 by Bragg [3].

2. Structure Determination

Formula (ideal): $CaCO_3$ (aragonite phase); *Unit Cell:* orthorhombic with $a=4.9598(5)$ Å, $b=7.9641(9)$ Å, $c=5.7379(6)$ Å at 25 °C (calculated by least squares from 12 2θ values observed on a diffractometer; volume: 226.65 Å^3; radiation, Mo($K_{\alpha 1}$), $\lambda=0.70926$ Å; monochromator: highly oriented graphite crystal; space-group: *Pmcn*; contents 4($CaCO_3$); reciprocal lattice extinctions, $hk0$: $h+k=2n+1$, $h0l$: $l=2n+1$; observed density, 2.947(2) g·cm^{-3} [4]; calculated density, 2.944 g·cm^{-3}; *Crystal:* material available was heavily twinned; a small wedge was the largest crystal fragment found which showed no evidence of twinning under optical and x-ray examination; this wedge was attached to thin borate glass fiber with clear household cement; fiber attached to insert in goniometer head with epoxy cement; origin of crystal, mineral sample #75538 from National Museum of Natural History, Smithsonian Institute, Washington, D.C. (Supplied by J. S. White, Jr.); linear absorption corrections made by $8\times8\times8$ Gaussian quadrature using subroutines written by C. W. Burnham [5] and adapted by B. Dickens; maximum and minimum corrections for absorption = 0.880 and 0.963 (transmission factors). *Intensity Data:* number of reflections, 2356 collected from 3 octants and merged into a unique set of 765, of which 619 are "observed" and 146 are "unobserved"; unobserved reflections are those less than 2σ above background; maximum $\sin\theta/\lambda$ for data 0.907 Å^{-1}; method used to estimate data: θ–2θ scan, scintillation counter; diffractometer: Picker[2] 4-circle single-crystal diffractometer automated by PDP 8/I computer through FACS–1 interface and adapted to include least significant digit of counts; *Computation:* setting programs, those of reference [6] as adapted by Picker Nuclear Corporation; scan range: $1.4°+114.6\,\frac{\Delta\lambda}{\lambda}$, $\Delta\lambda=0.692$, $\lambda=0.70926$ Å; scan parameters: backgrounds counted at higher and lower 2θ for 100 s each; θ–2θ scan at

*Research Associate from the American Dental Association at the National Bureau of Standards, Washington, D.C. 20234.

[1] Figures in brackets indicate the literature references at the end of this paper.

[2] Certain commercial equipment, instruments, or materials are identified in this paper in order to adequately specify the experimental procedure. In no case does such identification imply recommendation or endorsement by the National Bureau of Standards, nor does it imply that the material or equipment identified is necessarily the best available for the purpose.

0.25°/min for 2θ from one background position to the other; attenuators: 00.25 mm thick layers of Nb, 2 layers for first attenuator, 4 for second, 6 for third; scan range correction: table look-up method to obtain values recommended in reference [7]; intensity data on paper tape, processed by program written by B. Dickens for Univac 1108 computer; this program contains adaptations of subroutines written for similar program by F. A. Mauer (NBS), standard reflection plotting routine and extinct reflection editing routine from programs by J. M. Stewart, University of Maryland, and uses an intense standard reflection (at low 2θ angle) measured every 50 reflections to correct for any change in intensity of the primary x-ray beam. Counts in peak $= I = P - (T/2T_B)(B_L + B_H)$, $\sigma(I) = [P + (B_L + B_H)(T/(2T_B))^2]^{1/2}$, $F = [(AF)(LP)(I)]^{1/2}$, $\sigma(F) = (\sigma(I)/2)(LP/I)^{1/2}$, $LP = 2 \sin 2\theta_c/(\cos^2 2\theta_m + \cos^2 2\theta_c)$, $\beta = -1.58883 \times 10^6[\lambda^2(\cos^2 2\theta_m + \cos^4 2\theta_c) dA/d\mu]/[AV^2 \sin^2 \theta_c(\cos^2 2\theta_m + \cos^2 2\theta_c)]$ (for extinction corrections, calculated at same time as absorption correction). P = counts at the peak position, B_L and B_H = background counts at lower and higher 2θ respectively, T = time spend counting peak, T_B = time spent counting each background, AF = attenuator factor, LP = Lorentz-polarization correction, θ_c = Bragg angle for reflection under consideration, θ_m = Bragg angle for monochomator (= 6.005° here), A = transmission factor in the absorption correction, μ is the linear absorption coefficient, $dA/d\mu$ is in mm, V is the volume of the unit cell in Å^3. Data merging program for equivalent reflections, written by B. Dickens for Univac 1108 computer; in this program each set of equivalent reflections is treated as follows: Reflections which were all unobserved were averaged and given the largest individual standard deviation in the set. Unobserved reflections in the presence of at least one observed reflection were discarded. Observed reflections which occurred only once in the reflection list subsequent to this step were copied unchanged but their standard deviations were increased by a factor of three. Observed reflections with magnitudes which agreed within the counting statistics and reflections with magnitudes whose ratios fell within the range 0.95 to 1.06 were averaged and given as standard deviation the maximum of the standard deviation from counting statistics and the standard deviation from the range estimate [8, 9]. Under these circumstances, reflections whose magnitudes did not pass the criteria were discarded. If no members of a set of equivalent reflections passed the criteria, the highest magnitude was taken and the associated standard deviation multiplied by five. The justification for these arbitrary increases of standard deviation is that, without some corroboration, every reflection is suspect because of the possibilities of multiple reflection, including the "tail" of nearby intense reflections in its measurement, change in intensity of x-ray beam during reflection measurement, misalignment of crystal, etc. Since we usually measure three sets of equivalent reflections with care the number of standard deviations increased in this way is very small. Scattering factors: those for the neutral atoms in reference [10]; least-squares refinements: full-matrix, with $\Sigma w(|F_o| - |F_c|)^2$ minimized; refinements include unobserved reflections which calculate higher than 2σ above background; least-squares weights: $1/\sigma^2(F)$; $R_w = [\Sigma w(|F_o| - |F_c|)^2/\Sigma w|F_o|^2]^{1/2}$, $R = \Sigma||F_o| - |F_c||/\Sigma|F_o|$; thermal parameters have the form exp $[-1/4(a^{*2}B_{11}h^2 + b^{*2}B_{22}k^2 + c^{*2}B_{33}l^2 + 2a^*b^*B_{12}hk + 2a^*c^*B_{13}hl + 2b^*c^*B_{23}kl)]$. Most least squares and electron density synthesis calculations were carried out with the X-ray 67 system [11] of computing programs.

Final Refinement: $R_w = 0.024$; $R = 0.040$, average shift/error for last cycle = 0.0017; standard deviation of an observation of unit weight

$$= [\Sigma w(F_o - F_c)^2/(765 - 28)]^{1/2} = 0.775.$$

The structure was refined isotropically from the positions given by Bragg to $R_w = 0.031$, $R = 0.047$, and then anisotropically to $R_w = 0.024$, $R = 0.040$. The low value of R_w supports the earlier indications that the crystal used in the data collection is not twinned. The highest peak in an electron density difference synthesis calculated after anisotropic refinement to $R_w = 0.024$ corresponded to about 1/3 of an electron and was about 0.95 Å from C towards O(1). The largest correlation coefficients are 0.34–0.44 between the scale factor and the B_{11}, B_{22} and B_{33} temperature factors of Ca.

Two cycles of least squares refinement in which the isotropic secondary extinction parameter r in $F^2 = F^2_{unc}/(1 + \beta r|F_{unc}|^2)$ was varied [12] together with all other unconstrained parameters resulted in no change in R_w or R and gave a value of $-0.3(9) \times 10^{-8}$ for the extinction parameter. There was no significant change in the structural details or their standard deviations. Thus, we believe secondary extinction to be negligible in our crystal of aragonite. Only the observed reflections were used in these refinements. Three cycles of least squares refinement in which allowance was made for the anomalous scattering of Ca (values taken from reference 10) gave an increase from 0.024 to 0.025 for R_w. R was unchanged. There were no significant changes in the atomic positions.

The atomic parameters from the refinements without corrections for anomalous dispersion are given in table 1. The observed and calculated structure factors are given in table 2. The thermal parameters from the refinements which included corrections for the anomalous scattering of Ca are Ca: 0.71(1), 0.65(1), 0.65(1), 0.00, 0.00, −0.01(1); C: 0.67(5), 0.80(6), 0.43(5), 0.00, 0.00, 0.08(5); O(1): 1.45(5), 0.51(4), 1.01(5), 0.00, 0.00, 0.04(5); O(2): 0.67(3), 0.98(3), 1.00(3), −0.32(3), −0.02(3), −0.09(3). Only those for Ca are significantly different from the values in table 1. Distances and angles referred to in the paper were calculated using the values in table 1.

3. Description of the Structure

The structure of aragonite, the main points of which are well known, is shown in figure 1. The Ca ions lie in pseudohexagonal layers parallel to (001) and the layer sequence is ABAB. The Ca layers are separated by CO_3 groups which lie in two layers parallel to (001), and form columns parallel to [001].

TABLE 1. *Atomic parameters in aragonite* ($CaCO_3$)

Atoms	x	y	z	B_{11}*	B_{22}	B_{33}	B_{12}	B_{13}	B_{23}
Ca	0.25000	0.58507(5)	0.25974(6)	0.664(9)	0.599(9)	0.601(9)	0.0000	0.0000	−0.01(1)
C	.25000	.2386(2)	.4148(3)	.75(5)	.85(5)	.46(5)	.0000	.0000	.07(5)
O(1)	.25000	.0770(2)	.4043(2)	1.50(5)	.54(4)	1.04(4)	.0000	.0000	.03(4)
O(2)	.4737(2)	.3196(1)	.4131(2)	0.71(3)	1.03(3)	1.02(3)	−0.32(3)	−.02(3)	−.09(3)

Figures in parentheses are standard errors in last significant figure quoted, and were computed in the final cycle of full-matrix least-squares refinement.

*Thermal parameters are in Å².

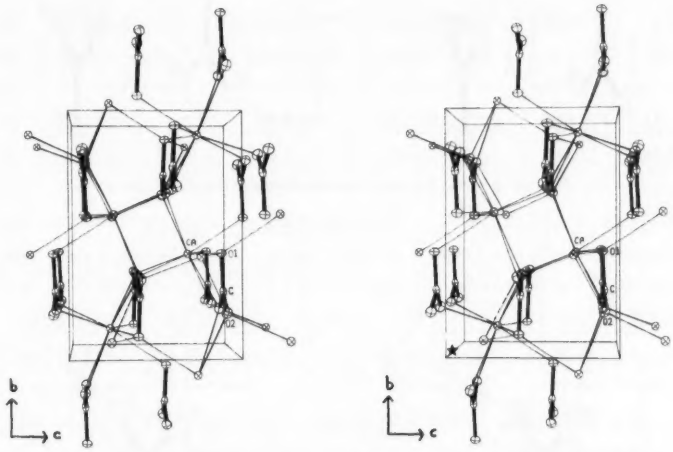

FIGURE 1. *A stereoscopic illustration of the crystal structure of aragonite* ($CaCO_3$).

A unique set of atoms is labeled. The origin of the crystallographic coordinate system is marked by *.

3.1. The Ca Ion Environments

The Ca ion lies on the mirror plane at $x = 1/4$. Its environment is shown in figure 2 and summarized in table 3. The coordination of nine oxygens to Ca consists of three CO_3 edges, O(1, 2), O(1^{I}, 2^{I}) and O(2^{IV}, 2^{V}) and three apexes, O(1^{II}, 2^{II}, 2^{III}). The apparent thermal motion of Ca is almost isotropic (table 1, fig. 2).

Corrections as given by Busing and Levy [13] to obtain the mean separation between atoms from the observed atomic positional and thermal parameters were calculated using a program written by Finger [12]. These corrections are included in tables 3 and 4.

3.2. The CO_3 Group

The details of the CO_3 group and its environment are given in table 4 and shown in figure 3. The positions reported by Bragg [3] give C–O distances of 1.26 Å and 1.30 Å, and O–C–O angles of 117°, 117° and 127°, which, under the circumstances, are all close to those reported here. The C–O distances and O–C–O angles reported here for the CO_3 group do not differ from each other significantly at the 95 percent confidence level; the same is true for the O–C–O angles. In view of the possibility of unknown systematic error, necessarily excluded from the calculations, our results therefore do not preclude trigonality of the CO_3 group. Because the oxygens in the CO_3 group have very similar environments, little deviation from trigonality is expected. The CO_3 group is nonplanar however. The carbon atom is 0.026(4) Å out of the plane of the oxygen atoms in the CO_3 group in aragonite. This displacement is approximately seven times the standard deviation and is clearly significant. The displacement is towards the nearest Ca layer and is presumably a result of polarization of each oxygen atom by the three bonded Ca ions. If the displacement were caused by Ca . . . C interactions, the C atom would not move towards the Ca layer.

The difference in the O–C–O angles, 119.6° and 120.13°, if real, is consistent with the O(2, 2^{I}) edge of the CO_3 group being coordinated slightly more strongly to Ca as judged from the Ca . . . O distances. However, this stronger coordination of O(2) to Ca would also suggest that C–O(2) should be longer than C–O(1). This is not the case. The average value of the C–O distances is 1.286 Å. This agrees well with the C–O distances of 1.283(2) A reported [14] for calcite in which 32 symmetry is forced on the CO_3 group by space-group $R\bar{3}c$. If the apparent thermal motions of the atoms in the CO_3 group are attributed to thermal motion rather than to slight positional disorder, there

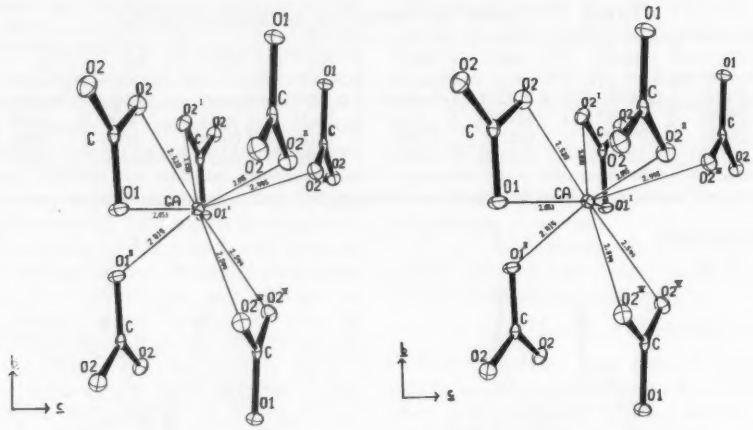

FIGURE 2. *The* Ca *environment in aragonite* ($CaCO_3$).

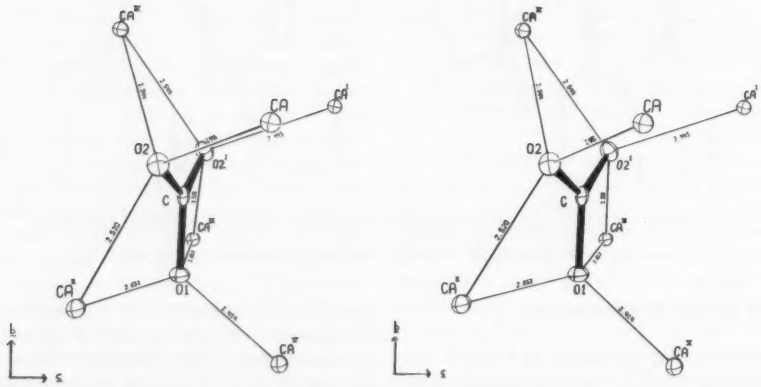

FIGURE 3. *The* CO_3 *group environment in aragonite* ($CaCO_3$).

The labels refer to atoms in table 4.

seems to be oscillation within the CO_3 layer, i.e., more or less perpendicular to the edge coordination to Ca. Similarly, O(1) may be undergoing some additional wagging out of the CO_3 layer.

TABLE 3. *The* Ca *environment in aragonite* ($CaCO_3$)

Atoms	Distance, Å raw	*Lower bound [13]	*Noncorrelated motion [13]
Ca, $O(1^{II})$	2.414(2)	2.414	2.423
Ca, $O(2^{II}, 2^{III})$	2.445(1)	2.445	2.454
Ca, O(2, 2^{I})	2.520(1)	2.520	2.527
Ca, $O(2^{IV}, 2^{V})$	2.544(1)	2.544	2.551
Ca, O(1, 1^{I})	2.653(1)	2.653	2.660

In all tables of interatomic distances and angles, the figures in parentheses are standard deviations in the last digit and were calculated from the standard deviations in the atomic positional parameters and the unit cell parameters.

*Mean separation between atoms when allowance is made for thermal motion.

TABLE 4. *The* CO_3 *group and its environment in aragonite* ($CaCO_3$)

Atoms	Distance, Å or angle, deg.	Lower bound [13]	Riding model [13]
C, O(1)	1.288(2) Å	1.289 Å	1.295 Å
C, O(2)	1.283(1)	1.284	1.288
O(1), O(2)	2.229(1)		
O(2), $O(2^{I})$	2.219(2)		
O(1), C, O(2)	120.13(8)°		
O(2), C, $O(2^{I})$	119.6(2)		
O(1), Ca^{V}	2.414(2) Å		
O(1), (Ca^{II}, Ca^{III})	2.653(1)		
O(2), Ca	2.445(1)		
$O(2^{I})$, Ca^{II}	2.520(1)		
O(2), Ca^{IV}	2.544(1)		

Table 2. Observed and calculated structure factors for aragonite ($CaCO_3$)

Columns are K, $10F_o$, $10F_c$. F_o and F_c are on an absolute scale. Reflections marked * are "unobserved".

We thank W. E. Brown for helpful discussions and P. B. Kingsbury for technical help. The ORTEP program of C. K. Johnson, Oak Ridge National Laboratory, was used to draw the figures. This investigation was supported in part by research grant DE–00572 to the American Dental Association from the National Institute of Dental Research, and is part of the dental research program conducted by the National Bureau of Standards in cooperation with the American Dental Association; the United States Army Medical Research and Development Command; the Dental Sciences Division of the School of Aerospace Medicine, USAF; the National Institute of Dental Research; and the Veterans Administration.

4. References

[1] Palache, C., Berman, H., and Frondel, C., Dana's system of mineralogy, vol. II, 7th ed., J. Wiley and Sons, N.Y. 1963, 182–193.

[2] Busing, W. R., An aid to the analysis of interionic and intermolecular forces in crystals. Abstract M1. American Crystallographic Association winter meeting, Tucson, Arizona (1968).

[3] Bragg, W. L., The structure of aragonite. Proc. Roy. Soc. London, **105,** 16–39 (1924).

[4] Reference [1], page 184.

[5] Burnham, C. W., Computation of absorption corrections and the significance of end effect. Am. Min., **51,** 159–167 (1966).

[6] Busing, W. R., Ellison, R. D., Levy, H. A., King, S. P., and Roseberry, R. T., The Oak Ridge Laboratory Computer-controlled X-ray Diffractometer. Oak Ridge National Laboratory Report ORNL 4143, January 1968.

[7] Alexander, L. E., and Smith, G. S., Single crystal intensity measurements with the three circle counter diffractometer. Acta Cryst., **15,** 983–1004 (1962).

[8] Ibers, J. A., Estimates of the standard deviations of the observed structure factors and of the electron density from intensity data. Acta Cryst., **9,** 652–654 (1956).

[9] Tippett, L. H. C., On the extreme individuals and the range of samples taken from a normal population. Biometrika, **17,** 364–387 (1925).

[10] International Tables for X-ray Crystallography, **3,** p. 202. The Kynoch Press, Birmingham, England, 1962.

[11] Stewart, J. M., Editor. X-ray 67 program system for X-ray crystallography. Technical report 67–58, University of Maryland, College Park, Maryland 20742, December (1967).

[12] Finger, L. W., Determination of cation distribution by least squares refinement of single crystal x-ray data. Carnegie Institute of Washington Year Book, **67,** 216–217 (1969).

[13] Busing, W. R., and Levy, H. A., The effect of thermal motion on the estimation of bond lengths from diffraction measurements. Acta Cryst., **17,** 142–146 (1964).

[14] Chessin, H., Hamilton, W. C., and Post, B., Position and thermal parameters of oxygen atoms in calcite. Acta Cryst., **18,** 689–693 (1965).

(Paper 75A1–647)

JOURNAL OF RESEARCH of the National Bureau of Standards—A. Physics and Chemistry
Vol. 75A, No. 1, January–February 1971

Simple Shearing Flows in Polyisobutylene Solutions

L. J. Zapas and J. C. Phillips

Institute for Basic Standards, National Bureau of Standards, Washington, D.C. 20234

(July 2, 1970)

Measurements of shear stress for various shearing flow histories at 25 °C are correlated through the BKZ elastic fluid theory. The data are on 10 percent PIB solution in cetane. The histories include single step stress relaxation, suddenly applied steady shear, steady shearing flow, stress relaxation after steady shear.

Key words: BKZ fluid; nonlinear behavior; polyisobutylene; stress relaxation; viscosity.

1. Introduction

In this paper we present the results of a series of experiments on a single sample of polyisobutylene solution subjected to various histories of simple shear. The work was done as a part of a larger program to study the appropriateness of a fairly general constitutive equation, the Bernstein, Kearsley, Zapas (BKZ) elastic fluid [1],[1] in describing a wide range of nonlinear viscoelastic behavior for a range of materials. This larger purpose influenced both the choice of test material and the choice of experiments. In the first place, the studies were confined to a single sample so as to provide a test of the correlations between experiments predicted by the assumed constitutive equation. The sample was chosen to show essentially complete relaxation within the time scale of the experiment, since earlier studies [2] had been made on materials with longer relaxation times. The deformations are various histories of simple shear, because they are experimentally convenient deformations and because they are convenient to analyze in terms of the assumed constitutive equation.

Some measurements of normal stresses were made on this sample, but we encountered serious discrepancies when we attempted to correlate them with the shear data. This trouble has been traced to the recently discovered "pressure hole error" [3] and the difficulty resolved, but we have postponed publication of the normal stress data to avoid further delay in the presentation of the shear stress measurements.

In the course of these studies some measurement errors, customarily ignored, were found to be surprisingly large and some correction methods were worked out and are presented here. A specialized form of the BKZ elastic fluid was used in this paper to correlate our experiments with very good success. Although this special form is neither unique nor exact, it has been chosen to be consistent with a wide range of phenomena beyond that described in this paper, and should be of considerable practical use.

2. General Considerations

The class of motions which we shall consider will be limited to simple shearing histories.

In the incompressible isothermal form of the BKZ theory [1, 4] the value of the shearing stress at time t is given by the following relation

$$\sigma(t) = -\int_{-\infty}^{t} W_*(\gamma(t)-\gamma(\tau),\, t-\tau)\,(\gamma(t)-\gamma(\tau))\,d\tau \tag{2.1}$$

where $\gamma(\tau)$ is the amount of shear at time τ and W_* is a function of strain and time.[2] If W_* is known, the shearing stress $\sigma(t)$ for any simple shearing flow can be calculated through eq (2.1). Of course, the form of W_* is not specified by the theory and in general the function W_* must be determined through experiments.

A good idea of the function W_* can be obtained from examining a single step stress relaxation history in simple shear. In such a deformation the shearing history is given by:

$$\begin{aligned} &\gamma(\tau) = 0 && \text{for } \tau < 0 \\ &\gamma(\tau) = \gamma = \text{constant} && \text{for } \tau > 0. \end{aligned} \tag{2.2}$$

By substituting $\xi = t-\tau$ and (2.2) in (2.1), we get

$$\frac{\sigma(t)}{\gamma} = -\int_{t}^{\infty} W_*(\gamma, \xi)\,d\xi = W(\gamma, t) \tag{2.3}$$

[1] Figures in brackets indicate the literature references at the end of this paper.

[2] Equation (2.1) is equivalent to eq (3.11) of Bernstein [4] except for a change of notation. W_* of this equation is equal to $-2(U_{i_1}+U_{i_2})$ of Bernstein, and our $\sigma(t)$ is Bernstein's σ_{12}.

408-434 O - 71 - 3

where

$$W_*(\gamma, t) = \frac{\partial W(\gamma, t)}{\partial t} \tag{2.4}$$

and

$$W(\gamma, \infty) = 0.$$

In this paper we shall refer to W as the relaxation function. From (2.3) it follows that W or W_* may be obtained from single step stress relaxation measurements in shear at different strains and from this the stress for any simple shearing flow history may be predicted. This approach is similar to the one used for simple extension histories [2].

Bernstein [5] has shown that the function

$$\mathscr{H}(\gamma, t) = W(\gamma, t)\left(1 + \frac{\partial \ln W(\gamma, t)}{\partial \ln \gamma}\right) \tag{2.5}$$

may also be obtained from experiments of suddenly applied steady shear. Thus, in principle, we should be able to obtain $W(\gamma, t)$ from a series of experiments, and then proceed to check the BKZ theory by comparing measured and predicted stress for simple shearing histories.

Of course, one can never realize experimentally these shearing histories exactly as assumed. From some of the experiments which approximated suddenly applied constant rate of shear history, discussed in section 6, we were able to get a rough approximation of the relaxation function. Applying corrections which will be discussed later using an iterative scheme, we recalculated a function W which is consistent with all our experiments which include measurements of viscosity as a function of the rate of shear, stress relaxation after shear (for different rates of shear), measurement of stress as a function of time for suddenly applied steady shear, and single step stress relaxation experiments. These results, we felt, justified the use of an expression for $W(\gamma, t)$ which can describe all our experiments and which is a special form of a more detailed expression consistent with the behavior of other materials and other deformations, viz:

$$W(\gamma, t) = G(t)\left\{\frac{1}{1+\frac{1}{3}\gamma^2} + \frac{0.145\,|\,\gamma\,|}{(1+0.06\gamma^2)^{5/2}}\right\} \tag{2.6}$$

where $G(t)$ is the shear stress relaxation modulus.[3] It is evident that there are many other forms which are consistent with our experimental data. Our motivation for choosing form (2.6) is its relative simplicity and its consistency with a strain potential function [1]. Furthermore, form (2.6) is useful in process control engineering since an immediate translation from the linear to the nonlinear behavior can be made as a function of temperature, molecular weight, and concentration.

[3] Notice that $G(t)$, the shear relaxation modulus, is the limit of relaxation function $W(\gamma, t)$ as γ goes to zero.

3. Experimental

The data reported in this paper were obtained on a 10-percent solution of polyisobutylene (vistanex L–100, Enjay Chemical Co.)[4] in cetane. A Weissenberg Rheogoniometer was used to shear the sample between a flat plate (7.5 cm diameter) and a cone such that the angle of the gap was 0.0268 radians. The cone was at the bottom and was connected to the driving shaft. The plate was at the top and was connected to a torsion bar which was used to measure the torque. For most of the experiments a torsion bar of 1/8-in diameter was used. The stress-time measurements and the dynamic response were recorded on an oscillograph.

The chamber enclosing the cone-plate assembly was kept at a temperature of 25.0 °C ± 0.1 °C. Ambient temperature was controlled at 25.0 °C ± 0.5 °C. An ambient temperature 3 degrees below the chamber temperature caused a noticeable change in the curve of viscosity versus rate of shear at high rates of shear. The zero shear viscosity at this temperature varies about 5 percent per degree.

Periodically, degradation checks were made on samples of 10-percent PIB by taking viscosity versus rate of shear data. No changes were observed over a 2 year period.

4. Behavior at Small Deformations

It is clear from eq (2.6) that the shear relaxation modulus, $G(t)$, plays an important role in our curve fitting scheme. Since stress relaxation measurements cannot be carried out using deformations small enough to yield an infinitesimal modulus, this is ordinarily obtained by some sort of extrapolation procedure. An alternate method, adopted here, is to calculate a curve from measured values of the dynamic modulus, $G'(\omega)$ [6]. We employed the conversion scheme given by Marvin [7],

$$G(t) = G'(\omega)\,|_{1/\omega = t} - \int_{-\infty}^{\infty} H(\tau)\left(\frac{\tau^2}{t^2+\tau^2} - e^{-t/\tau}\right) d \ln \tau, \tag{4.1}$$

using an approximation technique similar to the familiar derivative schemes [6] for the relaxation spectrum, $H(\tau)$. Even though we must depend on extrapolation for values of $H(\tau)$ at small τ, the effect on $G(t)$ is slight.

Figure 1 shows the dynamic data and figure 2 the derived values of $G(t)$. The dotted portion of figure 2 represents values extrapolated to times smaller than

[4] Certain commercial equipment, instruments, or materials are identified in this paper in order to adequately specify the experimental procedure. In no case does such identification imply recommendation or endorsement by the National Bureau of Standards, nor does it imply that the material or equipment identified is necessarily the best available for the purpose.

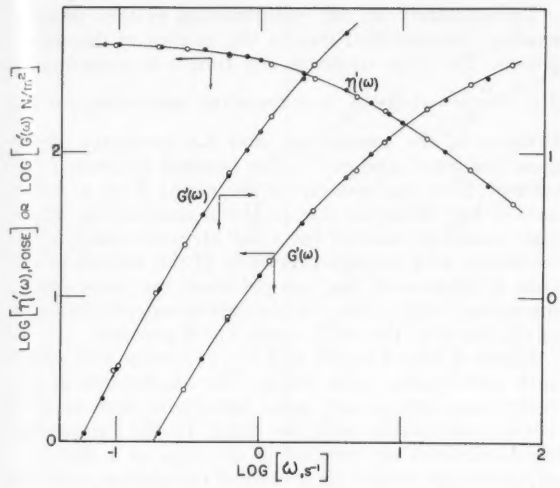

FIGURE 1: *Dynamic modulus* $G'(\omega)$ *and dynamic viscosity* $\eta'(\omega)$ *for a 10-percent PIB (L–100) solution in cetane.*

Solid circles are the calculated values from eqs (4.2) and (4.3).

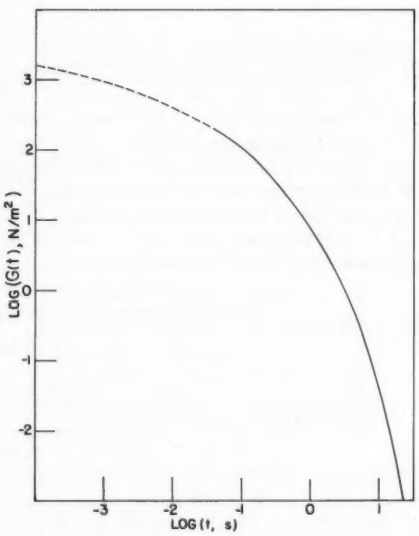

FIGURE 2: *Shear relaxation modulus,* G(t), *for a 10-percent PIB (L–100) solution in cetane.*

The dotted portion shows the extrapolated region.

$(1/\omega)$ for the highest measured frequency. As a critical check on both the conversion and the extrapolation, we calculated $G'(\omega)$ and $\eta'(\omega)$ from the well known relations [6]

$$G'(\omega) = \omega \int_{-\infty}^{\infty} tG(t) \qquad \sin \omega t \; d \ln t \qquad (4.2)$$

$$\eta'(\omega) = \int_{-\infty}^{\infty} tG(t) \qquad \cos \omega t \; d \ln t, \qquad (4.3)$$

where $\eta'(\omega)$ is the dynamic viscosity. The solid circles in figure 1 represent these values, which agree with the measured curve. For values of ω higher than $10\ s^{-1}$ the integrals in (4.2) and (4.3) depend strongly on the extrapolated region of $G(t)$. Some of the values of $G(t)$ calculated from (4.1) are given in table 1.

TABLE 1. *Shear relaxation modulus for 10 percent Vistanex L–100 (in cetane) at 25 °C*

t (s)	$G(t)$ (N/m^2)	t (s)	$G(t)$ (N/m^2)
1×10^{-5}	2.11×10^{3}	3×10^{-1}	3.85×10^{1}
2×10^{-5}	1.98×10^{3}	5×10^{-1}	2.02×10^{1}
5×10^{-5}	1.78×10^{3}	8×10^{-1}	1.05×10^{1}
1×10^{-4}	1.61×10^{3}	1.0	7.8
2×10^{-4}	1.45×10^{3}	2.0	2.57
5×10^{-4}	1.16×10^{3}	3.0	1.17
1×10^{-3}	9.5×10^{2}	4.6	4.1×10^{-1}
2×10^{-3}	7.4×10^{2}	8.0	7.9×10^{-2}
5×10^{-3}	5.2×10^{2}	10.0	4.0×10^{-2}
1×10^{-2}	3.8×10^{2}	1.4×10^{1}	1.2×10^{-2}
2×10^{-2}	2.85×10^{2}	1.8×10^{1}	3.9×10^{-3}
5×10^{-2}	1.8×10^{2}	2.0×10^{1}	2.0×10^{-3}
1×10^{-1}	1.08×10^{2}	3.0×10^{1}	9.87×10^{-5}
2×10^{-1}	5.92×10^{1}		

5. Single Step Stress Relaxation in Shear

In section 2 the definition of a single step stress relaxation history in simple shear was given in which the step is instantaneous. In practice, it takes a finite time to reach the desired deformation, and it can be shown that the measured stress is an upper bound of the stress relaxation function. At long times the difference between the relaxation function and the bound becomes small. With a knowledge of the actual strain history, one can estimate this difference and obtain a better bound for the relaxation function.

With the history

$$\gamma(\tau) = 0, \qquad \tau \leq 0$$

$$\gamma(\tau) = \frac{\gamma}{t_1}\tau, \qquad 0 \leq \tau \leq t_1 \qquad (5.1)$$

$$\gamma(\tau) = \gamma(t) = \gamma, \qquad t_1 \leq \tau \leq t$$

where t_1 is the time required to reach the maximum strain, eq (2.1) becomes

$$W(\gamma, t) = \frac{\sigma(t)}{\gamma} + \int_{t-t_1}^{t} W_*\left(\gamma\frac{t_1 - t + \xi}{t_1}, \xi\right)\left(\frac{\xi + t_1 - t}{t_1}\right) d\xi. \qquad (5.2)$$

Since the quantity given by the integral in (5.2) is negative, $\frac{\sigma(t)}{\gamma}$ is an upper bound of $W(\gamma, t)$. Since $-W_*(\gamma, t)$ is a monotone nonincreasing function of t, the ratio of

$\frac{\sigma(t)}{\gamma}/W(\gamma, t)$ goes to unity at high values of t.

For values of γ such that

$$|W_*(\gamma, t)| \geq |\alpha W_*(\alpha\gamma, t)|, \qquad 0 \leq \alpha \leq 1$$

a condition satisfied in the stress relaxation data reported here, it can be shown [8] that $\sigma(t+t_1)/\gamma$ for $t \geq t_1$ is a lower bound of $W(\gamma, t)$.[5]

An example of the two bounds and the function $W(\gamma, t)$ is shown in figure 3 for $\gamma = 0.2$ and $t_1 = 0.03$ s. The values of $W(\gamma, t)$ are the values that we used to correlate our different experiments. We see that even for values of $t = 10\ t_1$ the upper bound is high. The average of the two bounds gives agreement to within 1 percent. In the example in figure 3, a very good approximation of $W(\gamma, t)$ can be obtained by averaging the time of the two bounds, viz,

$$\frac{\sigma(t+\frac{1}{2}t_1)}{\gamma} \simeq W(\gamma, t).$$

In our experiments the strains were induced through a shaft of the rheogoniometer normally used for sinusoidal deformation histories. The motion of the cone was monitored with a transducer. The deformations were obtained by using a springloaded lever arm to drive the shaft through part of a cycle. This arrangement allowed us to obtain strains up to $\gamma = 1.8$. By using only a part of the sinusoidal deformation, we could obtain a motion of the cone very close to a ramp function. The time required to reach the maximum strain was of the order of 0.01 to 0.05 s.

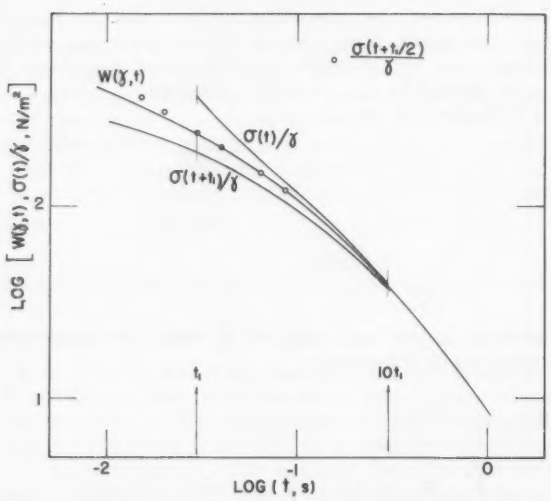

FIGURE 3: *Bounds of* $W(\gamma, t)$ *for* $\gamma = 0.2$ *and* $t_1 = 0.03$ *s.*

[5] This is equivalent to taking the relaxation from the instant of reaching the final shear value.

Unfortunately, in our experimental system there is another complication due to the motion of the upper platen. The true strain at any time t is more nearly $g(t) - \frac{\sigma(t)}{K}$ where K is a constant depending on the stiffness of the torsion bar and the geometry of the cone and plate, and $g(t)$ is the nominal strain at t calculated from the motion of the cone. With a stiffer torsion bar the error due to the motion of the upper plate would be smaller but small stresses could not be measured with enough precision. If the motion of the cone is monitored, one can calculate the error due to the motion of the plate. In our measurements the error in the stress at the early times was 6 percent.

Figure 4 shows a plot of $W(\gamma, t)$ versus γ in which both corrections were made. The isochrones at the early times are in very good agreement with eq (2.6) which corresponds with the lines. To the extent that the isochrones are parallel in this type of a plot, i.e., superposition occurs by a vertical translation, one can justify the representation of $W(\gamma, t)$ as a product of the stress relaxation modulus and a function of shear, γ, i.e., eq (2.6).

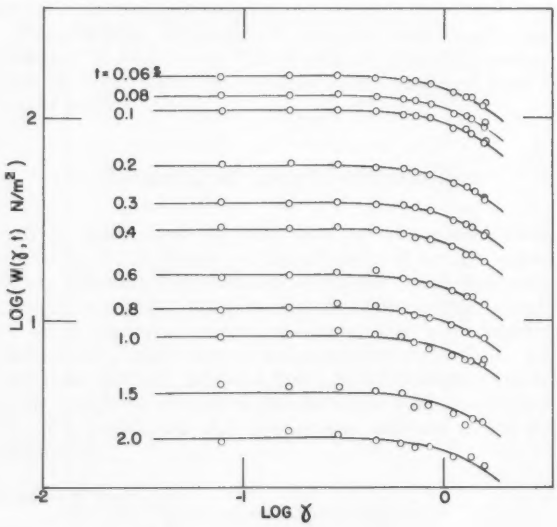

FIGURE 4: *Isochrones of* $W(\gamma, t)$ *versus* γ.

The lines indicate the calculated behavior from eq (2.6).

6. Suddenly Applied Constant Rate of Shear

With our experimental arrangement we found that we could not obtain an instantaneous constant rate of shear. For that reason we monitored and measured the motion of the cone with a transducer during the early part of the shearing. The monitoring arrangement prevented the use of the temperature control chamber. Therefore, the measurements were done at room tem-

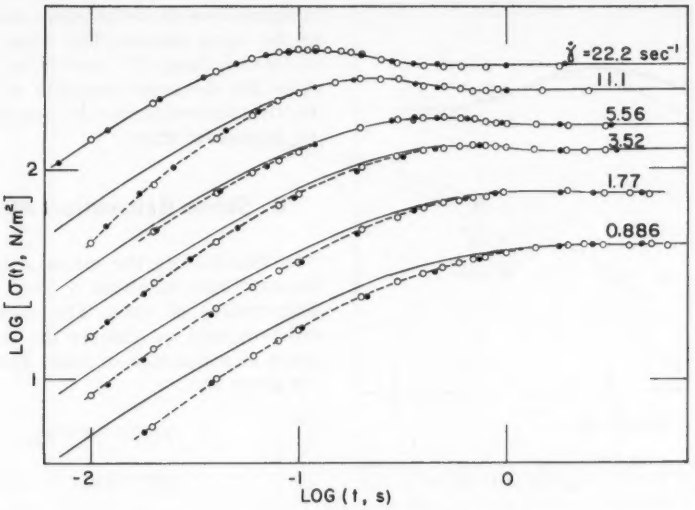

FIGURE 5: *The solid lines represent the stress calculated for a suddenly applied rate of shear for the rates of shear indicated.*

The open circles are experimental data, and the solid circles are calculated values using the true history of the motion.

perature. Since it took about 20 s to complete a run, the temperature variation was no more than ± 0.5 °C at 25 °C.

For these runs, due to the limitations of the transducer, we could monitor strains only up to $\gamma = 0.4$. On repeating an experiment, different strain histories were invariably obtained (over the early part of the time scale); this was probably caused by differing positions of the gear teeth. So, from each series of repetitive runs, we selected the one with the least deviation from a constant rate of shear.

Using eq (2.1) with the history

$$\gamma(\tau) = 0, \qquad \tau < 0$$
$$\gamma(\tau) = \dot{\gamma}\tau, \ \tau \geq 0; \qquad \dot{\gamma} = \text{constant} \tag{6.1}$$

we obtain [6]

$$\sigma(t) = \dot{\gamma} \int_0^t W(\dot{\gamma}\xi, \xi) \left(1 + \frac{\partial \ln W(\dot{\gamma}\xi, \xi)}{\partial \ln \gamma}\right) d\xi \tag{6.2}$$

where $\gamma = \dot{\gamma}\xi$ and $\dot{\gamma}$ is the rate of shear. In figure 5 we show the data as obtained. The lines represent the prediction of (6.2) and (2.6) which assume a suddenly applied steady shear (for the rates of shear indicated), and the black solid circles are values calculated from (2.1) and (2.6) using the true history of the motion. The agreement is very good. The inertia of the upper platen and assembly was not corrected for. We estimated for $\dot{\gamma} = 22.2$ s^{-1} that the inertial effect caused an error of less than 2 percent. Figure 5 shows at high rates of shear an overshoot of the stress $\sigma(t)$ as it approaches its limiting value.

From eq (6.2) the maximum value of the stress should occur when

$$\frac{\partial \ln W(\gamma, t)}{\partial \ln \gamma} = -1. \tag{6.3}$$

Our empirical form of $W(\gamma, t)$, eq (2.6), satisfies this condition at $\gamma = 2.44$.

In table 2 we show the strains at which the maximum of the stress occurs from other data.[7] Middleman's data [9] were estimated from the published graphs. The data of the more concentrated polyisobutylene solutions were obtained in our laboratory. The zero shear viscosities at 25 °C were 4460 poise for the 15.1 percent concentration and 17,760 poise for the 19.3-percent concentration. Assuming the principle of reduced variables with respect to concentration to be valid [10], we see that the rates of shear reported in table 2 for the higher concentrations will be 8 times as high when reduced to 10-percent concentration, for which the zero shear viscosity is 540 poise.[8]

The position of this overshoot can be used to study the error caused by the motion of the upper platen. It is easy to show this error by experiments with torsion bars of different diameters. In figure 6 we show the data obtained from a 15.1 percent solution at a nominal

[6] Throughout the paper we shall use the notation $\frac{\partial \ln W}{\partial \ln \gamma}$ to represent the derivative of $\ln W$ with respect to the derivative of the logarithm of the first argument.

[7] If eq (2.6) is correct for all concentrations, the maximum of the stress must occur at the same value of γ.

[8] The reduced rate of shear $\dot{\gamma}_R$ is given as

$$\dot{\gamma}_R = \dot{\gamma} \frac{\eta_1}{\eta_2} \left(\frac{c_1}{c_2}\right)^x$$

where η_1 is the zero shear viscosity at concentration c_1.

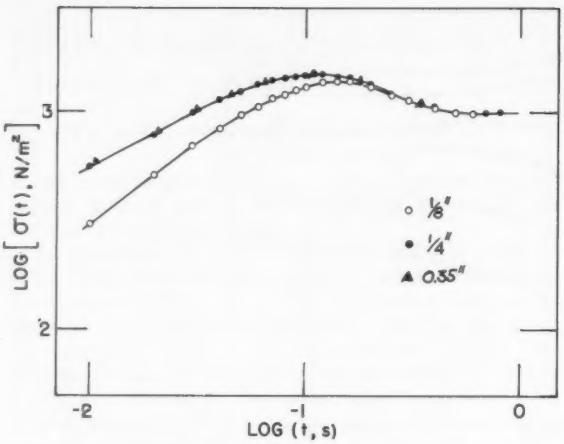

FIGURE 6: *Stress versus time, using different torsion bars for the same nominal rate of shear of 22.2 s^{-1} applied at t = 0, for a 15.1-percent solution of PIB in cetane.*

rate of shear of 22.2 s^{-1}. The open circles show the data obtained with a 0.125-in torsion bar. The solid circles are data obtained with a 0.25-in bar and the black triangles, with a 0.35-in bar. The histories of the motion of the cone for all the runs were almost identical, so that a direct comparison can be made of the effect of the motion of the upper platen. The maximum occurs at $t = 0.11$ s for the 0.25-in and 0.35-in bars and at $t = 0.16$ s for the 0.125-in bar.

TABLE 2. *Values of γ at which the maximum of the shearing stress occurs for the designated rates of shear*

$\dot{\gamma}$	15.1 percent Vistanex L-100 (in cetane) at 25 °C	19.3 percent Vistanex L-100 (in cetane) at 25 °C	Middleman's Data on Polyisobutylene BASF B-50 at 23.9 °C
0.0048	.....	.....	2.45
.012	.....	.....	2.4
.024	.....	.....	2.3
1.77	2..55	2.55	.....
5.56	2.55	2.55	.....
11.1	2.5	2.5	.....
22.2	2.5	2.55	.....

7. Steady State Shearing Flow

In the previous section we examined the stress from suddenly applied constant rate of shear. After a certain time, as can be observed, the shearing stress reaches a limiting value independent of time. The viscosity, $\eta(\dot{\gamma})$, which is the ratio of this shearing stress to the rate of shear, is given by

$$\eta(\dot{\gamma}) = \int_0^\infty W(\dot{\gamma}\xi, \xi)\left(1 + \frac{\partial \ln W(\dot{\gamma}\xi, \xi)}{\partial \ln \gamma}\right) d\xi. \tag{7.1}$$

In figure 7 we show the experimental values of viscosity as the open circles. The solid circles are the values calculated from (7.1) and (2.6). In the same figure we show the dynamic viscosity $\eta'(\omega)$. We observe that the two curves cannot be superposed by a shift along the horizontal axis.

8. Stress Relaxation After Steady Shear

In this history the material is initially sheared at a constant rate of shear $\dot{\gamma}$ until the shearing stress is independent of time. The motion stops at time we call zero, and we observe the subsequent decay of the stress as a function of time. The strain history at time τ is given by

$$\begin{aligned} \gamma(\tau) &= \dot{\gamma}\tau + \gamma_0, \qquad \tau \leq 0 \\ \gamma(\tau) &= \gamma_0, \qquad \tau \geq 0. \end{aligned} \tag{8.1}$$

From (2.1) and the conditions of (8.1) we obtain [9]

$$\sigma(t) = \dot{\gamma}\int_t^\infty W(\dot{\gamma}(\xi - t), \xi)\left(1 + \frac{\partial \ln W}{\partial \ln \gamma}\right) d\xi. \tag{8.2}$$

In figure 8 and figure 9 we show the experimental results with the open circles and the calculated results with the solid circles. The experimental points fall slightly higher than the calculated values, as the motion of the upper platen would lead one to expect.

At the limit of zero rate of shear, (8.2) reduces to

$$\frac{\sigma(t)}{\dot{\gamma}} = \int_t^\infty G(\xi)d\xi. \tag{8.3}$$

Differentiating (8.3) with respect to t we get

$$-\frac{\dot{\sigma}(t)}{\dot{\gamma}} = G(t). \tag{8.4}$$

In principle we can obtain $G(t)$ from this limit, but this method is not an accurate one. Since in the previous section we mentioned the errors due to the motion of the upper platen, it is interesting to look at an example where these errors are very pronounced. From (8.3) using an integration by parts we obtain

$$\frac{1}{\dot{\gamma}}\int_0^\infty \sigma(t)dt = \int_0^\infty G(t)t dt. \tag{8.5}$$

From eq (4.2) by taking the limit as ω goes to zero, we get

$$\lim_{\omega \to 0} \frac{G'(\omega)}{\omega^2} = \int_0^\infty G(t)t dt \tag{8.6}$$

[9] For brevity, when W appears in an integral without its arguments, it is understood that they are the same as for the preceding W.

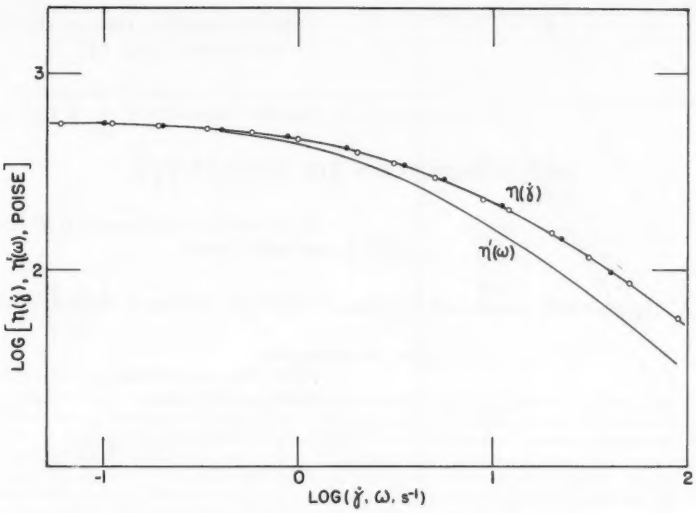

FIGURE 7: *The viscosity as a function of rate of shear.*

The open circles are experimental data, and the solid circles are calculated values. The dynamic viscosity is also shown for comparison.

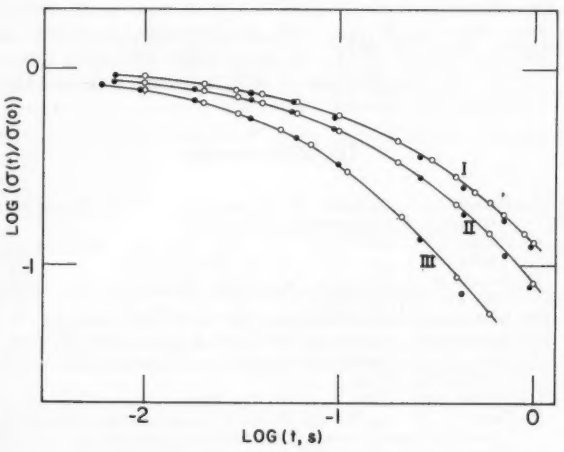

FIGURE 8: *Stress relaxation after steady shear, for rates of shear* $\dot{\gamma}=0.556\ s^{-1}(I)$, $\dot{\gamma}=1.77\ s^{-1}(II)$, *and* $\dot{\gamma}=11.1\ s^{-1}(III)$.

The open circles are experimental data, and the solid circles are calculated.

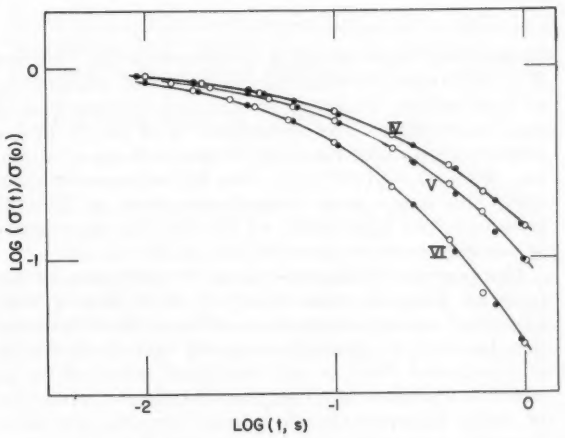

FIGURE 9: *Stress relaxation after steady shear, for rates of shear* $\dot{\gamma}=0.177\ s^{-1}(IV)$, $\dot{\gamma}=1.11\ s^{-1}(V)$, *and* $\dot{\gamma}=5.56\ s^{-1}(VI)$.

The open circles are experimental data, and the solid circles are calculated.

and from (8.5) and (8.6) we obtain

$$\frac{1}{\dot{\gamma}}\int_0^\infty \sigma(t)\,dt = \lim_{\omega\to 0}\frac{G'(\omega)}{\omega^2}. \tag{8.7}$$

In figure 10 we show a plot of

$$\dot{\gamma}\int_0^\infty \sigma(t)\,dt$$

versus $\dot{\gamma}$ using different torsion bars. The error introduced by the motion of the platen is very dramatic.

9. Discussion

The good agreement between the experimental data and the calculated values shows the validity of the BKZ theory even for materials where the shear relaxation modulus falls very quickly. The relatively

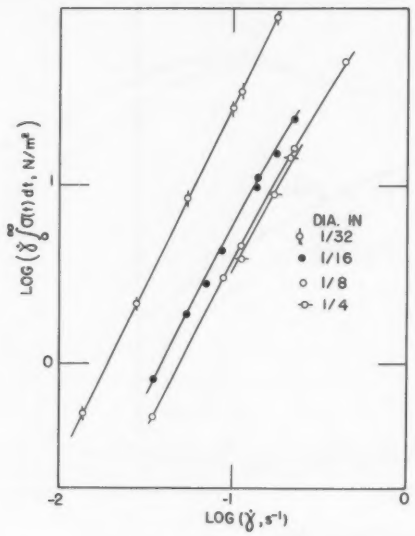

FIGURE 10. *Variation of* $\dot{\gamma}\int_0^\infty \sigma(t)dt$ *as a function of* $\dot{\gamma}$ *using different torsion bars, where* $\sigma(t)$ *is the measured stress after the cessation of steady shear.*

simple form that we used to represent the function $W(\gamma, t)$ seems to describe the behavior adequately, at least within the range of shearing deformations of our experiments. The separation of $W(\gamma, t)$ into a product of two functions, one of time and one of strain, i.e., $W(\gamma, t) = G(t)W_R(\gamma)$, may be an oversimplification. Although a more complicated form of $W(\gamma, t)$ gave us better agreement, we felt that the uncertainty in our experimental data did not justify its use.

Our purpose in this paper is not to establish a unique form of $W(\gamma, t)$, but rather to show how a wide variety of measurements from different shear histories can be related. Indeed, we know that the behavior of plasticized PVC is not consistent with a $W(\gamma, t)$ which is a product of a function of strain and a function of time. Experiments on normal stresses are more critically dependent on the values of $W(\gamma, t)$ at long times and large strains. For instance, the first normal stress difference, $\sigma_{11}(t) - \sigma_{22}(t)$, for a suddenly applied constant rate of shear, given by eq (6.1), can be calculated from [4]

$$\sigma_{11}(t) - \sigma_{22}(t) = \dot{\gamma}^2 \int_0^t W(\dot{\gamma}\xi, \xi)\left(2 + \frac{\partial \ln W}{\partial \ln \gamma}\right)\xi d\xi. \tag{9.1}$$

In general, if the function W is such that at high values of γ we have

$$\frac{\partial \ln W}{\partial \ln \gamma} < -2 \tag{9.2}$$

then the maximum of $\sigma_{11}(t) - \sigma_{22}(t)$ will occur at time t_m for which

$$\frac{\partial \ln W(\dot{\gamma}t_m, t_m)}{\partial \ln \gamma} = -2.$$

For longer times $\sigma_{11}(t) - \sigma_{22}(t)$ will tend to level to a lower value. This behavior of the first normal stress difference is roughly similar to that of the shear stress. There are clear differences however; a comparison of eq (9.1) with eq (6.2) shows that the overshoot for the shearing stress, if it occurs, must do so at an earlier time than t_m. It may well be possible, however, to find a form of $W(\gamma, t)$ compatible with the shear stress data of this paper which never satisfies the condition (9.2) for any value of γ.

10. References

[1] Bernstein, B., Kearsley, E. A., and Zapas, L. J., Trans. Soc. Rheol. **7**, 391–410 (1963).
[2] Zapas, L. J., and Craft, T., J. Res. Nat. Bur. Stand. (U.S.), **69A** (Phys. and Chem.), No. 6, 541–546 (1965).
[3] Broadbent, J. M., Kaye, A., Lodge, A. S., and Vale, D. G., Nature **217**, 55 (1968).
[4] Bernstein, B., Acta. Mechanica, **II**, No. 4, 329–354 (1966).
[5] Bernstein, B., and Fosdick, R. L., Rheologica Acta **9**, 106 (1970).
[6] Ferry, J. D., Viscoelastic Properties of Polymers (John Wiley, New York, 1961).
[7] Marvin, R. S., Phys. Rev. **86**, 644 (1952).
[8] Zapas, L. J., and Marvin, R. S., A Correction for a Non-Zero Loading Time in Stress Relaxation (in preparation).
[9] Middleman, S., Trans. Soc. Rheol. **13**, 123 (1969).
[10] DeWitt, T. W., Markovitz, H., Padden, F. J., and Zapas, L. J., J. Colloid Sci. **10**, 174–188 (1955).

(Paper 75A1–648)

JOURNAL OF RESEARCH of the National Bureau of Standards—A. Physics and Chemistry
Vol. 75A, No. 1, January–February 1971

Synthesis of Fluorodienes

James E. Fearn

Institute for Materials Research, National Bureau of Standards, Washington, D.C. 20234

(September 11, 1970)

In a comprehensive study of the cyclic, interintramolecular mechanism in diene polymerization, all of the completely fluorinated dienes from C_5 to C_8 have been prepared with a high degree of purity. Also prepared were 4-chloroperfluoro-1,6-heptadiene and perfluoro-1,11-dodecadiene, the latter inadvertently. The successful syntheses involved, in most cases, a telomerization which utilized, as the starting material, I_2, ICl, CF_2CFCl, or CF_2CF_2. From these telomers, not only the dienes but many new intermediate compounds were prepared; they were then purified and characterized. The chemistry of these compounds, especially that relating to their polymerization, is briefly discussed.

Key words: Cyclic inter-intramolecular mechanism; diene polymerization; fluorodienes; intermediates; polymerization; purity; synthesis; telomerization.

1. Introduction

Earlier reports from these laboratories have covered the synthesis and polymerization of 4-chloroperfluoro-1,6-heptadiene [1][1] and the chemistry involved in the preparation and polymerization of perfluoro-1,4-pentadiene [2,3]. These compounds were prepared according to the method of Park and Lacher [4]:

$$CF_2ClCFCl(CF_2CFCl)_nCF_2COOH + NaOH \longrightarrow CF_2ClCFCl(CF_2CFCl)_nCF_2COONa$$

$$CF_2ClCFCl(CF_2CFCl)_nCF_2COONa \xrightarrow[\text{Ether}]{\text{Zn, High boiling, } \triangle} CF_2CF(CF_2CFCl)_{n-1}CF_2CFCF_2$$

where n is 2 in the starting telomer acid, the resulting diene is 4-chloroperfluoro-1,6-heptadiene, and the acid in which $n=1$ produced perfluoro-1,4-pentadiene. To a marked extent, each of these fluorodienes polymerized according to an inter-intramolecular mechanism first postulated by Butler [5] after extensive investigations with allyl- and vinyl-amines and with quarternary ammonium salts. The general, idealized mechanism is:

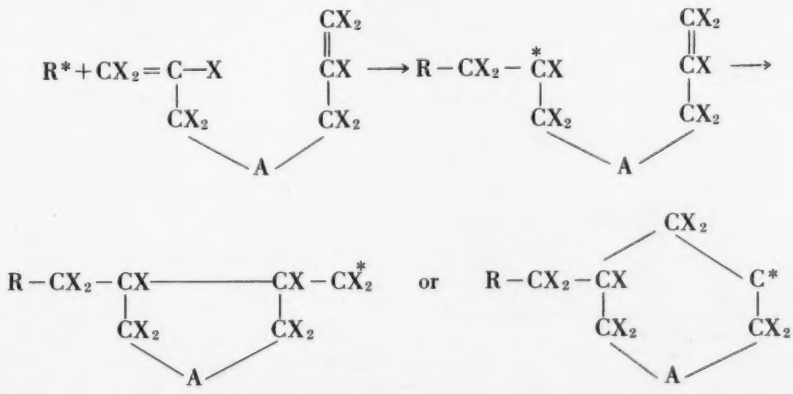

[1] Figures in brackets indicate the literature references at the end of this paper.

where X = H or F, and A = CH_2, CF_2, N, NR_1R_2, S, R_2 PH, or 0. With hydrocarbon compounds, the six-membered ring seems to be favored [5], but, with fluorocarbon compounds, this has not been established. A compound believed to have the structure $CF_2BrCFCF_2CFClCF_2CFBrCF_2$ could not be aromatized by passing it through a hot tube packed with KF, although thermal defluorination reactions resulting in aromatization are known to occur. Nuclear magnetic resonance studies of the compound obtained in the telomerization reaction between 4-chloroperfluoroheptadiene and bromine suggest that it has a five-membered ring [6]. Polymers of 4-chloroperfluoro-1,6-heptadiene are tough, slightly flexible materials of high thermal stability. They may be cast, or pressed into clear transparent films having good optical properties.

Polymers of perfluoro-1,4-pentadiene formed at ≥ 10,000 atm have the general formula

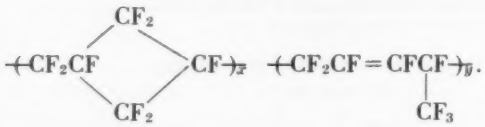

This structure is the result of the inward migration of one of the double bonds of the monomer, i.e., $CF_2 = CF - CF_2 - CF = CF_2 \rightleftarrows CF_2 = CF - CF = CF - CF_3$. The resulting 1,3-pentadiene copolymerizes with the 1,4-pentadiene to give the structure shown. When $\frac{x+y}{y}$ is ≥ 20, a powdery solid polymer of thermal stability is obtained, but when $\frac{x+y}{y}$ is 3 − 5, the product is rubbery and considerably less stable. Infrared and nuclear magnetic resonance results tend to support this correlation between structure and properties [2]. Polymerization of perfluoro-1,4-pentadiene is further complicated by the formation of four isomeric dimers under the conditions used for polymerization [2,3].

Efforts to prepare perfluoro-1,5-hexadiene, perfluoro-1,6-heptadiene, and perfluoro-1,7-octadiene were based on a synthesis that involved the telomerization of various fluoroiodoethanes, especially 1,2-dichlorotrifluoro 1-iodoethane with tetrafluoro-ethylene, e.g.,

$$CF_2ClCFClI + CF_2CF_2 \xrightarrow{\gamma} CF_2ClCFCl(CF_2CF_2)_n\,I$$

where $n = 1, 2, 3, 4$, etc. The work described here does not involve telomers higher than $n = 3$. The ethane derivative metioned was obtained by the addition of iodine monochloride to chlorotrifluoroethylene in such fashion that the ionic mode of addition was almost total. In a glass reaction-chamber, at temperatures ≤ 0 °C, the yield of the desired isomer is 98 percent. As the temperature rises, according to Hauptschein [7], the free-radical mechanism begins to compete with ionic addition, producing increasing proportions of the isomeric 1,1-dichloroethane as illustrated.

$$CF_2CFCl + ICl \begin{cases} \xrightarrow[< 0\ ^\circ C - Fe]{} CF_2ClCFClI & (A) \\ \xrightarrow[> 0\ ^\circ C \text{ and/or } Fe]{} CFCl_2CF_2I & (B) \end{cases}$$

Hauptschein [7] and Knunyants [8] have made extensive studies of this reaction, and have modified and extended the work of Haszeldine [9]. Knunyants asserted that isomer A is four times as active as isomer B in initiating telomerization and various other reactions. Telomers prepared from isomer A may be dechlorinated in the final step, to produce the second double bond in the diene, whereas, obviously, telomers produced from isomer B, having both chlorine atoms on the same carbon atom, will not. The efficiency of a telomerization in preparing perfluorodiene precursors is accordingly limited by the purity of the A isomer used as the starting material.

The telomerization illustrated may be adjusted to give maximal yields of the iodobutane, the iodohexane, or the iodooctane by varying the mole ratio of tetrafluoroethylene to the iodoethane, provided that there is a minimum of empty space in the reaction vessel. With a large vapor space in the reaction vessel, usually a steel bomb, and by use of gamma-ray initiation, much of the tetrafluoroethylene tends to polymerize in the vapor space, to form high polymer which drops into the liquid phase (consisting of the iodoethane and dissolved tetrafluoroethylene). High mole-ratios of tetrafluoroethylene to iodoethane produce high yields of hexane and octane, but, unfortunately, also increase the yields of telomers where $n \geq 4$ which are useless in the preparation of dienes that will undergo the cyclic mechanism of polymerization. All of the telomers used as precursors were clear, colorless liquids that turned violet and, finally, deep purple on standing. Their physical constants are shown in table 1.

TABLE 1. *Telomers of* $CF_2ClCFClI$ *and* CF_2CF_2

Compound	B.P. °C/mm	M.P. °C	N_D^{20}
$CF_2ClCFClI$	101°, 53/150		
$CF_2ClCFClCF_2CF_2I$	140°, 66/67		1.4046
$CF_2ClCFCl(CF_2CF_2)_2I$	83/35		1.3830
$CF_2ClCFCl(CF_2CF_2)_3I$	82/3	24	1.3710 (at 25°)
$CF_2ClCFCl(CF_2CF_2)_4I$	110/7	70	

By cross coupling 1,2-dichloro-heptafluoro-4-iodobutane and 1,2-dichloro-trifluoro-1-iodoethane, three products were obtained [10], namely, 1,2,3,4-tetrachlorohexafluorobutane, 1,2,5,6-tetrachloroperfluorohexane, and 1,2,7,8-tetrachloroperfluorooctane.

Dechlorination of these intermediates produced, respectively, perfluoro-1,3-butadiene, perfluoro-1,5-hexadiene, and perfluoro-1,7-octadiene. It is apparent that perfluoro-1,3-butadiene and perfluoro-1,7-octadiene may be prepared by homocoupling the iodoethane and/or the iodobutane mentioned, and by dechlorinating the respective tetrachloro compounds. Other syntheses of perfluoro-1,5-hexadiene are outlined later. Starting materials were, in all experiments, the telomers already discussed, listed in table 1.

1.

$$CF_2ClCFClCF_2CF_2I \xrightarrow{SO_3} CF_2ClCFClCF_2C(=O)F$$

$$CF_2ClCFClCF_2C(=O)F \xrightarrow[NaOH]{H_2O} CF_2ClCFClCF_2C(=O)ONa$$

$$CF_2ClCFClCF_2C(=O)ONa \xrightarrow{\Delta} CF_2ClCFCF_2$$

$$CF_2ClCFCF_2 \xrightarrow[MEK]{NaI} CF_2CFCF_2I$$

$$CF_2CFCF_2I \xrightarrow[Dioxane]{Zn} CF_2CFCF_2CF_2CFCF_2$$

2.

$$CF_2ClCFCl(CF_2)_4I \xrightarrow[Ether]{LiCH_3} CF_2ClCFCl(CF_2)_3CF_2Li$$

$$CF_2ClCFCl(CF_2)_3CF_2Li \xrightarrow{\Delta} CF_2ClCFClCF_2CF_2CFCF_2.$$

$$CF_2ClCFClCF_2CF_2CFCF_2 \xleftarrow{-Cl_2} CF_2ClCFClCF_2CF_2CFCF_2.$$

In reaction 1, the reaction with sulfur trioxide was reported by Knunyants [11] and the coupling of perfluoroallyiodide was described by Miller [12]. Efforts to prepare perfluoro-1,5-hexadiene by the following reaction were unsuccessful.

$$CF_2ClCFClCF_2CF_2CF_2CF_2Cl \xrightarrow[\text{High Boiling Ether}]{Zn} CF_2CFCF_2CF_2CFCF_2.$$

Instead of dechlorofluorination, inter-intramolecular dechlorination occurred, yielding perfluoro-1, 11-dodecadiene.

Efforts to synthesize perfluoro-1,6-hepatadiene, a previously unreported compound, resulted in a large number of interesting intermediates, some of which are also unreported compounds. The various syntheses are outlined.

1.

$$H(CF_2)_6CH_2OH \xrightarrow[H_2O+H_2SO_4]{Na_2Cr_2O_7} H(CF_2)_6C(F)(OH)_2 \xrightarrow{SF_4} H(CF_2)_7H$$

$$H(CF_2)_7H \xrightarrow{-2HF} CF_2CF(CF_2)_3CFCF_2.$$

This effort was unsuccessful. The oxidation step produced the aldehyde hydrate in good yield, but yields in the sulfur tetrafluoride reaction ranged from low to zero. Efforts to effect dehydrofluorination were completely unsuccessful. The intermediates were isolated, purified and characterized.

2.

$$CF_2ClCFCl(CF_2CF_2)_2I \xrightarrow{HSO_3Cl} CF_2ClCFClCF_2CF_2CF_2COOH$$

$$CF_2ClCFClCF_2CF_2CF_2COOH \xrightarrow[AgNO_3]{NH_4OH} CF_2ClCFClCF_2CF_2CF_2COOAg$$

$$CF_2ClCFClCF_2CF_2CF_2COOAg \xrightarrow[\Delta]{I_2} CF_2ClCFClCF_2CF_2CF_2I$$

$$CF_2ClCFClCF_2CF_2CF_2I + CF_2ClCFClI \xrightarrow{Zn} CF_2ClCFCl(CF_2)_3CFClCF_2Cl$$

$$CF_2ClCFCl(CF_2)_3CFClCF_2Cl \xrightarrow[\text{High Boiling Ether}]{Zn} CF_2CF(CF_2)_3CFCF_2$$

3.

$$CF_2ClCFClCF_2CF_2I \xrightarrow{SO_3} CF_2ClCFClCF_2COOH$$

$$\downarrow NH_4OH \quad AgNO_3$$

$$\overset{75\%}{CF_2CFCF_2Cl} + \overset{15\%}{CF_2ClCFClCF_2I} \xleftarrow{I_2} CF_2ClCFClCF_2COOAg$$

$$CF_2ClCFClCF_2I + CF_2ClCFClCF_2CF_2I \xrightarrow[CH_2Cl_2]{Zn} CF_2ClCFCl(CF_2)_3CFClCF_2Cl$$

$$\downarrow -2Cl_2$$

$$CF_2CF(CF_2)_3CFCF_2$$

4.

$$CF_2ClCFClCF_2CF_2I + CF_2CFCF_3 \longrightarrow CF_2ClCFCl(CF_2)_3\overset{I}{C}FCF_3 + \text{etc.}$$

$$\downarrow \text{Ethyl Ether} \quad CH_3Li$$

$$CF_2CF(CF_2)_3CFCF_2 \xleftarrow{-2Cl} CF_2ClCFCl(CF_2)_3CFCF_2.$$

5.

$$CF_2ClCFCl(CF_2)_6I \xrightarrow{HSO_3Cl} CF_2ClCFCl(CF_2)_5COOH$$

$$\downarrow H_2O \quad NaOH$$

$$CF_2ClCFCl(CF_2)_3CFCF_2 \xleftarrow{350°C} CF_2ClCFCl(CF_2)_5COONa$$

$$\downarrow -2Cl$$

$$CF_2CF(CF_2)_3CFCF_2.$$

The chlorosulfonic acid reaction utilized in syntheses 2 and 5 was reported by Hauptschein [13]. The high-boiling ether mentioned in synthesis 2 and used in all subsequent dechlorinations was *bis*[2-(2-methoxyethoxy)ethyl] ether. Fluorodienes prepared and their respective boiling points are listed in table 2.

TABLE 2. *Fluorodienes*

$CF_2CF(CF_2)_nCFCF_2$	B.P. °C
$n=0$	7
$n=1$	36
$n=2$	59
$n=3$	84
$n=4$	106

2. Experimental Procedure

2.1. Preparation of 4-Chloroperfluoro-1,6-heptadiene

4,6,7-Trichloroperfluoroheptene-1: This compound was prepared in the manner of Park and Lacher [4]. Eleven kilograms (5 mol) of 3,5,7,8-tetrachloroperfluorooctanoic acid was added to 200 g (5 mol) of sodium hydroxide dissolved in 3 liters of water. The mixture was carefully adjusted to pH 7 and chilled. The sodium salt was filtered with suction apparatus, dried in air, and placed in a strong vacuum for several days. The resulting salt was anhydrous and extremely hygroscopic.

Eleven kg of dry sodium salt was pyrolyzed under reduced pressure in a stainless steel tube connected through adapters to a series of dry ice acetone-cooled traps. The pyrolysis temperature was approximately 350 °C, produced by a furnace controlled by two 10-A variable voltage transformers. Pyrolysis proceeded rapidly and smoothly, producing 1,560 g of crude product or 83 percent. This was washed with three portions of 10 percent aqueous potassium hydroxide, each portion about 10 percent of the volume of fluorocarbon, then with similar portions of water. The washed material was dried over anhydrous sodium sulfate and distilled under reduced pressure. The yield was 1,400 g of pure 4,6,7-trichloroperfluoroheptene-1, or 75 percent. A higher boiling material which gave a single peak on the vapor-phase chromatograph amounted to 60 g B.P. 40 °C/1mm.

4-Chloroperfluoroheptadiene-1,6: In a 2-liter flask equipped with stirrer, reflux condenser, and dropping

funnel a mixture of 50 ml of *bis*[2(2-methoxyethoxy) ethyl] ether and 140 g of zinc dust, which had been treated with 100 ml of hydrochloric acid while suspended in acetone, filtered, and dried under vacuum for 4 h, was gently heated to about 60 °C with stirring. To this mixture was added 200 g (0.5 mol) of 4,6,7-trichloroperfluoroheptene-1 with continued stirring. Heating was increased until refluxing was observed, then discontinued until addition was complete. The mixture was then gently refluxed for 1 h and permitted to cool to room temperature. The heptene and heptadiene were removed from the mixture by attaching a series of dry ice acetone-cooled traps to the condenser and applying a vacuum of less than 1 mm of mercury to the system. The solvent did not distill. The mixture of heptene and heptadiene was distilled at 75 mm. Three fractions were collected, between 35 and 45, between 45 and 50, and between 50 and 70 °C. A vapor-phase study showed the first fraction to be two-thirds heptadiene and two lower boiling components. The 45–50 fraction was almost pure heptadiene, while the 50–70 fraction contained small amounts of heptadiene and two higher boiling components. Above 70 °C virtually pure starting material was recovered. About 10 percent of the starting material remained in the solvent, and upon distillation of the solvent was converted into tar. Approximately 60 g of dechlorination products was estimated to be the desired heptadiene, or about 35 percent conversion on each dechlorination. The starting material was recycled.

The purest fraction obtained from distillation was run through a vapor-phase chromatograph and was found to contain trace amounts of all other dechlorination products. These trace materials were carefully removed through preparatory-scale vapor-phase chromatography before any attempt to polymerize or telomerize the compound was made. The pure heptadiene boiled at 112 °C/760 mm, which compares well with Park's 103°/633 mm.

2.2. Preparation of Perfluoropentadiene

Preparation of Sodium 3,5,6-Trichlorooctafluorohexanoate. In a 4-liter beaker, 320 g (8 mol) of sodium hydroxide was dissolved in 2 liters of water. The solution was vigorously stirred and 2915 g (8 mol) of 3,5,6-trichlorooctafluorohexanoic acid was added. The solution became very viscous, but there was no precipitate. Chilling produced no precipitate, so the solution was poured into a clean vacuum desiccator and evaporated to near dryness by using an infrared lamp and an aspirator. The salt became syrupy, buttery, and then waxy, but did not crystallize. The salt was then dried at 10^{-2} mm (dry ice acetone trap) for three days. Water (500 ml) was removed, and the wax became a white, crystalline material. Drying was continued for two more days, with removal of water (200 ml), and the crystals became a fine, apparently amorphous, rather hygroscopic powder.

Pyrolysis of Sodium 3,5,6-Trichlorooctafluorohexanoate. 3,5,6-Trichlorooctafluorohexanoate (2.2 kg) was pyrolyzed under reduced pressure in a stainless steel tube connected, through adapters, to a series of cooled traps (dry ice acetone) and heated to approximately 350 °C in a furnace controlled by two 10 A, variable transformers. Pyrolysis took place smoothly, yielding 1520 g of products (theoretical yield, 1600 g). This was 95 percent based on the salt. The product was carefully distilled through a 10-in glass column packed with glass helices. A fraction boiling at 91 °C was collected as the desired product. It amounted to 1360 g (85%, based on the acid salt).

ANAL. Calcd. for $C_5Cl_2F_8$: C, 21.2%; Cl, 25.1%; F, 53.7%. Found: C, 21.0%; Cl, 24.8%.

In the same distillation, a second fraction was obtained, boiling at 120 °C. This amounted to 145 g (9% based on the acid salt). The remaining material would not distill at atmospheric pressure, and was assumed to be a coupling product. No further effort was made to characterize it. The 120 °C fraction showed three peaks on a gas-liquid chromatogram, and a deep, split band between 5 and 6 μ in its infrared spectrum. This appeared to be a mixture of the isomers of trichloroheptafluoropentene. This was supported by the elemental analysis and by conversion into a mixture of a three monochloroheptafluoropentadienes.

ANAL. Calcd. for $C_5Cl_3F_7$: C, 20.3%; Cl, 35.2%. Found: C, 20.1%; Cl, 34.9%.

Dechlorination of 4,5-Dichlorooctafluoro-1-pentene. Dechlorination was effected by a slight variation of the method of Park and Lacher [4]. In a beaker, 130 g (2.0 mol) of powdered zinc was suspended in acetone, and 100 ml of concentrated hydrochloric acid was added slowly with stirring. Stirring was continued for 30 min. The zinc was filtered off with suction, washed thoroughly with acetone, dried briefly in air, and then overnight in a vacuum oven at 70 °C. This activated zinc was placed in a 500-ml, three-necked flask (equipped with an efficient stirrer, a dropping funnel, and a 6-in glass column packed with glass helices and topped by a still-head) and 200 ml of *bis*[2-(2-methoxyethoxy)ethyl] ether was added. Stirring was commenced, and the flask was heated (Thermowell heater) to 70 °C. 4,5-Dichlorooctafluoro-1-pentene (284 g, 1 mol) was added in small portions until the reaction started, and then dropwise until addition was complete, Perfluoropentadiene distilled out of the column at about the same rate as the pentene was added. The rate of addition of the pentene and the heat applied to the flask were so controlled that the temperature of the distillate never exceeded 40 °C. The yield of crude pentadiene was 194 g (91%); this was distilled through a 10-in glass column, packed with glass helices, yielding a pure product, boiling at 36 °C, that showed one major peak (and two minor peaks with 1% and 0.3% of the area of the major peak) on an analytical gas-liquid chromatogram. The yield of pure compound was 160 g (89%). Recovered starting material (34 g) was recycled. Its infrared spectrum showed a single band at 5.6 μ, the band being somewhat broader and more intense

than that of the parent compound. Elemental analysis confirmed the composition of the diene.

ANAL. Calcd. for C_5F_8: C, 28.3%; F, 71.7%. Found: C, 28.1%; F, 70.9%.

Dechlorination of Trichloroheptafluoropentene Fraction. The dechlorination procedure described for the preparation of perfluoro-1,4-pentadiene was repeated. A 60 g (0.2 mol) portion of the trichloroheptafluoropentene fraction was added to the flask containing the high-boiling ether and activated zinc. During the dechlorination, the distillate came over below 70 °C. The crude yield was 42 g or 92%. Upon careful distillation at 65 °C, 39 g of a mixture of monochloroheptafluoropentadienes was obtained, which was 85 percent based on the pentene; 5 g of starting material was recovered and recycled.

ANAL. Calcd. for C_5ClF_7: C, 26.3%; Cl, 15.5%; F, 58.2%. Found: C, 26.6%; Cl, 15.2%; F, 58.1%.

2.3. Telomer Studies

Addition of Iodine Monochloride to Trifluoroethylene. In an 800-ml stainless steel bomb 238 g (2.9 m) of trifluoroethylene and 454 g (2.8 m) of iodine monochloride were shaken for 24 h at room temperature. The small excess of the ethylene was permitted to escape. The yield was 650 g of material boiling at 84 °C or 95 percent based on iodine monochloride.

Addition of Iodine Monochloride to Tetrafluoroethylene. In an 800-ml stainless steel bomb 100 g (1 m) of tetrafluoroethylene and 162 g (1 m) of iodine monochloride was shaken at room temperature for 24 h. The contents were removed from the bomb, shaken with aqueous sodium bisulfite, dried over anhydrous sodium sulfate and distilled. The yield was 200 g of clear liquid boiling at 56 °C or 76.5 percent based on either reagent.

Addition of Iodine to Tetrafluoroethylene. In a 1400-ml bomb was placed 254 g (1.0 m) of I_2 and 210 g (1.0 m) of CF_2Br_2. Through a vacuum line 100 g (1.0 m) of tetrafluoroethylene was distilled into the bomb. The bomb and its contents were rocked for 2 days at room temperature without diminution of pressure. The temperature was raised to 100° for 16 h and shaking was continued. The bomb was cooled to room temperature and the internal pressure was found to have decreased from 150 psi to atmospheric. A solution weighing 450 g was transferred from the bomb to a distilling flask. From this solution 140 g of dibromodifluoromethane and 40 g of iodine were recovered. The product, 1,2-diodotetrafluoroethane amounted to 210 g of a purple liquid boiling at 112 to 113 °C or 62.1 percent based on the tetrafluoroethylene.

Addition of Iodine Monochloride to Chlorotrifluoroethylene. A 12-liter three-neck flask equipped with a stirrer and dropping funnel was placed in a constant temperature bath set at −10 °C and fastened securely. Into it was poured 5000 ml of clean dry methylene chloride. Dropwise 2500 g 15.4 mol of iodine monochloride was added. The dropping funnel was replaced with a dry ice acetone-cooled condenser. Through the third neck 1830 g (16.0 m) of chlorotrifluoroethylene was distilled directly from the cylinder. Stirring and gentle refluxing of the ethylene was continued for six weeks. The flask was then removed from the bath and permitted to warm to room temperature. The unreacted ethylene was distilled into a dry ice acetone-cooled trap and saved for the next run. The contents of the flask were removed, the methylene chloride distilled and the product was fractionated through a 10-in column packed with helices. The forecut consisted of two fractions boiling at 46 °C and 54 °C. The desired product, $CF_2ClCFClI$, boiling at 101 °C amounted to 3100 g or 72.6 percent based on the iodine monochloride which was not chemically pure. A considerable quantity of iodine remained in the reaction flask.

Addition of Iodine Monochloride to Chlorotrifluoroethylene. In a 1400-ml steel bomb was placed 1000 g (6.2 m) of technical grade iodine monochloride. The bomb was cooled to −196° using liquid nitrogen and into it was distilled 727 g (6.25 m) of chlorotrifluoroethylene. The bomb was permitted to warm to room temperature while rocking. It was then rocked for 65 h at room temperature. At the end of this period the contents were removed, shaken with aqueous sodium bisulphite and dried over anhydrous sodium sulfate. The amount of crude product was 1510 g or 88 percent based on the impure iodine monochloride. Distillation produced a forecut boiling below 50 °C and 1415 g of product boiling at 101 °C or 82.5 percent based on iodine monochloride. This product was found to be a mixture of isomers $CF_2ClCFClI$ and CF_2ICFCl_2, but was largely the latter.

Telomerization of 1-Chloro-1,1.2-trifluoro-2-iodoethane with Tetrafluoroethylene. A glass tube containing 47.6 g (0.2 m) of $CF_2ClCFHI$ and 20 g (0.2 m) of CF_2CF_2 was subjected to ordinary room light for a brief period at 0 °C. Upon warming to 0° from −196 °C solid polymer began forming immediately. After all action had apparently ceased the tube was opened and any remaining CF_2CF_2 was permitted to escape. Resolution of the mixture yielded 33 g of the starting ethane, 3 g of very high boiling viscous liquid product and 5 g of solid polymer, both assumed to be low molecular weight polytetrafluoroethylene.

Telomerization of 1-Chloro-tetrafluoro 2-iodoethane with Tetrafluoroethylene. A glass tube charged with 49.6 g (0.19 m) of CF_2ICF_2Cl and 18.8 g (0.19 m) of CF_2CF_2 was permitted to warm from −195 °C to room temperature. It was subjected to ordinary fluorescent light for 8 h at room temperature then opened. Separation of the components of this mixture yielded 35 g of original ethane 3 g of material boiling between 60° and 120 °C and 11 g of polymer. Excess ethylene again was permitted to escape.

Telomerization of tetrafluoro 1,2-Diiodoethane with Tetrafluoroethylene. A glass tube containing 65.4 g (0.184 m) of CF_2ICF_2I and 18.4 g (0.184 m) of CF_2CF_2 was subjected for three days to radiation from a cobalt 60 source at a dose rate of 0.25 megarads/h. The yields were as follows:

B.P.	Postulated product	Yield
46 °C/65 mm	CF_2ICF_2I	16.0 g
55 °C/25	$I(CF_2)_4I$	11.5
52 °C/1	$I(CF_2)_6I$	4.0

Telomerization of 1,2-Dichlorotrifluoro-1-iodoethane with Tetrafluoroethylene. Into a thick-walled glass tube containing 500 g (1.8 m)$CF_2ClCFClI$ was distilled 192 g (1.9 m) of CF_2CF_2. The tube was thoroughly degassed and placed in a cobalt-60 source where it was subjected to a dose rate of 0.25 megorads/h for 20 h. It was then cooled to −196 °C with liquid nitrogen and opened. On warming to room temperature excess tetrafluoroethylene was permitted to escape. The liquid mixture was transferred to a distilling flask and distilled, first roughly then carefully through a 10-in column packed with glass helices. The yields of telomers were as follows:

99–101°	$CF_2ClCFClI$	91 g
101–140°		19
141	$CF_2ClCFCl(CF_2)_2I$	196
25–44/1 mm		20
46/1 mm	$CF_2ClCFCl(CF_2)_4I$	95
64/1 mm	$CF_2ClCFCl(CF_2)_6I$	30
> 64/1 mm	higher telomers	20

Telomerization of 3,4-Dichloroheptafluoro-1-iodobutane with Tetrafluoroethylene. A large thick-walled glass tube containing 495 g (1.31 m) of $CF_2ClCFCl(CF_2)_2I$ and 117 g (1.17 m) of tetrafluoroethylene was subjected to γ radiation at a dose rate of 2.5 megarads/h for 12 h. The tube was opened and its contents filtered. The liquid fraction was carefully distilled. The total yields are listed as follows:

Recovered	$CF_2ClCFCl(CF_2)_2I$	164 g
	$CF_2ClCFCl(CF_2)_4I$	127
	$CF_2ClCFCl(CF_2)_6I$	52
	$CF_2ClCFCl(CF_2)_nI$, $n \geq 8$	85
	High polymer	76

Telomerization of 1,2-Dichloro-trifluoro-1-iodoethane with Hexafluoropropylene. Into a 1400-ml bomb was poured 560 g (2 m) of 1,2-dichloro-1-iodotrifluoroethane. The bomb was attached to a vacuum line cooled to −196 °C and evacuated. Into it was distilled 800 g (5.3 m) of carefully degassed hexafluoropropylene. The bomb was sealed and placed in a heater-rocker assembly, heated to 200°, and rocked at this temperature for 294 h. It was then cooled to room temperature and 210 g of excess hexafluoropropylene was distilled into a dry ice-acetone cooled trap. The liquid product, 710 g of a dark oil was distilled and the following absolute yields were obtained. It is to be noted that percentage yields are not particularly informing in this type of telomerization.

< 100 °C	30 g	97–104/20 mm	88 g
		145–55/20 mm	
100–140	39	75–85/1 mm	154
56–61/20 mm	110	186–186/20 mm	122
61–96/20 mm	7	> 200/20 mm	157

Telomerization of 1,2-Dichloro-heptafluoro-4-iodobutane with Hexafluoropropylene. Into a 1400-ml bomb was placed 760 g (2 mm) of 1,2-dichloro-4-iodoheptafluorobutane. The bomb was attached to a vacuum line cooled to −195 °C and evacuated. Into it was distilled 470 g (3.14 m) of carefully degassed hexafluoropropylene. The bomb was sealed, placed in a heater-rocker mechanism, heated to 202 °C and rocked at this temperature for 411 h. It was then cooled to room temperature and attached to a dry ice acetone-cooled trap. In this way about 50 g of impure hexafluoropropylene was recovered. Total amount of liquid (or solid) product was 1071 g. The liquid was distilled roughly under reduced pressure giving the following yields.

< 130°/20 mm	546 g
> 130°/20 mm	247
Residue	170

A careful distillation of the first fraction yielded the following:

< 92°/20 mm	19 g	
92 − 94°/20 mm	372	$[CF_2ClCFCl(CF_2)_3\underset{I}{C}FCF_3]$
95 − 130°/20 mm	148	

Preparation of 1,5,6-Trichloroperfluorohexane. In each of two quartz tubes was placed 67 g (0.14 m) of $CF_2ClCFCl(CF_2)_4I$ and 28.4 g (0.4 m) of chlorine. The tubes were shaken and irradiated with ultraviolet light from a Hanovia type L burner for 13 h. The tubes were opened and the excess chlorine permitted to escape. The liquid mixtures were combined and distilled. The amount of desired product was 65 g or 61.8 percent conversion. Thirty nine grams of iodocompound were recovered unchanged. Taking this into consideration the yield was 84.1 percent. A small residue was not identified. Boiling point of the slightly impure material was 146 °C.

Dehalogenation of 1,5,6-Trichloroperfluorohexane. In a 1-liter flask equipped with a still head and stirrer 61 g (0.17 m) of $CF_2ClCFCl(CF_2)_4Cl$, 60 g (0.9 m of Z_n 90 ml of acetic anhydride and 270 ml of acetic acid was stirred and heated to 90°. The 6-chloroperfluoro-1-hexane distilled. The crude product was washed with water, dried over anhydrous sodium sulfate and redistilled. Yield of pure product was 27 g or 54 percent B.P. 89°.

Attempted Dechlorofluorination of 6-Chloroperfluoro-1-hexene. In a 1-liter flask equipped with a stirrer, reflux condenser, and a thermometer extending into the liquid were placed 30 g (0.09 m) of $CF_2=CF(CF_2)_4Cl$, 13 g (0.2 m) of Zn and 200 ml of diethylene glycol. The mixture was stirred and heated to 140 °C, the hexane refluxing vigorously. At 140° the contents of the flask began to seethe and froth and the refluxing subsided. No further reflux was observed until the temperature reached 190°. The reflux condenser was replaced with a still head and a product was distilled at 182 °C. This is the B.P. that Knunyants has reported for perfluoro-1,11-dodecadiene. The yield was 13 g or 50 percent.

Coupling of 1,2-Dichloro-heptafluoro 4-iodobutane (Haszeldine's Method). Three quartz tubes were prepared as described below.

	$CF_2ClCFClCF_2CF_2I$	H_4	Freom 112
No. 1	40 g (0.106 m)	215 g	32 g
No. 2	37 g (0.097 m)	190	35
No. 3	38 g (0.100 m)	170	33

These tubes were shaked and irradiated with ultraviolet rays from a Hanovia Type L burner for 35 h. The contents of the tubes were combined and the organic material was carefully separated from the mercury and distilled. The yield was 34 g of material, boiling at 68 °C/3 mm or 68.5 percent based on the fluorocarbon, since 40 g of fluorobutane was recovered.

(Knunyant's Method)

In a 250-ml 3-neck flask, complete with stirrer, reflux condenser and dropping funnel, was placed a mixture of 10 g (0.15 m) of powdered zinc in 31 g of acetic anhydride and 50 ml of methylene chloride. This mixture was stirred vigorously and heated to reflux. To it was added dropwise 57 g (0.15 m) of $CF_2ClCFClCF_2CF_2I$. During the addition, heating was discontinued but a vigorous reflux was maintained by the rate of addition. After addition, heating was resumed and reflux was maintained for 6 h. The flask was cooled and its contents were filtered and added dropwise to 1 liter of water. The organic layer was separated, dried over anhydrous sodium sulfate and distilled. Careful distilllation thorugh a 10-in column packed with glass helices yielded 22.4 g of a clear colorless liquid boiling at 68 °C/3 mm. This was 59.3 percent based on the dichloroiodoperfluorobutane.

Cross-coupling of 1,2-Dichlorotrifluoro-1-iodoethane and 1,2-Dichloro-perfluoro 4-iodobutane. Into a 3-liter, 3-neck flask equipped with a stirrer reflux condenser and dropping funnel was placed a mixture of 260 g (4.0 m) of zinc powder, 800 ml of acetic anhydride and 2000 ml of methylene chloride. This mixture was stirred and heated to reflux. To this refluxing mixture was added dropwise an intimate mixture of 556 g (2m) 1,2-dichloro-trifluoro-1-iodoethane and 760 g (2m) of 1,2-dichloro-4-iodoperfluorobutane. During the addition of the halocarbon mixture reflux was maintained without application of external heat. When addition was complete reflux and stirring were continued overnight. The contents of the flask were filtered and the residue discarded. The filtrate was added slowly with stirring to 5000 ml of water in two 4-liter beakers. The aqueous layer was discarded. The methylene chloride solution was dried over anhydrous sodium sulfate and distilled. It was then redistilled through an 18-in column packed with glass helices with the following results.

	B.P.	Yield
Forecut	41–130	78 g
1,2,3,4-Tetrachloroperfluorobutane	133	120
1,2,5,6-Tetrachloroperfluorohexane	43°/1 mm	132
1,2,7,8-Tetrachloroperfluorooctane	68°/3 mm	240
Residue	>68°/1 mm	210

Preparation of 7,8-Dichloroperfluorooctanoic Acid. Thirty g (0.05 m) of 1,2-dichloro-8-iodoperfluorooctane and 20 ml of 60 percent oleum were placed in a 100 ml steel bomb and the bomb sealed. The bomb was rocked and maintained at 250 °C for 18 h. The contents were removed from the bomb. The oily organic layer was separated and shaken with aqueous sodium bicarbonate until neutral to pH paper. The solution was then made acidic with dilute surfuric acid and extracted continuously with ether. The ether extract was dried over anhydrous sodium carbonate and distilled. The yield was 9.4 g of a colorless oil boiling at 155°/58 mm. This was 38 percent based on the iodooctane used as starting material. On standing the oil slowly solidified. This was consistent with the findings of Knunyants. This acid was later converted to the sodium salt and the salt dried by conventional means.

Preparation of Sodium 7,8-Dichloroperfluorooctanoate. A mixture of 145 g (0.25 m, 73 ml) of 7,8-dichloro-1-iodoperfluorooctane and 291 g (2.5 m 173 ml) of chlorosulfonic acid was placed in a glass tube of such size that the tube was about ⅔ full. The tube was placed in a metal bomb surrounded with carbon tetrachloride. The bomb was sealed and placed in a heater. The heater was inclined so that the glass tube was about 85° from vertical. The bomb and contents were maintained at 146–152° for 20 h after which the bomb was permitted to cool to room temperature. The glass tube was removed and cooled to −196 °C with liquid nitrogen. It was opened and permitted to warm to room temperature. Warming was accelerated by pouring warm water over the outside of the tube. The contents of the tube was poured on ice cubes. During this step most of the ice melted. On standing an oily layer separated. The aqueous layer was decanted. The oily layer, amounting to 127 g, was added dropwise to a hot solution of 40 g (1.0 m) of sodium hydroxide in 500 ml of

water. After addition heating was continued for two hours. The mixture was then permitted to cool to room temperature and refrigerated overnight. The crystals of 7,8-dichloroperfluorocaprylate were filtered and vacuum dried. The yield was 66 g or 56.3 percent based on the iodo compound. From the filtrate 35 g of oil was obtained. This was subjected to infrared analysis and was concluded to be 1,7,8-trichloroperfluoroheptane which Hauptschien suggested to be a byproduct in this type of reaction. The reaction was carried out six times with the yields varying between 44 and 56.5 percent. The product is a white microcrystalline material.

Preparation of 3,4-Dichloropentafluorobutyric Acid. In a 2-liter, 3-neck flask equipped with an efficient stirrer and a long stem thermometer, a mixture of 272 g (1.65 m) of potassium permanganate, 350 g (4.2 m) of sodium bicaronate, 100 ml of acetone and 400 ml of water was stirred and cooled to 4 °C. To this mixture was added dropwise 284 g (1.0 m) of

$$CClF_2CClFCF_2CF{=}CF_2.$$

The latter compound was obtained from the pyrolysis of $CClF_2CClFCF_2CFClCF_2COONa$ in a manner described in earlier work [1]. After addition the mixture was permitted to warm slowly to room temperature, care being exercised to prevent excessive foaming. Excess permanganate was destroyed with 5 percent aqueous sodium bisulphite. Manganese dioxide thus formed was filtered, washed with water, and discarded. The combined filtrate and washings were clear and colorless. To this was added 160 ml (294 g, 5 m) of 95 percent sulfuric acid. This acid solution was extracted continuously with ether for 50 h. The extract was dried over anhydrous sodium sulphate and distilled. The product was distilled under reduced pressure, yielding 121 g of a clear, colorless oil boiling at 100 °C/3 mm. This was 49 percent based on the pentene.

Preparation of 3,4-Dichloropentafluorobutyric Acid (Alternative Preparation). Into a 5-liter, 3-neck flask equipped with a condenser arranged for downward distillation was placed 570 g (1.5 m) of $CClF_2CClFCF_2CF_2I$ and 2000 g of 20 percent fuming sulfuric acid. This mixture was heated gently until the acid fluoride,

$$CClF_2CClFCF_2C(=O)F,$$

began to distill. Heating was then carefully adjusted so that the acid fluoride would continue to distill with a minimum of impurities. Sulfur trioxide which was evolved in copious quantities during the addition was vented from the system through a tube attached to an adapter between the condenser and the receiver. The crude acid fluoride-iodobutane layer, 283 g, was shaken with conc. sulfuric acid in a separatory funnel, removing dissolved sulfur trioxide, then distilled through a column. The yield was 158 g of

$$CClF_2CClFCF_2C(=O)F.$$

Approximately 107 g of butane was recovered. The yield of acid fluoride was 52.3 percent based on the iodobutane which reacted.

The acid fluoride was added dropwise to a solution of 80 g of sodium hydroxide in 200 ml of water. The mixture was heated to 90 °C and maintained at this temperature for 30 min. It was cooled and a small amount of oil separated. The aqueous alkali solution was acidified with 50 percent sulfuric acid and extracted continuously with ether for five days. The ether extract was dried over anhydrous sodium sulfate and distilled. The product, 3,4-dichloropentafluorobutyric acid was obtained by distillation under reduced pressure. It amounted to 149 g of a clear colorless liquid boiling at 100°/3 mm. This was 95 percent based on the acid fluoride or 49.5 percent based on the iodobutane.

Preparation of 3,4-Dichloropentafluorobutyric Acid (2nd Alternative Preparation). In a stainless steel bomb was placed 152 g (0.5 m, 76 ml) of 1,1,3,4,-tetrachlorohexafluorobutane (3M Kel-F Dimer No. 464) 72 ml of conc. sulfuric acid and 34 ml of 30 percent fuming sulfuric acid. The bomb was sealed. It was rocked, heated to 200 °C and maintained at this temperature for 96 h. It was cooled to −80 °C, opened and permitted to warm to room temperature. Intense foaming and evolution of gas occurred, but the contents of the bombs were successfully transferred to a beaker. On standing, the foaming and gas evolution subsided. This mixture was distilled under reduced pressure yielding 65 g of clear liquid boiling at 61°/1 mm or 53 percent based on the butane. It gave the same index of refraction as samples prepared in the other two ways. N_D^{20} 1.3470.

Preparation of 3-Chloropentafluoropropene. Fifty grams (0.21 m) of 3,4-dichloropentafluorobutyric acid were converted to the sodium salt by neutralizing an aqueous solution of the acid with sodium hydroxide so that the resulting solution had a pH of 7. This was evaporated to absolute dryness in a vacuum desiccator, yielding 56 g of anhydrous sodium 3,4-dichloropentafluorobutyrate. The salt was pyrolyzed in a 250 ml round-bottom flask which was connected by adapters to three liquid nitrogen-cooled traps connected in tandem. Heat was supplied by a microburner. The yield was 32 g or 91.5 percent based on the acid salt. This was distilled through a column packed with glass helices. The yield of pure compound was 30 g or 86.2 percent. B.P. 8 °C.

Preparation of Pentafluoro 3-Iodopropene. A 2-liter, 3-neck flask was equipped with a stirrer, a thermometer, and a reflux condenser topped by a dry ice acetone-cooled cold finger type condenser topped by a calcium chloride drying tube. Into the flask was placed 83 g (0.6 m) of sodium iodide and 300 ml of freshly distilled methyl-ethyl ketone. Stirring was commenced and into the flask was distilled 58 g (0.35 m) of 3-chloropentafluoropropene. The mixture was refluxed for 24 h. The reflux temperature rose from 20 to 60 °C. The product was removed from the flask, filtered, and the filtrate distilled. A fraction boiling between 50° and 55° was collected and redistilled through a 10-in column packed with glass helices. The yield was 40 g of a clear colorless liquid which slowly turned violet on standing. This was 44.2 percent based on the chloropentafluoropropene. B.P. 53 °C.

408-434 O - 71 - 4

Preparation of 1,2-Dichloro-pentafluoro 3-iodopropane. Seventy-four g (0.3 m) of 3,4-dichloropentafluorobutyric acid was carefully neutralized with 3.5 *N* ammonium hydroxide. To the solution was added a solution of 60 g of silver nitrate in 200 ml of water. Upon refrigeration, silver 3,4-dichloropentafluorobutyrate crystallized and was filtered. Concentration of the filtrate produced additional product. The salt was dried in a vacuum oven at 60 °C for a week. The yield was 104 g or 99 percent.

Seventy g (0.2 m) of powdered silver 3,4-dichloropentafluorobutyrate was mixed with 76 g (0.3 m) of powdered iodine. The mixture was sifted until homogeneous. It was placed in a metal tube attached to two dry ice acetone-cooled traps and a bubble counter in series. The silver salt-iodine mixture was pyrolyzed by heat from a micro burner, beginning with the end nearest the traps and keeping the evolution of carbon dioxide fairly constant as indicated by the bubble counter. The product was obtained from the first trap. It amounted to 16 g or 24 percent. The crude product was distilled through a 6-in column packed with glass helices. The yield of pure 1,2-dichloro-3-iodopentafluoropropane was 10 g or 15 percent based on the butyric acid. B.P. 119 °C. The predominant yield was 3-chloropentafluoropropene, the product described above in the pyrolysis of sodium 3,4-dichloropentafluorobutyrate.

Analysis of C_3ClF_5I

	C	Cl	I
Calculated	10.9	21.8	38.4
Found.....	11.2	22.5	38.0

Preparation of 5,6-Dichloroperfluorohexanoic Acid. In an 800-ml stainless steel bomb a mixture of 478 g (1.0 m) of 1,2-dichloro-6-iodoperfluorohexane and 654 g (5.6 m) of chlorosulfonic acid was rocked and heated to 150 °C. It was maintained at this temperature with rocking for 72 h. The liquid was removed from the bomb and added dropwise to 3000 ml of water in a beaker. The bomb was washed with two 500-ml portions of water and the washings were added to the beaker. An oil slowly separated. The aqueous layer was decanted. The oil was transferred to a separatory funnel diluted to three times its original volume with ether and washed with three 200-ml portions of water. The ether solution was dried over anhydrous sodium sulfate and distilled. The product was obtained by distillation under reduced pressure. It amounted to 254 g of a clear colorless liquid boiling at 138 °C/63 mm. This acid had the same index of refraction, N_D^{20} 1.3612, reported by Knunyants. The percentage yield was 73.5.

Preparation of 1,2-Dichloro-perfluoro 5-iodopentane. Thirty-eight g (0.11 m) of 5,6-dichloroperfluorocaproic acid was converted to the dry silver salt in the manner described above for 3,4-dichloropentafluorobutyric acid and pyrolyzed in the presence of a 100 percent molar excess of powdered iodine in a stainless steel tube attached through on an adapter to a large flask which was attached to a dry ice acetone-cooled trap and a vacuum pump. The pyrolysis was carried out under reduced pressure. Total pyrolysis products amounted to 40 g. This material was distilled through a column under reduced pressure. Yield of the iodopentane was 21 g or 44.5 percent based on the caproic acid. B.P. 68°/40 mm. There was a large solid residue.

Analysis for $C_5F_9Cl_2I$

	C	Cl	I
Calculated	14.0	16.6	29.6
Found	14.2	15.9	28.9

Preparation of 5,6-Dichloroperfluoro-1-hexene. A 2-liter resin flask was equipped with a stirrer, reflux condenser and a dropping funnel. It was evacuated and the wall thoroughly dehydrated by heating while a vacuum was maintained in the flask. Dry nitrogen was admitted to the flask and a slow nitrogen flow was maintained throughout the reaction. Into the flask was poured 240 g (0.5 m) of 5,6-dichloro-1-iodoperfluorohexane and 1000 ml of carefully dried ether. This was cooled to −80 °C with a dry ice acetone bath. With vigorous stirring a solution of 12 g (0.55 m) of methyl lithium was added dropwise. Stirring was continued and the reactants were permitted to warm to room temperature. To the mixture was added 200 ml of water followed by 200 ml of 20 percent hydrochloric acid. Stirring was continued for 2 h. The mixture was transferred to a separatory funnel; the aqueous layer was separated and discarded. The ether solution was dried over anhydrous sodium sulphate and distilled. Seventy grams of starting material was recovered. The yield was 80 g or 68 percent based on the hexane which reacted. B.P. 116 °C. Also obtained was 8.5 g of material boiling at 143°, which was not characterized and a small solid residue.

Preparation of Perfluoro 1,1,7-trihydroheptane. A 1400-ml silver lined bomb was charged with 498 g (1.5 m) of 1,1,7-trihydroperfluoroheptanol (Dupont fluoroalcohol C7) and sealed. Through copper tubing 256 g (238 m) of sulfur tetrafluoride was poured directly into the bomb from a cylinder as the bomb rested on a balance. The cylinder was gently heated to facilitate the transfer. A heater-rocker apparatus was heated to 100 °C. The bomb was placed in it and rocked. Heating was discontinued, but the temperature rose to 130°, then slowly subsided. Heating was resumed. The bomb was maintained at 100 °C for 4 h. Heating was again discontinued but the bomb was permitted to rock for an additional 18 h. When the bomb had cooled the gaseous contents were vented through a solution of 550 g of sodium hydroxide in 4000 ml of water, thus removing thionyl fluoride, hydrogen fluoride and excess sulfur tetrafluoride. Dry nitrogen was passed through the bomb in a further effort to remove corrosive gases. The bomb was opened. From a beaker 500 ml of cold potassium hydroxide solution was cautiously added to the bomb. The mixture was stirred manually until there was no further odor of sulfur tetrafluoride. The bomb contents were transferred to a 1500 ml beaker. The aqueous layer was decanted. The oily layer was washed with two 250 ml portions of cold water, then dried over anhydrous sodium sulfate and distilled

through an 18-in column packed with glass helices. In all 128 g of starting material was recovered. Yield of product was 272 g or 73 percent based on the telomer alcohol which reacted. B.P. 123–4°.

Analysis of $C_7F_{13}H_3$

	C	F	H
Calculated	25.1	74.0	0.9
Found.....	25.2	73.7	0.8

Preparation of Perfluoro 7-Hydroheptaldehyde. A 500-ml 3-neck flask was equipped with a dropping funnel, an 18-in column packed with glass helices and a still head. Into the flask was placed 83 g (0.25 m) of 1,1,7-hydroperfluoroheptanol (Dupont fluoroalcohol C7). This alcohol was heated until it boiled vigorously but did not distill through the column. A solution of 26 g (0.1 m) of sodium dichromate and 35 g (0.35 m) of sulfuric acid in 150 ml of water was added slowly through the funnel. 7-Hydroperfluoroheptaldehyde and water distilled through the column into the receiver forming two phases. The water layer was separated and extracted with three 100 ml portions of ether. The ether extracts were combined and added to the free aldehyde. The ether solution was dried over sodium sulfate and distilled. The fraction boiling at 121 to 122 °C was retained as the product. Higher boiling fractions were retained separately but not characterized further. The yield was 58 g or 70 percent. Upon standing in air the aldehyde slowly forms a monohydrate.

Preparation of Perfluoro 1,7-Dihydroheptane. An 800-ml stainless steel bomb was charged with 349 g (1.0 m) of 7-hydroperfluoroheptaldehyde-monohydrate. Through a valve attached to the bomb 275 g (2.5 m) of sulphur tetrafluoride was poured into the bomb from a measuring device. The bomb was rocked, heated to 150 °C and maintained at that temperature for 68 h. It was cooled to room temperature and the excess sulphur tetrafluoride was permitted to bubble through a large flask containing potassium hydroxide solution. The contents of the bomb were removed, treated with sodium fluoride and sodium sulphate, then filtered. The filtrate was distilled. A fraction boiling at 110 to 112 °C was retained as the product. This amounted to 15 g or 4.3 percent based on the aldehyde hydrate.

Analysis of $C_7F_{14}H_2$.

	C	H	F
Calculated	23.9	0.9	75.5
Found.....	23.8	0.6	75.3

Attempted Preparations of Perfluoro-1,6-Heptadiene. In a 100-ml flask a mixture of 7 g (0.02 m) $H(CF_2)_7H$, 2.3 g (0.04 m) of potassium hydroxide, and 50 ml of absolute alcohol was refluxed for five days. The components were separated and the starting material recovered unchanged.

In a 75-ml flask a mixture of 7 g (0.02 m) of $H(CF_2)_7H$ and 2.3 g (0.04 m) of potassium hydroxide was refluxed for 24 h. The mixture turned brown and the potassium hydroxide became coated with a dark substance. Five g of the heptane were recovered but no product was obtained.

Small amounts of 1,7-dihydroperfluoroheptane were put through steel tubes packed with (1) sodium fluoride, (2) steel wool, (3) nickel turnings, (4) platinum on carbon. This work was carried out under vacuum and under an atmosphere of dry nitrogen and at temperatures ranging between 300 and 600 °C at 50° intervals. Below 550 °C starting material was recovered unchanged. At 600° and above extensive carbonization occurred. Very little of the heptane was recovered and no unsaturated products were obtained under any combination of conditions.

Preparation of Perfluoro-1,7-octadiene. A 2-liter, 3-neck flask was equipped with a dropping funnel, an efficient stirrer and a still head. Into it was placed 134 g (2 m) of powdered zinc and 1000 ml of *bis*[2[(2-methoxy-ethoxy)ethyl] ether. This suspension was heated to 120 °C and maintained at this temperature. To it was added dropwise 504 g (1 m) of 1,2,7,8-tetrachloroperfluorooctane. Perfluoro-1,7-octadiene distilled at approximately the same rate as the octane was added after a short incubation period. The crude product was distilled through a 10-in column packed with glass helices. A clear colorless liquid boiling at 106 °C was obtained. The yield was 240 g or 66.5 percent based on the tetrachloroperfluorooctane.

Preparation of Perfluoro-1,5-hexadiene (Miller's Method) or (Method No. 1). In a 100-ml 3-neck flask equipped with a stirrer and reflux condenser was placed 5 g (0.077 m) of activated zinc suspended in 30 ml of carefully dried dioxane. The opening of the condenser was connected to a dry ice acetone-cooled trap. The apparatus was swept out with dry nitrogen. While stirring briskly, 14.1 g (0.055 m) of 3-iodopentafluoropropene (perfluoroallyl iodide) was added dropwise over a period of 1 h. After addition the contents of the flask were refluxed for 4 h and permitted to stand at room temperature for 68 h. The crude hexadiene was distilled directly from the flask. Distillate was collected up to 100 °C then distilled through a 10-in glass column packed with glass helices. The product was 4 g of clear colorless liquid boiling at 59 °C or 55.5 percent based on the 3-iodopentafluoropropene.

Preparation of Perfluoro-1,5-hexadiene (Knunyant's Method) or (Method No. 2). A 1-liter flask was equipped with a stirrer, a still head, and a dropping funnel. Into it was placed 52 g (0.8 m) of zinc powder, 360 ml of acetic acid and 90 ml of acetic anhydride. This mixture was stirred and heated to gentle reflux. Heating was discontinued and to the stirred suspension was added 73 g (0.18 m) of 1,2,5,6-tetrachloroperfluorohexane at a rate such that perfluorohexadiene distilled as rapidly as it formed. The crude hexadiene was distilled through a 10-in glass column packed with glass helices to produce 26 g (0.099 m) of clear colorless liquid boiling at 59 °C. This was 55 percent based on the hexane.

The acetic acid solution was poured into 3000 ml of water. Twenty-four g of fluorocarbon separated. This material was dried and distilled yielding 15 g (0.045 m) of material boiling at 115 °C which was assumed to be

either 5,6-dichloroperfluoro-1-hexene or 6,6-dichloroperfluoro-1-hexene and 8 g (0.02 m) of liquid boiling at 43°/1 mm or at 171° at atmospheric pressure. This was considered to be either 1,2,5,6-tetrachloroperfluorohexane or 1,1,6,6-tetrachloroperfluorohexane. 6,6-Dichloroperfluoro-1-hexene, and 1,1,6,6-tetrachloroperfluorohexane would arise from an isomeric impurity produced in the preparation of 1,2-dichloro-1-iodotrifluoroethane.

Preparation of Perfluoro-1,5-hexadiene (Fearn-Brown Method or Method No. 3). A 1-liter 3-neck flask was fitted with a stirrer, still head and dropping funnel as described above. Into it was placed 26 g (0.4 m) of powdered zinc, 360 ml of acetic acid and 90 ml of acetic anhydride. The mixture was stirred and heated to reflux. Heating was discontinued and 67 g (0.2 m) of 5,6-dichloroperfluoro-1-hexene was added dropwise. Perfluoro-1,5-hexadiene distilled at the same rate. The crude product was washed three times with cold dilute sodium carbonate solution, then three times with cold water. It was dried over anhydrous sodium sulfate and distilled. The yield was 34 g of clear colorless liquid boiling at 59 to 60 °C or 65 percent based on the dichloroperfluorohexene.

Preparation of Perfluoro-1,6-heptadiene (Method No. 1). Into a 1-liter 3-neck flask fitted with a stirrer, a reflux condenser, and a dropping funnel was placed a mixture of 13.1 g (0.2 m) of zinc powder, 400 ml of methylene chloride and 160 ml of acetic anhydride. The mixture was stirred and heated to reflux. To it was added dropwise a mixture of 19.3 g (0.045 m) of 1,2-dichloro-5-iodopentane and 55.9 g (0.2 m) of 1,2-dichloro-1-iodotrifluoroethane. After addition the mixture was stirred and refluxed for 24 h. The mixture was filtered and the filtrate added slowly to 4000 ml of cold water in a beaker. This mixture was stirred vigorously for 4 h. The organic layer was separated, dried, and distilled. The yields are recorded below.

	B.P.	Gms
(1) 1,2,3,4-Tetrachloroperfluorobutane.....	133°	16.8
(2) 1,2,6,7-Tetrachloroperfluoroheptane.....	74/19 mm	7.9
(3) 1,2,9,10-Tetrachloroperfluorodecane.....	94/5 mm	6.0

Compounds 1 and 3 are known.

Analysis for Compound 2 $C_7F_{12}Cl_{14}$

	C	Cl
Calculated	18.5	31.3
Found.....	18.4	30.9

Compound 2 was dehalogenated in the manner described above for perfluorooctadiene. Seven grams (0.015 m) of 1,2,6,7-tetrachloroperfluoroheptane yielded 3.5 g (0.011 m) of perfluoro-1,6-heptadiene or 75.5 percent based on the heptane. B.P. 86 °C.

Preparation of Perfluoro-1,6-heptadiene (Method No. 2). Into a 500-ml 3-neck flask fitted with a stirrer, a reflux condenser and a dropping funnel was placed a mixture of 6.5 g (0.1 m) of zinc powder, 200 ml of methylene chloride and 80 ml of acetic anhydride. The mixture was stirred and heated to gentle reflux. To it was added dropwise a mixture of 9 g (0.027 m) of 1,2-dichloro-3-iodopropane and 21 g (0.055 m) of 1,2-dichloro-4-iodobutane. After addition the mxiture was stirred and refluxed for 15 h. The mixture was filtered and the filtrate added to 2000 ml of water in a beaker. The mixture was stirred vigorously for 4 h. The organic layer was separated, dried, and distilled. Yields are recorded below.

	B.P.	Gms
(1) 1,2,5,6-Tetrachloroperfluorohexane.....	171°	4.5
(2) 1,2,6,7-Tetrachloroperfluoroheptane.....	74°/19 mm	5.1
(3) 1,2,7,8-Tetrachloroperfluorooctane.....	68°/1 mm	11.5

Compound 2 was again dehalogenated as described above. Five g (0.011 m) of 1,2,6,7-tetrachloroperfluoroheptane yielded 2.7 g (0.0087 m) of perfluoro-1,6-heptadiene or 79 percent. B.P. 86 °C.

Preparation of Perfluoro-1,6-heptadiene (Method No. 3). In a metal tube attached to two dry ice acetone-cooled traps connected in series and finally to a vacuum pump, 328 g (0.68 m) of sodium 6,7-dichloroperfluorocaprylate was pyrolyzed. Heat was applied by a cylindrical furnace surrounding the metal tube. Pyrolysis was carried out at 380 °C as indicated by a pyrometer. The product, crude 6,7-dichloroperfluoro-1-heptene was dried over anhydrous sodium sulfate and distilled through an 18-in column packed with glass helices under an atmosphere of dry nitrogen. The yield was 220 g or 84.5 percent based on the sodium salt. B.P. 138 °C.

Analysis for $C_7Cl_2F_{12}$

	C	Cl
Calculated	21.9	18.5
Found.....	21.8	18.4

In a 1000-ml 3-neck flask equipped with a stirrer, dropping funnel and still head, a mixture of 26 g (0.4 m) of zinc powder which had been previously activated by treatment with conc. hydrochloric acid in acetone and 500 ml of *bis*[2-(2-methoxyethoxy)ethyl] ether was stirred and heated to 75 °C. To this suspension was added dropwise 76.6 g (0.2 m) of 6,7-dichoroperfluoro-1-hexene. After a brief incubation period, perfluoro-1,6-heptadiene began to distill at the same rate as the hexene was added. The crude diene was treated with phosphorus pentoxide, filtered, then distilled under an atmosphere of dry nitrogen through a 10-in column packed with glass helices. The yield was 48 g (0.154 m) or 76 percent based on the heptene. B.P. 86°. Nine g of residue boiling above 90 °C was obtained but not studied.

Analysis for C_7F_{12}

	C
Calculated	26.9
Found.....	26.7

3. Discussion

3.1. Synthesis

The ethanes other than $CF_2ClCFClI$ mentioned in the introduction were prepared as follows:

1. $CF_2CF_2 + ICl \longrightarrow CF_2ClCF_2I$
2. $CF_2CF_2 + I_2 \xrightarrow{CF_2Br_2} CF_2ICF_2I$
3. $CF_2CFH + ICl \longrightarrow CF_2ClCFHI.$

All three addition reactions took place readily, giving yields which were virtually quantitative. Efforts to telomerize these materials with tetrafluoroethylene in the manner described above were abortive. 1-chlorotetrafluoroethane-2-iodo does not add tetrafluoroethylene to form a telomer nearly as readily as tetrafluoroethylene homopolymerizes. As a result efforts to carry out the reaction

$$CF_2ClCF_2I + CF_2CF_2 \longrightarrow CF_2ClCF_2(CF_2CF_2)_nI$$

resulted chiefly in the preparation of high polymer with only traces of liquid products. Attempts to telomerize 1-chloro-1,1,2-trifluoroethane-2 iodo with tetrafluoroethylene were even less successful, yielding only high polymer. If the telomers had formed the former would have proved very difficult to dechlorofluorinate but dehydrochlorination of the latter would have been feasible. The reaction $ICF_2CF_2I + CF_2CF_2 \longrightarrow I(CF_2CF_2)_nI$ was found to take place but Knunyants [14] asserted that this is not a telomerization but a coupling process which takes place according to the following mechanism.

$$ICF_2CF_2I \xrightarrow{250\,^\circ C} ICF_2CF_2^* + I^*$$

$$2ICF_2CF_2^* \longrightarrow I(CF_2CF_2)_2I$$

$$2I^* \longrightarrow I_2$$

The diiodobutane may then loose an iodine atom to form a radical which may couple with another iodobutyl radical or an iodoethyl radical to produce, respectively, a diiodooctane or a diodohexane. The stability of the molecule increases with the number of carbon atoms between the terminal iodines. The findings in all of this work tend to enhance the view that $R-CF_2I$ type compounds do not form radicals which either couple or initiate polymerization nearly as readily as $R-CFClI$ type structures. The telomerization of $CF_2ClCFClI$ with tetrafluoroethylene proceeded with gamma initiation in the same manner as Knunyants obtained using benzoyl peroxide catalysis [10].

The yields of perfluorohexadiene were acceptable in all three syntheses, the last preparation being superior in overall efficiency. The deiodofluorination reaction employing methyl lithium is a subject for further study since the exact conditions under which lithium fluoride splits out have not been precisely established. As of this writing efforts to prepare perfluoro-1,5-hexadiene by double deiodofluorination of $I(CF_2CF_2)_3I$ are continuing. Dechlorinations were in all cases routine.

Difficulties with the first proposed synthesis of perfluoro-1,6-heptadiene were discussed above. In the second effort the weakest link was the cross coupling reaction. The 1,2-dichloro-1-iodotrifluoroethane tends to homocouple for reasons indicated above. Another factor is the possibility of telomerizing the iodohexane used in preparing the iodopentane with tetrafluoroethylene to produce the iodooctane which is the starting material in the preferred synthesis. The hang-up in the third proposed synthesis is the pitifully small yield of 1,2-dichloro-3-iodopentafluoropropane in the mixed pyrolysis of silver 3,4-dichloropentafluorobutyrate and iodine. This results from the partial distillation of iodine from the reaction chamber before the pyrolysis temperature is reached. In this synthesis the cross coupling reaction proved reasonably efficacious. The fourth synthesis produced a quandry. The telomer obtained from 1,2-dichloro-4-iodobutane and hexafluoropropylene formed in good yield through the reaction scheme shown in the introduction. The deiodofluorination reaction, which was carried out experimentally in the manner described above for 5,6-dichloroperfluoro-1-hexane produced a multiplicity of compounds. These were separated on a preparative scale vapor phase chromatograph (VPC) and one of the major components was identified by analytical VPC and infrared studies as the desired 6,7-dichloroperfluoro-1-heptene. Evidence suggested strongly that another was 6,7-dichloroperfluoro-2-heptene. With the 1-heptene the VPC retention time and the infrared spectrum of the sample obtained was identical with that of a sample of this compound prepared in the manner described below. With the 2-heptene the retention time was slightly lower and the peak in the infrared spectrum usually associated with the double bond was displaced from 5.6 μ to 5.4 μ, the usual displacement between a terminal and an internal double bond. The mechanism through which each of these fluoroolefins is formed is illustrated below.

$$\begin{array}{l} CF_2ClCFClCF_2CF_2CF_2CFCF_3 \\ \qquad\qquad\qquad\qquad\qquad\qquad\quad\;\; | \\ \qquad\qquad\qquad\qquad\qquad\qquad\qquad\;\; I \\ \text{Ethyl Ether} \;\Big\downarrow\; CH_3Li \\ CF_2ClCFClCF_2CF_2CFCFCF_2 \\ \qquad\qquad\qquad\qquad\qquad\qquad\quad\;\; | \;\; | \;\; | \\ \qquad\qquad\qquad\qquad\qquad\qquad\quad\;\; F \;\; Li \; F \end{array}$$

If the lithium atom splits out with a fluorine atom from the terminal carbon atom the 1-heptene results, but if it selects a fluorine atom from the adjacent internal carbon atom the 2-heptene is produced. Results indi-

cate a competition between these two processes. A third component, whose infrared spectrum suggested a saturated compound was considered to be cyclic, possibly

$$CF_2ClCFClCFCF_2CF_2CFCF_3$$

The fact that this substance will undergo dechlorination militates against the five-member ring that one would expect. If the lithium atom attacked either the terminal or the penultimate carbon atom one would expect the chlorine atom to split off much easier than the fluorine atom, producing a compound which would not undergo intramolecular dechlorination as this compound does. The structure above remains a postulation since neither infrared, nuclear magnetic resonance (^{19}F) nor any other technique provided conclusive proof. The problem of separating the many products made this an unacceptable preparation for perfluoro-1,6-heptadiene. A possible explanation for the occurrence of some of these products many of which were not identificable by black box technique lay in the possibility that the initial telomerization reaction produced some head-to-head addition rather than uniformly head-to-tail addition predicted by the work of Hauptschein [15] on similar compounds, e.g.,

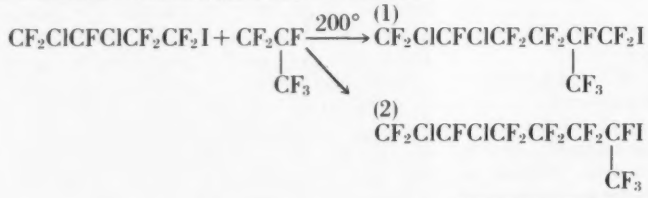

$$CF_2ClCFClCF_2CF_2I + CF_2CF \xrightarrow{200^\circ} \underset{(1)}{CF_2ClCFClCF_2CF_2CFCF_2I} + \underset{(2)}{CF_2ClCFClCF_2CF_2CF_2CFI}$$

CF_3 CF_3 CF_3

Deiodofluorination can then give rise to a compound with the formula $CF_2ClCFClCF_2CF_2CFCF_2$ which could not occur through a uniform head-to-tail telomerization. In the presence of fluoridation the double bond of this compound could consequently move inward, i.e.,

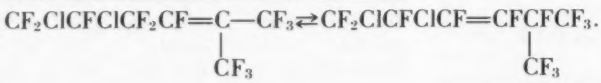

$$CF_2ClCFClCF_2CF{=}C{-}CF_3 \rightleftarrows CF_2ClCFClCF{=}CFCFCF_3.$$

CF_3 CF_3

In this way one head-to-head addition could result in three additional compounds.

The methods and principles employed in these investigations may be utilized in preparing any fluorodiene between perfluorobutadiene through $CF_2CF(CF_2)_{16}CFCF_2$. Terminal fluorodienes with more than eight carbon atoms are not suitable for the inter-intramolecular polymerization studies that provided the impetus for undertaking these syntheses. Perfluoro-1,8-nonadiene may be prepared from 1,2-dichloro-10-iodoperfluorodecane in the manner described in the fifth synthesis of perfluoro-1,6-heptadiene. In the same manner any perfluorodiene with an odd number of carbon atoms may be prepared from a telomer with one more carbon atom than the desired diene. All of the even numbered dienes may be prepared by cross-coupling and dechlorinating selected telomers. Telomers containing 12 carbon atoms or more are solid and virtually impossible to distill or selectively sublime. This makes the preparation of fluorodienes of 24 carbon atoms or more somewhat more difficult according to methods discussed above. Their preparation would involve the development of a sophisticated separation for the higher telomers.

3.2. Chemistry

Since perfluoropentadiene and 4-chloroperfluoro-1,6-heptadiene did not yield polymer of significant molecular weight except when polymerized at high pressure [1, 2, 3], no studies were made of perfluorodienes containing 6, 7, or 8 carbon atoms at pressures less than 5000 atm. Often at these pressures crystallization of monomer will occur. As this can greatly affect the nature of the polymerization reaction it is desirable to know the freezing pressure. This crystallization was detected by careful observation of isobaric volume changes during application of pressure [16]. Plotting the pressure at which isobaric volume changes occurred against temperature produced curves similar in slope for perfluoropentadiene and for perfluoro-1,7-octadiene, suggesting that perfluoro-1,5-hexadiene will show a similar slope when polymerization studies on it are completed. Perfluoro-1,6-heptadiene increased in viscosity during the application of pressure but showed no isobaric volume change, indicating that no freezing took place at 22° at even 10000 atm. The observed freezing temperatures were not found to vary monotonically with the number of carbon atoms in the compound but this is not unusual. Even with linear alkanes the pattern of variation is often complex.

Polymerization techniques did not differ from those previously described [17]. Initiation was effected by radiation from a ^{60}Co source. Preliminary investigations were carried out in bulk. The kinetic chain length was computed in the following fashion. At 0.045 Mrad/h about 5×10^{-3} percent per hour of the monomer was converted to initiating species, presumably radicals, if the G value (yield per 100 eV) for initiation is four. The kinetic chain length was taken as the ratio of the

percent of polymer formed to 5×10^{-3} times the irradiation time. For the purpose of these investigations this approximation is valid and sufficient. The ratio of polymerized monomer units to the number of perfluorovinyl groups in the polymer was obtained by a Beer's law computation from data obtained from infrared spectra. This type of computation proved very useful in earlier work [2, 3]. With perfluorohexadiene and perfluorooctadiene polymers these values are thought to have an uncertainty factor of about 2. With perfluoro-1,6-heptadiene polymer its crystallinity makes the accuracy of the $C_nF_{2n-2}/CF{=}CF_2$ ratio rather indeterminate.

When the kinetic chain length is much greater than the $C_nF_{2n-2}/CF{=}CF_2$ ratio, this ratio should be about equal to the ratio of cyclization to noncyclization, but when the kinetic chain length and the aforementioned ratio differ by a factor less than 10, it is probable that an appreciable fraction of the observed double bonds may represent chain ends. These considerations give rise to the concept that the ratio of cyclization to noncyclization is about 20 for the octadiene, 200 for the hexadiene and a still larger but not precisely established value for the heptadiene. For each polymer, similar values of $C_nF_{2n-2}/CF{=}CF_2$ were obtained under different polymerization conditions, suggesting that this ratio is not a strong function of either temperature or pressure.

Gelation occurs when a pendant vinyl group becomes incorporated in another chain, thus effecting a cross link between the two chains; thus, it may be used as a measure of the ratio of cyclization versus noncyclization. It is determined by extracting the polymer couple with boiling hexafluorobenzene and weighing both the soluble and insoluble fractions. The percent gelation is then determined by dividing the insoluble fraction by the weight of the total polymer sample. Polymer solution theory predicts that gelation will occur when the fraction of polymer formed is equal to the product of the ratio of cyclization to noncyclization and the reciprocal of the primary weight average degree of polymerization [18]. For cases where no gelation occurred a lower limit for the aforementioned ratio can be calculated by using 2γ as the weight average degree of polymerization and multiplying this value by the observed conversion. Cases in which gel formed may be used in the same way to compute an upper limit for the ratio. In this manner, R, the ratio of cyclization to noncyclization, has been computed for perfluoro-1,5-hexadiene, perfluoro-1,6-heptadiene, and perfluoro-1,7-octadiene. The values are $230 < R < 10^4$, $230 < R$, and $6 < R < 320$, respectively.

In cases where the polymer yield is fairly low, an additional check is possible since in such cases 2γ is a good estimate of the weight average degree of polymerization. For a most probable distribution the sol fraction may be used to compute the number of cross links per weight average molecule [19]. In this work computations of this sort tended to confirm values estimated through use of Beer's law computations.

Systematic studies with these monomers were hampered by sensitivity to impurities. The indicated results with perfluoro-1,7-octadiene were obtained with monomer which had not been purified on a prep scale vapor phase chromatograph. Polymer samples accordingly, gave values of γ below those of other materials studied. Other samples in all cases were prepared from monomer which had been carefully chromatographed on a long column. The double bond migration which takes place so readily with perfluoro-1,4-pentadiene [3] takes place less readily with the six, seven, and eight carbon fluorodienes. Whenever recovered monomer was used without chromatographic purification, lower rates were obtained. This diminution in rate was attributed to the presence of internal olefins resulting from double bond migration. Polymerization rates with pure monomer were about 200 to 500 times those obtained with perfluoro-1-heptene in the same conditions [20]. It is uncertain whether this is due to a difference in monomer rate constants, difference in monomer purity, or to some effect of gelation on rate where dienes are concerned.

Attempts were made to avoid gelation by polymerization in solvents such as perfluorocyclobutane. The intention here was to take advantage of the hypothesis that the cyclization rate should be independent of monomer concentration while propagation should be directly related to monomer concentration so that dilution should increase the ratio of cyclization to noncyclization. Calculations using spectra of these polymers gave values of $C_nF_{2n-2}/CF{=}CF_2$ of 10^3 or more. These spectra also showed intense absorption attributable to acid fluorides and internal double bonds. This is not easily explained since such absorptions were not observed with polymers prepared in bulk from highly purified monomer. A comprehensive study of the polymerization of these materials will be the subject of another communication.

4. References

[1] Fearn, J. E., and Wall, L. A., SPE Trans. **3,** 231 (1963).
[2] Fearn, J. E., Brown, D. W., and Wall, L. A., J. Polymer Sci. **4** Part A, 131–140 (1966).
[3] Brown, D. W., Fearn, J. E., and Lowry, R. E., J. Polymer Sci. **3** Part A, 1641–1660 (1965).
[4] Park, J. D., and Lacher, J. R., W.A.D.C. Tech. Report 56–590, Part 1, 21–22 (1957).
[5] Butler, G. B., and Agnello, R. J., J. Am. Chem. Soc. **79,** 3128 (1957).
[6] Miller, W. T., private communication.
[7] Hauptschein, M., and Fainberg, A. H., J. Am. Chem. Soc. **83,** 2495 (1961).
[8] Knunyants, I. L., Chai-yuan, Li, and Shokina, V. V., Doblady. Akad. Nauk. SSSR **136,** 610–12 (1961).
[9] Haszeldine, R. N., J. Chem. Soc. 4291–4305 (1955).
[10] Knunyants, I. L., Chai-yuan, Li, and Shokina, V. V., Izvestia Akad. Nauk. SSSR, Otdelenie Khimicheskikh Nauk. **10,** 1462–68 (1961).
[11] Knunyants, I. L., Chai-yuan, Li, and Shokina, V. V., Izvestia Akad. Nauk. SSSR, Otdelenie Khimicheskikh Nauk **10,** 1910–11 (1961).
[12] Miller, William T., U.S. Patent 2,668,182 (1954).
[13] Hauptschein, M., and Braid, M., J. Am. Chem. Soc. **83,** 2500 (1961).

[14] Knunyants, I. L., Khrlakyan, S. P., Zeifman, Yu. V., and Shokina, V. V., Doklady. Akad. Nauk. SSSR **2,** 384 (1964).
[15] Hauptschein, M., Braid, M., and Lawlor, F. E., J. Am. Chem. Soc. **79,** 2549 (1957).
[16] Brown, D. W., private communication.
[17] Wall, L. A., Brown, D. W., and Florin, R. E., Am. Chem. Soc. Polymer Preprints **4,** No. 2, 366 (Sept. 1961).
[18] Flory, P. J., Principles of Polymer Chemistry (Cornell Univ. Press, 1953) p. 391.
[19] Charlesby, A., Atomic Radiation and Polymers (Pergamon Press, 1960) p. 145.
[20] Brown, D. W., and Wall, L. A., SPE Trans. **3,** 300 (1963).

(Paper 75A1–649)

JOURNAL OF RESEARCH of the National Bureau of Standards—A. Physics and Chemistry
Vol. 75A, No. 1, January-February 1971

Quantum Corrections to the Second Virial Coefficient for the Lennard-Jones (*m*-6) Potential

Marjorie E. Boyd

**Institute for Basic Standards
National Bureau of Standards
Washington, D.C. 20234**

(September 18, 1970)

Tables are presented for the second virial coefficient of a Lennard-Jones (*m*-6) gas in reduced variables for seven values of *m*. A wide range of reduced temperatures, in a mesh chosen for ease of interpolation, is covered. Values are given for the classical term and three quantum corrections as well as the first two temperature derivatives of each of these terms. A discussion of the variation of behavior with *m*, especially at the limits $m=6$ and $m=\infty$, is included.

Key words: Lennard-Jones gas; (*m*-6) intermolecular potential; quantum corrections; second virial coefficient; statistical mechanics; thermodynamics.

For the temperature range in which one is approaching classical behavior the second virial coefficient, B, for a Boltzmann gas may be represented by an asymptotic series in powers of $\hbar^2$. [1][1] That is, we can express B as a classical term, $B^{(0)}$, plus quantum correction terms,

$$B=B^{(0)}+qB^{(1)}+q^2B^{(2)}+\ldots \quad (1)$$

where $q=\hbar^2/2\mu$, ($\hbar$ is Planck's constant divided by 2π, μ is the reduced mass of the molecule), and the $B^{(p)}$ are the quantum corrections of order p. Kihara, Midzuno and Shizume [2] give expressions for these terms up through third order as integrals over functions of the intermolecular potential and its derivatives.

This expansion of B will not be applicable in cases where the intermolecular potential function or its derivatives contain discontinuities, as, for example, the hard sphere or square well cases. It has also been shown [3] that the exchange term of the second virial coefficient cannot be represented by such an expansion, so eq (1) will not be adequate for calculating B at temperatures so low that spin and statistical effects are important. In practice, however, these temperatures will usually be below the range in which eq (1) converges.

At very low temperatures the second virial coefficient may be accurately calculated by means of the phase shift formulation, and we can examine the range of validity of eq (1) by comparing results obtained by both methods. In the case of He^4, for example, it has been shown [3] that eq (1) with three quantum corrections gives results within 1 percent of the exact values down to almost 50 K, while two quantum corrections are sufficient to give this accuracy above 70 K. In general, results become much poorer as one approaches a temperature corresponding to the well depth, and eq (1) tends to become divergent below this temperature. For the more classical gases, such as the heavier rare gases, eq (1) should give useful values down to nearly their melting temperatures.

If we introduce the reduced quantities:

$$\begin{aligned} B^*&=B/(b_0)\\ U^*&=U/\epsilon\\ T^*&=kT/\epsilon\\ R&=r/\sigma\\ \Lambda^*&=h/\sigma\sqrt{2\mu\epsilon} \end{aligned} \quad (2)$$

where $b_0=2/3\ \pi N\sigma^3$ is the classical hard sphere second virial coefficient, U is the intermolecular potential, ϵ is the depth of the potential well, T is the temperature, k is Boltzmann's constant, and σ is the molecular diameter, we can write eq (1) as:

$$B^*=B^{*(0)}+\Lambda^{*2}B^{*(1)}+\Lambda^{*4}B^{*(2)}+\ldots . \quad (3)$$

where the Kihara $B^{(p)}$'s become:

$$B^{*(0)}=-3\int_0^\infty (e^{-U^*/T^*}-1)R^2dR \quad (4)$$

$$B^{*(1)}=\frac{1}{16\pi^2T^{*3}}\int_0^\infty e^{-U^*/T^*}\ (U^{*\prime})^2R^2dR$$

[1] Figures in brackets indicate the literature references at the end of this paper.

$$B^{*(2)}=-\frac{1}{4(4\pi^2)^2T^{*4}}\int_0^\infty e^{-U^*/T^*}\left[\frac{(U^{*\prime\prime})^2}{10}+\frac{(U^{*\prime})^2}{4R^2}+\frac{(U^{*\prime})^3}{9T^*}-\frac{(U^{*\prime})^4}{72(T^*)^2}\right]R^2dR$$

$$B^{*(3)}=\frac{3}{2(4\pi^2)^3T^{*5}}\int_0^\infty e^{-U^*/T^*}\left[\frac{(U^{*\prime\prime\prime})^2}{840}+\frac{(U^{*\prime\prime})^2}{140R^2}+\frac{(U^{*\prime\prime})^3}{756T^*}+\frac{U^{*\prime}(U^{*\prime\prime})^2}{180T^*R}+\frac{(U^{*\prime})^3}{945T^*R^3}-\frac{(U^{*\prime})^2(U^{*\prime\prime})^2}{720(T^*)^2}-\frac{(U^{*\prime})^4}{6480(T^*)^2R^2}-\frac{(U^{*\prime})^5}{2160(T^*)^3R}+\frac{(U^{*\prime})^6}{25920(T^*)^4}\right]R^2dR.$$

For the case of the general Lennard-Jones $(m-6)$ potential in reduced variables,

$$U^*(r)=\frac{[R^{-m}-R^{-6}]}{C(m,6)} \tag{5}$$

where:

$$C(m,6)=\left(\frac{6}{m}\right)^{\frac{6}{m-6}}\left(1-\frac{6}{m}\right)$$

it has been shown [4] that when the part of the exponential containing the R^{-6} term is expanded in an infinite series, these expressions can be integrated term by term, giving power series. The resulting expressions for B through third order are given by Kihara et al. [2] and, when translated into reduced variables, are:

$$B^{*(p)}=\frac{(-)^{p+1}\cdot 3}{(2\pi)^{2p}}\sum_{t=0}^{\infty}T^{*[(\frac{6}{m}-1)t-p-\frac{p'}{m}]}\Gamma\left(\frac{6t-p'}{m}\right)\frac{1}{t!}\times\frac{m^{\left[t-1+\frac{p'}{m-6}\right]}\cdot J_t^{(p)}(6,m)}{(m-6)^{\left[(1-\frac{6}{m})t+\frac{p'}{m}\right]}\cdot 6^{\left[\frac{6}{m}t-\frac{p'}{m}+\frac{p'}{m-6}\right]}} \tag{6}$$

where $p'=3-2p$, and

$$J_t^{(0)}=1.$$

$$J_t^{(1)}=[(m-6)6t-(m-1)]/12.$$

$$J_t^{(2)}=[21(m-6)^2 6^2t^2+(6m^2+30m-42)(m-6)6t+6m^3-27m^2+30m+63]/4320.$$

$$J_t^{(3)}=[93(m-6)^3 6^3t^3+(82m^2+657m-741)(m-6)^2 6^2t^2+(24m^4+348m^3+93m^2-810m+2241)(m-6)6t+72m^5-126m^4-531m^3+1755m^2-405m-3645]/362880.$$

Since these corrections find wide applicability for Lennard-Jones $(m-6)$ type potentials, we have prepared numerical tables for a family of values of m(6, 9, 12, 15, 18, 24, 36) over a wide range of values of T^* for which eq (3) is useful. The first two temperature derivatives,

$$T^*\partial B^{(p)}/\partial T^* \quad \text{and} \quad (T^*)^2\frac{\partial^2 B^{(p)}}{\partial T^{*2}},$$

which are necessary for the calculation of thermodynamic quantities and sound velocities, are also given. They were obtained by differentiating eqs (4) with respect to T^* and numerically integrating the resulting expressions.

These tables were calculated by Simpson numerical integration of eqs (4) from a value of $R=R_s$ below which the exponential becomes negligibly small. The contribution to the classical term is then simply R_s^3 while this part of the integral gives a vanishingly small contribution to the quantum corrections and derivatives. The numerical integration is carried out from R_s to $R=10$, and the contributions from the large R region are obtained by expanding the exponential and integrating analytically a sufficient number of terms to give the desired numerical accuracy. The resulting values were tested for accuracy by decreasing the interval size used in the integration until no changes resulted. For the (6–6) and (9–6) the value 1/128 was sufficient, for (12–6) through (24–6), 1/256 was used, and for the (36–6), 1/320 was required. Higher order integration procedures than Simpson were also tried and found to be unnecessary. The numbers given in the tables are believed to be correct to within 1 in the last digit given.

$B^{*(0)}$ and its temperature derivatives could be checked against previous calculations for several of the potentials. For the (9–6) Epstein and Hibbert [5] give values for a number of T^*'s ranging from 0.5 to 100 calculated by means of the series expansions (eq 6). Bird and Spotz [6] give results obtained in the same way for the (12–6) for T^*'s covering our complete range, and Michels [7] also gives (12–6) results at low T^* values (below 10), including the first two quantum corrections, obtained in terms of confluent hypergeometric functions. In all cases our results were in complete agreement to all figures available.

For the (18–6) Saxena and Joshi [8] calculated values for $B^{*(0)}$ and its first derivative from the series, but in terms of $T^*_{SJ}=(8/3\sqrt{3})T^*$, so comparisons are somewhat difficult. Interpolating in our tables for a few values over their range ($T^*_{SJ}=0.5$ to 400) indicates approximate agreement. Values of $B^{*(0)}$ for a large number of values of m have been given by Sze and Hsu [9] but the formula they evaluated is incorrect except for $m=12$. For this case results are also in agreement. Spot checks of values for the other potentials were made by comparison with values calculated by means of eqs (6).

The T^* intervals have been chosen such that four-point Lagrangian interpolation will suffice to give

values correct to within 5 in the sixth digit given throughout the table, with the exception of some T^*'s < 1, and some higher order correction terms which have very small values and are given to fewer digits. We have included only a few small values of T^* as eq (1) is convergent here only for very small values of T^*, i.e. nearly classical systems.

In considering the behavior of B^* with m, it is useful to refer to figure 1 which shows the reduced potential

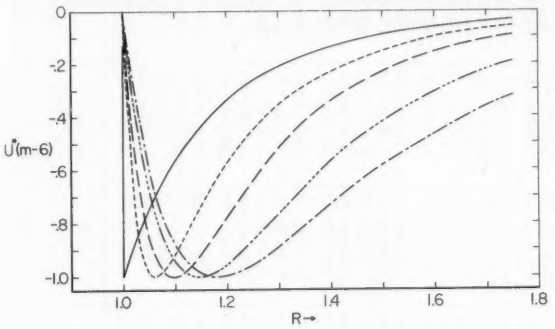

FIGURE 1. *Lennard-Jones* (m−6) *potential*, U*(m−6), *for various values of* m: —, m=∞; – – –, m=36; — — —, m=18; — — —, m=9; — – —, m=6.

function for selected values of m including the limiting cases $m=6$ and $m=\infty$. One notes that as m increases, the well becomes narrower and the strength of the well can thus be considered as weaker. As a consequence, the reduced Boyle temperature (where the repulsive effects cancel the attractive effects and B^* becomes zero) becomes lower as m increases. (It can also be noted from eq (4) that the first quantum correction is always positive and thus the more quantum mechanical the system, the more the Boyle temperature is lowered from the classical value.)

At higher T^*'s the repulsive effect, which predominates, is eventually dimmed somewhat by core penetration, as was pointed out by Lennard-Jones, and B^* passes through a maximum and then falls off as the system sees a smaller and smaller effective core size. This decrease is smaller the larger the m value, and the drop-off becomes less and less, until for $m=\infty$, no maximum occurs. The temperature at which the maximum occurs (T^*_{max}) is the result of a competition between the rise in B^* due to the loss of attractive effects from the declining strength of the well, and the drop in B^* due to decreasing effective core size. Thus T^*_{max} as a function of m passes through a minimum for m near 18.

Examination of the limiting cases is of interest to illustrate the caution which must be exercised in inferring the behavior of B in dimensioned units with m from that of B^*.

If we consider the most general Lennard-Jones potential in the usual dimensioned coordinates

$$U(r)=\lambda r^{-m}-\mu r^{-n} \tag{7}$$

it is apparent that a nonvanishing well appears at a finite r only if $m>n$. As $m\to n$, $U(r)$ becomes purely attractive or repulsive depending on the relative values of λ and μ, and it vanishes identically when they are equal. If we now change over into a representation in terms of (ϵ), the magnitude of the potential at the location where its derivative is zero, and (σ), the location of the zero of the potential, instead of λ and μ, we obtain

$$U(r)=\frac{\epsilon\left[\left(\frac{\sigma}{r}\right)^{-m}-\left(\frac{\sigma}{r}\right)^{-n}\right]}{C_{m,n}} \tag{8}$$

where

$$C_{m,n}=\left(\frac{n}{m}\right)^{\frac{n}{m-n}}\left(1-\frac{n}{m}\right). \tag{9}$$

In terms of reduced variables this becomes

$$U^*(R)=\frac{R^{-m}-R^{-n}}{C_{m,n}} \tag{10}$$

which, when $n=6$, becomes eq (5).

Now, however, because of the variables chosen, eq (10) will always contain a well at a finite R. If $m<n$, it is apparent from eq (9) that the coefficient changes sign and thus the larger exponent is always on the repulsive term. When $m\to n$, eq (10) approaches the limiting form

$$U^*(R)=-neR^{-n}\ln R \tag{11}$$

which has a zero at $R=1$ and a minimum at $R=e^{1/n}$.

For this limiting case it must be noted that the variables σ and ϵ are no longer appropriate quantities for parameterizing the potential function as, when $m\to n$, σ becomes infinite or indeterminate and ϵ is zero. Equation (11) cannot distinguish between the vanishing and purely attractive or repulsive limits of U having lost the information about λ and μ.

When $B^*(T^*)$ is calculated for the potential given by eq (11), it has the usual form, beginning at negative values for low T^* and becoming positive at higher T^*'s. Because of the loss of physical information in the potential function, however, these all correspond to $T=0$ and indeterminate B's. Thus these values, which we include in our tables, should be regarded as useful only as limiting values for interpolating with respect to m and one must keep in mind the peculiar nature of the limit.

When $m\to\infty$, eq (10) becomes

$$\begin{aligned} U^*(R)&=-R^{-n} && \text{for } R>1\\ &=\infty && R<1 \end{aligned} \tag{12}$$

which is the so-called Sutherland potential. The $B^{*(0)}$

has been calculated in this case by Sherwood and Prausnitz [10] over a range of T^* from 0.3 to 10, again by series expansion. The expressions for the quantum corrections given here blow up as the potential is no longer analytic and the expansion in eq (1) does not hold.

Interpolating with respect to m in these tables is more difficult for smaller m values since B^* changes more rapidly with m as $m \rightarrow 6$. For large m values it is necessary to use more widely spaced m values if one wishes to interpolate with equal intervals, but B is more slowly changing. Roughly, for low T^*'s, about 3 digits can be expected below $m = 9$ with 4 point Lagrange interpolation and for m between 9 and 18 with 3 point interpolation. At high T^*s (above the Boyle temperature) these same interpolation schemes would give about 4 digits.

A computer program giving the quantum corrections to B for the (12–6) potential was prepared and tested by S. Y. Larsen with the assistance of the author [3] and served as a starting point for the more generalized program used here. We also wish to thank M. Klein for use of a differencing program to examine the mesh size needed for interpolation as well as encouragement and support of these calculations.

(m = 6)

T^*	$B^{*(0)}$	$B^{*(1)}$	$B^{*(2)}$	$B^{*(3)}$	$T^*\frac{\partial B^{*(0)}}{\partial T^*}$	$T^*\frac{\partial B^{*(1)}}{\partial T^*}$	$T^*\frac{\partial B^{*(2)}}{\partial T^*}$	$T^*\frac{\partial B^{*(3)}}{\partial T^*}$	$T^{*2}\frac{\partial^2 B^{*(0)}}{\partial T^{*2}}$	$T^{*2}\frac{\partial^2 B^{*(1)}}{\partial T^{*2}}$	$T^{*2}\frac{\partial^2 B^{*(2)}}{\partial T^{*2}}$	$T^{*2}\frac{\partial^2 B^{*(3)}}{\partial T^{*2}}$
.300	−.5200306+02	.1808918+02	−.1083039+02	.8828317+01	.1352779+03	−.8837434+02	.7130301+02	−.7112935+02	−.6191167+03	.5804663+03	−.5788742+03	.6774773+03
.400	−.2687889+02	.5034017+01	−.1862926+01	.1004028+01	.5477869+02	−.2035962+02	.1060411+02	−.7124064+01	−.2058364+03	.1155539+03	−.7602279+02	.6063949+02
.500	−.1760689+02	.2166802+01	−.5573014+00	.2209051+00	.3122047+02	−.7644583+01	.2865666+01	−.1434309+01	−.1031736+03	.3914991+02	−.1884592+02	.1129137+02
.600	−.1292147+02	.1177066+01	−.2260761+00	.7031486−01	.2105902+02	−.3737462+01	.1077223+01	−.4271379+00	−.6373810+02	.1770730+02	−.6642625+01	.3171862+01
.700	−.1012043+02	.7362933+00	−.1108476+00	.2824571−01	.1563714+02	−.2148052+01	.4974850+00	−.1628252+00	−.4444770+02	.9566481+01	−.2916919+01	.1154970+01
.750	−.9106524+01	.6042573+00	−.8165069−01	.1906125−01	.1380438+02	−.1699538+01	.3572215+00	−.1074525+00	−.3827307+02	.7370382+01	−.2050108+01	.7474701+00
.775	−.8666709+01	.5514550+00	−.7079891−01	.1585957−01	.1303156+02	−.1524744+01	.3060960+00	−.8847997−01	−.3572874+02	.6530819+01	−.1739312+01	.6099395+00
.800	−.8264145+01	.5054719+00	−.6176610−01	.1329683−01	.1233613+02	−.1374918+01	.2640395+00	−.7345038−01	−.3347101+02	.5819563+01	−.1486170+01	.5019725+00
.825	−.7894325+01	.4651899+00	−.5419135−01	.1122733−01	.1170740+02	−.1245653+01	.2291677+00	−.6143328−01	−.3145674+02	.5212764+01	−.1278253+01	.4163896+00
.850	−.7553437+01	.4297086+00	−.4779541−01	.9542392−02	.1113652+02	−.1133450+01	.2000394+00	−.5174168−01	−.2965070+02	.4691705+01	−.1106150+01	.3479376+00
.875	−.7238237+01	.3982969+00	−.4236016−01	.8160038−02	.1061608+02	−.1035509+01	.1755415+00	−.4386263−01	−.2802390+02	.4241563+01	−.9626580+00	.2927274+00
.900	−.6945946+01	.3703563+00	−.3771366−01	.7017830−02	.1013989+02	−.9495703+00	.1548062+00	−.3740904−01	−.2655229+02	.3850497+01	−.8422134+00	.2478486+00
.925	−.6674169+01	.3453938+00	−.3371925−01	.6067750−02	.9702672+01	−.8737942+00	.1371507+00	−.3208590−01	−.2521577+02	.3508969+01	−.7404765+00	.2111010+00
.950	−.6420834+01	.3230000+00	−.3026749−01	.5272539−02	.9299966+01	−.8066742+00	.1220335+00	−.2766636−01	−.2399746+02	.3209239+01	−.6540348+00	.1808051+00
.975	−.6184137+01	.3028332+00	−.2727002−01	.4603047−02	.8927939+01	−.7469674+00	.1090218+00	−.2397440−01	−.2288307+02	.2944984+01	−.5801825+00	.1556676+00
1.000	−.5962500+01	.2846063+00	−.2465508−01	.4036291−02	.8583300+01	−.6936423+00	.9776733−01	−.2087236−01	−.2186046+02	.2711000+01	−.5167584+00	.1346841+00
1.020	−.5795098+01	.2712573+00	−.2279874−01	.3644458−02	.8325379+01	−.6549932+00	.8983730−01	−.1874178−01	−.2110142+02	.2542688+01	−.4723474+00	.1203541+00
1.040	−.5635814+01	.2588869+00	−.2112430−01	.3298998−02	.8081874+01	−.6194981+00	.8273007−01	−.1687391−01	−.2038981+02	.2389113+01	−.4327570+00	.1078523+00
1.060	−.5484075+01	.2474010+00	−.1961014−01	.2993507−02	.7851634+01	−.5868289+00	.7634321−01	−.1523118−01	−.1972151+02	.2248657+01	−.3973644+00	.9690966−01
1.080	−.5339360+01	.2367164+00	−.1823766−01	.2722584−02	.7633628+01	−.5566980+00	.7058903−01	−.1378209−01	−.1909284+02	.2119912+01	−.3656390+00	.8730156−01
1.100	−.5201197+01	.2267594+00	−.1699075−01	.2481658−02	.7426925+01	−.5288532+00	.6539216−01	−.1250013−01	−.1850054+02	.2001650+01	−.3371275+00	.7883983−01
1.120	−.5069153+01	.2174648+00	−.1585543−01	.2266841−02	.7230685+01	−.5030723+00	.6068764−01	−.1136288−01	−.1794165+02	.1892796+01	−.3114410+00	.7136620−01
1.140	−.4942833+01	.2087743+00	−.1481955−01	.2074822−02	.7044150+01	−.4791588+00	.5641927−01	−.1035133−01	−.1741354+02	.1792405+01	−.2882448+00	.6474703−01
1.160	−.4821874+01	.2006359+00	−.1387250−01	.1902763−02	.6866628+01	−.4569390+00	.5253828−01	−.9449285−02	−.1691384+02	.1699646+01	−.2672500+00	.5886910−01
1.180	−.4705946+01	.1930031+00	−.1300499−01	.1748233−02	.6697495+01	−.4362583+00	.4900223−01	−.8642939−02	−.1644040+02	.1613785+01	−.2482063+00	.5363610−01
1.200	−.4594743+01	.1858343+00	−.1220887−01	.1609135−02	.6536179+01	−.4169796+00	.4577407−01	−.7920441−02	−.1599127+02	.1534173+01	−.2308962+00	.4896588−01
1.220	−.4487984+01	.1790919+00	−.1147695−01	.1483658−02	.6382159+01	−.3989800+00	.4282138−01	−.7271613−02	−.1556470+02	.1460232+01	−.2151304+00	.4478812−01
1.240	−.4385409+01	.1727423+00	−.1080290−01	.1370235−02	.6234960+01	−.3821499+00	.4011571−01	−.6687678−02	−.1515909+02	.1391449+01	−.2007434+00	.4104243−01
1.260	−.4286779+01	.1667549+00	−.1018114−01	.1267503−02	.6094145+01	−.3663909+00	.3763202−01	−.6161045−02	−.1477298+02	.1327367+01	−.1875901+00	.3767682−01
1.280	−.4191873+01	.1611021+00	−.9606678−02	.1174277−02	.5959314+01	−.3516148+00	.3534823−01	−.5685136−02	−.1440505+02	.1267577+01	−.1755433+00	.3464638−01
1.300	−.4100485+01	.1557590+00	−.9075118−02	.1089520−02	.5830098+01	−.3377420+00	.3324481−01	−.5254229−02	−.1405408+02	.1211711+01	−.1644908+00	.3191220−01
1.320	−.4012424+01	.1507028+00	−.8582525−02	.1012326−02	.5706160+01	−.3247007+00	.3130446−01	−.4863339−02	−.1371897+02	.1159442+01	−.1543338+00	.2944052−01
1.340	−.3927514+01	.1459130+00	−.8125394−02	.9418981−03	.5587186+01	−.3124262+00	.2951182−01	−.4508109−02	−.1339869+02	.1110474+01	−.1449846+00	.2720193−01
1.360	−.3845590+01	.1413707+00	−.7700587−02	.8775369−03	.5472888+01	−.3008598+00	.2785321−01	−.4184722−02	−.1309232+02	.1064539+01	−.1363658+00	.2517076−01
1.380	−.3766497+01	.1370587+00	−.7305295−02	.8186250−03	.5363000+01	−.2899481+00	.2631644−01	−.3889827−02	−.1279899+02	.1021398+01	−.1284084+00	.2332456−01
1.400	−.3690094+01	.1329614+00	−.6936996−02	.7646175−03	.5257273+01	−.2796430+00	.2489059−01	−.3620475−02	−.1251791+02	.9808317+00	−.1210511+00	.2164364−01
1.420	−.3616247+01	.1290643+00	−.6593418−02	.7150316−03	.5155479+01	−.2699002+00	.2356591−01	−.3374066−02	−.1224836+02	.9426436+00	−.1142391+00	.2011068−01
1.440	−.3544829+01	.1253544+00	−.6272520−02	.6694390−03	.5057405+01	−.2606797+00	.2233365−01	−.3148301−02	−.1198965+02	.9066544+00	−.1079234+00	.1871044−01
1.460	−.3475725+01	.1218194+00	−.5972455−02	.6274592−03	.4962853+01	−.2519448+00	.2118594−01	−.2941146−02	−.1174117+02	.8727012+00	−.1020602+00	.1742947−01
1.480	−.3408825+01	.1184482+00	−.5691555−02	.5887531−03	.4871639+01	−.2436620+00	.2011568−01	−.2750794−02	−.1150233+02	.8406358+00	−.9661029−01	.1625585−01
1.500	−.3344026+01	.1152306+00	−.5428309−02	.5530182−03	.4783590+01	−.2358005+00	.1911649−01	−.2575640−02	−.1127260+02	.8103229+00	−.9153826−01	.1517905−01
1.540	−.3220351+01	.1092191+00	−.4949424−02	.4894089−03	.4616359+01	−.2212316+00	.1730879−01	−.2265358−02	−.1083852+02	.7544709+00	−.8240377−01	.1327944−01
1.580	−.3103994+01	.1037173+00	−.4526267−02	.4347880−03	.4459999+01	−.2080389+00	.1572291−01	−.2000599−02	−.1043532+02	.7042768+00	−.7443770−01	.1166733−01
1.620	−.2994332+01	.9866765−01	−.4150927−02	.3876680−03	.4313493+01	−.1960539+00	.1432595−01	−.1773586−02	−.1005991+02	.6590101+00	−.6746083−01	.1029231−01
1.660	−.2890808+01	.9402029−01	−.3816804−02	.3468411−03	.4175946+01	−.1851327+00	.1309071−01	−.1578045−02	−.9709564+01	.6180529+00	−.6132563−01	.9113914−02
1.700	−.2792925+01	.8973227−01	−.3518361−02	.3113207−03	.4046565+01	−.1751523+00	.1199449−01	−.1408884−02	−.9381905+01	.5808802+00	−.5591000−01	.8099470−02
1.740	−.2700241+01	.8576623−01	−.3250930−02	.2802961−03	.3924651+01	−.1660069+00	.1101831−01	−.1261943−02	−.9074843+01	.5470433+00	−.5111227−01	.7222444−02
1.780	−.2612356+01	.8208963−01	−.3010560−02	.2530977−03	.3809579+01	−.1576051+00	.1014621−01	−.1133807−02	−.8786530+01	.5161575+00	−.4684744−01	.6461157−02
1.820	−.2528910+01	.7867397−01	−.2793888−02	.2291698−03	.3700793+01	−.1498676+00	.9364685−02	−.1021659−02	−.8515330+01	.4878915+00	−.4304401−01	.5797800−02
1.860	−.2449581+01	.7549423−01	−.2598041−02	.2080486−03	.3597794+01	−.1427254+00	.8662282−02	−.9231578−03	−.8259790+01	.4619586+00	−.3964164−01	.5217671−02

(m=6)

T^*	$B^{*(0)}$	$B^{*(1)}$	$B^{*(2)}$	$B^{*(3)}$	$T^*\frac{\partial B^{*(0)}}{\partial T^*}$	$T^*\frac{\partial B^{*(1)}}{\partial T^*}$	$T^*\frac{\partial B^{*(2)}}{\partial T^*}$	$T^*\frac{\partial B^{*(3)}}{\partial T^*}$	$T^{*2}\frac{\partial^2 B^{*(0)}}{\partial T^{*2}}$	$T^{*2}\frac{\partial^2 B^{*(1)}}{\partial T^{*2}}$	$T^{*2}\frac{\partial^2 B^{*(2)}}{\partial T^{*2}}$	$T^{*2}\frac{\partial^2 B^{*(3)}}{\partial T^{*2}}$
1.900	−.2374074+01	.7252835−01	−.2420556−02	.1893456−03	.3500135+01	−.1361184+00	.8029235−02	−.8363557−03	−.8018614+01	.4381099+00	−.3658912−01	.4708568−02
1.940	−.2302122+01	.6975682−01	−.2259312−02	.1727337−03	.3407415+01	−.1299935+00	.7457184−02	−.7596199−03	−.7790643+01	.4161286+00	−.3384287−01	.4260322−02
1.980	−.2233485+01	.6716236−01	−.2112476−02	.1579364−03	.3319268+01	−.1243045+00	.6938948−02	−.6915776−03	−.7574839+01	.3958250+00	−.3136559−01	.3864415−02
2.020	−.2167940+01	.6472958−01	−.1978457−02	.1447192−03	.3235368+01	−.1190102+00	.6468333−02	−.6310696−03	−.7370267+01	.3770329+00	−.2912529−01	.3513687−02
2.060	−.2105287+01	.6244477−01	−.1855874−02	.1328821−03	.3155416+01	−.1140744+00	.6039982−02	−.5771131−03	−.7176084+01	.3596058+00	−.2709440−01	.3202091−02
2.100	−.2045341+01	.6029564−01	−.1743519−02	.1222544−03	.3079140+01	−.1094648+00	.5649242−02	−.5288717−03	−.6991530+01	.3434147+00	−.2524910−01	.2924502−02
2.140	−.1987932+01	.5827121−01	−.1640335−02	.1126894−03	.3006294+01	−.1051530+00	.5292061−02	−.4856311−03	−.6815915+01	.3283450+00	−.2356872−01	.2676560−02
2.180	−.1932906+01	.5636157−01	−.1545395−02	.1040610−03	.2936652+01	−.1011132+00	.4964900−02	−.4467791−03	−.6648614+01	.3142953+00	−.2203529−01	.2454541−02
2.220	−.1880120+01	.5455781−01	−.1457882−02	.9626009−04	.2870009+01	−.9732256−01	.4664658−02	−.4117892−03	−.6489056+01	.3011752+00	−.2063312−01	.2255256−02
2.260	−.1829440+01	.5285190−01	−.1377074−02	.8919243−04	.2806176+01	−.9376065−01	.4388609−02	−.3802074−03	−.6336723+01	.2889041+00	−.1934848−01	.2075964−02
2.300	−.1780747+01	.5123654−01	−.1302333−02	.8277596−04	.2744978+01	−.9040900−01	.4134354−02	−.3516407−03	−.6191141+01	.2774100+00	−.1816934−01	.1914300−02
2.340	−.1733927+01	.4970514−01	−.1233092−02	.7693923−04	.2686258+01	−.8725102−01	.3899772−02	−.3257482−03	−.6051874+01	.2666282+00	−.1708507−01	.1768221−02
2.380	−.1688876+01	.4825170−01	−.1168849−02	.7161983−04	.2629868+01	−.8427171−01	.3682986−02	−.3022331−03	−.5918526+01	.2565005+00	−.1608634−01	.1635954−02
2.420	−.1645497+01	.4687074−01	−.1109153−02	.6676309−04	.2575672+01	−.8145752−01	.3482329−02	−.2808366−03	−.5790731+01	.2469748+00	−.1516487−01	.1515956−02
2.460	−.1603701+01	.4555730−01	−.1053604−02	.6232099−04	.2523545+01	−.7879616−01	.3296320−02	−.2613322−03	−.5668152+01	.2380038+00	−.1431333−01	.1406882−02
2.500	−.1563404+01	.4430682−01	−.1001843−02	.5825127−04	.2473371+01	−.7627649−01	.3123637−02	−.2435210−03	−.5550479+01	.2295449+00	−.1352520−01	.1307556−02
2.600	−.1468722+01	.4142955−01	−.8869730−03	.4947191−04	.2355795+01	−.7053275−01	.2742779−02	−.2053053−03	−.5275938+01	.2103930+00	−.1179575−01	.1095428−02
2.700	−.1381859+01	.3886439−01	−.7896308−03	.4232295−04	.2248295+01	−.6547773−01	.2422803−02	−.1744211−03	−.5026414+01	.1936960+00	−.1035298−01	.9251034−03
2.800	−.1301902+01	.3656562−01	−.7065486−03	.3645015−04	.2149631+01	−.6100267−01	.2151922−02	−.1492313−03	−.4798660+01	.1790468+00	−.9139728−02	.7870350−03
2.900	−.1228075+01	.3449576−01	−.6351684−03	.3158642−04	.2058759+01	−.5701966−01	.1920992−02	−.1285114−03	−.4589966+01	.1661190+00	−.8111962−02	.6741272−03
3.000	−.1159714+01	.3262385−01	−.5734675−03	.2752812−04	.1974792+01	−.5345700−01	.1722845−02	−.1113344−03	−.4398048+01	.1546491+00	−.7235410−02	.5810440−03
3.100	−.1096245+01	.3092412−01	−.5198319−03	.2411828−04	.1896975+01	−.5025570−01	.1551807−02	−.9699097−04	−.4220973+01	.1444223+00	−.6483125−02	.5037266−03
3.200	−.1037175+01	.2937495−01	−.4729628−03	.2123478−04	.1824656+01	−.4736691−01	.1403348−02	−.8493295−04	−.4057093+01	.1352619+00	−.5833725−02	.4390558−03
3.300	−.9820703+00	.2795810−01	−.4318067−03	.1878168−04	.1757274+01	−.4474985−01	.1273819−02	−.7473253−04	−.3904992+01	.1270218+00	−.5270100−02	.3846114−03
3.400	−.9305557+00	.2665808−01	−.3955025−03	.1668303−04	.1694340+01	−.4237027−01	.1160261−02	−.6605298−04	−.3763449+01	.1195801+00	−.4778449−02	.3384982−03
3.500	−.8822999+00	.2546166−01	−.3633420−03	.1487818−04	.1635429+01	−.4019923−01	.1060256−02	−.5862710−04	−.3631407+01	.1128345+00	−.4347555−02	.2992199−03
3.600	−.8370113+00	.2435747−01	−.3347386−03	.1331835−04	.1580167+01	−.3821212−01	.9718142−03	−.5224121−04	−.3507943+01	.1066989+00	−.3968241−02	.2655858−03
3.700	−.7944319+00	.2333573−01	−.3092037−03	.1196405−04	.1528227+01	−.3638793−01	.8932885−03	−.4672320−04	−.3392251+01	.1011000+00	−.3632949−02	.2366413−03
3.800	−.7543325+00	.2238792−01	−.2863279−03	.1078309−04	.1479318+01	−.3470860−01	.8233075−03	−.4193353−04	−.3283621+01	.9597527−01	−.3335413−02	.2116158−03
3.900	−.7165088+00	.2150666−01	−.2657663−03	.9749061−05	.1433183+01	−.3315855−01	.7607223−03	−.3775831−04	−.3181429+01	.9127126−01	−.3070414−02	.1898830−03
4.000	−.6807783+00	.2068547−01	−.2472270−03	.8840179−05	.1389593+01	−.3172427−01	.7045662−03	−.3410405−04	−.3085119+01	.8694179−01	−.2833578−02	.1709313−03
4.100	−.6469775+00	.1991867−01	−.2304617−03	.8038378−05	.1348343+01	−.3039402−01	.6540211−03	−.3089359−04	−.2994199+01	.8294695−01	−.2621219−02	.1543396−03
4.200	−.6149590+00	.1920126−01	−.2152582−03	.7328593−05	.1309249+01	−.2915751−01	.6083918−03	−.2806287−04	−.2908230+01	.7925206−01	−.2430219−02	.1397599−03
4.300	−.5845903+00	.1852883−01	−.2014345−03	.6698203−05	.1272149+01	−.2800575−01	.5670847−03	−.2555843−04	−.2826819+01	.7582685−01	−.2257927−02	.1269031−03
4.400	−.5557513+00	.1789744−01	−.1888337−03	.6136582−05	.1236892+01	−.2693080−01	.5295910−03	−.2333550−04	−.2749614+01	.7264484−01	−.2102079−02	.1155277−03
4.500	−.5283334+00	.1730361−01	−.1773202−03	.5634747−05	.1203346+01	−.2592564−01	.4954726−03	−.2135635−04	−.2676297+01	.6968276−01	−.1960733−02	.1054308−03
4.600	−.5022379+00	.1674421−01	−.1667761−03	.5185069−05	.1171389+01	−.2498409−01	.4643510−03	−.1958909−04	−.2606584+01	.6692001−01	−.1832220−02	.9644166−04
4.700	−.4773749+00	.1621646−01	−.1570991−03	.4781047−05	.1140912+01	−.2410060−01	.4358982−03	−.1800662−04	−.2540214+01	.6433865−01	−.1715093−02	.8841569−04
4.800	−.4536624+00	.1571786−01	−.1481994−03	.4417116−05	.1111813+01	−.2327028−01	.4098284−03	−.1658585−04	−.2476953+01	.6192238−01	−.1608103−02	.8122998−04
4.900	−.4310254+00	.1524615−01	−.1399984−03	.4088494−05	.1084002+01	−.2248871−01	.3858925−03	−.1530702−04	−.2416588+01	.5965693−01	−.1510159−02	.7477969−04
5.000	−.4093955+00	.1479931−01	−.1324270−03	.3791065−05	.1057395+01	−.2175197−01	.3638719−03	−.1415316−04	−.2358925+01	.5752953−01	−.1420310−02	.6897503−04
5.100	−.3887095+00	.1437549−01	−.1254244−03	.3521265−05	.1031916+01	−.2105649−01	.3435751−03	−.1310962−04	−.2303787+01	.5552873−01	−.1337724−02	.6373887−04
5.200	−.3689097+00	.1397304−01	−.1189366−03	.3276003−05	.1007495+01	−.2039911−01	.3248329−03	−.1216378−04	−.2251012+01	.5364428−01	−.1261671−02	.5900470−04
5.300	−.3499427+00	.1359043−01	−.1129159−03	.3052591−05	.9840679+00	−.1977692−01	.3074961−03	−.1130465−04	−.2200451+01	.5186697−01	−.1191505−02	.5471497−04
5.400	−.3317593+00	.1322630−01	−.1073197−03	.2848682−05	.9615750+00	−.1918733−01	.2914326−03	−.1052269−04	−.2151967+01	.5018847−01	−.1126659−02	.5081978−04
5.500	−.3143142+00	.1287939−01	−.1021102−03	.2662222−05	.9399618+00	−.1862798−01	.2765249−03	−.9809570−05	−.2105436+01	.4860128−01	−.1066629−02	.4727568−04
5.600	−.2975654+00	.1254856−01	−.9725356−04	.2491408−05	.9191779+00	−.1809671−01	.2626687−03	−.9158011−05	−.2060742+01	.4709861−01	−.1010968−02	.4404476−04
5.800	−.2660038+00	.1193100−01	−.8848111−04	.2190563−05	.8799149+00	−.1711079−01	.2377474−03	−.8014773−05	−.1976446+01	.4432275−01	−.9112069−03	.3839386−04
6.000	−.2367954+00	.1136624−01	−.8079536−04	.1935557−05	.8434520+00	−.1621587−01	.2160343−03	−.7050463−05	−.1898320+01	.4181797−01	−.8246798−03	.3364719−04
6.200	−.2096988+00	.1084802−01	−.7402846−04	.1718080−05	.8095012+00	−.1540048−01	.1970181−03	−.6231898−05	−.1825711+01	.3954858−01	−.7492251−03	.2963388−04

(m=6)

T^*	$B^{*(0)}$	$B^{*(1)}$	$B^{*(2)}$	$B^{*(3)}$	$T^*\frac{\partial B^{*(0)}}{\partial T^*}$	$T^*\frac{\partial B^{*(1)}}{\partial T^*}$	$T^*\frac{\partial B^{*(2)}}{\partial T^*}$	$T^*\frac{\partial B^{*(3)}}{\partial T^*}$	$T^{*2}\frac{\partial^2 B^{*(0)}}{\partial T^{*2}}$	$T^{*2}\frac{\partial^2 B^{*(1)}}{\partial T^{*2}}$	$T^{*2}\frac{\partial^2 B^{*(2)}}{\partial T^{*2}}$	$T^{*2}\frac{\partial^2 B^{*(3)}}{\partial T^{*2}}$
6.400	−.1845043+00	.1037102−01	−.6804320−04	.1531549−05	.7778125+00	−.1465496−01	.1802833−03	−.5532934−05	−.1758055+01	.3748468−01	−.6830948−03	.2621991−04
6.600	−.1610284+00	.9930683−02	−.6272662−04	.1370708−05	.7481682+00	−.1397110−01	.1654899−03	−.4932799−05	−.1694861+01	.3560107−01	−.6248652−03	.2329925−04
6.800	−.1391105+00	.9523078−02	−.5798512−04	.1231329−05	.7203777+00	−.1334190−01	.1523576−03	−.4414860−05	−.1635704+01	.3387637−01	−.5733680−03	.2078734−04
7.000	−.1186090+00	.9144814−02	−.5374066−04	.1109983−05	.6942731+00	−.1276134−01	.1406541−03	−.3965698−05	−.1580209+01	.3229234−01	−.5276382−03	.1861623−04
7.200	−.9939856−01	.8792942−02	−.4992777−04	.1003876−05	.6697064+00	−.1222424−01	.1301852−03	−.3574415−05	−.1528046+01	.3083334−01	−.4868740−03	.1673090−04
7.400	−.8136819−01	.8464888−02	−.4649126−04	.9107121−06	.6465464+00	−.1172611−01	.1207883−03	−.3232099−05	−.1478924+01	.2948590−01	−.4504051−03	.1508656−04
7.600	−.6441900−01	.8158394−02	−.4338432−04	.8285945−06	.6246763+00	−.1126303−01	.1123261−03	−.2931420−05	−.1432586+01	.2823834−01	−.4176682−03	.1364648−04
7.800	−.4846267−01	.7871475−02	−.4056710−04	.7559488−06	.6039920+00	−.1083160−01	.1046820−03	−.2666312−05	−.1388800+01	.2708052−01	−.3881871−03	.1238037−04
8.000	−.3342010−01	.7602378−02	−.3800550−04	.6914603−06	.5844003+00	−.1042882−01	.9775682−04	−.2431731−05	−.1347363+01	.2600359−01	−.3615579−03	.1126311−04
8.200	−.1922021−01	.7349547−02	−.3567021−04	.6340256−06	.5658174+00	−.1005204−01	.9146574−04	−.2223458−05	−.1308091+01	.2499978−01	−.3374359−03	.1027377−04
8.400	−.5798995−02	.7111600−02	−.3353593−04	.5827144−06	.5481680+00	−.9698930−02	.8573574−04	−.2037950−05	−.1270818+01	.2406225−01	−.3155258−03	.9394820−05
8.600	.6901342−02	.6887305−02	−.3158076−04	.5367389−06	.5313840+00	−.9367422−02	.8050387−04	−.1872215−05	−.1235396+01	.2318498−01	−.2955737−03	.8611488−05
8.800	.1893313−01	.6675558−02	−.2978565−04	.4954288−06	.5154037+00	−.9055674−02	.7571558−04	−.1723718−05	−.1201690+01	.2236261−01	−.2773603−03	.7911298−05
9.000	.3034386−01	.6475371−02	−.2813397−04	.4582119−06	.5001714+00	−.8762044−02	.7132347−04	−.1590298−05	−.1169579+01	.2159040−01	−.2606955−03	.7283655−05
9.200	.4117670−01	.6285853−02	−.2661118−04	.4245975−06	.4856361+00	−.8485061−02	.6728617−04	−.1470111−05	−.1138953+01	.2086413−01	−.2454140−03	.6719527−05
9.400	.5147099−01	.6106201−02	−.2520449−04	.3941635−06	.4717516+00	−.8223407−02	.6356750−04	−.1361574−05	−.1109711+01	.2017999−01	−.2313714−03	.6211183−05
9.600	.6126268−01	.5935690−02	−.2390266−04	.3665453−06	.4584754+00	−.7975895−02	.6013566−04	−.1263324−05	−.1081762+01	.1953461−01	−.2184414−03	.5751986−05
9.800	.7058462−01	.5773664−02	−.2269572−04	.3414271−06	.4457689+00	−.7741455−02	.5696267−04	−.1174182−05	−.1055022+01	.1892494−01	−.2065131−03	.5336211−05
10.000	.7946694−01	.5619523−02	−.2157489−04	.3185343−06	.4335966+00	−.7519120−02	.5402382−04	−.1093128−05	−.1029414+01	.1834823−01	−.1954885−03	.4958910−05
10.200	.8793732−01	.5472726−02	−.2053231−04	.2976275−06	.4219258+00	−.7308013−02	.5129722−04	−.1019275−05	−.1004869+01	.1780200−01	−.1852815−03	.4615789−05
10.400	.9602119−01	.5332777−02	−.1956104−04	.2784975−06	.4107265+00	−.7107338−02	.4876343−04	−.9518475−06	−.9813206+00	.1728402−01	−.1758155−03	.4303110−05
10.600	.1037420+00	.5199222−02	−.1865484−04	.2609607−06	.3999710+00	−.6916372−02	.4640516−04	−.8901691−06	−.9587108+00	.1679224−01	−.1670225−03	.4017612−05
10.800	.1111214+00	.5071649−02	−.1780815−04	.2448558−06	.3896338+00	−.6734453−02	.4420697−04	−.8336454−06	−.9369843+00	.1632482−01	−.1588421−03	.3756440−05
11.000	.1181793+00	.4949677−02	−.1701597−04	.2300405−06	.3796912+00	−.6560981−02	.4215506−04	−.7817542−06	−.9160906+00	.1588008−01	−.1512203−03	.3517086−05
11.400	.1314034+00	.4721167−02	−.1557765−04	.2037900−06	.3609039+00	−.6237209−02	.3844185−04	−.6900798−06	−.8766177+00	.1505260−01	−.1374645−03	.3095274−05
11.800	.1435468+00	.4511220−02	−.1430904−04	.1813648−06	.3434522+00	−.5941168−02	.3518075−04	−.6120612−06	−.8399571+00	.1429902−01	−.1254254−03	.2737446−05
12.200	.1547237+00	.4317728−02	−.1318492−04	.1620963−06	.3272005+00	−.5669567−02	.3230287−04	−.5452673−06	−.8058197+00	.1361027−01	−.1148359−03	.2432036−05
12.600	.1650333+00	.4138888−02	−.1218455−04	.1454508−06	.3120307+00	−.5419605−02	.2975172−04	−.4877649−06	−.7739549+00	.1297866−01	−.1054782−03	.2169876−05
13.000	.1745621+00	.3973145−02	−.1129071−04	.1309988−06	.2978399+00	−.5188888−02	.2748074−04	−.4380047−06	−.7441439+00	.1239765−01	−.9717307−04	.1943647−05
13.400	.1833855+00	.3819155−02	−.1048906−04	.1183923−06	.2845376+00	−.4975352−02	.2545122−04	−.3947356−06	−.7161954+00	.1186164−01	−.8977231−04	.1747452−05
13.800	.1915701+00	.3675746−02	−.9767556−05	.1073470−06	.2720443+00	−.4777213−02	.2363083−04	−.3569399−06	−.6899411+00	.1136580−01	−.8315240−04	.1576514−05
14.200	.1991745+00	.3541896−02	−.9116045−05	.9762963−07	.2602897+00	−.4592923−02	.2199239−04	−.3237846−06	−.6652322+00	.1090596−01	−.7720988−04	.1426930−05
14.600	.2062506+00	.3416710−02	−.8525904−05	.8904721−07	.2492111+00	−.4421128−02	.2051295−04	−.2945834−06	−.6419371+00	.1047848−01	−.7185761−04	.1295496−05
15.000	.2128444+00	.3299396−02	−.7989787−05	.8143938−07	.2387529+00	−.4260644−02	.1917300−04	−.2687677−06	−.6199385+00	.1008021−01	−.6702178−04	.1179563−05
16.000	.2274778+00	.3036164−02	−.6846694−05	.6585596−07	.2150082+00	−.3902363−02	.1632991−04	−.2161164−06	−.5699546+00	.9194853−02	−.5680152−04	.9439779−06
17.000	.2398747+00	.2809030−02	−.5927342−05	.5400281−07	.1941961+00	−.3595291−02	.1405849−04	−.1763054−06	−.5260883+00	.8440350−02	−.4867999−04	.7667350−06
18.000	.2504438+00	.2611230−02	−.5177675−05	.4482980−07	.1758151+00	−.3329494−02	.1221758−04	−.1456636−06	−.4872894+00	.7790610−02	−.4213011−04	.6309396−06
19.000	.2595033+00	.2437568−02	−.4558886−05	.3762172−07	.1594715+00	−.3097413−02	.1070660−04	−.1217064−06	−.4527348+00	.7225927−02	−.3677845−04	.5252171−06
20.000	.2673046+00	.2283993−02	−.4042570−05	.3188027−07	.1448520+00	−.2893199−02	.9452408−05	−.1027125−06	−.4217703+00	.6731155−02	−.3235491−04	.4417262−06
21.000	.2740483+00	.2147298−02	−.3607563−05	.2725110−07	.1317041+00	−.2712261−02	.8400837−05	−.8746456−07	−.3938698+00	.6294480−02	−.2866049−04	.3749459−06
22.000	.2798964+00	.2024916−02	−.3237851−05	.2347769−07	.1198219+00	−.2550950−02	.7511148−05	−.7508569−07	−.3686046+00	.5906562−02	−.2554617−04	.3209156−06
23.000	.2849810+00	.1914770−02	−.2921145−05	.2037124−07	.1090363+00	−.2406327−02	.6752241−05	−.6493346−07	−.3456229+00	.5559926−02	−.2289870−04	.2767454−06
24.000	.2894107+00	.1815158−02	−.2647895−05	.1779075−07	.9920649−01	−.2276006−02	.6100064−05	−.5653018−07	−.3246322+00	.5248521−02	−.2063084−04	.2402941−06
25.000	.2932755+00	.1724678−02	−.2410589−05	.1562948−07	.9021490−01	−.2158026−02	.5535797−05	−.4951574−07	−.3053881+00	.4967407−02	−.1867458−04	.2099532−06
26.000	.2966508+00	.1642161−02	−.2203259−05	.1380565−07	.8196224−01	−.2050763−02	.5044550−05	−.4361525−07	−.2876847+00	.4712508−02	−.1697631−04	.1844988−06
27.000	.2995996+00	.1566628−02	−.2021117−05	.1225589−07	.7436420−01	−.1952863−02	.4614427−05	−.3861647−07	−.2713468+00	.4480435−02	−.1549335−04	.1629887−06
28.000	.3021756+00	.1497251−02	−.1860288−05	.1093056−07	.6734873−01	−.1863187−02	.4235834−05	−.3435379−07	−.2562249+00	.4268350−02	−.1419139−04	.1446901−06
29.000	.3044242+00	.1433327−02	−.1717605−05	.9790434−08	.6085389−01	−.1780770−02	.3900973−05	−.3069674−07	−.2421907+00	.4073857−02	−.1304259−04	.1290270−06
30.000	.3063844+00	.1374253−02	−.1590469−05	.8804238−08	.5482615−01	−.1704791−02	.3603450−05	−.2754160−07	−.2291329+00	.3894924−02	−.1202425−04	.1155429−06
32.000	.3095688+00	.1268660−02	−.1374568−05	.7197794−08	.4399182−01	−.1569424−02	.3100205−05	−.2242037−07	−.2055732+00	.3577032−02	−.1030725−04	.9372164−07

(m=6)

T^*	$B^{*(0)}$	$B^{*(1)}$	$B^{*(2)}$	$B^{*(3)}$	$T^*\frac{\partial B^{*(0)}}{\partial T^*}$	$T^*\frac{\partial B^{*(1)}}{\partial T^*}$	$T^*\frac{\partial B^{*(2)}}{\partial T^*}$	$T^*\frac{\partial B^{*(3)}}{\partial T^*}$	$T^{*2}\frac{\partial^2 B^{*(0)}}{\partial T^{*2}}$	$T^{*2}\frac{\partial^2 B^{*(1)}}{\partial T^{*2}}$	$T^{*2}\frac{\partial^2 B^{*(2)}}{\partial T^{*2}}$	$T^{*2}\frac{\partial^2 B^{*(3)}}{\partial T^{*2}}$
34.000	.3119458+00	.1177106−02	−.1199243−05	.5961402−08	.3453935−01	−.1452532−02	.2693583−05	−.1849664−07	−.1849099+00	.3303476−02	−.8925483−05	.7706617−07
36.000	.3136799+00	.1097030−02	−.1055014−05	.4994208−08	.2623158−01	−.1350668−02	.2360614−05	−.1543994−07	−.1666508+00	.3065836−02	−.7798169−05	.6413628−07
38.000	.3148973+00	.1026451−02	−.9350005−06	.4226632−08	.1888212−01	−.1261182−02	.2084720−05	−.1302342−07	−.1504087+00	.2857666−02	−.6867264−05	.5394714−07
40.000	.3156964+00	.9638141−03	−.8341128−06	.3609619−08	.1234250−01	−.1182007−02	.1853704−05	−.1108781−07	−.1358749+00	.2673954−02	−.6090235−05	.4581006−07
42.000	.3161544+00	.9078822−03	−.7485251−06	.3107905−08	.6493054−02	−.1111502−02	.1658437−05	−.9519107−08	−.1228005+00	.2510747−02	−.5435370−05	.3923371−07
44.000	.3163330+00	.8576589−03	−.6753167−06	.2695698−08	.1236256−02	−.1048353−02	.1491981−05	−.8234256−08	−.1109823+00	.2364887−02	−.4878656−05	.3386129−07
46.000	.3162816+00	.8123336−03	−.6122284−06	.2353841−08	−.3508120−02	−.9914972−03	.1348995−05	−.7171774−08	−.1002529+00	.2233824−02	−.4401653−05	.2942945−07
48.000	.3160400+00	.7712405−03	−.5574913−06	.2067895−08	−.7806670−02	−.9400620−03	.1225306−05	−.6285491−08	−.9047336−01	.2115477−02	−.3990022−05	.2574101−07
50.000	.3156408+00	.7338276−03	−.5097043−06	.1826846−08	−.1171511−01	−.8933278−03	.1117628−05	−.5540283−08	−.8152709−01	.2008132−02	−.3632482−05	.2264635−07
52.000	.3151108+00	.6996338−03	−.4677472−06	.1622184−08	−.1528042−01	−.8506952−03	.1023338−05	−.4909106−08	−.7331577−01	.1910366−02	−.3320064−05	.2003056−07
54.000	.3144721+00	.6682708−03	−.4307152−06	.1447269−08	−.1854244−01	−.8116610−03	.9403266−06	−.4370911−08	−.6575581−01	.1820986−02	−.3045570−05	.1780441−07
56.000	.3137428+00	.6394098−03	−.3978719−06	.1296865−08	−.2153522−01	−.7758001−03	.8668803−06	−.3909145−08	−.5877573−01	.1738988−02	−.2803171−05	.1589789−07
58.000	.3129385+00	.6127701−03	−.3686127−06	.1166807−08	−.2428797−01	−.7427507−03	.8015977−06	−.3510675−08	−.5231406−01	.1663518−02	−.2588106−05	.1425555−07
60.000	.3120717+00	.5881113−03	−.3424379−06	.1053752−08	−.2682593−01	−.7122034−03	.7433231−06	−.3164986−08	−.4631761−01	.1593849−02	−.2396461−05	.1283312−07
64.000	.3101925+00	.5439334−03	−.2977447−06	.8683421−09	−.3134227−01	−.6575860−03	.6441181−06	−.2599605−08	−.3554142−01	.1469496−02	−.2070990−05	.1051200−07
68.000	.3081729+00	.5055219−03	−.2612010−06	.7244138−09	−.3522822−01	−.6102153−03	.5633085−06	−.2162237−08	−.2614254−01	.1361870−02	−.1806671−05	.8721627−08
72.000	.3060618+00	.4718416−03	−.2309494−06	.6109358−09	−.3859492−01	−.5687723−03	.4966448−06	−.1818502−08	−.1788498−01	.1267891−02	−.1589224−05	.7318280−08
76.000	.3038947+00	.4420887−03	−.2056312−06	.5202255−09	−.4152947−01	−.5322359−03	.4410308−06	−.1544542−08	−.1058316−01	.1185181−02	−.1408284−05	.6202548−08
80.000	.3016977+00	.4156292−03	−.1842342−06	.4468196−09	−.4410100−01	−.4998042−03	.3941696−06	−.1323450−08	−.4089166−02	.1111878−02	−.1256182−05	.5304182−08
84.000	.2994900+00	.3919576−03	−.1659922−06	.3867592−09	−.4636508−01	−.4708387−03	.3543284−06	−.1143016−08	.1716279−02	.1046503−02	−.1127150−05	.4572573−08
88.000	.2972860+00	.3706651−03	−.1503168−06	.3371277−09	−.4836682−01	−.4448252−03	.3201811−06	−.9942670−09	.6930414−02	.9878690−03	−.1016785−05	.3970640−08
92.000	.2950960+00	.3514185−03	−.1367503−06	.2957433−09	−.5014319−01	−.4213452−03	.2906990−06	−.8705127−09	.1163327−01	.9350100−03	−.9216824−06	.3470782−08
96.000	.2929279+00	.3339433−03	−.1249321−06	.2609514−09	−.5172478−01	−.4000548−03	.2650747−06	−.7666915−09	.1589129−01	.8871344−03	−.8391733−06	.3052169−08
100.000	.2907872+00	.3180113−03	−.1145755−06	.2314817−09	−.5313707−01	−.3806687−03	.2426673−06	−.6789267−09	.1976009−01	.8435871−03	−.7671455−06	.2698881−08
105.000	.2881561+00	.2999784−03	−.1033381−06	.2006471−09	−.5469665−01	−.3587547−03	.2184091−06	−.5872889−09	.2411948−01	.7944153−03	−.6893079−06	.2330644−08
110.000	.2855794+00	.2837516−03	−.9367027−07	.1751277−09	−.5605959−01	−.3390620−03	.1975883−06	−.5116139−09	.2801980−01	.7502777−03	−.6226255−06	.2027105−08
115.000	.2830605+00	.2690786−03	−.8529370−07	.1538184−09	−.5725427−01	−.3212772−03	.1795883−06	−.4485535−09	.3152384−01	.7104578−03	−.5650785−06	.1774598−08
120.000	.2806011+00	.2557516−03	−.7798900−07	.1358795−09	−.5830410−01	−.3051423−03	.1639242−06	−.3955705−09	.3468366−01	.6743672−03	−.5150823−06	.1562785−08
125.000	.2782019+00	.2435976−03	−.7158136−07	.1206657−09	−.5922856−01	−.2904434−03	.1502106−06	−.3507179−09	.3754282−01	.6415184−03	−.4713800−06	.1383747−08
130.000	.2758627+00	.2324719−03	−.6593011−07	.1076747−09	−.6004394−01	−.2770017−03	.1381383−06	−.3124850−09	.4013799−01	.6115043−03	−.4329644−06	.1231351−08
135.000	.2735829+00	.2222523−03	−.6092106−07	.9651189−10	−.6076399−01	−.2646663−03	.1274566−06	−.2796865−09	.4250025−01	.5839823−03	−.3990212−06	.1100796−08
140.000	.2713613+00	.2128351−03	−.5646071−07	.8686428−10	−.6140039−01	−.2533094−03	.1179607−06	−.2513840−09	.4465614−01	.5586620−03	−.3688863−06	.9882823−09
145.000	.2691966+00	.2041315−03	−.5247196−07	.7848122−10	−.6196307−01	−.2428218−03	.1094824−06	−.2268277−09	.4662842−01	.5352962−03	−.3420139−06	.8907810−09
150.000	.2670874+00	.1960652−03	−.4889075−07	.7116048−10	−.6246058−01	−.2331098−03	.1018817−06	−.2054136−09	.4843672−01	.5136726−03	−.3179523−06	.8058547−09
160.000	.2630288+00	.1815898−03	−.4274522−07	.5907787−10	−.6328851−01	−.2157000−03	.8886582−07	−.1701394−09	.5162724−01	.4749447−03	−.2768157−06	.6661891−09
170.000	.2591718+00	.1689780−03	−.3768859−07	.4962276−10	−.6393204−01	−.2005516−03	.7818433−07	−.1426044−09	.5433944−01	.4412849−03	−.2431273−06	.5573891−09
180.000	.2555029+00	.1578990−03	−.3347844−07	.4211281−10	−.6442764−01	−.1872605−03	.6931243−07	−.1207840−09	.5665936−01	.4117818−03	−.2151998−06	.4713325−09
190.000	.2520089+00	.1480954−03	−.2993614−07	.3606863−10	−.6480342−01	−.1755124−03	.6186455−07	−.1032596−09	.5865428−01	.3857274−03	−.1917964−06	.4023394−09
200.000	.2486775+00	.1393637−03	−.2692774−07	.3114655−10	−.6508140−01	−.1650592−03	.5555234−07	−.8901654−10	.6037746−01	.3625643−03	−.1719941−06	.3463550−09
210.000	.2454971+00	.1315409−03	−.2435124−07	.2709564−10	−.6527897−01	−.1557028−03	.5015677−07	−.7731587−10	.6187160−01	.3418475−03	−.1550932−06	.3004346−09
220.000	.2424570+00	.1244953−03	−.2212784−07	.2372976−10	−.6541005−01	−.1472831−03	.4550904−07	−.6761047−10	.6317127−01	.3232179−03	−.1405556−06	.2623984−09
240.000	.2367598+00	.1123232−03	−.1850666−07	.1852568−10	−.6551550−01	−.1327537−03	.3795785−07	−.5263930−10	.6529529−01	.2911000−03	−.1169817−06	.2038359−09
260.000	.2315169+00	.1021886−03	−.1570785−07	.1476119−10	−.6546489−01	−.1206729−03	.3213912−07	−.4184059−10	.6692203−01	.2644252−03	−.9885953−07	.1616954−09
280.000	.2266707+00	.9362896−04	−.1350011−07	.1196725−10	−.6530381−01	−.1104819−03	.2756160−07	−.3384674−10	.6817207−01	.2419457−03	−.8463337−07	.1305664−09
300.000	.2221730+00	.8631089−04	−.1172805−07	.9847703−11	−.6506393−01	−.1017784−03	.2389636−07	−.2779646−10	.6913190−01	.2227640−03	−.7326421−07	.1070515−09

(m = 9)

T^*	$B^{*(0)}$	$B^{*(1)}$	$B^{*(2)}$	$B^{*(3)}$	$T^*\frac{\partial B^{*(0)}}{\partial T^*}$	$T^*\frac{\partial B^{*(1)}}{\partial T^*}$	$T^*\frac{\partial B^{*(2)}}{\partial T^*}$	$T^*\frac{\partial B^{*(3)}}{\partial T^*}$	$T^{*2}\frac{\partial^2 B^{*(0)}}{\partial T^{*2}}$	$T^{*2}\frac{\partial^2 B^{*(1)}}{\partial T^{*2}}$	$T^{*2}\frac{\partial^2 B^{*(2)}}{\partial T^{*2}}$	$T^{*2}\frac{\partial^2 B^{*(3)}}{\partial T^{*2}}$
.300	−.3502381+02	.2173459+02	−.2094497+02	.2703724+02	.9503545+02	−.1058401+03	.1375759+03	−.2176730+03	−.4415330+03	.6941081+03	−.1115171+04	.2072022+04
.400	−.1752750+02	.6080189+01	−.3619714+01	.3080385+01	.3768635+02	−.2446648+02	.2054056+02	−.2183749+02	−.1444092+03	.1385325+03	−.1469586+03	.1857509+03
.500	−.1119594+02	.2629996+01	−.1087318+01	.6786947+00	.2113078+02	−.9217033+01	.5570008+01	−.4402419+01	−.7133920+02	.4705443+02	−.3654083+02	.3463112+02
.600	−.8043546+01	.1435070+01	−.4426982+00	.2162764+00	.1407498+02	−.4520301+01	.2100225+01	−.1312468+01	−.4353453+02	.2133467+02	−.1291431+02	.9738379+01
.700	−.6180303+01	.9012830+00	−.2177729+00	.8696065−01	.1034877+02	−.2605507+01	.9726156+00	−.5007705+00	−.3005074+02	.1155307+02	−.5684819+01	.3549172+01
.750	−.5510663+01	.7410238+00	−.1606564+00	.5870844−01	.9097973+01	−.2064286+01	.6992919+00	−.3306050+00	−.2576154+02	.8910852+01	−.4000044+01	.2297850+01
.775	−.5221074+01	.6768685+00	−.1394067+00	.4885674−01	.8572180+01	−.1853204+01	.5995830+00	−.2722832+00	−.2399915+02	.7900117+01	−.3395514+01	.1875409+01
.800	−.4956506+01	.6209620+00	−.1217079+00	.4096961−01	.8099945+01	−.1672184+01	.5175181+00	−.2260737+00	−.2243806+02	.7043512+01	−.2902899+01	.1543717+01
.825	−.4713890+01	.5719555+00	−.1068571+00	.3459934−01	.7673790+01	−.1515932+01	.4494376+00	−.1891197+00	−.2104774+02	.6312424+01	−.2498106+01	.1280748+01
.850	−.4490634+01	.5287624+00	−.9430993−01	.2941188−01	.7287528+01	−.1380240+01	.3925416+00	−.1593119+00	−.1980327+02	.5684399+01	−.2162888+01	.1070382+01
.875	−.4284535+01	.4904999+00	−.8364122−01	.2515529−01	.6936001+01	−.1261742+01	.3446667+00	−.1350748+00	−.1868415+02	.5141642+01	−.1883277+01	.9006827+00
.900	−.4093710+01	.4564450+00	−.7451555−01	.2163759−01	.6614883+01	−.1157717+01	.3041250+00	−.1152194+00	−.1767342+02	.4669939+01	−.1648474+01	.7627180+00
.925	−.3916541+01	.4260019+00	−.6666622−01	.1871114−01	.6320518+01	−.1065953+01	.2695885+00	−.9883952−01	−.1675691+02	.4257836+01	−.1450057+01	.6497326+00
.950	−.3751627+01	.3986757+00	−.5987949−01	.1626133−01	.6049800+01	−.9846362+00	.2400035+00	−.8523804−01	−.1592273+02	.3896037+01	−.1281399+01	.5565701+00
.975	−.3597753+01	.3740531+00	−.5398283−01	.1419853−01	.5800072+01	−.9122690+00	.2145274+00	−.7387408−01	−.1516085+02	.3576943+01	−.1137247+01	.4792590+00
1.000	−.3453857+01	.3517866+00	−.4883598−01	.1245203−01	.5569055+01	−.8476090+00	.1924818+00	−.6432458−01	−.1446271+02	.3294301+01	−.1013399+01	.4147148+00
1.020	−.3345296+01	.3354710+00	−.4518053−01	.1124441−01	.5396381+01	−.8007269+00	.1769421+00	−.5776484−01	−.1394518+02	.3090924+01	−.9266466+00	.3706307+00
1.040	−.3242100+01	.3203451+00	−.4188191−01	.1017959−01	.5233529+01	−.7576564+00	.1630098+00	−.5201334−01	−.1346052+02	.2905302+01	−.8492869+00	.3321671+00
1.060	−.3143885+01	.3062947+00	−.3889786−01	.9237879−02	.5079708+01	−.7180019+00	.1504853+00	−.4695456−01	−.1300584+02	.2735490+01	−.7801082+00	.2984968+00
1.080	−.3050302+01	.2932191+00	−.3619195−01	.8402640−02	.4934205+01	−.6814168+00	.1391977+00	−.4249164−01	−.1257858+02	.2579794+01	−.7180786+00	.2689299+00
1.100	−.2961036+01	.2810290+00	−.3373263−01	.7659801−02	.4796381+01	−.6475966+00	.1289999+00	−.3854303−01	−.1217645+02	.2436736+01	−.6623160+00	.2428881+00
1.120	−.2875797+01	.2696452+00	−.3149255−01	.6997402−02	.4665657+01	−.6162733+00	.1197652+00	−.3503980−01	−.1179739+02	.2305024+01	−.6120636+00	.2198850+00
1.140	−.2794321+01	.2589971+00	−.2944789−01	.6405242−02	.4541511+01	−.5872099+00	.1113838+00	−.3192348−01	−.1143956+02	.2183520+01	−.5666699+00	.1995100+00
1.160	−.2716368+01	.2490215+00	−.2757787−01	.5874590−02	.4423470+01	−.5601966+00	.1037607+00	−.2914428−01	−.1110131+02	.2071223+01	−.5255723+00	.1814149+00
1.180	−.2641717+01	.2396622+00	−.2586426−01	.5397954−02	.4311104+01	−.5350470+00	.9681286−01	−.2665968−01	−.1078113+02	.1967251+01	−.4882833+00	.1653037+00
1.200	−.2570164+01	.2308684+00	−.2429108−01	.4968877−02	.4204022+01	−.5115951+00	.9046799−01	−.2443325−01	−.1047768+02	.1870821+01	−.4543793+00	.1509239+00
1.220	−.2501523+01	.2225946+00	−.2284426−01	.4581786−02	.4101868+01	−.4896928+00	.8466274−01	−.2243365−01	−.1018973+02	.1781237+01	−.4234912+00	.1380593+00
1.240	−.2435622+01	.2147999+00	−.2151137−01	.4231850−02	.4004316+01	−.4692076+00	.7934150−01	−.2063389−01	−.9916178+01	.1697881+01	−.3952966+00	.1265241+00
1.260	−.2372301+01	.2074471+00	−.2028141−01	.3914874−02	.3911068+01	−.4500207+00	.7445534−01	−.1901060−01	−.9656004+01	.1620203+01	−.3695127+00	.1161586+00
1.280	−.2311414+01	.2005029+00	−.1914465−01	.3627203−02	.3821850+01	−.4320252+00	.6996109−01	−.1754354−01	−.9408290+01	.1547709+01	−.3458914+00	.1068245+00
1.300	−.2252824+01	.1939367+00	−.1809241−01	.3365644−02	.3736412+01	−.4151252+00	.6582055−01	−.1621511−01	−.9172195+01	.1479958+01	−.3242140+00	.9840225−01
1.320	−.2196407+01	.1877210+00	−.1711697−01	.3127405−02	.3654522+01	−.3992337+00	.6199990−01	−.1500994−01	−.8946951+01	.1416553+01	−.3042876+00	.9078798−01
1.340	−.2142044+01	.1818307+00	−.1621145−01	.2910032−02	.3575967+01	−.3842725+00	.5846906−01	−.1391462−01	−.8731853+01	.1357137+01	−.2859413+00	.8389122−01
1.360	−.2089627+01	.1762429+00	−.1536968−01	.2711369−02	.3500552+01	−.3701704+00	.5520127−01	−.1291742−01	−.8526255+01	.1301390+01	−.2690238+00	.7763301−01
1.380	−.2039054+01	.1709367+00	−.1458614−01	.2529513−02	.3428094+01	−.3568632+00	.5217265−01	−.1200800−01	−.8329563+01	.1249019+01	−.2534005+00	.7194427−01
1.400	−.1990231+01	.1658930+00	−.1385587−01	.2362785−02	.3358426+01	−.3442922+00	.4936185−01	−.1117730−01	−.8141229+01	.1199764+01	−.2389517+00	.6676440−01
1.420	−.1943071+01	.1610942+00	−.1317439−01	.2209696−02	.3291393+01	−.3324042+00	.4674977−01	−.1041730−01	−.7960750+01	.1153385+01	−.2255704+00	.6204016−01
1.440	−.1897489+01	.1565243+00	−.1253770−01	.2068926−02	.3226849+01	−.3211505+00	.4431924−01	−.9720916−02	−.7787661+01	.1109667+01	−.2131610+00	.5772462−01
1.460	−.1853411+01	.1521687+00	−.1194215−01	.1939302−02	.3164660+01	−.3104868+00	.4205485−01	−.9081893−02	−.7621530+01	.1068413+01	−.2016379+00	.5377637−01
1.480	−.1810763+01	.1480135+00	−.1138447−01	.1819778−02	.3104703+01	−.3003725+00	.3994271−01	−.8494664−02	−.7461960+01	.1029444+01	−.1909244+00	.5015877−01
1.500	−.1769478+01	.1440465+00	−.1086168−01	.1709423−02	.3046859+01	−.2907703+00	.3797030−01	−.7954282−02	−.7308581+01	.9925968+00	−.1809513+00	.4683935−01
1.540	−.1690748+01	.1366313+00	−.9910205−02	.1512968−02	.2937089+01	−.2729688+00	.3440047−01	−.6996915−02	−.7019050+01	.9246828+00	−.1629839+00	.4098290−01
1.580	−.1616757+01	.1298410+00	−.9068955−02	.1344252−02	.2834565+01	−.2568412+00	.3126704−01	−.6179901−02	−.6750475+01	.8636224+00	−.1473073+00	.3601218−01
1.620	−.1547097+01	.1236050+00	−.8322331−02	.1198689−02	.2738601+01	−.2421830+00	.2850551−01	−.5479279−02	−.6500718+01	.8085330+00	−.1335711+00	.3177194−01
1.660	−.1481404+01	.1178625+00	−.7657314−02	.1072553−02	.2648593+01	−.2288197+00	.2606241−01	−.4875717−02	−.6267919+01	.7586676+00	−.1214865+00	.2813758−01
1.700	−.1419352+01	.1125612+00	−.7062977−02	.9627988−03	.2564009+01	−.2166021+00	.2389322−01	−.4353517−02	−.6050449+01	.7133914+00	−.1108145+00	.2500851−01
1.740	−.1360653+01	.1076553+00	−.6530108−02	.8669264−03	.2484377+01	−.2054017+00	.2196063−01	−.3899861−02	−.5846876+01	.6721619+00	−.1013559+00	.2230299−01
1.780	−.1305046+01	.1031051+00	−.6050899−02	.7828696−03	.2409280+01	−.1951075+00	.2023327−01	−.3504220−02	−.5655940+01	.6345136+00	−.9294435−01	.1995425−01
1.820	−.1252297+01	.9887558−01	−.5618706−02	.7089129−03	.2338342+01	−.1856232+00	.1868459−01	−.3157904−02	−.5476525+01	.6000455+00	−.8543963−01	.1790742−01
1.860	−.1202195+01	.9493623−01	−.5227849−02	.6436253−03	.2271232+01	−.1768650+00	.1729206−01	−.2853702−02	−.5307641+01	.5684104+00	−.7872345−01	.1611720−01

(m = 9)

T^*	$B^{*(0)}$	$B^{*(1)}$	$B^{*(2)}$	$B^{*(3)}$	$T^*\frac{\partial B^{*(0)}}{\partial T^*}$	$T^*\frac{\partial B^{*(1)}}{\partial T^*}$	$T^*\frac{\partial B^{*(2)}}{\partial T^*}$	$T^*\frac{\partial B^{*(3)}}{\partial T^*}$	$T^{*2}\frac{\partial^2 B^{*(0)}}{\partial T^{*2}}$	$T^{*2}\frac{\partial^2 B^{*(1)}}{\partial T^{*2}}$	$T^{*2}\frac{\partial^2 B^{*(2)}}{\partial T^{*2}}$	$T^{*2}\frac{\partial^2 B^{*(3)}}{\partial T^{*2}}$
1.900	−.1154549+01	.9126003−01	−.4873457−02	.5858073−03	.2207650+01	−.1687597+00	.1603647−01	−.2585603−02	−.5148404+01	.5393071+00	−.7269541−01	.1454600−01
1.940	−.1109186+01	.8782307−01	−.4551332−02	.5344493−03	.2147326+01	−.1612430+00	.1490135−01	−.2348573−02	−.4998029+01	.5124729+00	−.6726998−01	.1316248−01
1.980	−.1065949+01	.8460418−01	−.4257844−02	.4886976−03	.2090018+01	−.1542583+00	.1387257−01	−.2138376−02	−.4855807+01	.4876781+00	−.6237398−01	.1194038−01
2.020	−.1024695+01	.8158449−01	−.3989847−02	.4478280−03	.2035508+01	−.1477559+00	.1293792−01	−.1951437−02	−.4721107+01	.4647209+00	−.5794460−01	.1085764−01
2.060	−.9852936+00	.7874716−01	−.3744600−02	.4112232−03	.1983595+01	−.1416914+00	.1208685−01	−.1784725−02	−.4593356+01	.4434241+00	−.5392771−01	.9895622−02
2.100	−.9476245+00	.7607716−01	−.3519710−02	.3783557−03	.1934100+01	−.1360258+00	.1131019−01	−.1635658−02	−.4472040+01	.4236308+00	−.5027651−01	.9038515−02
2.140	−.9115787+00	.7356097−01	−.3313082−02	.3487728−03	.1886859+01	−.1307241+00	.1059994−01	−.1502033−02	−.4356692+01	.4052025+00	−.4695039−01	.8272880−02
2.180	−.8770556+00	.7118644−01	−.3122876−02	.3220845−03	.1841722+01	−.1257551+00	.9949117−02	−.1381960−02	−.4246890+01	.3880158+00	−.4391401−01	.7587237−02
2.220	−.8439630+00	.6894264−01	−.2947470−02	.2979544−03	.1798553+01	−.1210910+00	.9351609−02	−.1273814−02	−.4142248+01	.3719612+00	−.4113654−01	.6971750−02
2.260	−.8122157+00	.6681967−01	−.2785432−02	.2760909−03	.1757225+01	−.1167068+00	.8802033−02	−.1176195−02	−.4042416+01	.3569407+00	−.3859097−01	.6417966−02
2.300	−.7817352+00	.6480858−01	−.2635496−02	.2562405−03	.1717624+01	−.1125801+00	.8295650−02	−.1087889−02	−.3947076+01	.3428669+00	−.3625359−01	.5918502−02
2.340	−.7524490+00	.6290126−01	−.2496535−02	.2381826−03	.1679645+01	−.1086904+00	.7828271−02	−.1007844−02	−.3855934+01	.3296611+00	−.3410356−01	.5467325−02
2.380	−.7242899+00	.6109033−01	−.2367548−02	.2217243−03	.1643190+01	−.1050197+00	.7396187−02	−.9351434−03	−.3768723+01	.3172530+00	−.3212244−01	.5058692−02
2.420	−.6971957+00	.5936905−01	−.2247642−02	.2066966−03	.1608170+01	−.1015513+00	.6996102−02	−.8689883−03	−.3685198+01	.3055788+00	−.3029397−01	.4687938−02
2.460	−.6711087+00	.5773131−01	−.2136020−02	.1929511−03	.1574501+01	−.9827024−01	.6625088−02	−.8086792−03	−.3605131+01	.2945813+00	−.2860369−01	.4350912−02
2.500	−.6459752+00	.5617148−01	−.2031967−02	.1803572−03	.1542109+01	−.9516289−01	.6280529−02	−.7536023−03	−.3528316+01	.2842085+00	−.2703876−01	.4043985−02
2.600	−.5869934+00	.5258021−01	−.1800895−02	.1531869−03	.1466254+01	−.8807579−01	.5520133−02	−.6354168−03	−.3349278+01	.2607120+00	−.2360280−01	.3388410−02
2.700	−.5329750+00	.4937568−01	−.1604893−02	.1310598−03	.1396964+01	−.8183393−01	.4880739−02	−.5398908−03	−.3186778+01	.2402134+00	−.2073412−01	.2861946−02
2.800	−.4833354+00	.4650150−01	−.1437449−02	.1128806−03	.1333426+01	−.7630431−01	.4338998−02	−.4619674−03	−.3038644+01	.2222169+00	−.1831994−01	.2435118−02
2.900	−.4375776+00	.4391141−01	−.1293461−02	.9782353−04	.1274953+01	−.7137936−01	.3876783−02	−.3978630−03	−.2903069+01	.2063252+00	−.1627331−01	.2086022−02
3.000	−.3952766+00	.4156719−01	−.1168889−02	.8525875−04	.1220964+01	−.6697127−01	.3479872−02	−.3447136−03	−.2778531+01	.1922171+00	−.1452653−01	.1798182−02
3.100	−.3560670+00	.3943697−01	−.1060509−02	.7470081−04	.1170963+01	−.6300780−01	.3137001−02	−.3003271−03	−.2663745+01	.1796304+00	−.1302633−01	.1559064−02
3.200	−.3196326+00	.3749401−01	−.9657254−03	.6577187−04	.1124524+01	−.5942906−01	.2839171−02	−.2630090−03	−.2557615+01	.1683498+00	−.1173041−01	.1359034−02
3.300	−.2856988+00	.3571574−01	−.8824286−03	.5817521−04	.1081281+01	−.5618503−01	.2579131−02	−.2314368−03	−.2459204+01	.1581969+00	−.1060490−01	.1190615−02
3.400	−.2540257+00	.3408296−01	−.8088952−03	.5167577−04	.1040915+01	−.5323368−01	.2350994−02	−.2045695−03	−.2367704+01	.1490227+00	−.9622479−02	.1047953−02
3.500	−.2244029+00	.3257929−01	−.7437058−03	.4608589−04	.1003148+01	−.5053949−01	.2149947−02	−.1815810−03	−.2282414+01	.1407025+00	−.8760911−02	.9264238−03
3.600	−.1966450+00	.3119064−01	−.6856844−03	.4125465−04	.9677382+00	−.4807223−01	.1972027−02	−.1618103−03	−.2202726+01	.1331307+00	−.8002004−02	.8223479−03
3.700	−.1705883+00	.2990485−01	−.6338505−03	.3705980−04	.9344711+00	−.4580606−01	.1813953−02	−.1447254−03	−.2128109+01	.1262179+00	−.7330763−02	.7327748−03
3.800	−.1460874+00	.2871136−01	−.5873822−03	.3340169−04	.9031582+00	−.4371878−01	.1672990−02	−.1298945−03	−.2058093+01	.1198876+00	−.6734756−02	.6553227−03
3.900	−.1230129+00	.2760100−01	−.5455865−03	.3019860−04	.8736326+00	−.4179124−01	.1546846−02	−.1169653−03	−.1992269+01	.1140742+00	−.6203616−02	.5880561−03
4.000	−.1012493+00	.2656572−01	−.5078768−03	.2738308−04	.8457455+00	−.4000681−01	.1433591−02	−.1056487−03	−.1930271+01	.1087213+00	−.5728651−02	.5293925−03
4.100	−.8069299−01	.2559845−01	−.4737535−03	.2489920−04	.8193645+00	−.3835101−01	.1331592−02	−.9570586−04	−.1871777+01	.1037799+00	−.5302538−02	.4780304−03
4.200	−.6125092−01	.2469299−01	−.4427896−03	.2270031−04	.7943709+00	−.3681121−01	.1239459−02	−.8693858−04	−.1816499+01	.9920764−01	−.4919075−02	.4328937−03
4.300	−.4283928−01	.2384381−01	−.4146184−03	.2074735−04	.7706582+00	−.3537629−01	.1156007−02	−.7918151−04	−.1764178+01	.9496729−01	−.4572986−02	.3930881−03
4.400	−.2538237−01	.2304604−01	−.3889240−03	.1900740−04	.7481304+00	−.3403647−01	.1080216−02	−.7229601−04	−.1714584+01	.9102642−01	−.4259765−02	.3578664−03
4.500	−.8811610−02	.2229533−01	−.3654329−03	.1745265−04	.7267011+00	−.3278313−01	.1011211−02	−.6616535−04	−.1667510+01	.8735645−01	−.3975545−02	.3266017−03
4.600	.6935219−02	.2158779−01	−.3439076−03	.1605946−04	.7062918+00	−.3160859−01	.9482331−03	−.6069081−04	−.1622768+01	.8393221−01	−.3716997−02	.2987655−03
4.700	.2191473−01	.2091995−01	−.3241410−03	.1480772−04	.6868317+00	−.3050605−01	.8906257−03	−.5578854−04	−.1580191+01	.8073141−01	−.3481243−02	.2739106−03
4.800	.3617852−01	.2028868−01	−.3059522−03	.1368017−04	.6682560+00	−.2946943−01	.8378161−03	−.5138704−04	−.1539624+01	.7773427−01	−.3265786−02	.2516566−03
4.900	.4977375−01	.1969117−01	−.2891824−03	.1266202−04	.6505060+00	−.2849330−01	.7893046−03	−.4742512−04	−.1500928+01	.7492320−01	−.3068452−02	.2316792−03
5.000	.6274355−01	.1912488−01	−.2736920−03	.1174051−04	.6335278+00	−.2757279−01	.7446531−03	−.4385024−04	−.1463978+01	.7228247−01	−.2887345−02	.2137005−03
5.100	.7512749−01	.1858753−01	−.2593577−03	.1090459−04	.6172723+00	−.2670353−01	.7034767−03	−.4061710−04	−.1428658+01	.6979804−01	−.2720801−02	.1974819−03
5.200	.8696191−01	.1807702−01	−.2460705−03	.1014471−04	.6016943+00	−.2588156−01	.6654362−03	−.3768654−04	−.1394863+01	.6745727−01	−.2567360−02	.1828176−03
5.300	.9828027−01	.1759148−01	−.2337337−03	.9452523−05	.5867526+00	−.2510334−01	.6302319−03	−.3502460−04	−.1362495+01	.6524884−01	−.2425736−02	.1695294−03
5.400	.1091134+00	.1712918−01	−.2222612−03	.8820763−05	.5724088+00	−.2436562−01	.5975980−03	−.3260171−04	−.1331466+01	.6316251−01	−.2294792−02	.1574629−03
5.500	.1194897+00	.1668855−01	−.2115763−03	.8243069−05	.5586281+00	−.2366548−01	.5672987−03	−.3039208−04	−.1301695+01	.6118904−01	−.2173521−02	.1464836−03
5.600	.1294356+00	.1626816−01	−.2016105−03	.7713854−05	.5453778+00	−.2300028−01	.5391239−03	−.2837316−04	−.1273108+01	.5932007−01	−.2061029−02	.1364742−03
5.800	.1481315+00	.1548295−01	−.1835972−03	.6781791−05	.5203512+00	−.2176517−01	.4884171−03	−.2483064−04	−.1219210+01	.5586596−01	−.1859287−02	.1189669−03
6.000	.1653758+00	.1476428−01	−.1678011−03	.5991767−05	.4971145+00	−.2064334−01	.4442007−03	−.2184248−04	−.1169280+01	.5274729−01	−.1684166−02	.1042601−03
6.200	.1813192+00	.1410432−01	−.1538815−03	.5318029−05	.4754830+00	−.1962057−01	.4054446−03	−.1930590−04	−.1122895+01	.4992007−01	−.1531335−02	.9182488−04

(m = 9)

T^*	$B^{*(0)}$	$B^{*(1)}$	$B^{*(2)}$	$B^{*(3)}$	$T^*\frac{\partial B^{*(0)}}{\partial T^*}$	$T^*\frac{\partial B^{*(1)}}{\partial T^*}$	$T^*\frac{\partial B^{*(2)}}{\partial T^*}$	$T^*\frac{\partial B^{*(3)}}{\partial T^*}$	$T^{*2}\frac{\partial^2 B^{*(0)}}{\partial T^{*2}}$	$T^{*2}\frac{\partial^2 B^{*(1)}}{\partial T^{*2}}$	$T^{*2}\frac{\partial^2 B^{*(2)}}{\partial T^{*2}}$	$T^{*2}\frac{\partial^2 B^{*(3)}}{\partial T^{*2}}$
6.400	.1960928+00	.1349639−01	−.1415593−03	.4740182−05	.4552963+00	−.1868486−01	.3713111−03	−.1713991−04	−.1079691+01	.4734741−01	−.1397289−02	.8124626−04
6.600	.2098108+00	.1293475−01	−.1306050−03	.4241940−05	.4364149+00	−.1782604−01	.3411141−03	−.1528016−04	−.1039351+01	.4499820−01	−.1279171−02	.7219586−04
6.800	.2225734+00	.1241450−01	−.1208280−03	.3810198−05	.4187166+00	−.1703539−01	.3142880−03	−.1367512−04	−.1001600+01	.4284605−01	−.1174635−02	.6441180−04
7.000	.2344688+00	.1193135−01	−.1120691−03	.3434338−05	.4020940+00	−.1630546−01	.2903630−03	−.1228322−04	−.9661963+00	.4086841−01	−.1081742−02	.5768361−04
7.200	.2455746+00	.1148160−01	−.1041950−03	.3105694−05	.3864525+00	−.1562980−01	.2689469−03	−.1107067−04	−.9329271+00	.3904597−01	−.9988792−03	.5184092−04
7.400	.2559600+00	.1106202−01	−.9709314−04	.2817154−05	.3717080+00	−.1500282−01	.2497106−03	−.1000989−04	−.9016052+00	.3736206−01	−.9246991−03	.4674496−04
7.600	.2656862+00	.1066975−01	−.9066786−04	.2562841−05	.3577859+00	−.1441968−01	.2323760−03	−.9078135−05	−.8720645+00	.3580224−01	−.8580670−03	.4228193−04
7.800	.2748081+00	.1030230−01	−.8483778−04	.2337876−05	.3446198+00	−.1387610−01	.2167071−03	−.8256625−05	−.8441572+00	.3435396−01	−.7980244−03	.3835801−04
8.000	.2833745+00	.9957465−02	−.7953318−04	.2138184−05	.3321498+00	−.1336836−01	.2025030−03	−.7529725−05	−.8177515+00	.3300626−01	−.7437567−03	.3489538−04
8.200	.2914294+00	.9633271−02	−.7469411−04	.1960346−05	.3203228+00	−.1289318−01	.1895913−03	−.6884361−05	−.7927293+00	.3174950−01	−.6945690−03	.3182918−04
8.400	.2990125+00	.9327981−02	−.7026879−04	.1801480−05	.3090904+00	−.1244763−01	.1778241−03	−.6309551−05	−.7689848+00	.3057523−01	−.6498657−03	.2910508−04
8.600	.3061594+00	.9040037−02	−.6621237−04	.1659143−05	.2984093+00	−.1202915−01	.1670736−03	−.5796023−05	−.7464225+00	.2947597−01	−.6091340−03	.2667733−04
8.800	.3129022+00	.8768047−02	−.6248579−04	.1531259−05	.2882401+00	−.1163543−01	.1572288−03	−.5335917−05	−.7249563+00	.2844509−01	−.5719310−03	.2450726−04
9.000	.3192705+00	.8510759−02	−.5905499−04	.1416055−05	.2785472+00	−.1126443−01	.1481935−03	−.4922541−05	−.7045082+00	.2747670−01	−.5378727−03	.2256204−04
9.200	.3252906+00	.8267049−02	−.5589011−04	.1312011−05	.2692982+00	−.1091430−01	.1398836−03	−.4550177−05	−.6850075+00	.2656555−01	−.5066247−03	.2081368−04
9.400	.3309868+00	.8035903−02	−.5296490−04	.1217817−05	.2604635+00	−.1058342−01	.1322253−03	−.4213918−05	−.6663900+00	.2570694−01	−.4778951−03	.1923822−04
9.600	.3363811+00	.7816400−02	−.5025626−04	.1132346−05	.2520162+00	−.1027028−01	.1251540−03	−.3909539−05	−.6485969+00	.2489667−01	−.4514282−03	.1781509−04
9.800	.3414939+00	.7607710−02	−.4774375−04	.1054617−05	.2439314+00	−.9973562−02	.1186127−03	−.3633390−05	−.6315747+00	.2413094−01	−.4269993−03	.1652655−04
10.000	.3463434+00	.7409076−02	−.4540924−04	.9837797−06	.2361868+00	−.9692047−02	.1125510−03	−.3382306−05	−.6152746+00	.2340634−01	−.4044104−03	.1535727−04
10.200	.3509468+00	.7219809−02	−.4323665−04	.9190935−06	.2287613+00	−.9424642−02	.1069243−03	−.3153537−05	−.5996514+00	.2271981−01	−.3834863−03	.1429392−04
10.400	.3553194+00	.7039282−02	−.4121162−04	.8599096−06	.2216359+00	−.9170352−02	.1016930−03	−.2944682−05	−.5846640+00	.2206854−01	−.3640721−03	.1332494−04
10.600	.3594758+00	.6866921−02	−.3932134−04	.8056591−06	.2147930+00	−.8928270−02	.9682174−04	−.2753642−05	−.5702744+00	.2145001−01	−.3460299−03	.1244020−04
10.800	.3634291+00	.6702199−02	−.3755435−04	.7558424−06	.2082163+00	−.8697570−02	.9227902−04	−.2578576−05	−.5564475+00	.2086192−01	−.3292369−03	.1163087−04
11.000	.3671914+00	.6544634−02	−.3590035−04	.7100184−06	.2018908+00	−.8477498−02	.8803664−04	−.2417866−05	−.5431511+00	.2030216−01	−.3135837−03	.1088916−04
11.400	.3741877+00	.6249241−02	−.3289524−04	.6288359−06	.1899383+00	−.8066528−02	.8035436−04	−.2133965−05	−.5180322+00	.1926020−01	−.2853144−03	.9582102−05
11.800	.3805453+00	.5977598−02	−.3024235−04	.5594952−06	.1788357+00	−.7690488−02	.7360161−04	−.1892377−05	−.4947039+00	.1831069−01	−.2605519−03	.8473368−05
12.200	.3863337+00	.5727028−02	−.2788961−04	.4999257−06	.1684967+00	−.7345250−02	.6763738−04	−.1685569−05	−.4729817+00	.1744232−01	−.2387533−03	.7527102−05
12.600	.3916129+00	.5495234−02	−.2579414−04	.4484744−06	.1588462+00	−.7027304−02	.6234602−04	−.1507547−05	−.4527058+00	.1664552−01	−.2194749−03	.6714893−05
13.000	.3964354+00	.5280237−02	−.2392034−04	.4038112−06	.1498185+00	−.6733642−02	.5763203−04	−.1353512−05	−.4337367+00	.1591212−01	−.2023519−03	.6014044−05
13.400	.4008467+00	.5080324−02	−.2223851−04	.3648581−06	.1413563+00	−.6461674−02	.5341607−04	−.1219585−05	−.4159524+00	.1523514−01	−.1870820−03	.5406285−05
13.800	.4048871+00	.4894002−02	−.2072370−04	.3307354−06	.1334089+00	−.6209158−02	.4963176−04	−.1102613−05	−.3992458+00	.1460855−01	−.1734134−03	.4876800−05
14.200	.4085916+00	.4719966−02	−.1935486−04	.3007204−06	.1259315+00	−.5974147−02	.4622327−04	−.1000014−05	−.3835222+00	.1402714−01	−.1611348−03	.4413495−05
14.600	.4119916+00	.4557072−02	−.1811408−04	.2742158−06	.1188843+00	−.5754939−02	.4314341−04	−.9096612−06	−.3686976+00	.1348636−01	−.1500682−03	.4006436−05
15.000	.4151145+00	.4404311−02	−.1698614−04	.2507252−06	.1122319+00	−.5550042−02	.4035205−04	−.8297932−06	−.3546975+00	.1298226−01	−.1400628−03	.3647412−05
16.000	.4218646+00	.4061126−02	−.1457849−04	.2026234−06	.9712897−01	−.5092165−02	.3442288−04	−.6669358−06	−.3228845+00	.1186070−01	−.1188938−03	.2917949−05
17.000	.4273473+00	.3764500−02	−.1263913−04	.1660524−06	.8389259−01	−.4699195−02	.2967863−04	−.5438330−06	−.2949610+00	.1090375−01	−.1020463−03	.2369251−05
18.000	.4318049+00	.3505767−02	−.1105545−04	.1377634−06	.7220388−01	−.4358605−02	.2582806−04	−.4491127−06	−.2702592+00	.1007873−01	−.8843972−04	.1948958−05
19.000	.4354250+00	.3278261−02	−.9746496−05	.1155442−06	.6181245−01	−.4060848−02	.2266332−04	−.3750791−06	−.2482558+00	.9360928−02	−.7730733−04	.1621816−05
20.000	.4383549+00	.3076775−02	−.8652920−05	.9785371−07	.5251896−01	−.3798533−02	.2003305−04	−.3164022−06	−.2285350+00	.8731334−02	−.6809388−04	.1363527−05
21.000	.4407116+00	.2897184−02	−.7730458−05	.8359677−07	.4416276−01	−.3565852−02	.1782506−04	−.2693126−06	−.2107623+00	.8175111−02	−.6038979−04	.1156983−05
22.000	.4425889+00	.2736183−02	−.6945573−05	.7198050−07	.3661294−01	−.3358181−02	.1595484−04	−.2310957−06	−.1946657+00	.7680513−02	−.5388796−04	.9899137−06
23.000	.4440629+00	.2591090−02	−.6272496−05	.6242160−07	.2976175−01	−.3171799−02	.1435780−04	−.1997630−06	−.1800212+00	.7238136−02	−.4835475−04	.8533665−06
24.000	.4451956+00	.2459712−02	−.5691178−05	.5448456−07	.2351971−01	−.3003675−02	.1298393−04	−.1738364−06	−.1666433+00	.6840365−02	−.4360998−04	.7407090−06
25.000	.4460383+00	.2340234−02	−.5185837−05	.4783981−07	.1781192−01	−.2851323−02	.1179408−04	−.1522017−06	−.1543767+00	.6480971−02	−.3951307−04	.6469596−06
26.000	.4466335+00	.2231146−02	−.4743922−05	.4223487−07	.1257518−01	−.2712678−02	.1075722−04	−.1340086−06	−.1430904+00	.6154816−02	−.3595307−04	.5683282−06
27.000	.4470164+00	.2131179−02	−.4355349−05	.3747415−07	.7755798−02	−.2586018−02	.9848544−05	−.1186005−06	−.1326732+00	.5857624−02	−.3284157−04	.5018979−06
28.000	.4472171+00	.2039261−02	−.4011950−05	.3340455−07	.3307896−02	−.2469893−02	.9048038−05	−.1054656−06	−.1230301+00	.5585813−02	−.3010742−04	.4453997−06
29.000	.4472604+00	.1954478−02	−.3707051−05	.2990508−07	−.8079828−03	−.2363075−02	.8339406−05	−.9420033−07	−.1140795+00	.5336355−02	−.2769290−04	.3970509−06
30.000	.4471679+00	.1876049−02	−.3435158−05	.2687930−07	−.4625947−02	−.2264517−02	.7709282−05	−.8448417−07	−.1057507+00	.5106681−02	−.2555082−04	.3554383−06
32.000	.4466452+00	.1735654−02	−.2972929−05	.2195337−07	−.1148291−01	−.2088712−02	.6642257−05	−.6872063−07	−.9072116−01	.4698202−02	−.2193499−04	.2881215−06

(m = 9)

T^*	$B^{*(0)}$	$B^{*(1)}$	$B^{*(2)}$	$B^{*(3)}$	$T^*\frac{\partial B^{*(0)}}{\partial T^*}$	$T^*\frac{\partial B^{*(1)}}{\partial T^*}$	$T^*\frac{\partial B^{*(2)}}{\partial T^*}$	$T^*\frac{\partial B^{*(3)}}{\partial T^*}$	$T^{*2}\frac{\partial^2 B^{*(0)}}{\partial T^{*2}}$	$T^{*2}\frac{\partial^2 B^{*(1)}}{\partial T^{*2}}$	$T^{*2}\frac{\partial^2 B^{*(2)}}{\partial T^{*2}}$	$T^{*2}\frac{\partial^2 B^{*(3)}}{\partial T^{*2}}$
34.000	.4457657+00	.1613697−02	−.2597044−05	.1816511−07	−.1745827−01	−.1936660−02	.5778850−05	−.5665040−07	−.7753734−01	.4346201−02	−.1902086−04	.2367660−06
36.000	.4446162+00	.1506841−02	−.2287423−05	.1520392−07	−.2270324−01	−.1803959−02	.5070880−05	−.4725301−07	−.6588615−01	.4040008−02	−.1664011−04	.1969174−06
38.000	.4432621+00	.1412498−02	−.2029469−05	.1285564−07	−.2733668−01	−.1687218−02	.4483521−05	−.3982810−07	−.5552127−01	.3771443−02	−.1467160−04	.1655306−06
40.000	.4417531+00	.1328638−02	−.1812376−05	.1096935−07	−.3145332−01	−.1583785−02	.3991117−05	−.3388427−07	−.4624632−01	.3534143−02	−.1302649−04	.1404770−06
42.000	.4401279+00	.1253638−02	−.1628006−05	.9436634−08	−.3512951−01	−.1491558−02	.3574441−05	−.2906988−07	−.3790277−01	.3323079−02	−.1163843−04	.1202384−06
44.000	.4384162+00	.1186194−02	−.1470143−05	.8178240−08	−.3842751−01	−.1408850−02	.3218868−05	−.2512884−07	−.3036129−01	.3134236−02	−.1045713−04	.1037125−06
46.000	.4366414+00	.1125240−02	−.1333970−05	.7135319−08	−.4139853−01	−.1334294−02	.2913118−05	−.2187167−07	−.2351528−01	.2964365−02	−.9443916−05	.9008619−07
48.000	.4348218+00	.1069903−02	−.1215715−05	.6263556−08	−.4408510−01	−.1266767−02	.2648380−05	−.1915613−07	−.1727615−01	.2810814−02	−.8568701−05	.7875075−07
50.000	.4329719+00	.1019456−02	−.1112385−05	.5529147−08	−.4652282−01	−.1205342−02	.2417698−05	−.1687406−07	−.1156961−01	.2671395−02	−.7807781−05	.6924438−07
52.000	.4311034+00	.9732907−03	−.1021585−05	.4906001−08	−.4874168−01	−.1149247−02	.2215522−05	−.1494219−07	−.6332967−02	.2544292−02	−.7142294−05	.6121259−07
54.000	.4292253+00	.9308957−03	−.9413803−06	.4373761−08	−.5076715−01	−.1097833−02	.2037379−05	−.1329577−07	−.1512904−02	.2427980−02	−.6557087−05	.5438019−07
56.000	.4273450+00	.8918364−03	−.8701936−06	.3916388−08	−.5262097−01	−.1050549−02	.1879637−05	−.1188388−07	.2936185−02	.2321175−02	−.6039879−05	.4853129−07
58.000	.4254684+00	.8557422−03	−.8067293−06	.3521125−08	−.5432183−01	−.1006930−02	.1739322−05	−.1066612−07	.7053544−02	.2222785−02	−.5580632−05	.4349500−07
60.000	.4236001+00	.8222947−03	−.7499156−06	.3177742−08	−.5588585−01	−.9665737−03	.1613976−05	−.9610189−08	.1087312−01	.2131877−02	−.5171084−05	.3913489−07
64.000	.4199024+00	.7622763−03	−.6528122−06	.2615072−08	−.5865756−01	−.8943189−03	.1400371−05	−.7884406−08	.1773326−01	.1969412−02	−.4474807−05	.3202441−07
68.000	.4162734+00	.7099855−03	−.5733165−06	.2178782−08	−.6102812−01	−.8315393−03	.1226145−05	−.6550633−08	.2371123−01	.1828572−02	−.3908580−05	.2654422−07
72.000	.4127259+00	.6640469−03	−.5074324−06	.1835172−08	−.6306859−01	−.7765225−03	.1082241−05	−.5503352−08	.2895790−01	.1705399−02	−.3442173−05	.2225211−07
76.000	.4092675+00	.6233904−03	−.4522332−06	.1560793−08	−.6483463−01	−.7279411−03	.9620516−06	−.4669401−08	.3359198−01	.1596836−02	−.3053605−05	.1884227−07
80.000	.4059020+00	.5871713−03	−.4055359−06	.1338983−08	−.6637042−01	−.6847511−03	.8606685−06	−.3996967−08	.3770814−01	.1500484−02	−.2726601−05	.1609878−07
84.000	.4026306+00	.5547140−03	−.3656866−06	.1157681−08	−.6771146−01	−.6461201−03	.7743855−06	−.3448648−08	.4138274−01	.1414438−02	−.2448902−05	.1386621−07
88.000	.3994529+00	.5254722−03	−.3314135−06	.1008005−08	−.6888657−01	−.6113771−03	.7003626−06	−.2996990−08	.4467809−01	.1337162−02	−.2211142−05	.1203065−07
92.000	.3963675+00	.4989997−03	−.3017261−06	.8833173−09	−.6991935−01	−.5799751−03	.6363947−06	−.2621525−08	.4764547−01	.1267410−02	−.2006066−05	.1050742−07
96.000	.3933721+00	.4749281−03	−.2758440−06	.7785887−09	−.7082934−01	−.5514640−03	.5807491−06	−.2306783−08	.5032748−01	.1204158−02	−.1827987−05	.9232682−08
100.000	.3904641+00	.4529512−03	−.2531455−06	.6899601−09	−.7163279−01	−.5254705−03	.5320495−06	−.2040919−08	.5275978−01	.1146558−02	−.1672397−05	.8157570−08
105.000	.3869474+00	.4280383−03	−.2284969−06	.5973168−09	−.7250787−01	−.4960473−03	.4792815−06	−.1763554−08	.5549440−01	.1081435−02	−.1504103−05	.7037772−08
110.000	.3835566+00	.4055839−03	−.2072730−06	.5207241−09	−.7325975−01	−.4695679−03	.4339491−06	−.1534712−08	.5793454−01	.1022901−02	−.1359789−05	.6115483−08
115.000	.3802854+00	.3852478−03	−.1888691−06	.4568329−09	−.7390651−01	−.4456203−03	.3947240−06	−.1344184−08	.6012049−01	.9700239−03	−.1235132−05	.5348842−08
120.000	.3771279+00	.3667492−03	−.1728080−06	.4031014−09	−.7446304−01	−.4238649−03	.3605612−06	−.1184243−08	.6208570−01	.9220387−03	−.1126738−05	.4706226−08
125.000	.3740783+00	.3498546−03	−.1587091−06	.3575761−09	−.7494171−01	−.4040201−03	.3306289−06	−.1048958−08	.6385815−01	.8783109−03	−.1031911−05	.4163476−08
130.000	.3711308+00	.3343678−03	−.1462661−06	.3187392−09	−.7535288−01	−.3858497−03	.3042591−06	−.9337335−09	.6546139−01	.8383098−03	−.9484893−06	.3701824−08
135.000	.3682801+00	.3201231−03	−.1352298−06	.2853987−09	−.7570526−01	−.3691545−03	.2809102−06	−.8349660−09	.6691542−01	.8015884−03	−.8747246−06	.3306606−08
140.000	.3655213+00	.3069797−03	−.1253964−06	.2566097−09	−.7600625−01	−.3537656−03	.2601395−06	−.7498053−09	.6823729−01	.7677678−03	−.8091890−06	.2966236−08
145.000	.3628496+00	.2948169−03	−.1165974−06	.2316161−09	−.7626213−01	−.3395384−03	.2415821−06	−.6759726−09	.6944161−01	.7365245−03	−.7507083−06	.2671498−08
150.000	.3602604+00	.2835311−03	−.1086930−06	.2098086−09	−.7647829−01	−.3263489−03	.2249355−06	−.6116351−09	.7054103−01	.7075809−03	−.6983099−06	.2414944−08
160.000	.3553134+00	.2632430−03	−.9511794−07	.1738603−09	−.7680940−01	−.3026678−03	.1964038−06	−.5057694−09	.7246746−01	.6556665−03	−.6086450−06	.1993414−08
170.000	.3506498+00	.2455273−03	−.8393691−07	.1457747−09	−.7702970−01	−.2820211−03	.1729632−06	−.4232484−09	.7408844−01	.6104601−03	−.5351286−06	.1665468−08
180.000	.3462427+00	.2299320−03	−.7461890−07	.1235017−09	−.7716206−01	−.2638710−03	.1534736−06	−.3579415−09	.7545928−01	.5707648−03	−.4741170−06	.1406389−08
190.000	.3420689+00	.2161044−03	−.6677221−07	.1056026−09	−.7722403−01	−.2477985−03	.1370966−06	−.3055616−09	.7662324−01	.5356494−03	−.4229367−06	.1198916−08
200.000	.3381074+00	.2037651−03	−.6010282−07	.9104730−10	−.7722932−01	−.2334728−03	.1232043−06	−.2630427−09	.7761453−01	.5043796−03	−.3795901−06	.1030772−08
210.000	.3343402+00	.1926902−03	−.5438659−07	.7908487−10	−.7718870−01	−.2206289−03	.1113193−06	−.2281560−09	.7846061−01	.4763684−03	−.3425614−06	.8929961−09
220.000	.3307511+00	.1826983−03	−.4945023−07	.6915869−10	−.7711073−01	−.2090523−03	.1010735−06	−.1992527−09	.7918366−01	.4511414−03	−.3106835−06	.7789927−09
240.000	.3240512+00	.1653943−03	−.4140280−07	.5384026−10	−.7686896−01	−.1890308−03	.8440909−07	−.1547421−09	.8033005−01	.4075580−03	−.2589310−06	.6037489−09
260.000	.3179107+00	.1509423−03	−.3517549−07	.4278647−10	−.7654483−01	−.1723363−03	.7155058−07	−.1227058−09	.8116433−01	.3712637−03	−.2190891−06	.4778814−09
280.000	.3122518+00	.1387016−03	−.3025799−07	.3460149−10	−.7616570−01	−.1582162−03	.6142260−07	−.9903975−10	.8176368−01	.3406011−03	−.1877718−06	.3850921−09
300.000	.3070109+00	.1282085−03	−.2630705−07	.2840582−10	−.7575026−01	−.1461274−03	.5330403−07	−.8116234−10	.8218336−01	.3143756−03	−.1627138−06	.3151118−09

(m = 12)

T^*	$B^{*(0)}$	$B^{*(1)}$	$B^{*(2)}$	$B^{*(3)}$	$T^*\frac{\partial B^{*(0)}}{\partial T^*}$	$T^*\frac{\partial B^{*(1)}}{\partial T^*}$	$T^*\frac{\partial B^{*(2)}}{\partial T^*}$	$T^*\frac{\partial B^{*(3)}}{\partial T^*}$	$T^{*2}\frac{\partial^2 B^{*(0)}}{\partial T^{*2}}$	$T^{*2}\frac{\partial^2 B^{*(1)}}{\partial T^{*2}}$	$T^{*2}\frac{\partial^2 B^{*(2)}}{\partial T^{*2}}$	$T^{*2}\frac{\partial^2 B^{*(3)}}{\partial T^{*2}}$
.300	−.2788058+02	.2495831+02	−.3392134+02	.6183245+02	.7660726+02	−.1211236+03	.2219993+03	−.4958473+03	−.3568768+03	.7929995+03	−.1795084+04	.4705947+04
.400	−.1379884+02	.7019887+01	−.5906112+01	.7112688+01	.3026708+02	−.2810116+02	.3335049+02	−.5017340+02	−.1163660+03	.1587144+03	−.2378388+03	.4252021+03
.500	−.8720205+01	.3051606+01	−.1785792+01	.1579906+01	.1692369+02	−.1062264+02	.9092938+01	−.1018874+02	−.5733952+02	.5405480+02	−.5941938+02	.7980465+02
.600	−.6197971+01	.1672560+01	−.7313444+00	.5070168+00	.1124885+02	−.5226202+01	.3445280+01	−.3056777+01	−.3491869+02	.2457106+02	−.2108967+02	.2257221+02
.700	−.4710037+01	.1054610+01	−.3616675+00	.2051313+00	.8257115+01	−.3021161+01	.1602553+01	−.1172858+01	−.2406266+02	.1333733+02	−.9319556+01	.8269089+01
.750	−.4175928+01	.8686635+00	−.2674671+00	.1388823+00	.7254013+01	−.2396856+01	.1154577+01	−.7763107+00	−.2061311+02	.1029868+02	−.6569467+01	.5366455+01
.775	−.3945069+01	.7941485+00	−.2323654+00	.1157352+00	.6832553+01	−.2153180+01	.9909381+00	−.6401557+00	−.1919640+02	.9135545+01	−.5581520+01	.4384905+01
.800	−.3734225+01	.7291720+00	−.2031005+00	.9718115−01	.6454140+01	−.1944108+01	.8561437+00	−.5321575+00	−.1794190+02	.8149382+01	−.4775874+01	.3613422+01
.825	−.3540935+01	.6721787+00	−.1785209+00	.8217750−01	.6112751+01	−.1763553+01	.7442278+00	−.4456972+00	−.1682495+02	.7307384+01	−.4113379+01	.3001166+01
.850	−.3363119+01	.6219150+00	−.1577345+00	.6994541−01	.5803406+01	−.1606684+01	.6506231+00	−.3758826+00	−.1582546+02	.6583797+01	−.3564363+01	.2510901+01
.875	−.3199015+01	.5773619+00	−.1400435+00	.5989685−01	.5521956+01	−.1469627+01	.5717978+00	−.3190567+00	−.1492689+02	.5958211+01	−.3106099+01	.2115033+01
.900	−.3047114+01	.5376846+00	−.1248975+00	.5158333−01	.5264918+01	−.1349257+01	.5049953+00	−.2724570+00	−.1411557+02	.5414313+01	−.2721011+01	.1792892+01
.925	−.2906119+01	.5021948+00	−.1118581+00	.4465956−01	.5029352+01	−.1243026+01	.4480448+00	−.2339760+00	−.1338007+02	.4938958+01	−.2395379+01	.1528833+01
.950	−.2774910+01	.4703204+00	−.1005741+00	.3885733−01	.4812761+01	−.1148847+01	.3992229+00	−.2019913+00	−.1271081+02	.4521473+01	−.2118404+01	.1310906+01
.975	−.2652514+01	.4415835+00	−.9076144−01	.3396659−01	.4613008+01	−.1064998+01	.3571510+00	−.1752427+00	−.1209970+02	.4153131+01	−.1881518+01	.1129899+01
1.000	−.2538081+01	.4155824+00	−.8218929−01	.2982151−01	.4428262+01	−.9900469+00	.3207182+00	−.1527442+00	−.1153985+02	.3826750+01	−.1677869+01	.9786521+00
1.020	−.2451766+01	.3965210+00	−.7609649−01	.2695279−01	.4290198+01	−.9356827+00	.2950205+00	−.1372767+00	−.1112492+02	.3591823+01	−.1535138+01	.8752701+00
1.040	−.2369731+01	.3788421+00	−.7059485−01	.2442131−01	.4160009+01	−.8857221+00	.2719683+00	−.1237052+00	−.1073641+02	.3377346+01	−.1407796+01	.7850083+00
1.060	−.2291669+01	.3624134+00	−.6561464−01	.2218075−01	.4037058+01	−.8397090+00	.2512341+00	−.1117598+00	−.1037200+02	.3181082+01	−.1293865+01	.7059429+00
1.080	−.2217301+01	.3471184+00	−.6109571−01	.2019200−01	.3920774+01	−.7972439+00	.2325372+00	−.1012141+00	−.1002962+02	.3001083+01	−.1191659+01	.6364680+00
1.100	−.2146374+01	.3328534+00	−.5698601−01	.1842103−01	.3810642+01	−.7579757+00	.2156365+00	−.9187724−01	−.9707435+01	.2835651+01	−.1099735+01	.5752370+00
1.120	−.2078658+01	.3195268+00	−.5324035−01	.1684236−01	.3706199+01	−.7215953+00	.2003238+00	−.8358793−01	−.9403782+01	.2683297+01	−.1016856+01	.5211167+00
1.140	−.2013943+01	.3070564+00	−.4981935−01	.1542925−01	.3607024+01	−.6878293+00	.1864188+00	−.7620918−01	−.9117182+01	.2542714+01	−.9419546+00	.4731497+00
1.160	−.1952035+01	.2953694+00	−.4668863−01	.1416200−01	.3512739+01	−.6564356+00	.1737652+00	−.6962433−01	−.8846301+01	.2412751+01	−.8741108+00	.4305239+00
1.180	−.1892758+01	.2844001+00	−.4381805−01	.1302295−01	.3422999+01	−.6271992+00	.1622266+00	−.6373367−01	−.8589936+01	.2292390+01	−.8125261+00	.3925486+00
1.200	−.1835949+01	.2740898+00	−.4118116−01	.1199683−01	.3337489+01	−.5999282+00	.1516840+00	−.5845169−01	−.8347000+01	.2180731+01	−.7565068+00	.3586341+00
1.220	−.1781460+01	.2643858+00	−.3875463−01	.1107048−01	.3255924+01	−.5744519+00	.1420333+00	−.5370487−01	−.8116508+01	.2076974+01	−.7054479+00	.3282751+00
1.240	−.1729153+01	.2552403+00	−.3651788−01	.1023247−01	.3178042+01	−.5506170+00	.1331828+00	−.4942976−01	−.7897567+01	.1980406+01	−.6588208+00	.3010377+00
1.260	−.1678902+01	.2466103+00	−.3445269−01	.9472884−02	.3103605+01	−.5282863+00	.1250521+00	−.4557148−01	−.7689364+01	.1890393+01	−.6161620+00	.2765479+00
1.280	−.1630589+01	.2384569+00	−.3254290−01	.8783066−02	.3032393+01	−.5073365+00	.1175698+00	−.4208240−01	−.7491158+01	.1806367+01	−.5770641+00	.2544825+00
1.300	−.1584105+01	.2307448+00	−.3077412−01	.8155455−02	.2964204+01	−.4876565+00	.1106731+00	−.3892111−01	−.7302275+01	.1727819+01	−.5411685+00	.2345616+00
1.320	−.1539350+01	.2234419+00	−.2913354−01	.7583428−02	.2898854+01	−.4691459+00	.1043063+00	−.3605145−01	−.7122096+01	.1654292+01	−.5081584+00	.2165418+00
1.340	−.1496231+01	.2165190+00	−.2760972−01	.7061171−02	.2836173+01	−.4517142+00	.9841961−01	−.3344186−01	−.6950054+01	.1585375+01	−.4777532+00	.2002111+00
1.360	−.1454661+01	.2099494+00	−.2619242−01	.6583564−02	.2776002+01	−.4352793+00	.9296899−01	−.3106463−01	−.6785631+01	.1520697+01	−.4497044+00	.1853844+00
1.380	−.1414558+01	.2037089+00	−.2487244−01	.6146092−02	.2718196+01	−.4197665+00	.8791498−01	−.2889545−01	−.6628348+01	.1459924+01	−.4237907+00	.1718996+00
1.400	−.1375848+01	.1977752+00	−.2364155−01	.5744764−02	.2662621+01	−.4051083+00	.8322235−01	−.2691289−01	−.6477768+01	.1402752+01	−.3998153+00	.1596146+00
1.420	−.1338460+01	.1921279+00	−.2249231−01	.5376044−02	.2609152+01	−.3912428+00	.7885951−01	−.2509806−01	−.6333484+01	.1348907+01	−.3776023+00	.1484043+00
1.440	−.1302330+01	.1867483+00	−.2141804−01	.5036791−02	.2557673+01	−.3781139+00	.7479811−01	−.2343424−01	−.6195123+01	.1298140+01	−.3569946+00	.1381586+00
1.460	−.1267394+01	.1816192+00	−.2041267−01	.4724215−02	.2508077+01	−.3656702+00	.7101266−01	−.2190662−01	−.6062339+01	.1250223+01	−.3378512+00	.1287801+00
1.480	−.1233597+01	.1767249+00	−.1947075−01	.4435827−02	.2460264+01	−.3538646+00	.6748020−01	−.2050207−01	−.5934813+01	.1204950+01	−.3200458+00	.1201827+00
1.500	−.1200883+01	.1720507+00	−.1858731−01	.4169406−02	.2414140+01	−.3426541+00	.6418001−01	−.1920888−01	−.5812247+01	.1162133+01	−.3034645+00	.1122900+00
1.540	−.1138509+01	.1633099+00	−.1697829−01	.3694723−02	.2326621+01	−.3218635+00	.5820327−01	−.1691601−01	−.5580918+01	.1083191+01	−.2735749+00	.9835469−01
1.580	−.1079904+01	.1553010+00	−.1555428−01	.3286610−02	.2244890+01	−.3030191+00	.5295278−01	−.1495727−01	−.5366373+01	.1012186+01	−.2474766+00	.8651556−01
1.620	−.1024742+01	.1479417+00	−.1428923−01	.2934116−02	.2168400+01	−.2858836+00	.4832164−01	−.1327588−01	−.5166900+01	.9480973+00	−.2245916+00	.7640667−01
1.660	−.9727319+00	.1411613+00	−.1316140−01	.2628338−02	.2096665+01	−.2702550+00	.4422121−01	−.1182599−01	−.4981004+01	.8900628+00	−.2044437+00	.6773420−01
1.700	−.9236164+00	.1348984+00	−.1215251−01	.2361997−02	.2029262+01	−.2559599+00	.4057760−01	−.1057033−01	−.4807378+01	.8373483+00	−.1866381+00	.6026066−01
1.740	−.8771644+00	.1290996+00	−.1124715−01	.2129103−02	.1965812+01	−.2428494+00	.3732890−01	−.9478450−02	−.4644875+01	.7893267+00	−.1708462+00	.5379298−01
1.780	−.8331688+00	.1237184+00	−.1043223−01	.1924707−02	.1905982+01	−.2307946+00	.3442294−01	−.8525322−02	−.4492484+01	.7454595+00	−.1567925+00	.4817328−01
1.820	−.7914434+00	.1187141+00	−.9696623−02	.1744693−02	.1849471+01	−.2196837+00	.3181562−01	−.7690260−02	−.4349310+01	.7052827+00	−.1442454+00	.4327174−01
1.860	−.7518202+00	.1140508+00	−.9030805−02	.1585628−02	.1796014+01	−.2094193+00	.2946946−01	−.6956089−02	−.4214559+01	.6683947+00	−.1330092+00	.3898109−01

(m = 12)

T^*	$B^{*(0)}$	$B^{*(1)}$	$B^{*(2)}$	$B^{*(3)}$	$T^*\frac{\partial B^{*(0)}}{\partial T^*}$	$T^*\frac{\partial B^{*(1)}}{\partial T^*}$	$T^*\frac{\partial B^{*(2)}}{\partial T^*}$	$T^*\frac{\partial B^{*(3)}}{\partial T^*}$	$T^{*2}\frac{\partial^2 B^{*(0)}}{\partial T^{*2}}$	$T^{*2}\frac{\partial^2 B^{*(1)}}{\partial T^{*2}}$	$T^{*2}\frac{\partial^2 B^{*(2)}}{\partial T^{*2}}$	$T^{*2}\frac{\partial^2 B^{*(3)}}{\partial T^{*2}}$
1.900	−.7141474+00	.1096969+00	−.8426594−02	.1444628−02	.1745372+01	−.1999163+00	.2735246−01	−.6308482−02	−.4087525+01	.6344467+00	−.1229176+00	.3521224−01
1.940	−.6782872+00	.1056245+00	−.7876941−02	.1319265−02	.1697330+01	−.1911000+00	.2543722−01	−.5735427−02	−.3967576+01	.6031344+00	−.1138289+00	.3189088−01
1.980	−.6441147+00	.1018087+00	−.7375747−02	.1207486−02	.1651692+01	−.1829046+00	.2370016−01	−.5226818−02	−.3854146+01	.5741918+00	−.1056219+00	.2895470−01
2.020	−.6115159+00	.9822746−01	−.6917715−02	.1107545−02	.1608286+01	−.1752722+00	.2212095−01	−.4774109−02	−.3746729+01	.5473852+00	−.9819238−01	.2635130−01
2.060	−.5803871+00	.9486102−01	−.6498235−02	.1017955−02	.1566951+01	−.1681514+00	.2068197−01	−.4370051−02	−.3644865+01	.5225090+00	−.9145058−01	.2403636−01
2.100	−.5506332+00	.9169174−01	−.6113277−02	.9374420−03	.1527544+01	−.1614964+00	.1936790−01	−.4008471−02	−.3548144+01	.4993815+00	−.8531878−01	.2197232−01
2.140	−.5221672+00	.8870378−01	−.5759309−02	.8649136−03	.1489934+01	−.1552668+00	.1816540−01	−.3684089−02	−.3456192+01	.4778419+00	−.7972955−01	.2012717−01
2.180	−.4949092+00	.8588287−01	−.5433227−02	.7994278−03	.1454002+01	−.1494261+00	.1706280−01	−.3392379−02	−.3368670+01	.4577472+00	−.7462418−01	.1847359−01
2.220	−.4687858+00	.8321618−01	−.5132295−02	.7401705−03	.1419637+01	−.1439420+00	.1604986−01	−.3129446−02	−.3285269+01	.4389702+00	−.6995139−01	.1698813−01
2.260	−.4437295+00	.8069209−01	−.4854096−02	.6864361−03	.1386740+01	−.1387853+00	.1511759−01	−.2891926−02	−.3205711+01	.4213975+00	−.6566627−01	.1565063−01
2.300	−.4196777+00	.7830009−01	−.4596487−02	.6376109−03	.1355219+01	−.1339297+00	.1425805−01	−.2676908−02	−.3129740+01	.4049272+00	−.6172938−01	.1444370−01
2.340	−.3965730+00	.7603064−01	−.4357567−02	.5931598−03	.1324990+01	−.1293518+00	.1346421−01	−.2481861−02	−.3057120+01	.3894683+00	−.5810598−01	.1335228−01
2.380	−.3743618+00	.7387505−01	−.4135640−02	.5526152−03	.1295976+01	−.1250301+00	.1272988−01	−.2304585−02	−.2987639+01	.3749388+00	−.5476540−01	.1236331−01
2.420	−.3529949+00	.7182543−01	−.3929196−02	.5155669−03	.1268105+01	−.1209454+00	.1204952−01	−.2143154−02	−.2921100+01	.3612649+00	−.5168051−01	.1146540−01
2.460	−.3324263+00	.6987456−01	−.3736883−02	.4816546−03	.1241310+01	−.1170801+00	.1141822−01	−.1995886−02	−.2857322+01	.3483799+00	−.4882722−01	.1064864−01
2.500	−.3126134+00	.6801585−01	−.3557489−02	.4505607−03	.1215532+01	−.1134184+00	.1083159−01	−.1861303−02	−.2796139+01	.3362235+00	−.4618411−01	.9904331−02
2.600	−.2661336+00	.6373381−01	−.3158658−02	.3833958−03	.1155169+01	−.1050628+00	.9535684−02	−.1572176−02	−.2653555+01	.3086740+00	−.4037567−01	.8312807−02
2.700	−.2235863+00	.5990966−01	−.2819816−02	.3286025−03	.1100035+01	−.9769845−01	.8444458−02	−.1338101−02	−.2524164+01	.2846236+00	−.3551996−01	.7032729−02
2.800	−.1845074+00	.5647691−01	−.2529895−02	.2835099−03	.1049480+01	−.9117006−01	.7518625−02	−.1146856−02	−.2406232+01	.2634955+00	−.3142845−01	.5993349−02
2.900	−.1485023+00	.5338104−01	−.2280210−02	.2461010−03	.1002957+01	−.8535177−01	.6727650−02	−.9892867−03	−.2298314+01	.2448272+00	−.2795565−01	.5142016−02
3.000	−.1152340+00	.5057690−01	−.2063880−02	.2148352−03	.9600032+00	−.8014082−01	.6047548−02	−.8584507−03	−.2199196+01	.2282442+00	−.2498813−01	.4439073−02
3.100	−.8441244−01	.4802687−01	−.1875402−02	.1885233−03	.9202229+00	−.7545263−01	.5459305−02	−.7490291−03	−.2107850+01	.2134413+00	−.2243658−01	.3854313−02
3.200	−.5578704−01	.4569934−01	−.1710340−02	.1662384−03	.8832775+00	−.7121703−01	.4947710−02	−.6569042−03	−.2023402+01	.2001670+00	−.2022998−01	.3364491−02
3.300	−.2913991−01	.4356762−01	−.1565087−02	.1472516−03	.8488746+00	−.6737540−01	.4500494−02	−.5788584−03	−.1945105+01	.1882134+00	−.1831146−01	.2951542−02
3.400	−.4280856−02	.4160901−01	−.1436693−02	.1309847−03	.8167606+00	−.6387846−01	.4107688−02	−.5123557−03	−.1872313+01	.1774066+00	−.1663504−01	.2601304−02
3.500	.1895689−01	.3980408−01	−.1322723−02	.1169755−03	.7867145+00	−.6068450−01	.3761132−02	−.4553811−03	−.1804467+01	.1676008+00	−.1516331−01	.2302583−02
3.600	.4072019−01	.3813616−01	−.1221158−02	.1048517−03	.7585429+00	−.5775805−01	.3454102−02	−.4063207−03	−.1741083+01	.1586727+00	−.1386563−01	.2046456−02
3.700	.6113885−01	.3659084−01	−.1130315−02	.9431160−04	.7320758+00	−.5506877−01	.3181023−02	−.3638734−03	−.1681735+01	.1505178+00	−.1271670−01	.1825764−02
3.800	.8032801−01	.3515559−01	−.1048780−02	.8510878−04	.7071630+00	−.5259058−01	.2937246−02	−.3269826−03	−.1626052+01	.1430467+00	−.1169555−01	.1634719−02
3.900	.9839019−01	.3381952−01	−.9753583−03	.7704094−04	.6836714+00	−.5030095−01	.2718870−02	−.2947854−03	−.1573706+01	.1361826+00	−.1078467−01	.1468614−02
4.000	.1154169+00	.3257308−01	−.9090400−03	.6994101−04	.6614830+00	−.4818032−01	.2522610−02	−.2665721−03	−.1524405+01	.1298595+00	−.9969359−02	.1323595−02
4.100	.1314902+00	.3140788−01	−.8489628−03	.6367022−04	.6404922+00	−.4621169−01	.2345679−02	−.2417567−03	−.1477892+01	.1240201+00	−.9237238−02	.1196493−02
4.200	.1466837+00	.3031653−01	−.7943893−03	.5811276−04	.6206045+00	−.4438015−01	.2185708−02	−.2198518−03	−.1433938+01	.1186145+00	−.8577802−02	.1084680−02
4.300	.1610638+00	.2929249−01	−.7446857−03	.5317145−04	.6017352+00	−.4267264−01	.2040669−02	−.2004505−03	−.1392337+01	.1135995+00	−.7982114−02	.9859742−03
4.400	.1746904+00	.2832993−01	−.6993052−03	.4876444−04	.5838082+00	−.4107763−01	.1908824−02	−.1832116−03	−.1352906+01	.1089367+00	−.7442531−02	.8985486−03
4.500	.1876177+00	.2742369−01	−.6577741−03	.4482242−04	.5667545+00	−.3958494−01	.1788673−02	−.1678472−03	−.1315479+01	.1045929+00	−.6952493−02	.8208698−03
4.600	.1998951+00	.2656915−01	−.6196807−03	.4128647−04	.5505118+00	−.3818555−01	.1678919−02	−.1541137−03	−.1279908+01	.1005384+00	−.6506345−02	.7516440−03
4.700	.2115673+00	.2576215−01	−.5846659−03	.3810635−04	.5350237+00	−.3687142−01	.1578436−02	−.1418040−03	−.1246058+01	.9674705−01	−.6099197−02	.6897747−03
4.800	.2226751+00	.2499897−01	−.5524153−03	.3523898−04	.5202387+00	−.3563539−01	.1486241−02	−.1307414−03	−.1213807+01	.9319570−01	−.5726803−02	.6343294−03
4.900	.2332558+00	.2427628−01	−.5226530−03	.3264736−04	.5061101+00	−.3447106−01	.1401478−02	−.1207745−03	−.1183045+01	.8986366−01	−.5385465−02	.5845118−03
5.000	.2433435+00	.2359104−01	−.4951361−03	.3029953−04	.4925951+00	−.3337266−01	.1323395−02	−.1117732−03	−.1153670+01	.8673246−01	−.5071949−02	.5396394−03
5.100	.2529696+00	.2294051−01	−.4696500−03	.2816786−04	.4796546+00	−.3233503−01	.1251329−02	−.1036252−03	−.1125592+01	.8378560−01	−.4783425−02	.4991251−03
5.200	.2621627+00	.2232221−01	−.4460048−03	.2622834−04	.4672527+00	−.3135351−01	.1184699−02	−.9623328−04	−.1098725+01	.8100825−01	−.4517402−02	.4624626−03
5.300	.2709493+00	.2173388−01	−.4240317−03	.2446008−04	.4553567+00	−.3042390−01	.1122987−02	−.8951323−04	−.1072994+01	.7838706−01	−.4271684−02	.4292132−03
5.400	.2793537+00	.2117348−01	−.4035807−03	.2284480−04	.4439360+00	−.2954237−01	.1065736−02	−.8339158−04	−.1048327+01	.7591002−01	−.4044330−02	.3989961−03
5.500	.2873986+00	.2063912−01	−.3845179−03	.2136651−04	.4329629+00	−.2870548−01	.1012541−02	−.7780421−04	−.1024661+01	.7356625−01	−.3833620−02	.3714799−03
5.600	.2951045+00	.2012910−01	−.3667233−03	.2001117−04	.4224115+00	−.2791007−01	.9630377−03	−.7269496−04	−.1001934+01	.7134592−01	−.3638027−02	.3463746−03
5.800	.3095754+00	.1917589−01	−.3345208−03	.1762128−04	.4024803+00	−.2643251−01	.8738486−03	−.6371956−04	−.9590868+00	.6724063−01	−.3286890−02	.3024136−03
6.000	.3229044+00	.1830278−01	−.3062380−03	.1559243−04	.3839722+00	−.2508962−01	.7959636−03	−.5613717−04	−.9193931+00	.6353189−01	−.2981678−02	.2654300−03
6.200	.3352105+00	.1750037−01	−.2812770−03	.1385961−04	.3667401+00	−.2386455−01	.7276010−03	−.4969117−04	−.8825170+00	.6016787−01	−.2714965−02	.2341137−03

(m = 12)

T^*	$B^{*(0)}$	$B^{*(1)}$	$B^{*(2)}$	$B^{*(3)}$	$T^*\frac{\partial B^{*(0)}}{\partial T^*}$	$T^*\frac{\partial B^{*(1)}}{\partial T^*}$	$T^*\frac{\partial B^{*(2)}}{\partial T^*}$	$T^*\frac{\partial B^{*(3)}}{\partial T^*}$	$T^{*2}\frac{\partial^2 B^{*(0)}}{\partial T^{*2}}$	$T^{*2}\frac{\partial^2 B^{*(1)}}{\partial T^{*2}}$	$T^{*2}\frac{\partial^2 B^{*(2)}}{\partial T^{*2}}$	$T^{*2}\frac{\partial^2 B^{*(3)}}{\partial T^{*2}}$
6.400	.3465971+00	.1676067−01	−.2591483−03	.1237126−04	.3506568+00	−.2274311−01	.6673107−03	−.4417907−04	−.8481685+00	.5710510−01	−.2480737−02	.2074358−03
6.600	.3571546+00	.1607681−01	−.2394479−03	.1108614−04	.3356111+00	−.2171322−01	.6139031−03	−.3943978−04	−.8160961+00	.5430689−01	−.2274084−02	.1845811−03
6.800	.3669619+00	.1544289−01	−.2218402−03	.9971037−05	.3215062+00	−.2076456−01	.5663964−03	−.3534412−04	−.7860805+00	.5174210−01	−.2090972−02	.1648983−03
7.000	.3760885+00	.1485378−01	−.2060451−03	.8998987−05	.3082566+00	−.1988828−01	.5239744−03	−.3178772−04	−.7579298+00	.4938413−01	−.1928064−02	.1478638−03
7.200	.3845958+00	.1430503−01	−.1918269−03	.8147967−05	.2957870+00	−.1907672−01	.4859549−03	−.2868571−04	−.7314752+00	.4721016−01	−.1782579−02	.1330530−03
7.400	.3925381+00	.1379275−01	−.1789866−03	.7399870−05	.2840307+00	−.1832325−01	.4517645−03	−.2596860−04	−.7065677+00	.4520051−01	−.1652193−02	.1201195−03
7.600	.3999640+00	.1331351−01	−.1673553−03	.6739724−05	.2729285+00	−.1762209−01	.4209184−03	−.2357917−04	−.6830753+00	.4333811−01	−.1534946−02	.1087791−03
7.800	.4069164+00	.1286433−01	−.1567886−03	.6155079−05	.2624274+00	−.1696820−01	.3930051−03	−.2147002−04	−.6608806+00	.4160812−01	−.1429180−02	.9879723−04
8.000	.4134340+00	.1244252−01	−.1471630−03	.5635528−05	.2524801+00	−.1635712−01	.3676731−03	−.1960167−04	−.6398787+00	.3999758−01	−.1333488−02	.8997903−04
8.200	.4195513+00	.1204573−01	−.1383721−03	.5172326−05	.2430441+00	−.1578495−01	.3446214−03	−.1794108−04	−.6199759+00	.3849509−01	−.1246665−02	.8216198−04
8.400	.4252996+00	.1167186−01	−.1303237−03	.4758094−05	.2340811+00	−.1524822−01	.3235909−03	−.1646046−04	−.6010880+00	.3709063−01	−.1167678−02	.7520973−04
8.600	.4307069+00	.1131903−01	−.1229382−03	.4386575−05	.2255566+00	−.1474387−01	.3043574−03	−.1513631−04	−.5831393+00	.3577536−01	−.1095639−02	.6900744−04
8.800	.4357987+00	.1098557−01	−.1161460−03	.4052442−05	.2174394+00	−.1426915−01	.2867268−03	−.1394871−04	−.5660614+00	.3454142−01	−.1029777−02	.6345789−04
9.000	.4405978+00	.1066996−01	−.1098863−03	.3751141−05	.2097012+00	−.1382164−01	.2705298−03	−.1288067−04	−.5497922+00	.3338183−01	−.9694263−03	.5847847−04
9.200	.4451254+00	.1037084−01	−.1041058−03	.3478762−05	.2023161+00	−.1339912−01	.2556187−03	−.1191766−04	−.5342756+00	.3229037−01	−.9140043−03	.5399867−04
9.400	.4494002+00	.1008700−01	−.9875775−04	.3231941−05	.1952606+00	−.1299966−01	.2418639−03	−.1104721−04	−.5194605+00	.3126147−01	−.8630030−03	.4995812−04
9.600	.4534398+00	.9817314−02	−.9380078−04	.3007767−05	.1885135+00	−.1262147−01	.2291517−03	−.1025855−04	−.5053004+00	.3029014−01	−.8159770−03	.4630489−04
9.800	.4572600+00	.9560785−02	−.8919830−04	.2803718−05	.1820549+00	−.1226296−01	.2173815−03	−.9542394−05	−.4917528+00	.2937188−01	−.7725343−03	.4299419−04
10.000	.4608753+00	.9316495−02	−.8491788−04	.2617599−05	.1758670+00	−.1192268−01	.2064645−03	−.8890667−05	−.4787786+00	.2850264−01	−.7323295−03	.3998725−04
10.200	.4642990+00	.9083612−02	−.8093065−04	.2447495−05	.1699332+00	−.1159934−01	.1963222−03	−.8296348−05	−.4663423+00	.2767877−01	−.6950568−03	.3725041−04
10.400	.4675432+00	.8861377−02	−.7721087−04	.2291730−05	.1642383+00	−.1129174−01	.1868843−03	−.7753306−05	−.4544111+00	.2689696−01	−.6604451−03	.3475432−04
10.600	.4706194+00	.8649093−02	−.7373554−04	.2148832−05	.1587682+00	−.1099880−01	.1780887−03	−.7256174−05	−.4429547+00	.2615421−01	−.6282536−03	.3247338−04
10.800	.4735378+00	.8446124−02	−.7048404−04	.2017508−05	.1535101+00	−.1071952−01	.1698794−03	−.6800242−05	−.4319455+00	.2544777−01	−.5982672−03	.3038513−04
11.000	.4763080+00	.8251887−02	−.6743786−04	.1896614−05	.1484520+00	−.1045302−01	.1622067−03	−.6381364−05	−.4213577+00	.2477516−01	−.5702943−03	.2846987−04
11.400	.4814386+00	.7887498−02	−.6189648−04	.1682195−05	.1388921+00	−.9955076−02	.1482962−03	−.5640552−05	−.4013531+00	.2352253−01	−.5197185−03	.2509087−04
11.800	.4860743+00	.7552116−02	−.5699665−04	.1498782−05	.1300091+00	−.9499135−02	.1360500−03	−.5009209−05	−.3827712+00	.2238034−01	−.4753510−03	.2222025−04
12.200	.4902696+00	.7242488−02	−.5264441−04	.1340991−05	.1217343+00	−.9080259−02	.1252174−03	−.4467973−05	−.3654655+00	.2133513−01	−.4362376−03	.1976675−04
12.600	.4940715+00	.6955828−02	−.4876220−04	.1204518−05	.1140082+00	−.8694242−02	.1155931−03	−.4001430−05	−.3493090+00	.2037551−01	−.4015981−03	.1765790−04
13.000	.4975209+00	.6689728−02	−.4528560−04	.1085895−05	.1067784+00	−.8337479−02	.1070069−03	−.3597205−05	−.3341911+00	.1949175−01	−.3707896−03	.1583572−04
13.400	.5006536+00	.6442105−02	−.4216076−04	.9823073−06	.9999925−01	−.8006865−02	.9931732−04	−.3245294−05	−.3200148+00	.1867553−01	−.3432793−03	.1425353−04
13.800	.5035008+00	.6211141−02	−.3934237−04	.8914540−06	.9363051−01	−.7699710−02	.9240588−04	−.2937549−05	−.3066950+00	.1791965−01	−.3186222−03	.1287334−04
14.200	.5060901+00	.5995250−02	−.3679216−04	.8114432−06	.8763652−01	−.7413678−02	.8617282−04	−.2667292−05	−.2941566+00	.1721790−01	−.2964450−03	.1166420−04
14.600	.5084457+00	.5793034−02	−.3447757−04	.7407097−06	.8198565−01	−.7146723−02	.8053367−04	−.2429015−05	−.2823328+00	.1656486−01	−.2764328−03	.1060060−04
15.000	.5105892+00	.5603263−02	−.3237079−04	.6779507−06	.7664973−01	−.6897056−02	.7541653−04	−.2218148−05	−.2711645+00	.1595581−01	−.2583181−03	.9661421−05
16.000	.5151403+00	.5176435−02	−.2786452−04	.5492089−06	.6452900−01	−.6338601−02	.6452532−04	−.1787379−05	−.2457780+00	.1459962−01	−.2199176−03	.7749635−05
17.000	.5187265+00	.4806915−02	−.2422430−04	.4510865−06	.5389813−01	−.5858676−02	.5578634−04	−.1460928−05	−.2234846+00	.1344112−01	−.1892733−03	.6307851−05
18.000	.5215359+00	.4484104−02	−.2124370−04	.3750107−06	.4450317−01	−.5442196−02	.4867489−04	−.1209142−05	−.2037538+00	.1244123−01	−.1644605−03	.5200773−05
19.000	.5237139+00	.4199838−02	−.1877391−04	.3151300−06	.3614466−01	−.5077655−02	.4281555−04	−.1011905−05	−.1861700+00	.1157036−01	−.1441105−03	.4337094−05
20.000	.5253742+00	.3947731−02	−.1670558−04	.2673591−06	.2866377−01	−.4756135−02	.3793432−04	−.8552527−06	−.1704027+00	.1080573−01	−.1272295−03	.3653724−05
21.000	.5266070+00	.3722721−02	−.1495693−04	.2287877−06	.2193242−01	−.4470622−02	.3382759−04	−.7292875−06	−.1561863+00	.1012955−01	−.1130832−03	.3106154−05
22.000	.5274845+00	.3520744−02	−.1346588−04	.1973051−06	.1584626−01	−.4215527−02	.3034170−04	−.6268658−06	−.1433044+00	.9527718−02	−.1011195−03	.2662381−05
23.000	.5280651+00	.3338501−02	−.1218462−04	.1713555−06	.1031932−01	−.3986347−02	.2735895−04	−.5427465−06	−.1315792+00	.8988941−02	−.9091788−04	.2299023−05
24.000	.5283962+00	.3173289−02	−.1107588−04	.1497748−06	.5280227−02	−.3779415−02	.2478805−04	−.4730245−06	−.1208630+00	.8504065−02	−.8215323−04	.1998724−05
25.000	.5285169+00	.3022872−02	−.1011025−04	.1316811−06	.6691794−03	−.3591715−02	.2255737−04	−.4147523−06	−.1110324+00	.8065600−02	−.7457149−04	.1748417−05
26.000	.5284595+00	.2885384−02	−.9264321−05	.1163973−06	−.3564282−02	−.3420745−02	.2061006−04	−.3656757−06	−.1019832+00	.7667359−02	−.6797180−04	.1538140−05
27.000	.5282509+00	.2759259−02	−.8519232−05	.1033982−06	−.7463032−02	−.3264415−02	.1890058−04	−.3240526−06	−.9362699−01	.7304195−02	−.6219380−04	.1360228−05
28.000	.5279135+00	.2643169−02	−.7859686−05	.9227201−07	−.1106373−01	−.3120963−02	.1739213−04	−.2885211−06	−.8588821−01	.6971788−02	−.5710829−04	.1208702−05
29.000	.5274664+00	.2535985−02	−.7273163−05	.8269299−07	−.1439792−01	−.2988898−02	.1605469−04	−.2580077−06	−.7870187−01	.6666489−02	−.5261027−04	.1078857−05
30.000	.5269255+00	.2436739−02	−.6749343−05	.7440099−07	−.1749286−01	−.2866944−02	.1486361−04	−.2316570−06	−.7201179−01	.6385197−02	−.4861372−04	.9669516−06
32.000	.5256147+00	.2258837−02	−.5856936−05	.6088018−07	−.2305682−01	−.2649153−02	.1284237−04	−.1888315−06	−.5993132−01	.5884391−02	−.4185321−04	.7855962−06

(m = 12)

T^*	$B^{*(0)}$	$B^{*(1)}$	$B^{*(2)}$	$B^{*(3)}$	$T^*\frac{\partial B^{*(0)}}{\partial T^*}$	$T^*\frac{\partial B^{*(1)}}{\partial T^*}$	$T^*\frac{\partial B^{*(2)}}{\partial T^*}$	$T^*\frac{\partial B^{*(3)}}{\partial T^*}$	$T^{*2}\frac{\partial^2 B^{*(0)}}{\partial T^{*2}}$	$T^{*2}\frac{\partial^2 B^{*(1)}}{\partial T^{*2}}$	$T^{*2}\frac{\partial^2 B^{*(2)}}{\partial T^{*2}}$	$T^{*2}\frac{\partial^2 B^{*(3)}}{\partial T^{*2}}$
34.000	.5240679+00	.2104026−02	−.5129256−05	.5046093−07	−.2791186−01	−.2460503−02	.1120233−04	−.1559669−06	−.4932497−01	.5452243−02	−.3638969−04	.6469184−06
36.000	.5223492+00	.1968157−02	−.4528332−05	.4230123−07	−.3217905−01	−.2295624−02	.9854069−05	−.1303274−06	−.3994337−01	.5075846−02	−.3191465−04	.5390801−06
38.000	.5205062+00	.1848011−02	−.4026492−05	.3581926−07	−.3595363−01	−.2150377−02	.8732782−05	−.1100309−06	−.3159028−01	.4745298−02	−.2820552−04	.4539702−06
40.000	.5185750+00	.1741052−02	−.3603197−05	.3060420−07	−.3931154−01	−.2021518−02	.7790609−05	−.9375421−07	−.2410914−01	.4452883−02	−.2509860−04	.3859056−06
42.000	.5165830+00	.1645257−02	−.3242947−05	.2636037−07	−.4231404−01	−.1906476−02	.6991607−05	−.8054852−07	−.1737355−01	.4192504−02	−.2247142−04	.3308249−06
44.000	.5145512+00	.1558994−02	−.2933870−05	.2287126−07	−.4501111−01	−.1803184−02	.6308370−05	−.6972160−07	−.1128032−01	.3959281−02	−.2023094−04	.2857742−06
46.000	.5124958+00	.1480930−02	−.2666755−05	.1997583−07	−.4744390−01	−.1709963−02	.5719716−05	−.6076036−07	−.5744390−02	.3749269−02	−.1830548−04	.2485698−06
48.000	.5104293+00	.1409969−02	−.2434367−05	.1755265−07	−.4964657−01	−.1625437−02	.5209072−05	−.5327901−07	−.6950254−03	.3559239−02	−.1663913−04	.2175745−06
50.000	.5083614+00	.1345200−02	−.2230960−05	.1550892−07	−.5164776−01	−.1548467−02	.4763326−05	−.4698371−07	.3927095−02	.3386530−02	−.1518777−04	.1915443−06
52.000	.5062997+00	.1285859−02	−.2051926−05	.1377296−07	−.5347162−01	−.1478103−02	.4371994−05	−.4164797−07	.8172074−02	.3228927−02	−.1391626−04	.1695227−06
54.000	.5042499+00	.1231303−02	−.1893535−05	.1228875−07	−.5513864−01	−.1413544−02	.4026621−05	−.3709533−07	.1208252−01	.3084572−02	−.1279628−04	.1507660−06
56.000	.5022167+00	.1180984−02	−.1752741−05	.1101209−07	−.5666636−01	−.1354116−02	.3720321−05	−.3318690−07	.1569491−01	.2951898−02	−.1180487−04	.1346901−06
58.000	.5002033+00	.1134436−02	−.1627040−05	.9907802−08	−.5806983−01	−.1299240−02	.3447449−05	−.2981236−07	.1904063−01	.2829571−02	−.1092322−04	.1208319−06
60.000	.4982126+00	.1091257−02	−.1514356−05	.8947636−08	−.5936206−01	−.1248423−02	.3203337−05	−.2688334−07	.2214685−01	.2716452−02	−.1013582−04	.1088213−06
64.000	.4943063+00	.1013664−02	−.1321390−05	.7372454−08	−.6165656−01	−.1157320−02	.2786495−05	−.2208969−07	.2773230−01	.2514048−02	−.8794379−05	.8920497−07
68.000	.4905078+00	.9459353−03	−.1163023−05	.6149271−08	−.6362420−01	−.1078030−02	.2445616−05	−.1837848−07	.3260716−01	.2338311−02	−.7700600−05	.7405750−07
72.000	.4868219+00	.8863288−03	−.1031470−05	.5184639−08	−.6532246−01	−.1008434−02	.2163379−05	−.1545981−07	.3689236−01	.2184392−02	−.6797403−05	.6217304−07
76.000	.4832497+00	.8334875−03	−.9210157−06	.4413427−08	−.6679641−01	−.9468850−03	.1927117−05	−.1313230−07	.4068313−01	.2048538−02	−.6043188−05	.5271630−07
80.000	.4797901+00	.7863385−03	−.8273854−06	.3789283−08	−.6808188−01	−.8920869−03	.1727397−05	−.1125304−07	.4405545−01	.1927802−02	−.5407072−05	.4509622−07
84.000	.4764405+00	.7440225−03	−.7473338−06	.3278601−08	−.6920767−01	−.8430053−03	.1557080−05	−.9718752−08	.4707068−01	.1819841−02	−.4865747−05	.3888654−07
88.000	.4731977+00	.7058435−03	−.6783609−06	.2856609−08	−.7019720−01	−.7988047−03	.1410686−05	−.8453483−08	.4977891−01	.1722764−02	−.4401364−05	.3377452−07
92.000	.4700576+00	.6712321−03	−.6185155−06	.2504765−08	−.7106968−01	−.7588037−03	.1283947−05	−.7400534−08	.5222138−01	.1635034−02	−.4000069−05	.2952725−07
96.000	.4670163+00	.6397181−03	−.5662574−06	.2209006−08	−.7184100−01	−.7224409−03	.1173509−05	−.6516993−08	.5443241−01	.1555388−02	−.3650982−05	.2596872−07
100.000	.4640695+00	.6109095−03	−.5203574−06	.1958530−08	−.7252443−01	−.6892497−03	.1076697−05	−.5769971−08	.5644073−01	.1482778−02	−.3345461−05	.2296433−07
105.000	.4605125+00	.5782075−03	−.4704335−06	.1696508−08	−.7327191−01	−.6516316−03	.9716155−06	−.4989866−08	.5870264−01	.1400588−02	−.3014401−05	.1983212−07
110.000	.4570886+00	.5486893−03	−.4273725−06	.1479715−08	−.7391740−01	−.6177310−03	.8811743−06	−.4345579−08	.6072499−01	.1326618−02	−.2729967−05	.1724849−07
115.000	.4537902+00	.5219184−03	−.3899727−06	.1298744−08	−.7447568−01	−.5870317−03	.8027811−06	−.3808729−08	.6254030−01	.1259715−02	−.2483830−05	.1509910−07
120.000	.4506101+00	.4975337−03	−.3572840−06	.1146450−08	−.7495895−01	−.5591079−03	.7343915−06	−.3357612−08	.6417563−01	.1198930−02	−.2269433−05	.1329568−07
125.000	.4475414+00	.4752345−03	−.3285474−06	.1017340−08	−.7537737−01	−.5336055−03	.6743765−06	−.2975743−08	.6565358−01	.1143474−02	−.2081561−05	.1177039−07
130.000	.4445779+00	.4547681−03	−.3031507−06	.9071359−09	−.7573945−01	−.5102278−03	.6214248−06	−.2650240−08	.6699325−01	.1092689−02	−.1916027−05	.1047235−07
135.000	.4417134+00	.4359207−03	−.2805958−06	.8124812−09	−.7605235−01	−.4887240−03	.5744720−06	−.2371094−08	.6821082−01	.1046019−02	−.1769436−05	.9360309−08
140.000	.4389426+00	.4185103−03	−.2604739−06	.7307096−09	−.7632217−01	−.4688812−03	.5326463−06	−.2130198−08	.6932012−01	.1002990−02	−.1639010−05	.8401887−08
145.000	.4362602+00	.4023811−03	−.2424473−06	.6596886−09	−.7655410−01	−.4505172−03	.4952284−06	−.1921217−08	.7033303−01	.9632014−03	−.1522464−05	.7571149−08
150.000	.4336614+00	.3873986−03	−.2262348−06	.5976975−09	−.7675259−01	−.4334753−03	.4616210−06	−.1739026−08	.7125980−01	.9263056−03	−.1417900−05	.6847202−08
160.000	.4286974+00	.3604239−03	−.1983466−06	.4954542−09	−.7706408−01	−.4028332−03	.4039175−06	−.1438981−08	.7288936−01	.8600368−03	−.1238638−05	.5657030−08
170.000	.4240185+00	.3368231−03	−.1753301−06	.4155222−09	−.7728163−01	−.3760678−03	.3564040−06	−.1204901−08	.7426727−01	.8022286−03	−.1091313−05	.4730649−08
180.000	.4195968+00	.3160087−03	−.1561126−06	.3521004−09	−.7742423−01	−.3524975−03	.3168166−06	−.1019475−08	.7543863−01	.7513823−03	−.9687768−06	.3997413−08
190.000	.4154083+00	.2975212−03	−.1399012−06	.3011103−09	−.7750653−01	−.3315907−03	.2834867−06	−.8706522−09	.7643876−01	.7063309−03	−.8657735−06	.3409618−08
200.000	.4114317+00	.2809962−03	−.1260996−06	.2596290−09	−.7753999−01	−.3129264−03	.2551620−06	−.7497787−09	.7729567−01	.6661523−03	−.7783685−06	.2933189−08
210.000	.4076485+00	.2661412−03	−.1142524−06	.2255255−09	−.7753364−01	−.2961674−03	.2308886−06	−.6505243−09	.7803181−01	.6301085−03	−.7035667−06	.2542506−08
220.000	.4040424+00	.2527185−03	−.1040068−06	.1972203−09	−.7749469−01	−.2810404−03	.2099291−06	−.5682559−09	.7866540−01	.5976022−03	−.6390587−06	.2218722−08
240.000	.3973054+00	.2294242−03	−.8727155−07	.1535232−09	−.7734111−01	−.2548258−03	.1757646−06	−.4414903−09	.7968199−01	.5413341−03	−.5340892−06	.1721063−08
260.000	.3911234+00	.2099177−03	−.7428995−07	.1219822−09	−.7711387−01	−.2329114−03	.1493304−06	−.3501691−09	.8043653−01	.4943611−03	−.4530393−06	.1362862−08
280.000	.3854186+00	.1933552−03	−.6401646−07	.9862171−10	−.7683630−01	−.2143327−03	.1284579−06	−.2826818−09	.8099280−01	.4545860−03	−.3891622−06	.1098891−08
300.000	.3801279+00	.1791249−03	−.5574592−07	.8093777−10	−.7652453−01	−.1983914−03	.1116887−06	−.2316691−09	.8139661−01	.4204942−03	−.3379267−06	.8993717−09

(m = 15)

T^*	$B^{*(0)}$	$B^{*(1)}$	$B^{*(2)}$	$B^{*(3)}$	$T^*\frac{\partial B^{*(0)}}{\partial T^*}$	$T^*\frac{\partial B^{*(1)}}{\partial T^*}$	$T^*\frac{\partial B^{*(2)}}{\partial T^*}$	$T^*\frac{\partial B^{*(3)}}{\partial T^*}$	$T^{*2}\frac{\partial^2 B^{*(0)}}{\partial T^{*2}}$	$T^{*2}\frac{\partial^2 B^{*(1)}}{\partial T^{*2}}$	$T^{*2}\frac{\partial^2 B^{*(2)}}{\partial T^{*2}}$	$T^{*2}\frac{\partial^2 B^{*(3)}}{\partial T^{*2}}$
.300	−.2383783+02	.2792413+02	−.4977022+02	.1199448+03	.6579973+02	−.1350680+03	.3243963+03	−.9569529+03	−.3063799+03	.8828146+03	−.2615871+04	.9047238+04
.400	−.1173909+02	.7894737+01	−.8737634+01	.1396994+02	.2601603+02	−.3144757+02	.4906947+02	−.9791091+02	−.9995191+02	.1771844+03	−.3486811+03	.8257908+03
.500	−.7372564+01	.3447935+01	−.2661179+01	.3135784+01	.1455559+02	−.1192669+02	.1345948+02	−.2007029+02	−.4927675+02	.6050365+02	−.8757185+02	.1563294+03
.600	−.5202771+01	.1897584+01	−.1096896+01	.1015491+01	.9679453+01	−.5885352+01	.5127201+01	−.6070656+01	−.3002249+02	.2756952+02	−.3122864+02	.4454941+02
.700	−.3922199+01	.1200845+01	−.5455957+00	.4141459+00	.7107760+01	−.3411438+01	.2396484+01	−.2346104+01	−.2069694+02	.1499867+02	−.1385904+02	.1642911+02
.750	−.3462400+01	.9907516+00	−.4045769+00	.2814219+00	.6245248+01	−.2709892+01	.1730483+01	−.1558034+01	−.1773303+02	.1159380+02	−.9788922+01	.1069487+02
.775	−.3263638+01	.9064795+00	−.3519383+00	.2349304+00	.5882810+01	−.2435869+01	.1486846+01	−.1286824+01	−.1651565+02	.1028969+02	−.8324863+01	.8751642+01
.800	−.3082096+01	.8329509+00	−.3080051+00	.1976056+00	.5557364+01	−.2200650+01	.1285971+01	−.1071393+01	−.1543757+02	.9183572+01	−.7129991+01	.7222270+01
.825	−.2915657+01	.7684186+00	−.2710664+00	.1673765+00	.5263735+01	−.1997424+01	.1119041+01	−.8986845+00	−.1447765+02	.8238794+01	−.6146646+01	.6006979+01
.850	−.2762535+01	.7114734+00	−.2397957+00	.1426945+00	.4997648+01	−.1820779+01	.9793008+00	−.7590366+00	−.1361861+02	.7426576+01	−.5331102+01	.5032605+01
.875	−.2621212+01	.6609698+00	−.2131547+00	.1223887+00	.4755536+01	−.1666378+01	.8615228+00	−.6452183+00	−.1284626+02	.6724105+01	−.4649845+01	.4244868+01
.900	−.2490390+01	.6159687+00	−.1903232+00	.1055650+00	.4534407+01	−.1530717+01	.7616243+00	−.5517609+00	−.1214886+02	.6113140+01	−.4076941+01	.3603064+01
.925	−.2368955+01	.5756954+00	−.1706482+00	.9153402−01	.4331737+01	−.1410941+01	.6763880+00	−.4744875+00	−.1151659+02	.5578979+01	−.3592133+01	.3076358+01
.950	−.2255944+01	.5395061+00	−.1536053+00	.7975973−01	.4145377+01	−.1304712+01	.6032581+00	−.4101792+00	−.1094124+02	.5109683+01	−.3179469+01	.2641165+01
.975	−.2150518+01	.5068624+00	−.1387708+00	.6982178−01	.3973495+01	−.1210095+01	.5401885+00	−.3563332+00	−.1041584+02	.4695486+01	−.2826280+01	.2279291+01
1.000	−.2051947+01	.4773116+00	−.1257997+00	.6138796−01	.3814514+01	−.1125486+01	.4855294+00	−.3109883+00	−.9934485+01	.4328349+01	−.2522434+01	.1976577+01
1.020	−.1977594+01	.4556385+00	−.1165726+00	.5554432−01	.3695699+01	−.1064095+01	.4469490+00	−.2797811+00	−.9577709+01	.4064007+01	−.2309344+01	.1769458+01
1.040	−.1906925+01	.4355295+00	−.1082348+00	.5038243−01	.3583655+01	−.1007660+01	.4123191+00	−.2523741+00	−.9243637+01	.3822611+01	−.2119127+01	.1588469+01
1.060	−.1839677+01	.4168357+00	−.1006819+00	.4580918−01	.3477834+01	−.9556684+00	.3811525+00	−.2282290+00	−.8930275+01	.3601656+01	−.1948852+01	.1429797+01
1.080	−.1775610+01	.3994253+00	−.9382382−01	.4174593−01	.3377747+01	−.9076715+00	.3530318+00	−.2068940+00	−.8635848+01	.3398962+01	−.1796018+01	.1290255+01
1.100	−.1714507+01	.3831816+00	−.8758249−01	.3812598−01	.3282950+01	−.8632752+00	.3275976+00	−.1879880+00	−.8358769+01	.3212623+01	−.1658488+01	.1167170+01
1.120	−.1656167+01	.3680009+00	−.8189013−01	.3489256−01	.3193046+01	−.8221320+00	.3045398+00	−.1711886+00	−.8097619+01	.3040972+01	−.1534425+01	.1058291+01
1.140	−.1600411+01	.3537907+00	−.7668769−01	.3199718−01	.3107673+01	−.7839347+00	.2835899+00	−.1562217+00	−.7851125+01	.2882544+01	−.1422248+01	.9617138+00
1.160	−.1547073+01	.3404684+00	−.7192353−01	.2939829−01	.3026505+01	−.7484112+00	.2645144+00	−.1428539+00	−.7618141+01	.2736048+01	−.1320589+01	.8758233+00
1.180	−.1496001+01	.3279601+00	−.6755238−01	.2706015−01	.2949246+01	−.7153195+00	.2471103+00	−.1308853+00	−.7397633+01	.2600343+01	−.1228263+01	.7992440+00
1.200	−.1447054+01	.3161993+00	−.6353448−01	.2495196−01	.2875627+01	−.6844443+00	.2311997+00	−.1201447+00	−.7188667+01	.2474419+01	−.1144239+01	.7308010+00
1.220	−.1400105+01	.3051264+00	−.5983476−01	.2304707−01	.2805400+01	−.6555931+00	.2166271+00	−.1104845+00	−.6990398+01	.2357379+01	−.1067617+01	.6694871+00
1.240	−.1355036+01	.2946874+00	−.5642225−01	.2132234−01	.2738342+01	−.6285938+00	.2032557+00	−.1017774+00	−.6802057+01	.2248423+01	−.9976127+00	.6144367+00
1.260	−.1311737+01	.2848337+00	−.5326953−01	.1975768−01	.2674247+01	−.6032918+00	.1909650+00	−.9391297−01	−.6622947+01	.2146840+01	−.9335354+00	.5649031+00
1.280	−.1270107+01	.2755213+00	−.5035223−01	.1833552−01	.2612926+01	−.5795483+00	.1796487+00	−.8679559−01	−.6452431+01	.2051992+01	−.8747793+00	.5202409+00
1.300	−.1230053+01	.2667102+00	−.4764869−01	.1704054−01	.2554207+01	−.5572384+00	.1692127+00	−.8034190−01	−.6289929+01	.1963307+01	−.8208104+00	.4798901+00
1.320	−.1191488+01	.2583640+00	−.4513960−01	.1585927−01	.2497930+01	−.5362489+00	.1595734+00	−.7447916−01	−.6134909+01	.1880274+01	−.7711569+00	.4433642+00
1.340	−.1154332+01	.2504497+00	−.4280770−01	.1477990−01	.2443949+01	−.5164780+00	.1506565+00	−.6914374−01	−.5986886+01	.1802429+01	−.7254008+00	.4102389+00
1.360	−.1118510+01	.2429371+00	−.4063752−01	.1379202−01	.2392127+01	−.4978330+00	.1423960+00	−.6427980−01	−.5845412+01	.1729356+01	−.6831717+00	.3801436+00
1.380	−.1083953+01	.2357988+00	−.3861520−01	.1288644−01	.2342341+01	−.4802301+00	.1347327+00	−.5983830−01	−.5710079+01	.1660680+01	−.6441397+00	.3527534+00
1.400	−.1050596+01	.2290094+00	−.3672829−01	.1205503−01	.2294475+01	−.4635928+00	.1276139+00	−.5577599−01	−.5580507+01	.1596061+01	−.6080112+00	.3277833+00
1.420	−.1018377+01	.2225459+00	−.3496554−01	.1129058−01	.2248420+01	−.4478517+00	.1209922+00	−.5205471−01	−.5456349+01	.1535189+01	−.5745239+00	.3049825+00
1.440	−.9872417+00	.2163871+00	−.3331685−01	.1058669−01	.2204079+01	−.4329434+00	.1148250+00	−.4864068−01	−.5337284+01	.1477784+01	−.5434430+00	.2841297+00
1.460	−.9571359+00	.2105135+00	−.3177306−01	.9937658−02	.2161357+01	−.4188099+00	.1090740+00	−.4550395−01	−.5223015+01	.1423591+01	−.5145583+00	.2650295+00
1.480	−.9280104+00	.2049071+00	−.3032590−01	.9338405−02	.2120170+01	−.4053982+00	.1037049+00	−.4261792−01	−.5113266+01	.1372379+01	−.4876809+00	.2475087+00
1.500	−.8998190+00	.1995515+00	−.2896785−01	.8784392−02	.2080437+01	−.3926598+00	.9868644−01	−.3995892−01	−.5007784+01	.1323934+01	−.4626408+00	.2314138+00
1.540	−.8460668+00	.1895325+00	−.2649244−01	.7796247−02	.2005039+01	−.3690279+00	.8959166−01	−.3523976−01	−.4808687+01	.1234591+01	−.4174754+00	.2029704+00
1.580	−.7955618+00	.1803477+00	−.2429935−01	.6945475−02	.1934625+01	−.3475989+00	.8159472−01	−.3120298−01	−.4624026+01	.1154199+01	−.3780067+00	.1787756+00
1.620	−.7480230+00	.1719037+00	−.2234906−01	.6209629−02	.1868720+01	−.3281052+00	.7453480−01	−.2773334−01	−.4452327+01	.1081611+01	−.3433696+00	.1580917+00
1.660	−.7032009+00	.1641200+00	−.2060855−01	.5570439−02	.1806909+01	−.3103185+00	.6827844−01	−.2473764−01	−.4292305+01	.1015855+01	−.3128510+00	.1403259+00
1.700	−.6608730+00	.1569270+00	−.1905005−01	.5012946−02	.1748827+01	−.2940431+00	.6271430−01	−.2214006−01	−.4142837+01	.9561057+00	−.2858595+00	.1249983+00
1.740	−.6208404+00	.1502638+00	−.1765011−01	.4524832−02	.1694148+01	−.2791106+00	.5774901−01	−.1987856−01	−.4002937+01	.9016561+00	−.2619021+00	.1117186+00
1.780	−.5829248+00	.1440778+00	−.1638882−01	.4095900−02	.1642585+01	−.2653752+00	.5330389−01	−.1790211−01	−.3871735+01	.8518997+00	−.2405658+00	.1001671+00
1.820	−.5469657+00	.1383224+00	−.1524921−01	.3717666−02	.1593881+01	−.2527107+00	.4931233−01	−.1616848−01	−.3748463+01	.8063137+00	−.2215027+00	.9008073−01
1.860	−.5128183+00	.1329569+00	−.1421677−01	.3383038−02	.1547806+01	−.2410068+00	.4571768−01	−.1464257−01	−.3632438+01	.7644453+00	−.2044189+00	.8124198−01

(m = 15)

T^*	$B^{*(0)}$	$B^{*(1)}$	$B^{*(2)}$	$B^{*(3)}$	$T^*\frac{\partial B^{*(0)}}{\partial T^*}$	$T^*\frac{\partial B^{*(1)}}{\partial T^*}$	$T^*\frac{\partial B^{*(2)}}{\partial T^*}$	$T^*\frac{\partial B^{*(3)}}{\partial T^*}$	$T^{*2}\frac{\partial^2 B^{*(0)}}{\partial T^{*2}}$	$T^{*2}\frac{\partial^2 B^{*(1)}}{\partial T^{*2}}$	$T^{*2}\frac{\partial^2 B^{*(2)}}{\partial T^{*2}}$	$T^{*2}\frac{\partial^2 B^{*(3)}}{\partial T^{*2}}$
1.900	−.4803519+00	.1279453+00	−.1327901−01	.3086060−02	.1504155+01	−.2301672+00	.4247158−01	−.1329507−01	−.3523051+01	.7259012+00	−.1890644+00	.7346996−01
1.940	−.4494478+00	.1232557+00	−.1242516−01	.2821709−02	.1462741+01	−.2201073+00	.3953256−01	−.1210138−01	−.3419760+01	.6903383+00	−.1752261+00	.6661362−01
1.980	−.4199984+00	.1188598+00	−.1164591−01	.2585730−02	.1423400+01	−.2107529+00	.3686494−01	−.1104080−01	−.3322078+01	.6574563+00	−.1627216+00	.6054627−01
2.020	−.3919055+00	.1147325+00	−.1093315−01	.2374505−02	.1385979+01	−.2020381+00	.3443790−01	−.1009579−01	−.3229570+01	.6269918+00	−.1513940+00	.5516118−01
2.060	−.3650796+00	.1108512+00	−.1027983−01	.2184946−02	.1350343+01	−.1939048+00	.3222473−01	−.9251465−02	−.3141841+01	.5987125+00	−.1411080+00	.5036807−01
2.100	−.3394389+00	.1071958+00	−.9679784−02	.2014409−02	.1316367+01	−.1863012+00	.3020221−01	−.8495128−02	−.3058537+01	.5724133+00	−.1317464+00	.4609030−01
2.140	−.3149084+00	.1037483+00	−.9127586−02	.1860620−02	.1283939+01	−.1791813+00	.2835008−01	−.7815922−02	−.2979337+01	.5479126+00	−.1232077+00	.4226258−01
2.180	−.2914192+00	.1004923+00	−.8618480−02	.1721619−02	.1252955+01	−.1725039+00	.2665061−01	−.7204526−02	−.2903950+01	.5250489+00	−.1154031+00	.3882904−01
2.220	−.2689082+00	.9741322−01	−.8148268−02	.1595708−02	.1223322+01	−.1662322+00	.2508825−01	−.6652908−02	−.2832111+01	.5036786+00	−.1082553+00	.3574175−01
2.260	−.2473169+00	.9449776−01	−.7713235−02	.1481417−02	.1194953+01	−.1603332+00	.2364932−01	−.6154131−02	−.2763578+01	.4836732+00	−.1016964+00	.3295946−01
2.300	−.2265917+00	.9173390−01	−.7310091−02	.1377465−02	.1167770+01	−.1547772+00	.2232174−01	−.5702181−02	−.2698132+01	.4649179+00	−.9566676−01	.3044654−01
2.340	−.2066829+00	.8911074−01	−.6935908−02	.1282733−02	.1141700+01	−.1495373+00	.2109484−01	−.5291834−02	−.2635572+01	.4473095+00	−.9011388−01	.2817213−01
2.380	−.1875445+00	.8661836−01	−.6588079−02	.1196243−02	.1116676+01	−.1445893+00	.1995915−01	−.4918532−02	−.2575713+01	.4307555+00	−.8499135−01	.2610942−01
2.420	−.1691339+00	.8424772−01	−.6264279−02	.1117136−02	.1092637+01	−.1399113+00	.1890624−01	−.4578295−02	−.2518386+01	.4151722+00	−.8025808−01	.2423505−01
2.460	−.1514116+00	.8199057−01	−.5962423−02	.1044658−02	.1069526+01	−.1354834+00	.1792863−01	−.4267634−02	−.2463436+01	.4004842+00	−.7587760−01	.2252864−01
2.500	−.1343408+00	.7983935−01	−.5680645−02	.9781429−03	.1047290+01	−.1312876+00	.1701961−01	−.3983484−02	−.2410720+01	.3866234+00	−.7181745−01	.2097233−01
2.600	−.9429550−01	.7488080−01	−.5053431−02	.8342447−03	.9952186+00	−.1217090+00	.1500940−01	−.3372157−02	−.2287861+01	.3551980+00	−.6288622−01	.1763989−01
2.700	−.5764079−01	.7044912−01	−.4519648−02	.7165968−03	.9476527+00	−.1132615+00	.1331412−01	−.2876208−02	−.2176360+01	.3277479+00	−.5540959−01	.1495430−01
2.800	−.2397646−01	.6646815−01	−.4062174−02	.6195746−03	.9040327+00	−.1057683+00	.1187367−01	−.2470200−02	−.2074727+01	.3036194+00	−.4910113−01	.1276953−01
2.900	.7037441−02	.6287534−01	−.3667558−02	.5389222−03	.8638877+00	−.9908634−01	.1064127−01	−.2135039−02	−.1981716+01	.2822883+00	−.4373962−01	.1097673−01
3.000	.3569159−01	.5961890−01	−.3325127−02	.4713824−03	.8268187+00	−.9309849−01	.9580161−02	−.1856224−02	−.1896282+01	.2633301+00	−.3915236−01	.9493780−02
3.100	.6223596−01	.5665562−01	−.3026334−02	.4144368−03	.7924853+00	−.8770842−01	.8661131−02	−.1622623−02	−.1817543+01	.2463982+00	−.3520320−01	.8258014−02
3.200	.8688667−01	.5394921−01	−.2764279−02	.3661187−03	.7605957+00	−.8283616−01	.7860801−02	−.1425605−02	−.1744745+01	.2312075+00	−.3178383−01	.7221138−02
3.300	.1098316+00	.5146896−01	−.2533347−02	.3248787−03	.7308980+00	−.7841485−01	.7160291−02	−.1258413−02	−.1677245+01	.2175215+00	−.2880736−01	.6345564−02
3.400	.1312346+00	.4918877−01	−.2328934−02	.2894859−03	.7031736+00	−.7438827−01	.6544243−02	−.1115715−02	−.1614486+01	.2051428+00	−.2620350−01	.5601780−02
3.500	.1512396+00	.4708629−01	−.2147241−02	.2589547−03	.6772321+00	−.7070881−01	.6000070−02	−.9932667−03	−.1555988+01	.1939057+00	−.2391502−01	.4966420−02
3.600	.1699732+00	.4514232−01	−.1985115−02	.2324901−03	.6529069+00	−.6733599−01	.5517391−02	−.8876635−03	−.1501334+01	.1836702+00	−.2189496−01	.4420838−02
3.700	.1875473+00	.4334026−01	−.1839917−02	.2094464−03	.6300515+00	−.6423512−01	.5087590−02	−.7961568−03	−.1450157+01	.1743170+00	−.2010455−01	.3950048−02
3.800	.2040612+00	.4166568−01	−.1709433−02	.1892957−03	.6085364+00	−.6137640−01	.4703473−02	−.7165118−03	−.1402138+01	.1657446+00	−.1851159−01	.3541923−02
3.900	.2196033+00	.4010601−01	−.1591793−02	.1716041−03	.5882470+00	−.5873408−01	.4359003−02	−.6469002−03	−.1356993+01	.1578656+00	−.1708920−01	.3186583−02
4.000	.2342526+00	.3865024−01	−.1485407−02	.1560126−03	.5690815+00	−.5628579−01	.4049084−02	−.5858171−03	−.1314472+01	.1506047+00	−.1581477−01	.2875933−02
4.100	.2480797+00	.3728869−01	−.1388922−02	.1422226−03	.5509488+00	−.5401207−01	.3769393−02	−.5320171−03	−.1274355+01	.1438968+00	−.1466925−01	.2603301−02
4.200	.2611482+00	.3601283−01	−.1301176−02	.1299845−03	.5337677+00	−.5189586−01	.3516251−02	−.4844641−03	−.1236441+01	.1376850+00	−.1363646−01	.2363156−02
4.300	.2735153+00	.3481509−01	−.1221173−02	.1190889−03	.5174651+00	−.4992220−01	.3286508−02	−.4422917−03	−.1200556+01	.1319198+00	−.1270264−01	.2150892−02
4.400	.2852327+00	.3368876−01	−.1148049−02	.1093587−03	.5019752+00	−.4807789−01	.3077456−02	−.4047721−03	−.1166541+01	.1265579+00	−.1185599−01	.1962656−02
4.500	.2963472+00	.3262785−01	−.1081056−02	.1006442−03	.4872388+00	−.4635127−01	.2886761−02	−.3712909−03	−.1134254+01	.1215609+00	−.1108638−01	.1795203−02
4.600	.3069013+00	.3162702−01	−.1019546−02	.9281771−04	.4732020+00	−.4473199−01	.2712401−02	−.3413274−03	−.1103565+01	.1168952+00	−.1038508−01	.1645796−02
4.700	.3169335+00	.3068147−01	−.9629491−03	.8577031−04	.4598162+00	−.4321084−01	.2552620−02	−.3144387−03	−.1074360+01	.1125310+00	−.9744525−02	.1512112−02
4.800	.3264791+00	.2978690−01	−.9107686−03	.7940851−04	.4470371+00	−.4177961−01	.2405886−02	−.2902460−03	−.1046533+01	.1084417+00	−.9158144−02	.1392174−02
4.900	.3355703+00	.2893942−01	−.8625673−03	.7365186−04	.4348244+00	−.4043093−01	.2270859−02	−.2684249−03	−.1019990+01	.1046038+00	−.8620213−02	.1284289−02
5.000	.3442364+00	.2813555−01	−.8179600−03	.6843088−04	.4231411+00	−.3915822−01	.2146362−02	−.2486958−03	−.9946423+00	.1009961+00	−.8125721−02	.1187009−02
5.100	.3525045+00	.2737209−01	−.7766062−03	.6368535−04	.4119536+00	−.3795554−01	.2031361−02	−.2308177−03	−.9704121+00	.9759977−01	−.7670277−02	.1099083−02
5.200	.3603994+00	.2664618−01	−.7382041−03	.5936295−04	.4012309+00	−.3681754−01	.1924942−02	−.2145814−03	−.9472267+00	.9439788−01	−.7250015−02	.1019433−02
5.300	.3679438+00	.2595520−01	−.7024857−03	.5541802−04	.3909447+00	−.3573938−01	.1826297−02	−.1998055−03	−.9250200+00	.9137517−01	−.6861526−02	.9471245−03
5.400	.3751587+00	.2529676−01	−.6692121−03	.5181068−04	.3810688+00	−.3471669−01	.1734708−02	−.1863315−03	−.9037312+00	.8851788−01	−.6501794−02	.8813445−03
5.500	.3820637+00	.2466870−01	−.6381701−03	.4850594−04	.3715791+00	−.3374548−01	.1649537−02	−.1740211−03	−.8833045+00	.8581359−01	−.6168145−02	.8213848−03
5.600	.3886765+00	.2406902−01	−.6091688−03	.4547303−04	.3624534+00	−.3282215−01	.1570216−02	−.1627531−03	−.8636885+00	.8325102−01	−.5858199−02	.7666260−03
5.800	.4010909+00	.2294767−01	−.5566207−03	.4011743−04	.3452135+00	−.3110623−01	.1427139−02	−.1429306−03	−.8267028+00	.7851111−01	−.5301168−02	.6706057−03
6.000	.4125210+00	.2191983−01	−.5103940−03	.3556239−04	.3292019+00	−.2954583−01	.1302006−02	−.1261535−03	−.7924364+00	.7422686−01	−.4816298−02	.5896769−03
6.200	.4230695+00	.2097460−01	−.4695330−03	.3166496−04	.3142920+00	−.2812158−01	.1192012−02	−.1118651−03	−.7605997+00	.7033890−01	−.4392001−02	.5210281−03

(m = 15)

T^*	$B^{*(0)}$	$B^{*(1)}$	$B^{*(2)}$	$B^{*(3)}$	$T^*\frac{\partial B^{*(0)}}{\partial T^*}$	$T^*\frac{\partial B^{*(1)}}{\partial T^*}$	$T^*\frac{\partial B^{*(2)}}{\partial T^*}$	$T^*\frac{\partial B^{*(3)}}{\partial T^*}$	$T^{*2}\frac{\partial^2 B^{*(0)}}{\partial T^{*2}}$	$T^{*2}\frac{\partial^2 B^{*(1)}}{\partial T^{*2}}$	$T^{*2}\frac{\partial^2 B^{*(2)}}{\partial T^{*2}}$	$T^{*2}\frac{\partial^2 B^{*(3)}}{\partial T^{*2}}$
6.400	.4328256+00	.2010267−01	−.4332534−03	.2831157−04	.3003738+00	−.2681712−01	.1094867−02	−.9962568−04	−.7309427+00	.6679742−01	−.4018879−02	.4624467−03
6.600	.4418671+00	.1929606−01	−.4009076−03	.2541124−04	.2873516+00	−.2561854−01	.1008694−02	−.8908460−04	−.7032485+00	.6356035−01	−.3689253−02	.4121772−03
6.800	.4502622+00	.1854790−01	−.3719568−03	.2289054−04	.2751418+00	−.2451395−01	.9319387−03	−.7996028−04	−.6773283+00	.6059198−01	−.3396805−02	.3688150−03
7.000	.4580707+00	.1785222−01	−.3459503−03	.2068978−04	.2636706+00	−.2349314−01	.8633092−03	−.7202491−04	−.6530165+00	.5786178−01	−.3136299−02	.3312284−03
7.200	.4653456+00	.1720382−01	−.3225089−03	.1876012−04	.2528731+00	−.2254730−01	.8017239−03	−.6509288−04	−.6301677+00	.5534357−01	−.2903375−02	.2984988−03
7.400	.4721339+00	.1659817−01	−.3013118−03	.1706136−04	.2426917+00	−.2166875−01	.7462726−03	−.5901203−04	−.6086533+00	.5301472−01	−.2694377−02	.2698758−03
7.600	.4784772+00	.1603129−01	−.2820860−03	.1556019−04	.2330753+00	−.2085084−01	.6961849−03	−.5365688−04	−.5883596+00	.5085566−01	−.2506224−02	.2447428−03
7.800	.4844127+00	.1549966−01	−.2645987−03	.1422888−04	.2239782+00	−.2008773−01	.6508061−03	−.4892330−04	−.5691853+00	.4884931−01	−.2336306−02	.2225898−03
8.000	.4899737+00	.1500018−01	−.2486496−03	.1304422−04	.2153595+00	−.1937429−01	.6095768−03	−.4472450−04	−.5510402+00	.4698076−01	−.2182401−02	.2029929−03
8.200	.4951901+00	.1453008−01	−.2340665−03	.1198669−04	.2071825+00	−.1870599−01	.5720167−03	−.4098769−04	−.5338433+00	.4523693−01	−.2042612−02	.1855981−03
8.400	.5000887+00	.1408692−01	−.2207001−03	.1103977−04	.1994144+00	−.1807884−01	.5377125−03	−.3765159−04	−.5175221+00	.4360629−01	−.1915307−02	.1701078−03
8.600	.5046937+00	.1366849−01	−.2084209−03	.1018946−04	.1920251+00	−.1748928−01	.5063061−03	−.3466436−04	−.5020111+00	.4207865−01	−.1799080−02	.1562713−03
8.800	.5090270+00	.1327284−01	−.1971159−03	.9423800−05	.1849879+00	−.1693415−01	.4774870−03	−.3198193−04	−.4872515+00	.4064497−01	−.1692714−02	.1438759−03
9.000	.5131086+00	.1289820−01	−.1866862−03	.8732581−05	.1782781+00	−.1641063−01	.4509843−03	−.2956671−04	−.4731898+00	.3929722−01	−.1595151−02	.1327407−03
9.200	.5169562+00	.1254298−01	−.1770450−03	.8107012−05	.1718736+00	−.1591617−01	.4265613−03	−.2738649−04	−.4597775+00	.3802823−01	−.1505471−02	.1227112−03
9.400	.5205865+00	.1220574−01	−.1681161−03	.7539520−05	.1657541+00	−.1544852−01	.4040104−03	−.2541360−04	−.4469706+00	.3683158−01	−.1422866−02	.1136549−03
9.600	.5240144+00	.1188518−01	−.1598320−03	.7023551−05	.1599010+00	−.1500561−01	.3831486−03	−.2362415−04	−.4347289+00	.3570152−01	−.1346630−02	.1054576−03
9.800	.5272534+00	.1158013−01	−.1521329−03	.6553414−05	.1542975+00	−.1458560−01	.3638148−03	−.2199746−04	−.4230158+00	.3463286−01	−.1276139−02	.9802094−04
10.000	.5303162+00	.1128951−01	−.1449657−03	.6124155−05	.1489280+00	−.1418682−01	.3458662−03	−.2051557−04	−.4117977+00	.3362095−01	−.1210844−02	.9125944−04
10.200	.5332142+00	.1101235−01	−.1382834−03	.5731443−05	.1437782+00	−.1380775−01	.3291760−03	−.1916284−04	−.4010438+00	.3266156−01	−.1150258−02	.8509892−04
10.400	.5359579+00	.1074775−01	−.1320436−03	.5371488−05	.1388349+00	−.1344702−01	.3136314−03	−.1792559−04	−.3907259+00	.3175088−01	−.1093949−02	.7947467−04
10.600	.5385571+00	.1049490−01	−.1262087−03	.5040957−05	.1340862+00	−.1310336−01	.2991321−03	−.1679183−04	−.3808179+00	.3088542−01	−.1041534−02	.7433011−04
10.800	.5410207+00	.1025304−01	−.1207449−03	.4736916−05	.1295207+00	−.1277563−01	.2855880−03	−.1575104−04	−.3712958+00	.3006205−01	−.9926691−03	.6961561−04
11.000	.5433568+00	.1002150−01	−.1156218−03	.4456774−05	.1251282+00	−.1246279−01	.2729185−03	−.1479394−04	−.3621375+00	.2927789−01	−.9470482−03	.6528753−04
11.400	.5476769+00	.9586894−02	−.1062907−03	.3959265−05	.1168246+00	−.1187799−01	.2499213−03	−.1309899−04	−.3448319+00	.2781689−01	−.8644681−03	.5764130−04
11.800	.5515718+00	.9186585−02	−.9802671−04	.3532984−05	.1091065+00	−.1134220−01	.2296434−03	−.1165196−04	−.3287545+00	.2648399−01	−.7919133−03	.5113391−04
12.200	.5550884+00	.8816754−02	−.9067492−04	.3165662−05	.1019148+00	−.1084967−01	.2116792−03	−.1040937−04	−.3137791+00	.2526361−01	−.7278554−03	.4556248−04
12.600	.5582673+00	.8474118−02	−.8410734−04	.2847475−05	.9519773−01	−.1039552−01	.1956950−03	−.9336523−05	−.2997959+00	.2414259−01	−.6710429−03	.4076574−04
13.000	.5611437+00	.8155844−02	−.7821748−04	.2570495−05	.8891037−01	−.9975545−02	.1814146−03	−.8405536−05	−.2867096+00	.2310968−01	−.6204432−03	.3661449−04
13.400	.5637483+00	.7859475−02	−.7291619−04	.2328276−05	.8301313−01	−.9586144−02	.1686078−03	−.7593818−05	−.2744365+00	.2215523−01	−.5751991−03	.3300437−04
13.800	.5661081+00	.7582871−02	−.6812839−04	.2115543−05	.7747120−01	−.9224181−02	.1570816−03	−.6882947−05	−.2629032+00	.2127093−01	−.5345943−03	.2985055−04
14.200	.5682468+00	.7324156−02	−.6379052−04	.1927951−05	.7225379−01	−.8886934−02	.1466732−03	−.6257799−05	−.2520448+00	.2044958−01	−.4980268−03	.2708359−04
14.600	.5701853+00	.7081683−02	−.5984848−04	.1761900−05	.6733355−01	−.8572023−02	.1372447−03	−.5705882−05	−.2418037+00	.1968490−01	−.4649879−03	.2464627−04
15.000	.5719421+00	.6854001−02	−.5625600−04	.1614388−05	.6268612−01	−.8277357−02	.1286786−03	−.5216819−05	−.2321288+00	.1897141−01	−.4350458−03	.2249121−04
16.000	.5756430+00	.6341402−02	−.4855652−04	.1311187−05	.5212376−01	−.7617708−02	.1104098−03	−.4215627−05	−.2101311+00	.1738149−01	−.3714467−03	.1809478−04
17.000	.5785189+00	.5897027−02	−.4231963−04	.1079468−05	.4285262−01	−.7050169−02	.9571030−04	−.3454672−05	−.1908062+00	.1602194−01	−.3205532−03	.1476914−04
18.000	.5807315+00	.5508327−02	−.3719971−04	.8993597−06	.3465303−01	−.6557120−02	.8371711−04	−.2866170−05	−.1736960+00	.1484738−01	−.2792375−03	.1220833−04
19.000	.5824058+00	.5165625−02	−.3294701−04	.7572629−06	.2735239−01	−.6125110−02	.7381125−04	−.2404006−05	−.1584417+00	.1382343−01	−.2452697−03	.1020528−04
20.000	.5836395+00	.4861343−02	−.2937750−04	.6436573−06	.2081324−01	−.5743706−02	.6553984−04	−.2036076−05	−.1447580+00	.1292359−01	−.2170271−03	.8616503−05
21.000	.5845101+00	.4589468−02	−.2635326−04	.5517443−06	.1492472−01	−.5404692−02	.5856559−04	−.1739569−05	−.1324154+00	.1212716−01	−.1933076−03	.7340499−05
22.000	.5850794+00	.4345166−02	−.2376933−04	.4765821−06	.9596441−02	−.5101521−02	.5263335−04	−.1497984−05	−.1212270+00	.1141773−01	−.1732059−03	.6304136−05
23.000	.5853974+00	.4124513−02	−.2154471−04	.4145198−06	.4753970−02	−.4828911−02	.4754732−04	−.1299183−05	−.1110391+00	.1078211−01	−.1560308−03	.5453825−05
24.000	.5855050+00	.3924288−02	−.1961615−04	.3628213−06	.3354561−03	−.4582556−02	.4315532−04	−.1134105−05	−.1017244+00	.1020966−01	−.1412469−03	.4749707−05
25.000	.5854355+00	.3741825−02	−.1793363−04	.3194082−06	−.3710919−02	−.4358915−02	.3933768−04	−.9958979−06	−.9317601−01	.9691609−02	−.1284350−03	.4161725−05
26.000	.5852165+00	.3574897−02	−.1645725−04	.2826832−06	−.7428895−02	−.4155047−02	.3599928−04	−.8793098−06	−.8530401−01	.9220754−02	−.1172633−03	.3666926−05
27.000	.5848710+00	.3421634−02	−.1515483−04	.2514046−06	−.1085565−01	−.3968495−02	.3306381−04	−.7802743−06	−.7803197−01	.8791074−02	−.1074663−03	.3247586−05
28.000	.5844182+00	.3280448−02	−.1400022−04	.2245975−06	−.1402297−01	−.3797185−02	.3046946−04	−.6956085−06	−.7129455−01	.8397522−02	−.9882958−04	.2889868−05
29.000	.5838743+00	.3149990−02	−.1297198−04	.2014892−06	−.1695821−01	−.3639360−02	.2816576−04	−.6227971−06	−.6503558−01	.8035829−02	−.9117886−04	.2582867−05
30.000	.5832528+00	.3029100−02	−.1205240−04	.1814620−06	−.1968505−01	−.3493518−02	.2611118−04	−.5598351−06	−.5920649−01	.7702367−02	−.8437103−04	.2317912−05
32.000	.5818221+00	.2812163−02	−.1048275−04	.1487529−06	−.2459317−01	−.3232809−02	.2261751−04	−.4573188−06	−.4867442−01	.7108145−02	−.7283108−04	.1887658−05

(m = 15)

T^*	$B^{*(0)}$	$B^{*(1)}$	$B^{*(2)}$	$B^{*(3)}$	$T^*\frac{\partial B^{*(0)}}{\partial T^*}$	$T^*\frac{\partial B^{*(1)}}{\partial T^*}$	$T^*\frac{\partial B^{*(2)}}{\partial T^*}$	$T^*\frac{\partial B^{*(3)}}{\partial T^*}$	$T^{*2}\frac{\partial^2 B^{*(0)}}{\partial T^{*2}}$	$T^{*2}\frac{\partial^2 B^{*(1)}}{\partial T^{*2}}$	$T^{*2}\frac{\partial^2 B^{*(2)}}{\partial T^{*2}}$	$T^{*2}\frac{\partial^2 B^{*(3)}}{\partial T^{*2}}$
34.000	.5801996+00	.2623117−02	−.9199716−05	.1234952−06	−.2888299−01	−.3006696−02	.1977537−04	−.3784628−06	−.3942005−01	.6594790−02	−.6348018−04	.1557818−05
36.000	.5784395+00	.2456981−02	−.8137777−05	.1036781−06	−.3265970−01	−.2808838−02	.1743320−04	−.3168103−06	−.3122764−01	.6147166−02	−.5580197−04	.1300729−05
38.000	.5765823+00	.2309886−02	−.7249067−05	.8790860−07	−.3600608−01	−.2634337−02	.1548092−04	−.2679088−06	−.2392739−01	.5753652−02	−.4942300−04	.1097386−05
40.000	.5746581+00	.2178779−02	−.6497975−05	.7520139−07	−.3898815−01	−.2479356−02	.1383699−04	−.2286206−06	−.1738380−01	.5405182−02	−.4406796−04	.9344408−06
42.000	.5726901+00	.2061224−02	−.5857566−05	.6484574−07	−.4165924−01	−.2340848−02	.1244009−04	−.1966910−06	−.1148744−01	.5094589−02	−.3953039−04	.8023322−06
44.000	.5706957+00	.1955251−02	−.5307173−05	.5632032−07	−.4406284−01	−.2216362−02	.1124332−04	−.1704715−06	−.6148966−02	.4816131−02	−.3565310−04	.6940910−06
46.000	.5686883+00	.1859252−02	−.4830725−05	.4923677−07	−.4623480−01	−.2103907−02	.1021037−04	−.1487382−06	−.1294700−02	.4565162−02	−.3231476−04	.6045557−06
48.000	.5666783+00	.1771902−02	−.4415577−05	.4330170−07	−.4820490−01	−.2001846−02	.9312801−05	−.1305689−06	.3136649−02	.4337876−02	−.2942055−04	.5298487−06
50.000	.5646735+00	.1692097−02	−.4051670−05	.3829068−07	−.4999810−01	−.1908827−02	.8528037−05	−.1152603−06	.7196485−02	.4131136−02	−.2689551−04	.4670183−06
52.000	.5626802+00	.1618913−02	−.3730921−05	.3403000−07	−.5163548−01	−.1823717−02	.7838018−05	−.1022694−06	.1092824−01	.3942326−02	−.2467978−04	.4137913−06
54.000	.5607029+00	.1551572−02	−.3446780−05	.3038378−07	−.5313493−01	−.1745566−02	.7228144−05	−.9117249−07	.1436886−01	.3769255−02	−.2272514−04	.3683974−06
56.000	.5587453+00	.1489408−02	−.3193889−05	.2724472−07	−.5451176−01	−.1673567−02	.6686513−05	−.8163554−07	.1754997−01	.3610068−02	−.2099232−04	.3294442−06
58.000	.5568100+00	.1431856−02	−.2967837−05	.2452724−07	−.5577913−01	−.1607033−02	.6203348−05	−.7339299−07	.2049882−01	.3463190−02	−.1944917−04	.2958261−06
60.000	.5548990+00	.1378428−02	−.2764961−05	.2216260−07	−.5694841−01	−.1545374−02	.5770555−05	−.6623178−07	.2323896−01	.3327272−02	−.1806913−04	.2666581−06
64.000	.5511555+00	.1282308−02	−.2416989−05	.1827927−07	−.5903101−01	−.1434717−02	.5030202−05	−.5449631−07	.2817261−01	.3083829−02	−.1571362−04	.2189481−06
68.000	.5475216+00	.1198288−02	−.2130832−05	.1525982−07	−.6082465−01	−.1338277−02	.4423393−05	−.4539590−07	.3248628−01	.2872186−02	−.1378835−04	.1820376−06
72.000	.5439999+00	.1124244−02	−.1892683−05	.1287585−07	−.6237970−01	−.1253517−02	.3919916−05	−.3822828−07	.3628504−01	.2686591−02	−.1219498−04	.1530284−06
76.000	.5405901+00	.1058520−02	−.1692382−05	.1096792−07	−.6373574−01	−.1178466−02	.3497627−05	−.3250470−07	.3965168−01	.2522588−02	−.1086165−04	.1299090−06
80.000	.5372900+00	.9998059−03	−.1522318−05	.9422385−08	−.6492423−01	−.1111570−02	.3140000−05	−.2787778−07	.4265229−01	.2376674−02	−.9734896−05	.1112529−06
84.000	.5340964+00	.9470496−03	−.1376700−05	.8156750−08	−.6597051−01	−.1051586−02	.2834501−05	−.2409596−07	.4534025−01	.2246059−02	−.8774284−05	.9602977−07
88.000	.5310057+00	.8993990−03	−.1251058−05	.7110121−08	−.6689522−01	−.9975100−03	.2571489−05	−.2097404−07	.4775919−01	.2128494−02	−.7948782−05	.8348229−07
92.000	.5280137+00	.8561562−03	−.1141899−05	.6236876−08	−.6771527−01	−.9485223−03	.2343446−05	−.1837355−07	.4994505−01	.2022145−02	−.7234262−05	.7304552−07
96.000	.5251160+00	.8167439−03	−.1046461−05	.5502371−08	−.6844471−01	−.9039469−03	.2144447−05	−.1618955−07	.5192772−01	.1925505−02	−.6611737−05	.6429203−07
100.000	.5223085+00	.7806808−03	−.9625377−06	.4879972−08	−.6909525−01	−.8632215−03	.1969767−05	−.1434153−07	.5373228−01	.1837323−02	−.6066106−05	.5689443−07
105.000	.5189196+00	.7397018−03	−.8711443−06	.4228512−08	−.6981236−01	−.8170182−03	.1779893−05	−.1241010−07	.5576944−01	.1737410−02	−.5473943−05	.4917308−07
110.000	.5156572+00	.7026724−03	−.7922129−06	.3689190−08	−.7043748−01	−.7753363−03	.1616226−05	−.1081361−07	.5759566−01	.1647396−02	−.4964348−05	.4279945−07
115.000	.5125138+00	.6690543−03	−.7235756−06	.3238753−08	−.7098376−01	−.7375519−03	.1474162−05	−.9482161−08	.5923940−01	.1565901−02	−.4522683−05	.3749070−07
120.000	.5094824+00	.6384024−03	−.6635161−06	.2859522−08	−.7146202−01	−.7031500−03	.1350061−05	−.8362698−08	.6072428−01	.1491788−02	−.4137410−05	.3303246−07
125.000	.5065565+00	.6103454−03	−.6106614−06	.2537886−08	−.7188132−01	−.6717017−03	.1241018−05	−.7414450−08	.6207013−01	.1424111−02	−.3799338−05	.2926028−07
130.000	.5037299+00	.5845709−03	−.5639026−06	.2263254−08	−.7224923−01	−.6428474−03	.1144695−05	−.6605732−08	.6329363−01	.1362079−02	−.3501070−05	.2604650−07
135.000	.5009970+00	.5608145−03	−.5223362−06	.2027293−08	−.7257217−01	−.6162830−03	.1059187−05	−.5911665−08	.6440901−01	.1305025−02	−.3236604−05	.2329104−07
140.000	.4983525+00	.5388509−03	−.4852202−06	.1823390−08	−.7285558−01	−.5917499−03	.9829340−06	−.5312522−08	.6542837−01	.1252380−02	−.3001023−05	.2091464−07
145.000	.4957915+00	.5184870−03	−.4519405−06	.1646248−08	−.7310412−01	−.5690268−03	.9146473−06	−.4792529−08	.6636216−01	.1203660−02	−.2790274−05	.1885397−07
150.000	.4933094+00	.4995561−03	−.4219855−06	.1491591−08	−.7332178−01	−.5479232−03	.8532545−06	−.4338964−08	.6721937−01	.1158448−02	−.2600990−05	.1705802−07
160.000	.4885654+00	.4654348−03	−.3704000−06	.1236442−08	−.7367782−01	−.5099360−03	.7477009−06	−.3591646−08	.6873436−01	.1077154−02	−.2275994−05	.1410229−07
170.000	.4840903+00	.4355390−03	−.3277652−06	.1036913−08	−.7394622−01	−.4767076−03	.6606382−06	−.3008176−08	.7002480−01	.1006140−02	−.2008388−05	.1179789−07
180.000	.4798578+00	.4091376−03	−.2921215−06	.8785560−09	−.7414417−01	−.4474068−03	.5879851−06	−.2545782−08	.7113047−01	.9435959−03	−.1785420−05	.9974028−08
190.000	.4758450+00	.3856582−03	−.2620176−06	.7512167−09	−.7428497−01	−.4213841−03	.5267269−06	−.2174456−08	.7208255−01	.8881107−03	−.1597689−05	.8511110−08
200.000	.4720321+00	.3646463−03	−.2363605−06	.6476144−09	−.7437908−01	−.3981250−03	.4745979−06	−.1872719−08	.7290580−01	.8385683−03	−.1438144−05	.7323647−08
210.000	.4684016+00	.3457364−03	−.2143142−06	.5624334−09	−.7443476−01	−.3772165−03	.4298689−06	−.1624914−08	.7362013−01	.7940744−03	−.1301413−05	.6349410−08
220.000	.4649382+00	.3286316−03	−.1952305−06	.4917301−09	−.7445864−01	−.3583236−03	.3912015−06	−.1419444−08	.7424169−01	.7539042−03	−.1183343−05	.5542358−08
240.000	.4584600+00	.2989032−03	−.1640195−06	.3825858−09	−.7443146−01	−.3255336−03	.3280732−06	−.1102702−08	.7525727−01	.6842661−03	−.9908700−06	.4299786−08
260.000	.4525059+00	.2739621−03	−.1397716−06	.3038111−09	−.7432972−01	−.2980704−03	.2791340−06	−.8744863−09	.7603368−01	.6260219−03	−.8419307−06	.3405855−08
280.000	.4470029+00	.2527489−03	−.1205560−06	.2454815−09	−.7417533−01	−.2747467−03	.2404248−06	−.7057559−09	.7662797−01	.5766167−03	−.7243144−06	.2745816−08
300.000	.4418917+00	.2344937−03	−.1050680−06	.2013357−09	−.7398359−01	−.2547017−03	.2092773−06	−.5782263−09	.7708123−01	.5342020−03	−.6298095−06	.2247538−08

(m = 18)

T^*	$B^{*(0)}$	$B^{*(1)}$	$B^{*(2)}$	$B^{*(3)}$	$T^*\frac{\partial B^{*(0)}}{\partial T^*}$	$T^*\frac{\partial B^{*(1)}}{\partial T^*}$	$T^*\frac{\partial B^{*(2)}}{\partial T^*}$	$T^*\frac{\partial B^{*(3)}}{\partial T^*}$	$T^{*2}\frac{\partial^2 B^{*(0)}}{\partial T^{*2}}$	$T^{*2}\frac{\partial^2 B^{*(1)}}{\partial T^{*2}}$	$T^{*2}\frac{\partial^2 B^{*(2)}}{\partial T^{*2}}$	$T^{*2}\frac{\partial^2 B^{*(3)}}{\partial T^{*2}}$
.300	−.2120540+02	.3071437+02	−.6855396+02	.2092694+03	.5861919+02	−.1480976+03	.4449520+03	−.1660300+04	−.2724983+03	.9664111+03	−.3577858+04	.1563089+05
.400	−.1041668+02	.8725622+01	−.1213756+02	.2470386+02	.2322975+02	−.3459806+02	.6778122+02	−.1719307+03	−.8906154+02	.1944879+03	−.4798693+03	.1442535+04
.500	−.6514690+01	.3827153+01	−.3723993+01	.5608167+01	.1301943+02	−.1316194+02	.1870643+02	−.3560218+02	−.4397747+02	.6657806+02	−.1211715+03	.2756394+03
.600	−.4572671+01	.2114170+01	−.1544986+01	.1833868+01	.8669428+01	−.6512882+01	.7164832+01	−.1086331+02	−.2682924+02	.3040683+02	−.4341814+02	.7918637+02
.700	−.3425153+01	.1342277+01	−.7729564+00	.7542897+00	.6372644+01	−.3784566+01	.3365309+01	−.4230798+01	−.1851574+02	.1657687+02	−.1935217+02	.2941188+02
.750	−.3012822+01	.1109077+01	−.5747157+00	.5145510+00	.5601747+01	−.3009732+01	.2435596+01	−.2819597+01	−.1587168+02	.1282627+02	−.1369641+02	.1920921+02
.775	−.2834522+01	.1015455+01	−.5005892+00	.4303456+00	.5277698+01	−.2706879+01	.2094985+01	−.2332740+01	−.1478533+02	.1138891+02	−.1165930+02	.1574377+02
.800	−.2671639+01	.9337243+00	−.4386544+00	.3626293+00	.4986662+01	−.2446802+01	.1813897+01	−.1945422+01	−.1382311+02	.1016933+02	−.9995371+01	.1301251+02
.825	−.2522279+01	.8619553+00	−.3865246+00	.3076968+00	.4724028+01	−.2222006+01	.1580098+01	−.1634452+01	−.1296618+02	.9127272+01	−.8624903+01	.1083915+02
.850	−.2384845+01	.7985916+00	−.3423478+00	.2627730+00	.4485982+01	−.2026533+01	.1384206+01	−.1382644+01	−.1219917+02	.8231111+01	−.7487397+01	.9094286+01
.875	−.2257980+01	.7423671+00	−.3046732+00	.2257569+00	.4269344+01	−.1855607+01	.1218959+01	−.1177119+01	−.1150945+02	.7455773+01	−.6536458+01	.7681778+01
.900	−.2140525+01	.6922438+00	−.2723536+00	.1950417+00	.4071447+01	−.1705367+01	.1078679+01	−.1008127+01	−.1088654+02	.6781207+01	−.5736156+01	.6529460+01
.925	−.2031481+01	.6473650+00	−.2444749+00	.1693873+00	.3890037+01	−.1572670+01	.9588872+00	−.8682098+00	−.1032172+02	.6191245+01	−.5058414+01	.5582597+01
.950	−.1929985+01	.6070183+00	−.2203027+00	.1478279+00	.3723200+01	−.1454936+01	.8560261+00	−.7516137+00	−.9807651+01	.5672756+01	−.4481102+01	.4799283+01
.975	−.1835290+01	.5706079+00	−.1992429+00	.1296051+00	.3569299+01	−.1350035+01	.7672441+00	−.6538601+00	−.9338143+01	.5214996+01	−.3986642+01	.4147147+01
1.000	−.1746741+01	.5376325+00	−.1808113+00	.1141190+00	.3426927+01	−.1256195+01	.6902408+00	−.5714351+00	−.8907933+01	.4809118+01	−.3560962+01	.3600979+01
1.020	−.1679939+01	.5134382+00	−.1676893+00	.1033758+00	.3320511+01	−.1188085+01	.6358508+00	−.5146450+00	−.8589017+01	.4516801+01	−.3262240+01	.3226894+01
1.040	−.1616442+01	.4909824+00	−.1558234+00	.9387576−01	.3220147+01	−.1125456+01	.5870004+00	−.4647213+00	−.8290362+01	.4249795+01	−.2995438+01	.2899704+01
1.060	−.1556012+01	.4700998+00	−.1450670+00	.8545029−01	.3125348+01	−.1067743+01	.5430091+00	−.4206972+00	−.8010189+01	.4005339+01	−.2756476+01	.2612600+01
1.080	−.1498436+01	.4506445+00	−.1352932+00	.7795670−01	.3035675+01	−.1014449+01	.5032933+00	−.3817598+00	−.7746916+01	.3781033+01	−.2541878+01	.2359886+01
1.100	−.1443518+01	.4324870+00	−.1263924+00	.7127388−01	.2950733+01	−.9651406+00	.4673507+00	−.3472234+00	−.7499128+01	.3574778+01	−.2348666+01	.2136783+01
1.120	−.1391080+01	.4155123+00	−.1182690+00	.6529868−01	.2870166+01	−.9194331+00	.4347475+00	−.3165069+00	−.7265560+01	.3384739+01	−.2174284+01	.1939258+01
1.140	−.1340960+01	.3996178+00	−.1108398+00	.5994291−01	.2793653+01	−.8769876+00	.4051078+00	−.2891163+00	−.7045076+01	.3209298+01	−.2016528+01	.1763903+01
1.160	−.1293010+01	.3847119+00	−.1040320+00	.5513091−01	.2720901+01	−.8375033+00	.3781050+00	−.2646303+00	−.6836655+01	.3047035+01	−.1873491+01	.1607821+01
1.180	−.1247093+01	.3707125+00	−.9778181−01	.5079761−01	.2651646+01	−.8007129+00	.3534542+00	−.2426882+00	−.6639375+01	.2896691+01	−.1743520+01	.1468545+01
1.200	−.1203084+01	.3575458+00	−.9203300−01	.4688680−01	.2585647+01	−.7663783+00	.3309065+00	−.2229802+00	−.6452403+01	.2757152+01	−.1625178+01	.1343966+01
1.220	−.1160868+01	.3451456+00	−.8673610−01	.4334986−01	.2522684+01	−.7342868+00	.3102437+00	−.2052395+00	−.6274984+01	.2627430+01	−.1517210+01	.1232274+01
1.240	−.1120339+01	.3334519+00	−.8184736−01	.4014453−01	.2462557+01	−.7042480+00	.2912740+00	−.1892356+00	−.6106434+01	.2506643+01	−.1418518+01	.1131912+01
1.260	−.1081399+01	.3224108+00	−.7732801−01	.3723405−01	.2405081+01	−.6760911+00	.2738282+00	−.1747687+00	−.5946129+01	.2394006+01	−.1328139+01	.1041537+01
1.280	−.1043958+01	.3119732+00	−.7314359−01	.3458633−01	.2350089+01	−.6496625+00	.2577570+00	−.1616652+00	−.5793503+01	.2288814+01	−.1245226+01	.9599880+00
1.300	−.1007932+01	.3020947+00	−.6926346−01	.3217326−01	.2297425+01	−.6248238+00	.2429283+00	−.1497741+00	−.5648036+01	.2190439+01	−.1169033+01	.8862551+00
1.320	−.9732430+00	.2927350+00	−.6566027−01	.2997020−01	.2246948+01	−.6014502+00	.2292247+00	−.1389632+00	−.5509256+01	.2098313+01	−.1098900+01	.8194613+00
1.340	−.9398193+00	.2838573+00	−.6230956−01	.2795548−01	.2198526+01	−.5794285+00	.2165417+00	−.1291169+00	−.5376727+01	.2011927+01	−.1034243+01	.7588413+00
1.360	−.9075938+00	.2754279+00	−.5918943−01	.2610999−01	.2152037+01	−.5586566+00	.2047864+00	−.1201338+00	−.5250052+01	.1930821+01	−.9745426+00	.7037258+00
1.380	−.8765040+00	.2674164+00	−.5628022−01	.2441685−01	.2107372+01	−.5390413+00	.1938756+00	−.1119245+00	−.5128864+01	.1854580+01	−.9193376+00	.6535283+00
1.400	−.8464919+00	.2597946+00	−.5356426−01	.2286112−01	.2064425+01	−.5204981+00	.1837351+00	−.1044105+00	−.5012827+01	.1782829+01	−.8682165+00	.6077335+00
1.420	−.8175030+00	.2525368+00	−.5102561−01	.2142953−01	.2023101+01	−.5029502+00	.1742980+00	−.9752208−01	−.4901630+01	.1715226+01	−.8208118+00	.5658876+00
1.440	−.7894868+00	.2456195+00	−.4864990−01	.2011031−01	.1983311+01	−.4863272+00	.1655045+00	−.9119778−01	−.4794985+01	.1651461+01	−.7767948+00	.5275902+00
1.460	−.7623958+00	.2390208+00	−.4642414−01	.1889296−01	.1944972+01	−.4705649+00	.1573006+00	−.8538293−01	−.4692628+01	.1591254+01	−.7358704+00	.4924874+00
1.480	−.7361855+00	.2327209+00	−.4433656−01	.1776811−01	.1908008+01	−.4556046+00	.1496379+00	−.8002898−01	−.4594313+01	.1534347+01	−.6977739+00	.4602655+00
1.500	−.7108145+00	.2267013+00	−.4237649−01	.1672737−01	.1872346+01	−.4413925+00	.1424723+00	−.7509267−01	−.4499813+01	.1480506+01	−.6622667+00	.4306459+00
1.540	−.6624364+00	.2154363+00	−.3880095−01	.1486906−01	.1804668+01	−.4150191+00	.1294774+00	−.6632270−01	−.4321427+01	.1381185+01	−.5981823+00	.3782501+00
1.580	−.6169764+00	.2051045+00	−.3562990−01	.1326673−01	.1741455+01	−.3910950+00	.1180409+00	−.5881056−01	−.4155951+01	.1291783+01	−.5421351+00	.3336227+00
1.620	−.5741823+00	.1956018+00	−.3280709−01	.1187886−01	.1682284+01	−.3693235+00	.1079355+00	−.5234514−01	−.4002069+01	.1211032+01	−.4929097+00	.2954228+00
1.660	−.5338302+00	.1868385+00	−.3028540−01	.1067161−01	.1626782+01	−.3494512+00	.9897259−01	−.4675554−01	−.3858635+01	.1137857+01	−.4495033+00	.2625712+00
1.700	−.4957204+00	.1787367+00	−.2802522−01	.9617217−02	.1574622+01	−.3312610+00	.9099455−01	−.4190256−01	−.3724644+01	.1071345+01	−.4110839+00	.2341938+00
1.740	−.4596741+00	.1712287+00	−.2599304−01	.8692806−02	.1525513+01	−.3145659+00	.8386922−01	−.3767217−01	−.3599216+01	.1010714+01	−.3769574+00	.2095785+00
1.780	−.4255312+00	.1642555+00	−.2416043−01	.7879414−02	.1479198+01	−.2992041+00	.7748513−01	−.3397044−01	−.3481572+01	.9552905+00	−.3465418+00	.1881415+00
1.820	−.3931477+00	.1577652+00	−.2250310−01	.7161244−02	.1435446+01	−.2850352+00	.7174783−01	−.3071957−01	−.3371026+01	.9044973+00	−.3193471+00	.1694021+00
1.860	−.3623936+00	.1517122+00	−.2100026−01	.6525075−02	.1394053+01	−.2719369+00	.6657695−01	−.2785484−01	−.3266967+01	.8578325+00	−.2949582+00	.1529622+00

(m = 18)

T^*	$B^{*(0)}$	$B^{*(1)}$	$B^{*(2)}$	$B^{*(3)}$	$T^*\frac{\partial B^{*(0)}}{\partial T^*}$	$T^*\frac{\partial B^{*(1)}}{\partial T^*}$	$T^*\frac{\partial B^{*(2)}}{\partial T^*}$	$T^*\frac{\partial B^{*(3)}}{\partial T^*}$	$T^{*2}\frac{\partial^2 B^{*(0)}}{\partial T^{*2}}$	$T^{*2}\frac{\partial^2 B^{*(1)}}{\partial T^{*2}}$	$T^{*2}\frac{\partial^2 B^{*(2)}}{\partial T^{*2}}$	$T^{*2}\frac{\partial^2 B^{*(3)}}{\partial T^{*2}}$
1.900	−.3331512+00	.1460564+00	−.1963405−01	.5959791−02	.1354833+01	−.2598021+00	.6190383−01	−.2532213−01	−.3168851+01	.8148601+00	−.2730227+00	.1384904+00
1.940	−.3053142+00	.1407620+00	−.1838901−01	.5456007−02	.1317621+01	−.2485367+00	.5766956−01	−.2307599−01	−.3076194+01	.7752001+00	−.2532395+00	.1257099+00
1.980	−.2787856+00	.1357975+00	−.1725177−01	.5005763−02	.1282267+01	−.2380581+00	.5382341−01	−.2107808−01	−.2988561+01	.7385197+00	−.2353508+00	.1143881+00
2.020	−.2534774+00	.1311346+00	−.1621071−01	.4602286−02	.1248637+01	−.2282931+00	.5032154−01	−.1929593−01	−.2905561+01	.7045265+00	−.2191349+00	.1043289+00
2.060	−.2293090+00	.1267482+00	−.1525568−01	.4239786−02	.1216607+01	−.2191771+00	.4712594−01	−.1770196−01	−.2826841+01	.6729631+00	−.2044003+00	.9536635−01
2.100	−.2062070+00	.1226158+00	−.1437781−01	.3913300−02	.1186068+01	−.2106523+00	.4420352−01	−.1627259−01	−.2752086+01	.6436021+00	−.1909812+00	.8735941−01
2.140	−.1841040+00	.1187170+00	−.1356931−01	.3618558−02	.1156917+01	−.2026676+00	.4152542−01	−.1498767−01	−.2681007+01	.6162418+00	−.1787337+00	.8018776−01
2.180	−.1629380+00	.1150337+00	−.1282332−01	.3351872−02	.1129063+01	−.1951772+00	.3906636−01	−.1382985−01	−.2613344+01	.5907031+00	−.1675321+00	.7374840−01
2.220	−.1426523+00	.1115493+00	−.1213379−01	.3110050−02	.1102421+01	−.1881400+00	.3680415−01	−.1278420−01	−.2548860+01	.5668265+00	−.1572667+00	.6795289−01
2.260	−.1231944+00	.1082491+00	−.1149536−01	.2890319−02	.1076915+01	−.1815192+00	.3471926−01	−.1183779−01	−.2487339+01	.5444694+00	−.1478412+00	.6272503−01
2.300	−.1045159+00	.1051196+00	−.1090330−01	.2690262−02	.1052472+01	−.1752817+00	.3279444−01	−.1097941−01	−.2428585+01	.5235043+00	−.1391711+00	.5799894−01
2.340	−.8657231−01	.1021485+00	−.1035336−01	.2507770−02	.1029029+01	−.1693976+00	.3101442−01	−.1019930−01	−.2372417+01	.5038166+00	−.1311817+00	.5371753−01
2.380	−.6932218−01	.9932468−01	−.9841789−02	.2340992−02	.1006525+01	−.1638400+00	.2936566−01	−.9488955−02	−.2318671+01	.4853033+00	−.1238072+00	.4983115−01
2.420	−.5272723−01	.9663804−01	−.9365219−02	.2188306−02	.9849058+00	−.1585844+00	.2783613−01	−.8840937−02	−.2267195+01	.4678718+00	−.1169891+00	.4629654−01
2.460	−.3675190−01	.9407927−01	−.8920636−02	.2048283−02	.9641194+00	−.1536086+00	.2641508−01	−.8248717−02	−.2217849+01	.4514381+00	−.1106755+00	.4307585−01
2.500	−.2136313−01	.9163993−01	−.8505338−02	.1919660−02	.9441190+00	−.1488925+00	.2509293−01	−.7706555−02	−.2170506+01	.4359264+00	−.1048203+00	.4013595−01
2.600	.1473918−01	.8601461−01	−.7579850−02	.1640970−02	.8972781+00	−.1381217+00	.2216606−01	−.6538402−02	−.2060158+01	.4007449+00	−.9192812−01	.3383193−01
2.700	.4778841−01	.8098372−01	−.6790931−02	.1412620−02	.8544843+00	−.1286176+00	.1969409−01	−.5588724−02	−.1959996+01	.3699979+00	−.8112095−01	.2874122−01
2.800	.7814456−01	.7646162−01	−.6113725−02	.1223909−02	.8152353+00	−.1201828+00	.1759070−01	−.4809693−02	−.1868684+01	.3429579+00	−.7199031−01	.2459174−01
2.900	.1061135+00	.7237798−01	−.5528675−02	.1066719−02	.7791087+00	−.1126571+00	.1578863−01	−.4165343−02	−.1785108+01	.3190411+00	−.6422032−01	.2118028−01
3.000	.1319568+00	.6867448−01	−.5020240−02	.9348302−03	.7457462+00	−.1059100+00	.1423494−01	−.3628307−02	−.1708331+01	.2977751+00	−.5756411−01	.1835326−01
3.100	.1558995+00	.6530249−01	−.4575963−02	.8234200−03	.7148423+00	−.9983354−01	.1288753−01	−.3177538−02	−.1637562+01	.2787735+00	−.5182688−01	.1599328−01
3.200	.1781360+00	.6222111−01	−.4185770−02	.7287176−03	.6861349+00	−.9433831−01	.1171266−01	−.2796690−02	−.1572125+01	.2617185+00	−.4685347−01	.1400973−01
3.300	.1988355+00	.5939574−01	−.3841454−02	.6477466−03	.6593979+00	−.8934948−01	.1068306−01	−.2472947−02	−.1511442+01	.2463464+00	−.4251928−01	.1233197−01
3.400	.2181455+00	.5679694−01	−.3536279−02	.5781385−03	.6344349+00	−.8480409−01	.9776514−02	−.2196174−02	−.1455017+01	.2324371+00	−.3872346−01	.1090443−01
3.500	.2361956+00	.5439950−01	−.3264680−02	.5179934−03	.6110751+00	−.8064884−01	.8974802−02	−.1958295−02	−.1402418+01	.2198056+00	−.3538374−01	.9683088−02
3.600	.2530997+00	.5218173−01	−.3022028−02	.4657766−03	.5891686+00	−.7683832−01	.8262878−02	−.1752822−02	−.1353270+01	.2082955+00	−.3243261−01	.8632724−02
3.700	.2689588+00	.5012489−01	−.2804451−02	.4202395−03	.5685839+00	−.7333368−01	.7628244−02	−.1574507−02	−.1307245+01	.1977738+00	−.2981427−01	.7725010−02
3.800	.2838621+00	.4821269−01	−.2608695−02	.3803602−03	.5492046+00	−.7010149−01	.7060453−02	−.1419079−02	−.1264056+01	.1881269+00	−.2748233−01	.6936982−02
3.900	.2978893+00	.4643091−01	−.2432005−02	.3452968−03	.5309278+00	−.6711286−01	.6550728−02	−.1283036−02	−.1223449+01	.1792572+00	−.2539801−01	.6249913−02
4.000	.3111115+00	.4476712−01	−.2272042−02	.3143521−03	.5136619+00	−.6434271−01	.6091656−02	−.1163495−02	−.1185200+01	.1710807+00	−.2352871−01	.5648434−02
4.100	.3235925+00	.4321036−01	−.2126807−02	.2869455−03	.4973252+00	−.6176916−01	.5676943−02	−.1058064−02	−.1149109+01	.1635243+00	−.2184691−01	.5119860−02
4.200	.3353894+00	.4175096−01	−.1994589−02	.2625911−03	.4818445+00	−.5937308−01	.5301226−02	−.9647531−03	−.1114999+01	.1565246+00	−.2032921−01	.4653668−02
4.300	.3465538+00	.4038038−01	−.1873912−02	.2408801−03	.4671542+00	−.5713764−01	.4959908−02	−.8818937−03	−.1082711+01	.1500261+00	−.1895569−01	.4241081−02
4.400	.3571322+00	.3909101−01	−.1763501−02	.2214671−03	.4531952+00	−.5504805−01	.4649039−02	−.8080834−03	−.1052104+01	.1439802+00	−.1770928−01	.3874742−02
4.500	.3671669+00	.3787606−01	−.1662248−02	.2040591−03	.4399142+00	−.5309116−01	.4365205−02	−.7421372−03	−.1023049+01	.1383443+00	−.1657530−01	.3548459−02
4.600	.3766961+00	.3672949−01	−.1569192−02	.1884064−03	.4272628+00	−.5125536−01	.4105450−02	−.6830494−03	−.9954320+00	.1330804+00	−.1554109−01	.3256994−02
4.700	.3857546+00	.3564586−01	−.1483488−02	.1742955−03	.4151973+00	−.4953030−01	.3867204−02	−.6299631−03	−.9691480+00	.1281553+00	−.1459567−01	.2995901−02
4.800	.3943742+00	.3462028−01	−.1404400−02	.1615429−03	.4036778+00	−.4790671−01	.3648221−02	−.5821454−03	−.9441030+00	.1235391+00	−.1372950−01	.2761390−02
4.900	.4025838+00	.3364835−01	−.1331276−02	.1499905−03	.3926680+00	−.4637634−01	.3446538−02	−.5389670−03	−.9202115+00	.1192055+00	−.1293425−01	.2550214−02
5.000	.4104099+00	.3272610−01	−.1263545−02	.1395018−03	.3821348+00	−.4493175−01	.3260429−02	−.4998860−03	−.8973954+00	.1151308+00	−.1220265−01	.2359589−02
5.100	.4178769+00	.3184994−01	−.1200700−02	.1299583−03	.3720479+00	−.4356626−01	.3088374−02	−.4644338−03	−.8755838+00	.1112938+00	−.1152829−01	.2187113−02
5.200	.4250072+00	.3101659−01	−.1142291−02	.1212567−03	.3623795+00	−.4227386−01	.2929032−02	−.4322039−03	−.8547116+00	.1076756+00	−.1090555−01	.2030710−02
5.300	.4318212+00	.3022308−01	−.1087919−02	.1133071−03	.3531039+00	−.4104909−01	.2781213−02	−.4028430−03	−.8347194+00	.1042589+00	−.1032945−01	.1888578−02
5.400	.4383379+00	.2946670−01	−.1037228−02	.1060305−03	.3441978+00	−.3988702−01	.2643861−02	−.3760425−03	−.8155527+00	.1010285+00	−.9795613−02	.1759150−02
5.500	.4445749+00	.2874499−01	−.9898983−03	.9935796−04	.3356394+00	−.3878317−01	.2516037−02	−.3515326−03	−.7971612+00	.9797034−01	−.9300119−02	.1641059−02
5.600	.4505482+00	.2805569−01	−.9456457−03	.9322849−04	.3274088+00	−.3773346−01	.2396903−02	−.3290767−03	−.7794988+00	.9507175−01	−.8839499−02	.1533109−02
5.800	.4617627+00	.2676616−01	−.8653726−03	.8239022−04	.3118582+00	−.3578196−01	.2181780−02	−.2895181−03	−.7461943+00	.8970845−01	−.8010822−02	.1343555−02
6.000	.4720888+00	.2558349−01	−.7946516−03	.7315578−04	.2974137+00	−.3400647−01	.1993371−02	−.2559766−03	−.7153358+00	.8485859−01	−.7288515−02	.1183505−02
6.200	.4816190+00	.2449525−01	−.7320502−03	.6524112−04	.2839614+00	−.3238514−01	.1827527−02	−.2273612−03	−.6866629+00	.8045543−01	−.6655610−02	.1047504−02

(m = 18)

T^*	$B^{*(0)}$	$B^{*(1)}$	$B^{*(2)}$	$B^{*(3)}$	$T^*\frac{\partial B^{*(0)}}{\partial T^*}$	$T^*\frac{\partial B^{*(1)}}{\partial T^*}$	$T^*\frac{\partial B^{*(2)}}{\partial T^*}$	$T^*\frac{\partial B^{*(3)}}{\partial T^*}$	$T^{*2}\frac{\partial^2 B^{*(0)}}{\partial T^{*2}}$	$T^{*2}\frac{\partial^2 B^{*(1)}}{\partial T^{*2}}$	$T^{*2}\frac{\partial^2 B^{*(2)}}{\partial T^{*2}}$	$T^{*2}\frac{\partial^2 B^{*(3)}}{\partial T^{*2}}$
6.400	.4904338+00	.2349086−01	−.6763913−03	.5842016−04	.2714023+00	−.3089950−01	.1680863−02	−.2028083−03	−.6599508+00	.7644298−01	−.6098329−02	.9312524−03
6.600	.4986035+00	.2256123−01	−.6267012−03	.5251149−04	.2596503+00	−.2953385−01	.1550595−02	−.1816283−03	−.6350048+00	.7277395−01	−.5605402−02	.8313335−03
6.800	.5061894+00	.2169850−01	−.5821693−03	.4736847−04	.2486300+00	−.2827475−01	.1434419−02	−.1632666−03	−.6116549+00	.6940814−01	−.5167542−02	.7450090−03
7.000	.5132457+00	.2089589−01	−.5421165−03	.4287170−04	.2382752+00	−.2711067−01	.1330416−02	−.1472734−03	−.5897523+00	.6631123−01	−.4777052−02	.6700688−03
7.200	.5198201+00	.2014748−01	−.5059706−03	.3892335−04	.2285273+00	−.2603163−01	.1236978−02	−.1332822−03	−.5691661+00	.6345370−01	−.4427508−02	.6047166−03
7.400	.5259549+00	.1944808−01	−.4732469−03	.3544274−04	.2193345+00	−.2502898−01	.1152750−02	−.1209918−03	−.5497810+00	.6081011−01	−.4113520−02	.5474829−03
7.600	.5316878+00	.1879314−01	−.4435330−03	.3236296−04	.2106508+00	−.2409516−01	.1076584−02	−.1101534−03	−.5314945+00	.5835839−01	−.3830543−02	.4971582−03
7.800	.5370524+00	.1817866−01	−.4164759−03	.2962822−04	.2024351+00	−.2322359−01	.1007504−02	−.1005604−03	−.5142155+00	.5607931−01	−.3574722−02	.4527412−03
8.000	.5420786+00	.1760107−01	−.3917724−03	.2719175−04	.1946505+00	−.2240844−01	.9446748−03	−.9204029−04	−.4978628+00	.5395605−01	−.3342772−02	.4133981−03
8.200	.5467934+00	.1705724−01	−.3691611−03	.2501416−04	.1872640+00	−.2164460−01	.8873780−03	−.8444829−04	−.4823638+00	.5197386−01	−.3131884−02	.3784318−03
8.400	.5512211+00	.1654436−01	−.3484154−03	.2306211−04	.1802460+00	−.2092754−01	.8349952−03	−.7766228−04	−.4676530+00	.5011975−01	−.2939642−02	.3472557−03
8.600	.5553835+00	.1605990−01	−.3293383−03	.2130726−04	.1735695+00	−.2025324−01	.7869906−03	−.7157879−04	−.4536716+00	.4838221−01	−.2763960−02	.3193748−03
8.800	.5593003+00	.1560164−01	−.3117577−03	.1972542−04	.1672103+00	−.1961809−01	.7428985−03	−.6610984−04	−.4403667+00	.4675105−01	−.2603033−02	.2943687−03
9.000	.5629896+00	.1516753−01	−.2955232−03	.1829587−04	.1611463+00	−.1901891−01	.7023126−03	−.6118025−04	−.4276901+00	.4521719−01	−.2455291−02	.2718795−03
9.200	.5664676+00	.1475577−01	−.2805025−03	.1700079−04	.1553575+00	−.1845282−01	.6648775−03	−.5672555−04	−.4155983+00	.4377255−01	−.2319364−02	.2516011−03
9.400	.5697490+00	.1436472−01	−.2665790−03	.1582478−04	.1498257+00	−.1791724−01	.6302810−03	−.5269025−04	−.4040516+00	.4240987−01	−.2194051−02	.2332706−03
9.600	.5728474+00	.1399287−01	−.2536497−03	.1475451−04	.1445341+00	−.1740984−01	.5982481−03	−.4902644−04	−.3930138+00	.4112266−01	−.2078301−02	.2166616−03
9.800	.5757752+00	.1363888−01	−.2416234−03	.1377841−04	.1394675+00	−.1692854−01	.5685360−03	−.4569257−04	−.3824520+00	.3990506−01	−.1971184−02	.2015782−03
10.000	.5785436+00	.1330152−01	−.2304187−03	.1288637−04	.1346119+00	−.1647142−01	.5409297−03	−.4265254−04	−.3723360+00	.3875180−01	−.1871881−02	.1878506−03
10.200	.5811630+00	.1297966−01	−.2199634−03	.1206956−04	.1299544+00	−.1603678−01	.5152380−03	−.3987485−04	−.3626380+00	.3765811−01	−.1779666−02	.1753309−03
10.400	.5836429+00	.1267230−01	−.2101929−03	.1132023−04	.1254832+00	−.1562303−01	.4912908−03	−.3733195−04	−.3533326+00	.3661967−01	−.1693893−02	.1638902−03
10.600	.5859920+00	.1237848−01	−.2010494−03	.1063159−04	.1211875+00	−.1522876−01	.4689362−03	−.3499968−04	−.3443964+00	.3563256−01	−.1613990−02	.1534156−03
10.800	.5882186+00	.1209735−01	−.1924808−03	.9997614−05	.1170570+00	−.1485266−01	.4480384−03	−.3285678−04	−.3358079+00	.3469321−01	−.1539442−02	.1438079−03
11.000	.5903299+00	.1182813−01	−.1844406−03	.9413007−05	.1130826+00	−.1449355−01	.4284754−03	−.3088452−04	−.3275470+00	.3379837−01	−.1469791−02	.1349798−03
11.400	.5942339+00	.1132255−01	−.1697808−03	.8373613−05	.1055679+00	−.1382198−01	.3929268−03	−.2738748−04	−.3119357+00	.3213057−01	−.1343578−02	.1193638−03
11.800	.5977533+00	.1085658−01	−.1567794−03	.7481709−05	.9858153−01	−.1320638−01	.3615372−03	−.2439719−04	−.2974309+00	.3060826−01	−.1232530−02	.1060515−03
12.200	.6009305+00	.1042584−01	−.1451977−03	.6712079−05	.9207001−01	−.1264019−01	.3336910−03	−.2182545−04	−.2839187+00	.2921385−01	−.1134354−02	.9463567−04
12.600	.6038021+00	.1002655−01	−.1348381−03	.6044500−05	.8598683−01	−.1211787−01	.3088814−03	−.1960178−04	−.2713005+00	.2793239−01	−.1047168−02	.8479216−04
13.000	.6063999+00	.9655446−02	−.1255361−03	.5462628−05	.8029140−01	−.1163462−01	.2866882−03	−.1766942−04	−.2594903+00	.2675114−01	−.9694169−03	.7626071−04
13.400	.6087517+00	.9309696−02	−.1171537−03	.4953153−05	.7494808−01	−.1118634−01	.2667606−03	−.1598235−04	−.2484128+00	.2565916−01	−.8998099−03	.6883087−04
13.800	.6108820+00	.8986836−02	−.1095745−03	.4505169−05	.6992548−01	−.1076947−01	.2488043−03	−.1450297−04	−.2380019+00	.2464702−01	−.8372657−03	.6233128−04
14.200	.6128121+00	.8684706−02	−.1027000−03	.4109680−05	.6519582−01	−.1038088−01	.2325708−03	−.1320036−04	−.2281991+00	.2370656−01	−.7808750−03	.5662145−04
14.600	.6145609+00	.8401404−02	−.9644608−04	.3759222−05	.6073445−01	−.1001788−01	.2178492−03	−.1204897−04	−.2189526+00	.2283064−01	−.7298688−03	.5158550−04
15.000	.6161452+00	.8135256−02	−.9074086−04	.3447568−05	.5651942−01	−.9678068−02	.2044596−03	−.1102752−04	−.2102164+00	.2201305−01	−.6835930−03	.4712728−04
16.000	.6194801+00	.7535581−02	−.7849267−04	.2805905−05	.4693567−01	−.8916829−02	.1758537−03	−.8932545−05	−.1903492+00	.2019000−01	−.5851244−03	.3801432−04
17.000	.6220676+00	.7015150−02	−.6854813−04	.2314389−05	.3851824−01	−.8261249−02	.1527804−03	−.7336180−05	−.1728911+00	.1862974−01	−.5061323−03	.3110207−04
18.000	.6240542+00	.6559454−02	−.6036704−04	.1931547−05	.3106897−01	−.7691191−02	.1339122−03	−.6098685−05	−.1574295+00	.1728064−01	−.4418574−03	.2576609−04
19.000	.6255529+00	.6157293−02	−.5355807−04	.1628918−05	.2443215−01	−.7191271−02	.1182947−03	−.5124734−05	−.1436411+00	.1610359−01	−.3888984−03	.2158254−04
20.000	.6266521+00	.5799887−02	−.4783226−04	.1386538−05	.1848374−01	−.6749543−02	.1052280−03	−.4347802−05	−.1312689+00	.1506843−01	−.3447752−03	.1825701−04
21.000	.6274220+00	.5480266−02	−.4297262−04	.1190117−05	.1312368−01	−.6356598−02	.9418976−04	−.3720515−05	−.1201060+00	.1415156−01	−.3076466−03	.1558074−04
22.000	.6279187+00	.5192821−02	−.3881368−04	.1029248−05	.8270375−02	−.6004930−02	.8478400−04	−.3208525−05	−.1099841+00	.1333427−01	−.2761234−03	.1340295−04
23.000	.6281874+00	.4932993−02	−.3522753−04	.8962281−06	.3856636−02	−.5688480−02	.7670637−04	−.2786518−05	−.1007648+00	.1260153−01	−.2491427−03	.1161294−04
24.000	.6282651+00	.4697040−02	−.3211406−04	.7852743−06	−.1733935−03	−.5402307−02	.6971988−04	−.2435562−05	−.9233300−01	.1194117−01	−.2258800−03	.1012820−04
25.000	.6281821+00	.4481860−02	−.2939406−04	.6919874−06	−.3866513−02	−.5142344−02	.6363784−04	−.2141307−05	−.8459267−01	.1134320−01	−.2056886−03	.8886394−05
26.000	.6279634+00	.4284863−02	−.2700416−04	.6129805−06	−.7262231−02	−.4905212−02	.5831165−04	−.1892745−05	−.7746265−01	.1079938−01	−.1880556−03	.7839828−05
27.000	.6276298+00	.4103869−02	−.2489324−04	.5456173−06	−.1039413−01	−.4688084−02	.5362186−04	−.1681334−05	−.7087403−01	.1030283−01	−.1725700−03	.6951613−05
28.000	.6271988+00	.3937030−02	−.2301965−04	.4878252−06	−.1329095−01	−.4488576−02	.4947161−04	−.1500380−05	−.6476794−01	.9847765−02	−.1588999−03	.6192908−05
29.000	.6266849+00	.3782771−02	−.2134924−04	.4379594−06	−.1597742−01	−.4304664−02	.4578170−04	−.1344584−05	−.5909372−01	.9429314−02	−.1467743−03	.5540946−05
30.000	.6261007+00	.3639740−02	−.1985374−04	.3947030−06	−.1847491−01	−.4134619−02	.4248687−04	−.1209717−05	−.5380758−01	.9043319−02	−.1359711−03	.4977595−05
32.000	.6247614+00	.3382848−02	−.1729721−04	.3239678−06	−.2297503−01	−.3830399−02	.3687484−04	−.9897980−06	−.4425208−01	.8354963−02	−.1176261−03	.4061264−05

(m = 18)

T^*	$B^{*(0)}$	$B^{*(1)}$	$B^{*(2)}$	$B^{*(3)}$	$T^*\frac{\partial B^{*(0)}}{\partial T^*}$	$T^*\frac{\partial B^{*(1)}}{\partial T^*}$	$T^*\frac{\partial B^{*(2)}}{\partial T^*}$	$T^*\frac{\partial B^{*(3)}}{\partial T^*}$	$T^{*2}\frac{\partial^2 B^{*(0)}}{\partial T^{*2}}$	$T^{*2}\frac{\partial^2 B^{*(1)}}{\partial T^{*2}}$	$T^{*2}\frac{\partial^2 B^{*(2)}}{\partial T^{*2}}$	$T^{*2}\frac{\partial^2 B^{*(3)}}{\partial T^{*2}}$
34.000	.6232478+00	.3158739−02	−.1520353−04	.2692626−06	−.2691402−01	−.3566274−02	.3229965−04	−.8203190−06	−.3585046−01	.7759704−02	−.1027275−03	.3357318−05
36.000	.6216090+00	.2961586−02	−.1346761−04	.2262812−06	−.3038704−01	−.3334926−02	.2852188−04	−.6875893−06	−.2840814−01	.7240183−02	−.9046827−04	.2807585−05
38.000	.6198819+00	.2786859−02	−.1201251−04	.1920360−06	−.3346899−01	−.3130700−02	.2536718−04	−.5821483−06	−.2177196−01	.6783060−02	−.8026356−04	.2372013−05
40.000	.6180939+00	.2630980−02	−.1078089−04	.1644094−06	−.3621968−01	−.2949158−02	.2270622−04	−.4973152−06	−.1581966−01	.6377923−02	−.7168119−04	.2022410−05
42.000	.6162660+00	.2491091−02	−.9729291−05	.1418720−06	−.3868739−01	−.2786775−02	.2044147−04	−.4282814−06	−.1045250−01	.6016533−02	−.6439645−04	.1738545−05
44.000	.6144141+00	.2364880−02	−.8824326−05	.1233003−06	−.4091155−01	−.2640713−02	.1849827−04	−.3715254−06	−.5589842−02	.5692285−02	−.5816168−04	.1505642−05
46.000	.6125503+00	.2250456−02	−.8039984−05	.1078561−06	−.4292463−01	−.2508665−02	.1681871−04	−.3244281−06	−.1165186−02	.5399829−02	−.5278535−04	.1312742−05
48.000	.6106842+00	.2146263−02	−.7355768−05	.9490562−07	−.4475366−01	−.2388735−02	.1535731−04	−.2850140−06	.2876799−02	.5134786−02	−.4811755−04	.1151596−05
50.000	.6088230+00	.2051001−02	−.6755353−05	.8396347−07	−.4642128−01	−.2279351−02	.1407797−04	−.2517738−06	.6582527−02	.4893536−02	−.4403958−04	.1015917−05
52.000	.6069721+00	.1963582−02	−.6225606−05	.7465350−07	−.4794661−01	−.2179200−02	.1295174−04	−.2235411−06	.9991221−02	.4673066−02	−.4045651−04	.9008557−06
54.000	.6051360+00	.1883088−02	−.5755865−05	.6668124−07	−.4934592−01	−.2087177−02	.1195520−04	−.1994045−06	.1313625−01	.4470845−02	−.3729172−04	.8026313−06
56.000	.6033178+00	.1808736−02	−.5337405−05	.5981386−07	−.5063310−01	−.2002344−02	.1106921−04	−.1786450−06	.1604619−01	.4284734−02	−.3448280−04	.7182658−06
58.000	.6015200+00	.1739857−02	−.4963029−05	.5386564−07	−.5182011−01	−.1923903−02	.1027804−04	−.1606901−06	.1874565−01	.4112911−02	−.3197853−04	.6453924−06
60.000	.5997445+00	.1675875−02	−.4626759−05	.4868716−07	−.5291730−01	−.1851166−02	.9568669−05	−.1450801−06	.2125593−01	.3953819−02	−.2973654−04	.5821139−06
64.000	.5962652+00	.1560673−02	−.4049331−05	.4017720−07	−.5487704−01	−.1720518−02	.8353535−05	−.1194757−06	.2578076−01	.3668636−02	−.2590410−04	.4784947−06
68.000	.5928862+00	.1459864−02	−.3573798−05	.3355506−07	−.5657158−01	−.1606534−02	.7355873−05	−.9959810−07	.2974307−01	.3420447−02	−.2276574−04	.3982199−06
72.000	.5896100+00	.1370935−02	−.3177525−05	.2832300−07	−.5804681−01	−.1506253−02	.6526795−05	−.8392649−07	.3323789−01	.3202588−02	−.2016386−04	.3350514−06
76.000	.5864362+00	.1291924−02	−.2843827−05	.2413315−07	−.5933879−01	−.1417375−02	.5830396−05	−.7140100−07	.3634010−01	.3009894−02	−.1798308−04	.2846518−06
80.000	.5833630+00	.1221276−02	−.2560188−05	.2073736−07	−.6047627−01	−.1338081−02	.5239834−05	−.6126734−07	.3910954−01	.2838302−02	−.1613740−04	.2439413−06
84.000	.5803875+00	.1157743−02	−.2317070−05	.1795527−07	−.6148239−01	−.1266920−02	.4734719−05	−.5297867−07	.4159456−01	.2684570−02	−.1456166−04	.2106916−06
88.000	.5775063+00	.1100313−02	−.2107104−05	.1565367−07	−.6237602−01	−.1202715−02	.4299341−05	−.4613188−07	.4383464−01	.2546086−02	−.1320575−04	.1832631−06
92.000	.5747157+00	.1048155−02	−.1924521−05	.1373267−07	−.6317266−01	−.1144505−02	.3921436−05	−.4042534−07	.4586239−01	.2420718−02	−.1203069−04	.1604313−06
96.000	.5720117+00	.1000582−02	−.1764756−05	.1211639−07	−.6388517−01	−.1091500−02	.3591321−05	−.3563025−07	.4770489−01	.2306710−02	−.1100574−04	.1412686−06
100.000	.5693906+00	.9570218−03	−.1624156−05	.1074644−07	−.6452429−01	−.1043037−02	.3301268−05	−.3157088−07	.4938488−01	.2202606−02	−.1010639−04	.1250638−06
105.000	.5662249+00	.9074866−03	−.1470917−05	.9312151−08	−.6523366−01	−.9880142−03	.2985665−05	−.2732628−07	.5128533−01	.2084564−02	−.9129229−05	.1081389−06
110.000	.5631756+00	.8626899−03	−.1338461−05	.8124466−08	−.6585713−01	−.9383350−03	.2713334−05	−.2381609−07	.5299300−01	.1978130−02	−.8287296−05	.9415891−07
115.000	.5602357+00	.8219894−03	−.1223189−05	.7132327−08	−.6640677−01	−.8932660−03	.2476713−05	−.2088742−07	.5453374−01	.1881695−02	−.7556768−05	.8250771−07
120.000	.5573990+00	.7848533−03	−.1122248−05	.6296891−08	−.6689260−01	−.8522010−03	.2269818−05	−.1842411−07	.5592904−01	.1793929−02	−.6918836−05	.7271789−07
125.000	.5546594+00	.7508374−03	−.1033356−05	.5588246−08	−.6732294−01	−.8146351−03	.2087871−05	−.1633686−07	.5719690−01	.1713728−02	−.6358497−05	.6443054−07
130.000	.5520114+00	.7195682−03	−.9546656−06	.4983098−08	−.6770482−01	−.7801441−03	.1927014−05	−.1455623−07	.5835253−01	.1640166−02	−.5863666−05	.5736688−07
135.000	.5494497+00	.6907292−03	−.8846713−06	.4463124−08	−.6804417−01	−.7483696−03	.1784108−05	−.1302763−07	.5940885−01	.1572462−02	−.5424519−05	.5130812−07
140.000	.5469695+00	.6640503−03	−.8221356−06	.4013770−08	−.6834603−01	−.7190063−03	.1656576−05	−.1170780−07	.6037691−01	.1509952−02	−.5033007−05	.4608093−07
145.000	.5445664+00	.6393001−03	−.7660337−06	.3623378−08	−.6861473−01	−.6917928−03	.1542289−05	−.1056209−07	.6126621−01	.1452066−02	−.4682481−05	.4154673−07
150.000	.5422361+00	.6162786−03	−.7155108−06	.3282532−08	−.6885397−01	−.6665040−03	.1439472−05	−.9562569−08	.6208498−01	.1398317−02	−.4367415−05	.3759384−07
160.000	.5377790+00	.5747513−03	−.6284455−06	.2720218−08	−.6925656−01	−.6209456−03	.1262537−05	−.7915350−08	.6353853−01	.1301592−02	−.3825886−05	.3108570−07
170.000	.5335704+00	.5383297−03	−.5564254−06	.2280506−08	−.6957481−01	−.5810523−03	.1116433−05	−.6628986−08	.6478457−01	.1217007−02	−.3379394−05	.2600937−07
180.000	.5295863+00	.5061347−03	−.4961680−06	.1931560−08	−.6982481−01	−.5458393−03	.9943847−06	−.5609382−08	.6585949−01	.1142436−02	−.3006928−05	.2199013−07
190.000	.5258056+00	.4774774−03	−.4452403−06	.1650999−08	−.7001907−01	−.5145367−03	.8913817−06	−.4790497−08	.6679182−01	.1076218−02	−.2692977−05	.1876529−07
200.000	.5222102+00	.4518102−03	−.4018077−06	.1422774−08	−.7016743−01	−.4865336−03	.8036534−06	−.4125033−08	.6760428−01	.1017040−02	−.2425891−05	.1614701−07
210.000	.5187839+00	.4286923−03	−.3644656−06	.1235163−08	−.7027771−01	−.4613395−03	.7283188−06	−.3578498−08	.6831515−01	.9638471−03	−.2196778−05	.1399846−07
220.000	.5155126+00	.4077653−03	−.3321241−06	.1079471−08	−.7035622−01	−.4385560−03	.6631455−06	−.3125332−08	.6893929−01	.9157844−03	−.1998762−05	.1221832−07
240.000	.5093867+00	.3713558−03	−.2791931−06	.8392094−09	−.7043741−01	−.3989700−03	.5566400−06	−.2426798−08	.6997408−01	.8323700−03	−.1675586−05	.9477108−08
260.000	.5037481+00	.3407695−03	−.2380360−06	.6658854−09	−.7044183−01	−.3657690−03	.4739753−06	−.1923570−08	.7078355−01	.7625050−03	−.1425147−05	.7504779−08
280.000	.4985294+00	.3147234−03	−.2053966−06	.5376127−09	−.7039068−01	−.3375364−03	.4085224−06	−.1551592−08	.7142046−01	.7031655−03	−.1227127−05	.6048451−08
300.000	.4936759+00	.2922844−03	−.1790722−06	.4405843−09	−.7029889−01	−.3132441−03	.3558074−06	−.1270519−08	.7192298−01	.6521610−03	−.1067839−05	.4949085−08

(m = 24)

T^*	$B^{*(0)}$	$B^{*(1)}$	$B^{*(2)}$	$B^{*(3)}$	$T^*\frac{\partial B^{*(0)}}{\partial T^*}$	$T^*\frac{\partial B^{*(1)}}{\partial T^*}$	$T^*\frac{\partial B^{*(2)}}{\partial T^*}$	$T^*\frac{\partial B^{*(3)}}{\partial T^*}$	$T^{*2}\frac{\partial^2 B^{*(0)}}{\partial T^{*2}}$	$T^{*2}\frac{\partial^2 B^{*(1)}}{\partial T^{*2}}$	$T^{*2}\frac{\partial^2 B^{*(2)}}{\partial T^{*2}}$	$T^{*2}\frac{\partial^2 B^{*(3)}}{\partial T^{*2}}$
.300	−.1794584+02	.3594153+02	−.1153001+03	.5197400+03	.4957408+02	−.1723089+03	.7421625+03	−.4076358+04	−.2294472+03	.1121002+04	−.5934254+04	.3804531+05
.400	−.8799016+01	.1029929+02	−.2075408+02	.6305114+02	.1976169+02	−.4050556+02	.1146331+03	−.4325930+03	−.7536302+02	.2267450+03	−.8057004+03	.3591109+04
.500	−.5472878+01	.4551343+01	−.6458740+01	.1464080+02	.1112450+02	−.1549468+02	.3201639+02	−.9142552+02	−.3736669+02	.7797563+02	−.2056035+03	.6992436+03
.600	−.3810922+01	.2530452+01	−.2713016+01	.4880402+01	.7432031+01	−.7704739+01	.1239195+02	−.2838833+02	−.2287233+02	.3575892+02	−.7435987+02	.2041624+03
.700	−.2825992+01	.1615514+01	−.1372319+01	.2041055+01	.5476885+01	−.4496566+01	.5875153+01	−.1122589+02	−.1582763+02	.1956713+02	−.3342053+02	.7691655+02
.750	−.2471435+01	.1338177+01	−.1025525+01	.1402877+01	.4819420+01	−.3583055+01	.4270474+01	−.7533580+01	−.1358315+02	.1516603+02	−.2374474+02	.5056244+02
.775	−.2317999+01	.1226669+01	−.8954227+00	.1177530+01	.4542826+01	−.3225573+01	.3680916+01	−.6253514+01	−.1266025+02	.1347764+02	−.2025082+02	.4157000+02
.800	−.2177764+01	.1129233+01	−.7864944+00	.9957141+00	.4294285+01	−.2918353+01	.3193527+01	−.5232089+01	−.1184240+02	.1204414+02	−.1739242+02	.3446271+02
.825	−.2049114+01	.1043595+01	−.6946263+00	.8477511+00	.4069890+01	−.2652616+01	.2787433+01	−.4409597+01	−.1111369+02	.1081851+02	−.1503451+02	.2879165+02
.850	−.1930686+01	.9679191+00	−.6166207+00	.7263705+00	.3866408+01	−.2421377+01	.2446608+01	−.3741678+01	−.1046115+02	.9763828+01	−.1307443+02	.2422646+02
.875	−.1821322+01	.9007118+00	−.5499683+00	.6260529+00	.3681144+01	−.2219036+01	.2158624+01	−.3195005+01	−.9874097+01	.8850786+01	−.1143341+02	.2052119+02
.900	−.1720030+01	.8407472+00	−.4926823+00	.5425660+00	.3511834+01	−.2041063+01	.1913756+01	−.2744280+01	−.9343685+01	.8055938+01	−.1005033+02	.1749072+02
.925	−.1625956+01	.7870127+00	−.4431767+00	.4726342+00	.3356566+01	−.1883767+01	.1704321+01	−.2370111+01	−.8862532+01	.7360375+01	−.8877383+01	.1499437+02
.950	−.1538365+01	.7386661+00	−.4001758+00	.4137000+00	.3213715+01	−.1744116+01	.1524207+01	−.2057499+01	−.8424435+01	.6748727+01	−.7876854+01	.1292418+02
.975	−.1456614+01	.6950022+00	−.3626454+00	.3637504+00	.3081889+01	−.1619608+01	.1368509+01	−.1794742+01	−.8024156+01	.6208416+01	−.7018738+01	.1119657+02
1.000	−.1380145+01	.6554278+00	−.3297421+00	.3211886+00	.2959896+01	−.1508160+01	.1233266+01	−.1572639+01	−.7657241+01	.5729079+01	−.6278991+01	.9746306+01
1.020	−.1322440+01	.6263722+00	−.3062811+00	.2915922+00	.2868682+01	−.1427225+01	.1137612+01	−.1419276+01	−.7385156+01	.5383689+01	−.5759253+01	.8750930+01
1.040	−.1267577+01	.5993888+00	−.2850378+00	.2653672+00	.2782633+01	−.1352768+01	.1051602+01	−.1284199+01	−.7130282+01	.5068069+01	−.5294567+01	.7878773+01
1.060	−.1215352+01	.5742814+00	−.2657555+00	.2420617+00	.2701333+01	−.1284122+01	.9740592+00	−.1164861+01	−.6891113+01	.4778985+01	−.4877943+01	.7112118+01
1.080	−.1165581+01	.5508770+00	−.2482121+00	.2212928+00	.2624410+01	−.1220704+01	.9039742+00	−.1059119+01	−.6666308+01	.4513619+01	−.4503418+01	.6436126+01
1.100	−.1118098+01	.5290219+00	−.2322152+00	.2027351+00	.2551527+01	−.1162002+01	.8404776+00	−.9651579+00	−.6454669+01	.4269511+01	−.4165881+01	.5838320+01
1.120	−.1072750+01	.5085795+00	−.2175972+00	.1861107+00	.2482382+01	−.1107562+01	.7828177+00	−.8814410+00	−.6255124+01	.4044502+01	−.3860938+01	.5308164+01
1.140	−.1029397+01	.4894278+00	−.2042119+00	.1711817+00	.2416700+01	−.1056985+01	.7303425+00	−.8066581+00	−.6066708+01	.3836698+01	−.3584800+01	.4836731+01
1.160	−.9879128+00	.4714579+00	−.1919313+00	.1577438+00	.2354233+01	−.1009917+01	.6824850+00	−.7396903+00	−.5888556+01	.3644426+01	−.3334188+01	.4416430+01
1.180	−.9481795+00	.4545723+00	−.1806429+00	.1456207+00	.2294755+01	−.9660413+00	.6387505+00	−.6795781+00	−.5719886+01	.3466210+01	−.3106253+01	.4040783+01
1.200	−.9100902+00	.4386831+00	−.1702478+00	.1346601+00	.2238061+01	−.9250771+00	.5987059+00	−.6254963+00	−.5559990+01	.3300740+01	−.2898518+01	.3704243+01
1.220	−.8735459+00	.4237114+00	−.1606587+00	.1247298+00	.2183964+01	−.8867734+00	.5619715+00	−.5767330+00	−.5408229+01	.3146853+01	−.2708818+01	.3402046+01
1.240	−.8384556+00	.4095860+00	−.1517983+00	.1157151+00	.2132293+01	−.8509052+00	.5282131+00	−.5326722+00	−.5264021+01	.3003514+01	−.2535258+01	.3130089+01
1.260	−.8047353+00	.3962424+00	−.1435980+00	.1075157+00	.2082891+01	−.8172707+00	.4971359+00	−.4927795+00	−.5126838+01	.2869796+01	−.2376174+01	.2884824+01
1.280	−.7723072+00	.3836224+00	−.1359970+00	.1000440+00	.2035614+01	−.7856883+00	.4684795+00	−.4565898+00	−.4996196+01	.2744874+01	−.2230103+01	.2663179+01
1.300	−.7410993+00	.3716729+00	−.1289409+00	.9322332−01	.1990330+01	−.7559944+00	.4420128+00	−.4236973+00	−.4871656+01	.2628005+01	−.2095752+01	.2462484+01
1.320	−.7110448+00	.3603457+00	−.1223814+00	.8698612−01	.1946919+01	−.7280412+00	.4175307+00	−.3937473+00	−.4752816+01	.2518521+01	−.1971980+01	.2280413+01
1.340	−.6820818+00	.3495970+00	−.1162748+00	.8127300−01	.1905267+01	−.7016950+00	.3948508+00	−.3664286+00	−.4639306+01	.2415825+01	−.1857773+01	.2114934+01
1.360	−.6541526+00	.3393868+00	−.1105825+00	.7603153−01	.1865273+01	−.6768347+00	.3738102+00	−.3414677+00	−.4530788+01	.2319372+01	−.1752232+01	.1964269+01
1.380	−.6272036+00	.3296785+00	−.1052694+00	.7121529−01	.1826839+01	−.6533501+00	.3542631+00	−.3186238+00	−.4426950+01	.2228676+01	−.1654556+01	.1826857+01
1.400	−.6011847+00	.3204384+00	−.1003040+00	.6678315−01	.1789879+01	−.6311413+00	.3360794+00	−.2976843+00	−.4327506+01	.2143291+01	−.1564032+01	.1701324+01
1.420	−.5760492+00	.3116360+00	−.9565813−01	.6269855−01	.1754309+01	−.6101168+00	.3191419+00	−.2784609+00	−.4232192+01	.2062817+01	−.1480019+01	.1586461+01
1.440	−.5517535+00	.3032430+00	−.9130602−01	.5892895−01	.1720055+01	−.5901936+00	.3033454+00	−.2607869+00	−.4140764+01	.1986888+01	−.1401947+01	.1481197+01
1.460	−.5282567+00	.2952335+00	−.8722452−01	.5544534−01	.1687045+01	−.5712955+00	.2885952+00	−.2445140+00	−.4052996+01	.1915171+01	−.1329302+01	.1384586+01
1.480	−.5055207+00	.2875835+00	−.8339263−01	.5222177−01	.1655213+01	−.5533529+00	.2748058+00	−.2295105+00	−.3968679+01	.1847365+01	−.1261623+01	.1295788+01
1.500	−.4835097+00	.2802709+00	−.7979128−01	.4923503−01	.1624499+01	−.5363019+00	.2619000+00	−.2156587+00	−.3887619+01	.1783193+01	−.1198494+01	.1214056+01
1.540	−.4415299+00	.2665785+00	−.7321237−01	.4389087−01	.1566198+01	−.5046447+00	.2384658+00	−.1910008+00	−.3734566+01	.1664758+01	−.1084427+01	.1069205+01
1.580	−.4020719+00	.2540109+00	−.6736673−01	.3927027−01	.1511728+01	−.4759091+00	.2178075+00	−.1698245+00	−.3592544+01	.1558088+01	−.9845133+00	.9455222+00
1.620	−.3649185+00	.2424433+00	−.6215345−01	.3525742−01	.1460727+01	−.4497426+00	.1995238+00	−.1515525+00	−.3460432+01	.1461684+01	−.9966298+00	.8393956+00
1.660	−.3298765+00	.2317680+00	−.5748790−01	.3175772−01	.1412878+01	−.4258441+00	.1832812+00	−.1357165+00	−.3337252+01	.1374275+01	−.8190216+00	.7479107+00
1.700	−.2967738+00	.2218917+00	−.5329882−01	.2869339−01	.1367898+01	−.4039554+00	.1688008+00	−.1219341+00	−.3222148+01	.1294781+01	−.7502313+00	.6687020+00
1.740	−.2654563+00	.2127331+00	−.4952584−01	.2600018−01	.1325541+01	−.3838540+00	.1558482+00	−.1098915+00	−.3114370+01	.1222275+01	−.6890414+00	.5998380+00
1.780	−.2357858+00	.2042211+00	−.4611761−01	.2362470−01	.1285584+01	−.3653476+00	.1442255+00	−.9932944−01	−.3013254+01	.1155963+01	−.6344300+00	.5397326+00
1.820	−.2076379+00	.1962935+00	−.4303028−01	.2152238−01	.1247830+01	−.3482688+00	.1337650+00	−.9003286−01	−.2918214+01	.1095159+01	−.5855352+00	.4870765+00
1.860	−.1809006+00	.1888955+00	−.4022622−01	.1965581−01	.1212105+01	−.3324719+00	.1243235+00	−.8182243−01	−.2828729+01	.1039268+01	−.5416269+00	.4407833+00

(m = 24)

T^*	$B^{*(0)}$	$B^{*(1)}$	$B^{*(2)}$	$B^{*(3)}$	$T^*\frac{\partial B^{*(0)}}{\partial T^*}$	$T^*\frac{\partial B^{*(1)}}{\partial T^*}$	$T^*\frac{\partial B^{*(2)}}{\partial T^*}$	$T^*\frac{\partial B^{*(3)}}{\partial T^*}$	$T^{*2}\frac{\partial^2 B^{*(0)}}{\partial T^{*2}}$	$T^{*2}\frac{\partial^2 B^{*(1)}}{\partial T^{*2}}$	$T^{*2}\frac{\partial^2 B^{*(2)}}{\partial T^{*2}}$	$T^{*2}\frac{\partial^2 B^{*(3)}}{\partial T^{*2}}$
1.900	−.1554722+00	.1819785+00	−.3767301−01	.1799350−01	.1178248+01	−.3178292+00	.1157788+00	−.7454788−01	−.2744335+01	.9877748+00	−.5020836+00	.3999474+00
1.940	−.1312609+00	.1754997+00	−.3534264−01	.1650878−01	.1146119+01	−.3042287+00	.1080256+00	−.6808276−01	−.2664617+01	.9402273+00	−.4663745+00	.3638100+00
1.980	−.1081830+00	.1694210+00	−.3321080−01	.1517901−01	.1115589+01	−.2915716+00	.1009735+00	−.6232022−01	−.2589204+01	.8962310+00	−.4340442+00	.3317330+00
2.020	−.8616238−01	.1637083+00	−.3125633−01	.1398485−01	.1086543+01	−.2797706+00	.9454392−01	−.5716958−01	−.2517763+01	.8554389+00	−.4047005+00	.3031774+00
2.060	−.6512949−01	.1583314+00	−.2946073−01	.1290977−01	.1058874+01	−.2687485+00	.8866890−01	−.5255359−01	−.2449993+01	.8175453+00	−.3780048+00	.2776859+00
2.100	−.4502079−01	.1532629+00	−.2780782−01	.1193955−01	.1032488+01	−.2584365+00	.8328913−01	−.4840624−01	−.2385622+01	.7822800+00	−.3536632+00	.2548693+00
2.140	−.2577801−01	.1484785+00	−.2628337−01	.1106193−01	.1007298+01	−.2487733+00	.7835280−01	−.4467086−01	−.2324405+01	.7494033+00	−.3314204+00	.2343950+00
2.180	−.7347686−02	.1439560+00	−.2487482−01	.1026632−01	.9832255+00	−.2397041+00	.7381450−01	−.4129867−01	−.2266119+01	.7187023+00	−.3110534+00	.2159779+00
2.220	.1031938−01	.1396757+00	−.2357111−01	.9543528−02	.9601968+00	−.2311799+00	.6963432−01	−.3824757−01	−.2210561+01	.6899872+00	−.2923672+00	.1993726+00
2.260	.2726850−01	.1356195+00	−.2236240−01	.8885545−02	.9381462+00	−.2231566+00	.6577708−01	−.3548105−01	−.2157547+01	.6630884+00	−.2751906+00	.1843675+00
2.300	.4354148−01	.1317712+00	−.2123997−01	.8285388−02	.9170127+00	−.2155946+00	.6221171−01	−.3296740−01	−.2106908+01	.6378541+00	−.2593728+00	.1707792+00
2.340	.5917698−01	.1281159+00	−.2019607−01	.7736948−02	.8967406+00	−.2084580+00	.5891067−01	−.3067900−01	−.2058490+01	.6141479+00	−.2447810+00	.1584485+00
2.380	.7421075−01	.1246401+00	−.1922375−01	.7234860−02	.8772784+00	−.2017146+00	.5584949−01	−.2859170−01	−.2012152+01	.5918472+00	−.2312975+00	.1472369+00
2.420	.8867597−01	.1213316+00	−.1831682−01	.6774408−02	.8585784+00	−.1953350+00	.5300641−01	−.2668433−01	−.1967764+01	.5708413+00	−.2188181+00	.1370234+00
2.460	.1026034+00	.1181792+00	−.1746972−01	.6351432−02	.8405970+00	−.1892927+00	.5036200−01	−.2493832−01	−.1925207+01	.5510305+00	−.2072500+00	.1277020+00
2.500	.1160216+00	.1151725+00	−.1667746−01	.5962254−02	.8232936+00	−.1835635+00	.4789889−01	−.2333731−01	−.1884371+01	.5323241+00	−.1965106+00	.1191797+00
2.600	.1475099+00	.1082335+00	−.1490829−01	.5116683−02	.7827610+00	−.1704705+00	.4243603−01	−.1987838−01	−.1789166+01	.4898705+00	−.1728230+00	.1008572+00
2.700	.1763468+00	.1020212+00	−.1339585−01	.4421160−02	.7457208+00	−.1589065+00	.3780996−01	−.1705559−01	−.1702721+01	.4527354+00	−.1529172+00	.8600552−01
2.800	.2028440+00	.9643136−01	−.1209397−01	.3844232−02	.7117404+00	−.1486345+00	.3386359−01	−.1473151−01	−.1623889+01	.4200500+00	−.1360590+00	.7385609−01
2.900	.2272669+00	.9137854−01	−.1096625−01	.3361961−02	.6804560+00	−.1394620+00	.3047418−01	−.1280242−01	−.1551715+01	.3911167+00	−.1216797+00	.6383278−01
3.000	.2498420+00	.8679175−01	−.9983685−02	.2955929−02	.6515589+00	−.1312316+00	.2754491−01	−.1118915−01	−.1485394+01	.3653700+00	−.1093339+00	.5549876−01
3.100	.2707644+00	.8261171−01	−.9122965−02	.2611816−02	.6247859+00	−.1238135+00	.2499866−01	−.9830590−02	−.1424246+01	.3423476+00	−.9866926−01	.4851907−01
3.200	.2902030+00	.7878854−01	−.8365204−02	.2318383−02	.5999110+00	−.1170998+00	.2277347−01	−.8679132−02	−.1367693+01	.3216687+00	−.8940487−01	.4263433−01
3.300	.3083045+00	.7528002−01	−.7694980−02	.2066734−02	.5767391+00	−.1110004+00	.2081916−01	−.7697339−02	−.1315237+01	.3030174+00	−.8131456−01	.3764173−01
3.400	.3251969+00	.7205018−01	−.7099604−02	.1849765−02	.5551010+00	−.1054392+00	.1909476−01	−.6855518−02	−.1266450+01	.2861295+00	−.7421494−01	.3338134−01
3.500	.3409926+00	.6906821−01	−.6568574−02	.1661762−02	.5348491+00	−.1003518+00	.1756663−01	−.6129931−02	−.1220963+01	.2707830+00	−.6795622−01	.2972596−01
3.600	.3557906+00	.6630759−01	−.6093135−02	.1498096−02	.5158542+00	−.9568338−01	.1620692−01	−.5501461−02	−.1178451+01	.2567901+00	−.6241519−01	.2657368−01
3.700	.3696786+00	.6374535−01	−.5665951−02	.1354989−02	.4980026+00	−.9138694−01	.1499246−01	−.4954603−02	−.1138635+01	.2439909+00	−.5748989−01	.2384225−01
3.800	.3827341+00	.6136155−01	−.5280840−02	.1229344−02	.4811940+00	−.8742201−01	.1390385−01	−.4476699−02	−.1101265+01	.2322489+00	−.5309540−01	.2146484−01
3.900	.3950263+00	.5913877−01	−.4932564−02	.1118599−02	.4653394+00	−.8375362−01	.1292476−01	−.4057352−02	−.1066123+01	.2214468+00	−.4916061−01	.1938681−01
4.000	.4066171+00	.5706173−01	−.4616661−02	.1020629−02	.4503597+00	−.8035139−01	.1204137−01	−.3687972−02	−.1033017+01	.2114831+00	−.4562567−01	.1756320−01
4.100	.4175618+00	.5511700−01	−.4329320−02	.9336604−03	.4361843+00	−.7718879−01	.1124193−01	−.3361424−02	−.1001774+01	.2022700+00	−.4243991−01	.1595683−01
4.200	.4279101+00	.5329271−01	−.4067262−02	.8562032−03	.4227501+00	−.7424262−01	.1051643−01	−.3071749−02	−.9722418+00	.1937312+00	−.3956030−01	.1453677−01
4.300	.4377069+00	.5157834−01	−.3827663−02	.7870028−03	.4100001+00	−.7149248−01	.9856237−02	−.2813945−02	−.9442840+00	.1857997+00	−.3695005−01	.1327717−01
4.400	.4469927+00	.4996454−01	−.3608074−02	.7249963−03	.3978835+00	−.6892037−01	.9253956−02	−.2583798−02	−.9177777+00	.1784169+00	−.3457764−01	.1215631−01
4.500	.4558042+00	.4844297−01	−.3406368−02	.6692797−03	.3863540+00	−.6651037−01	.8703175−02	−.2377737−02	−.8926129+00	.1715313+00	−.3241591−01	.1115587−01
4.600	.4641746+00	.4700617−01	−.3220688−02	.6190815−03	.3753698+00	−.6424834−01	.8198330−02	−.21[illegible]−02	−.8686903+00	.1650972+00	−.3044140−01	.1026034−01
4.700	.4721342+00	.4564745−01	−.3049412−02	.5737398−03	.3648932+00	−.6212168−01	.7734578−02	−.2026173−02	−.8459201+00	.1590742+00	−.2863374−01	.9456492−02
4.800	.4797107+00	.4436079−01	−.2891112−02	.5326854−03	.3548897+00	−.6011915−01	.7307686−02	−.1875857−02	−.8242209+00	.1534266+00	−.2697521−01	.8733054−02
4.900	.4869293+00	.4314077−01	−.2744532−02	.4954269−03	.3453278+00	−.5823069−01	.6913940−02	−.1739866−02	−.8035189+00	.1481222+00	−.2545033−01	.8080347−02
5.000	.4938131+00	.4198247−01	−.2608563−02	.4615385−03	.3361789+00	−.5644726−01	.6550078−02	−.1616551−02	−.7837469+00	.1431325+00	−.2404553−01	.7490045−02
5.100	.5003833+00	.4088147−01	−.2482221−02	.4306499−03	.3274167+00	−.5476071−01	.6213221−02	−.1504483−02	−.7648435+00	.1384320+00	−.2274889−01	.6954958−02
5.200	.5066592+00	.3983371−01	−.2364633−02	.4024387−03	.3190172+00	−.5316371−01	.5900823−02	−.1402421−02	−.7467527+00	.1339975+00	−.2154990−01	.6468860−02
5.300	.5126589+00	.3883554−01	−.2255022−02	.3766228−03	.3109582+00	−.5164961−01	.5610625−02	−.1309284−02	−.7294230+00	.1298084+00	−.2043928−01	.6026339−02
5.400	.5183988+00	.3788360−01	−.2152693−02	.3529546−03	.3032195+00	−.5021241−01	.5340620−02	−.1224125−02	−.7128075+00	.1258460+00	−.1940878−01	.5622677−02
5.500	.5238941+00	.3697485−01	−.2057025−02	.3312169−03	.2957823+00	−.4884663−01	.5089019−02	−.1146116−02	−.6968627+00	.1220934+00	−.1845109−01	.5253750−02
5.600	.5291590+00	.3610647−01	−.1967462−02	.3112177−03	.2886293+00	−.4754731−01	.4854223−02	−.1074529−02	−.6815488+00	.1185352+00	−.1755971−01	.4915947−02
5.800	.5390486+00	.3448081−01	−.1804694−02	.2757769−03	.2751128+00	−.4513028−01	.4429466−02	−.9481279−03	−.6526694+00	.1119478+00	−.1595318−01	.4321378−02
6.000	.5481612+00	.3298849−01	−.1660948−02	.2454940−03	.2625555+00	−.4292952−01	.4056557−02	−.8406289−03	−.6259071+00	.1059866+00	−.1454956−01	.3817792−02
6.200	.5565774+00	.3161412−01	−.1533410−02	.2194681−03	.2508587+00	−.4091831−01	.3727547−02	−.7486521−03	−.6010369+00	.1005706+00	−.1331687−01	.3388598−02

(m = 24)

T^*	$B^{*(0)}$	$B^{*(1)}$	$B^{*(2)}$	$B^{*(3)}$	$T^*\frac{\partial B^{*(0)}}{\partial T^*}$	$T^*\frac{\partial B^{*(1)}}{\partial T^*}$	$T^*\frac{\partial B^{*(2)}}{\partial T^*}$	$T^*\frac{\partial B^{*(3)}}{\partial T^*}$	$T^{*2}\frac{\partial^2 B^{*(0)}}{\partial T^{*2}}$	$T^{*2}\frac{\partial^2 B^{*(1)}}{\partial T^{*2}}$	$T^{*2}\frac{\partial^2 B^{*(2)}}{\partial T^{*2}}$	$T^{*2}\frac{\partial^2 B^{*(3)}}{\partial T^{*2}}$
6.400	.5643674+00	.3034455−01	−.1419761−02	.1969799−03	.2399368+00	−.3907406−01	.3435932−02	−.6695134−03	−.5778646+00	.9563187−01	−.1222907−01	.3020678−02
6.600	.5715925+00	.2916850−01	−.1318081−02	.1774506−03	.2297150+00	−.3737754−01	.3176355−02	−.6010640−03	−.5562216+00	.9111278−01	−.1126484−01	.2703575−02
6.800	.5783063+00	.2807622−01	−.1226767−02	.1604111−03	.2201281+00	−.3581231−01	.2944372−02	−.5415700−03	−.5359611+00	.8696449−01	−.1040655−01	.2428886−02
7.000	.5845560+00	.2705927−01	−.1144472−02	.1454783−03	.2111187+00	−.3436422−01	.2736275−02	−.4896225−03	−.5169543+00	.8314522−01	−.9639573−02	.2189810−02
7.200	.5903833+00	.2611026−01	−.1070060−02	.1323377−03	.2026359+00	−.3302103−01	.2548947−02	−.4440693−03	−.4990880+00	.7961903−01	−.8951681−02	.1980807−02
7.400	.5958251+00	.2522276−01	−.1002568−02	.1207290−03	.1946350+00	−.3177214−01	.2379762−02	−.4039616−03	−.4822624+00	.7635492−01	−.8332593−02	.1797330−02
7.600	.6009144+00	.2439108−01	−.9411713−03	.1104362−03	.1870759+00	−.3060827−01	.2226488−02	−.3685140−03	−.4663888+00	.7332596−01	−.7773620−02	.1635628−02
7.800	.6056805+00	.2361023−01	−.8851665−03	.1012785−03	.1799231+00	−.2952131−01	.2087223−02	−.3370726−03	−.4513884+00	.7050871−01	−.7267383−02	.1492589−02
8.000	.6101495+00	.2287578−01	−.8339467−03	.9310411−04	.1731446+00	−.2850412−01	.1960336−02	−.3090900−03	−.4371909+00	.6788265−01	−.6807585−02	.1365617−02
8.200	.6143451+00	.2218378−01	−.7869873−03	.8578481−04	.1667117+00	−.2755041−01	.1844427−02	−.2841056−03	−.4237333+00	.6542976−01	−.6388827−02	.1252533−02
8.400	.6182885+00	.2153075−01	−.7438334−03	.7921196−04	.1605988+00	−.2665460−01	.1738283−02	−.2617304−03	−.4109591+00	.6313416−01	−.6006461−02	.1151502−02
8.600	.6219987+00	.2091353−01	−.7040886−03	.7329300−04	.1547824+00	−.2581173−01	.1640854−02	−.2416341−03	−.3988173+00	.6098180−01	−.5656471−02	.1060971−02
8.800	.6254931+00	.2032931−01	−.6674066−03	.6794878−04	.1492417+00	−.2501739−01	.1551226−02	−.2235351−03	−.3872620+00	.5896021−01	−.5335371−02	.9796202−03
9.000	.6287874+00	.1977558−01	−.6334835−03	.6311134−04	.1439573+00	−.2426763−01	.1468599−02	−.2071923−03	−.3762516+00	.5705830−01	−.5040127−02	.9063214−03
9.200	.6318958+00	.1925003−01	−.6020520−03	.5872212−04	.1389119+00	−.2355891−01	.1392273−02	−.1923988−03	−.3657482+00	.5526615−01	−.4768085−02	.8401089−03
9.400	.6348312+00	.1875062−01	−.5728761−03	.5473048−04	.1340898+00	−.2288805−01	.1321632−02	−.1789758−03	−.3557176+00	.5357489−01	−.4516920−02	.7801517−03
9.600	.6376055+00	.1827548−01	−.5457469−03	.5109249−04	.1294763+00	−.2225218−01	.1256133−02	−.1667689−03	−.3461285+00	.5197657−01	−.4284588−02	.7257326−03
9.800	.6402295+00	.1782291−01	−.5204790−03	.4776989−04	.1250584+00	−.2164871−01	.1195296−02	−.1556440−03	−.3369521+00	.5046400−01	−.4069285−02	.6762302−03
10.000	.6427131+00	.1739137−01	−.4969074−03	.4472927−04	.1208238+00	−.2107530−01	.1138693−02	−.1454842−03	−.3281625+00	.4903074−01	−.3869415−02	.6311045−03
10.200	.6450653+00	.1697945−01	−.4748849−03	.4194140−04	.1167613+00	−.2052982−01	.1085948−02	−.1361874−03	−.3197354+00	.4767092−01	−.3683563−02	.5898850−03
10.400	.6472946+00	.1658587−01	−.4542797−03	.3938057−04	.1128607+00	−.2001033−01	.1036720−02	−.1276642−03	−.3116490+00	.4637926−01	−.3510470−02	.5521601−03
10.600	.6494086+00	.1620945−01	−.4349738−03	.3702416−04	.1091125+00	−.1951507−01	.9907081−03	−.1198361−03	−.3038829+00	.4515092−01	−.3349013−02	.5175691−03
10.800	.6514143+00	.1584911−01	−.4168610−03	.3485220−04	.1055081+00	−.1904243−01	.9476418−03	−.1126338−03	−.2964184+00	.4398155−01	−.3198189−02	.4857947−03
11.000	.6533184+00	.1550385−01	−.3998457−03	.3284700−04	.1020392+00	−.1859093−01	.9072778−03	−.1059962−03	−.2892381+00	.4286713−01	−.3057100−02	.4565574−03
11.400	.6568451+00	.1485504−01	−.3687711−03	.2927586−04	.9547883−01	−.1774608−01	.8338031−03	−.9420463−04	−.2756678+00	.4078887−01	−.2800980−02	.4047337−03
11.800	.6600320+00	.1425652−01	−.3411536−03	.2620477−04	.8937776−01	−.1697097−01	.7687778−03	−.8409698−04	−.2630576+00	.3889046−01	−.2575113−02	.3604383−03
12.200	.6629161+00	.1370276−01	−.3165021−03	.2354924−04	.8368953−01	−.1625752−01	.7109676−03	−.7538370−04	−.2513088+00	.3715025−01	−.2374980−02	.3223575−03
12.600	.6655298+00	.1318898−01	−.2944092−03	.2124129−04	.7837378−01	−.1559883−01	.6593539−03	−.6783287−04	−.2403359+00	.3554987−01	−.2196869−02	.2894421−03
13.000	.6679009+00	.1271108−01	−.2745348−03	.1922588−04	.7339523−01	−.1498896−01	.6130906−03	−.6125725−04	−.2300644+00	.3407359−01	−.2037704−02	.2608482−03
13.400	.6700540+00	.1226548−01	−.2565933−03	.1745810−04	.6872293−01	−.1442281−01	.5714698−03	−.5550463−04	−.2204289+00	.3270797−01	−.1894926−02	.2358913−03
13.800	.6720105+00	.1184905−01	−.2403433−03	.1590104−04	.6432962−01	−.1389594−01	.5338964−03	−.5045034−04	−.2113720+00	.3144136−01	−.1766387−02	.2140128−03
14.200	.6737892+00	.1145906−01	−.2255798−03	.1452421−04	.6019117−01	−.1340448−01	.4998668−03	−.4599170−04	−.2028431+00	.3026368−01	−.1650279−02	.1947536−03
14.600	.6754068+00	.1109311−01	−.2121279−03	.1330226−04	.5628617−01	−.1294507−01	.4689529−03	−.4204357−04	−.1947972+00	.2916615−01	−.1545068−02	.1777342−03
15.000	.6768780+00	.1074908−01	−.1998374−03	.1221400−04	.5259553−01	−.1251473−01	.4407889−03	−.3853502−04	−.1871943+00	.2814108−01	−.1449447−02	.1626389−03
16.000	.6799984+00	.9972997−02	−.1733864−03	.9968084−05	.4419912−01	−.1154963−01	.3804539−03	−.3131921−04	−.1699006+00	.2585306−01	−.1245398−02	.1316895−03
17.000	.6824518+00	.9298383−02	−.1518376−03	.8242191−05	.3681811−01	−.1071722−01	.3316054−03	−.2580010−04	−.1546989+00	.2389209−01	−.1081064−02	.1081167−03
18.000	.6843676+00	.8706784−02	−.1340547−03	.6893993−05	.3028026−01	−.9992375−02	.2915206−03	−.2150705−04	−.1412313+00	.2219427−01	−.9468569−03	.8985027−04
19.000	.6858456+00	.8183938−02	−.1192118−03	.5825467−05	.2445020−01	−.9355849−02	.2582343−03	−.1811768−04	−.1292170+00	.2071108−01	−.8358995−03	.7547890−04
20.000	.6869644+00	.7718651−02	−.1066967−03	.4967610−05	.1922006−01	−.8792692−02	.2303005−03	−.1540616−04	−.1184330+00	.1940511−01	−.7431583−03	.6401820−04
21.000	.6877861+00	.7302021−02	−.9604845−04	.4270889−05	.1450284−01	−.8291116−02	.2066365−03	−.1321109−04	−.1086997+00	.1824705−01	−.6648840−03	.5476749−04
22.000	.6883605+00	.6926877−02	−.8691435−04	.3699121−05	.1022756−01	−.7841702−02	.1864188−03	−.1141509−04	−.9987096−01	.1721361−01	−.5982388−03	.4721897−04
23.000	.6887279+00	.6587384−02	−.7902113−04	.3225457−05	.6335746−02	−.7436844−02	.1690126−03	−.9931364−05	−.9182649−01	.1628612−01	−.5410445−03	.4099854−04
24.000	.6889213+00	.6278745−02	−.7215432−04	.2829689−05	.2778805−02	−.7070329−02	.1539223−03	−.8694835−05	−.8446653−01	.1544939−01	−.4916071−03	.3582651−04
25.000	.6889677+00	.5996982−02	−.6614378−04	.2496409−05	−.4839969−03	−.6737040−02	.1407563−03	−.7656039−05	−.7770756−01	.1469098−01	−.4485939−03	.3149096−04
26.000	.6888894+00	.5738767−02	−.6085314−04	.2213730−05	−.3487056−02	−.6432721−02	.1292023−03	−.6776934−05	−.7147914−01	.1400059−01	−.4109453−03	.2782935−04
27.000	.6887051+00	.5501299−02	−.5617209−04	.1972380−05	−.6259617−02	−.6153809−02	.1190085−03	−.6027937−05	−.6572141−01	.1336963−01	−.3778102−03	.2471558−04
28.000	.6884305+00	.5282199−02	−.5201061−04	.1765058−05	−.8826701−02	−.5897295−02	.1099703−03	−.5385806−05	−.6038325−01	.1279089−01	−.3484991−03	.2205086−04
29.000	.6880786+00	.5079439−02	−.4829470−04	.1585956−05	−.1120984−01	−.5660624−02	.1019201−03	−.4832112−05	−.5542065−01	.1225826−01	−.3224489−03	.1975699−04
30.000	.6876608+00	.4891273−02	−.4496305−04	.1430421−05	−.1342769−01	−.5441613−02	.9471953−04	−.4352113−05	−.5079556−01	.1176653−01	−.2991956−03	.1777159−04
32.000	.6866635+00	.4552907−02	−.3925618−04	.1175699−05	−.1743025−01	−.5049311−02	.8242556−04	−.3567890−05	−.4242986−01	.1088861−01	−.2596061−03	.1453487−04

(m = 24)

T^*	$B^{*(0)}$	$B^{*(1)}$	$B^{*(2)}$	$B^{*(3)}$	$T^*\frac{\partial B^{*(0)}}{\partial T^*}$	$T^*\frac{\partial B^{*(1)}}{\partial T^*}$	$T^*\frac{\partial B^{*(2)}}{\partial T^*}$	$T^*\frac{\partial B^{*(3)}}{\partial T^*}$	$T^{*2}\frac{\partial^2 B^{*(0)}}{\partial T^{*2}}$	$T^{*2}\frac{\partial^2 B^{*(1)}}{\partial T^{*2}}$	$T^{*2}\frac{\partial^2 B^{*(2)}}{\partial T^{*2}}$	$T^{*2}\frac{\partial^2 B^{*(3)}}{\partial T^{*2}}$
34.000	.6854992+00	.4257263−02	−.3457068−04	.9783382−06	−.2094135−01	−.4708186−02	.7237273−04	−.2962077−05	−.3506810−01	.1012827−01	−.2273474−03	.1204126−04
36.000	.6842126+00	.3996802−02	−.3067684−04	.8230211−06	−.2404398−01	−.4408955−02	.6404900−04	−.2486603−05	−.2854121−01	.9463735−02	−.2007223−03	.1008894−04
38.000	.6828373+00	.3765651−02	−.2740599−04	.6990938−06	−.2680350−01	−.4144437−02	.5708033−04	−.2108148−05	−.2271610−01	.8878227−02	−.1784963−03	.8538444−05
40.000	.6813985+00	.3559170−02	−.2463208−04	.5989891−06	−.2927212−01	−.3908995−02	.5118840−04	−.1803127−05	−.1748651−01	.8358643−02	−.1597546−03	.7291337−05
42.000	.6799157+00	.3373644−02	−.2225935−04	.5172310−06	−.3149201−01	−.3698137−02	.4616273−04	−.1554517−05	−.1276663−01	.7894598−02	−.1438074−03	.6276771−05
44.000	.6784036+00	.3206064−02	−.2021406−04	.4497894−06	−.3349761−01	−.3508250−02	.4184176−04	−.1349827−05	−.8486337−02	.7477763−02	−.1301273−03	.5442877−05
46.000	.6768738+00	.3053970−02	−.1843861−04	.3936533−06	−.3531733−01	−.3336386−02	.3809986−04	−.1179746−05	−.4587825−02	.7101381−02	−.1183053−03	.4751082−05
48.000	.6753352+00	.2915327−02	−.1688757−04	.3465421−06	−.3697481−01	−.3180127−02	.3483815−04	−.1037240−05	−.1022974−02	.6759914−02	−.1080205−03	.4172300−05
50.000	.6737946+00	.2788444−02	−.1552464−04	.3067067−06	−.3848986−01	−.3037461−02	.3197795−04	−.9169234−06	.2248583−02	.6448784−02	−.9901812−04	.3684312−05
52.000	.6722575+00	.2671896−02	−.1432059−04	.2727903−06	−.3987924−01	−.2906708−02	.2945606−04	−.8146279−06	.5260963−02	.6164174−02	−.9109399−04	.3269948−05
54.000	.6707282+00	.2564482−02	−.1325164−04	.2437295−06	−.4115719−01	−.2786453−02	.2722119−04	−.7270920−06	.8043202−02	.5902876−02	−.8408294−04	.2915796−05
56.000	.6692098+00	.2465177−02	−.1229832−04	.2186823−06	−.4233589−01	−.2675493−02	.2523144−04	−.6517389−06	.1062016−01	.5662175−02	−.7785017−04	.2611277−05
58.000	.6677049+00	.2373105−02	−.1144452−04	.1969767−06	−.4342584−01	−.2572803−02	.2345226−04	−.5865142−06	.1301326−01	.5439758−02	−.7228484−04	.2347969−05
60.000	.6662155+00	.2287509−02	−.1067685−04	.1780713−06	−.4443612−01	−.2477500−02	.2185497−04	−.5297661−06	.1524103−01	.5233646−02	−.6729512−04	.2119110−05
64.000	.6632884+00	.2133214−02	−.9356828−05	.1469854−06	−.4624827−01	−.2306113−02	.1911406−04	−.4365943−06	.1926316−01	.4863734−02	−.5874845−04	.1743868−05
68.000	.6604363+00	.1997999−02	−.8267868−05	.1227792−06	−.4782443−01	−.2156357−02	.1685872−04	−.3641765−06	.2279312−01	.4541310−02	−.5173180−04	.1452707−05
72.000	.6576627+00	.1878557−02	−.7358998−05	.1036437−06	−.4920500−01	−.2024417−02	.1498071−04	−.3070244−06	.2591371−01	.4257879−02	−.4590105−04	.1223275−05
76.000	.6549691+00	.1772301−02	−.6592564−05	.8831315−07	−.5042176−01	−.1907320−02	.1340035−04	−.2613058−06	.2869022−01	.4006845−02	−.4100352−04	.1039997−05
80.000	.6523548+00	.1677177−02	−.5940261−05	.7588362−07	−.5150008−01	−.1802718−02	.1205789−04	−.2242897−06	.3117481−01	.3783011−02	−.3685036−04	.8917945−06
84.000	.6498185+00	.1591536−02	−.5380486−05	.6569760−07	−.5246041−01	−.1708730−02	.1090788−04	−.1939932−06	.3340966−01	.3582231−02	−.3329811−04	.7706362−06
88.000	.6473578+00	.1514038−02	−.4896514−05	.5726899−07	−.5331946−01	−.1623832−02	.9915213−05	−.1689529−06	.3542926−01	.3401153−02	−.3023627−04	.6706052−06
92.000	.6449703+00	.1443583−02	−.4475237−05	.5023310−07	−.5409095−01	−.1546779−02	.9052427−05	−.1480726−06	.3726205−01	.3237042−02	−.2757859−04	.5872749−06
96.000	.6426533+00	.1379259−02	−.4106263−05	.4431261−07	−.5478631−01	−.1476541−02	.8297807−05	−.1305200−06	.3893173−01	.3087645−02	−.2525696−04	.5172889−06
100.000	.6404039+00	.1320306−02	−.3781271−05	.3929409−07	−.5541508−01	−.1412260−02	.7633991−05	−.1156551−06	.4045816−01	.2951088−02	−.2321705−04	.4580703−06
105.000	.6376828+00	.1253200−02	−.3426746−05	.3403975−07	−.5611957−01	−.1339198−02	.6910824−05	−.1001067−06	.4219011−01	.2796077−02	−.2099740−04	.3961831−06
110.000	.6350574+00	.1192450−02	−.3120019−05	.2968887−07	−.5674564−01	−.1273158−02	.6286024−05	−.8724449−07	.4375175−01	.2656150−02	−.1908204−04	.3450346−06
115.000	.6325224+00	.1137200−02	−.2852859−05	.2605452−07	−.5730410−01	−.1213183−02	.5742515−05	−.7651036−07	.4516571−01	.2529228−02	−.1741779−04	.3023848−06
120.000	.6300728+00	.1086740−02	−.2618731−05	.2299448−07	−.5780387−01	−.1158480−02	.5266773−05	−.6748010−07	.4645082−01	.2413595−02	−.1596259−04	.2665331−06
125.000	.6277038+00	.1040479−02	−.2412399−05	.2039916−07	−.5825246−01	−.1108389−02	.4847971−05	−.5982729−07	.4762288−01	.2307822−02	−.1468282−04	.2361722−06
130.000	.6254111+00	.9979164−03	−.2229623−05	.1818322−07	−.5865617−01	−.1062355−02	.4477365−05	−.5329792−07	.4869524−01	.2210713−02	−.1355137−04	.2102858−06
135.000	.6231905+00	.9586293−03	−.2066945−05	.1627949−07	−.5902033−01	−.1019910−02	.4147826−05	−.4769235−07	.4967926−01	.2121254−02	−.1254616−04	.1880761−06
140.000	.6210380+00	.9222562−03	−.1921516−05	.1463462−07	−.5934950−01	−.9806512−03	.3853497−05	−.4285212−07	.5058464−01	.2038584−02	−.1164908−04	.1689101−06
145.000	.6189501+00	.8884869−03	−.1790979−05	.1320588−07	−.5964760−01	−.9442371−03	.3589529−05	−.3865041−07	.5141976−01	.1961965−02	−.1084515−04	.1522818−06
150.000	.6169233+00	.8570534−03	−.1673363−05	.1195874−07	−.5991798−01	−.9103715−03	.3351880−05	−.3498485−07	.5219185−01	.1890762−02	−.1012189−04	.1377829−06
160.000	.6130408+00	.8002937−03	−.1470538−05	.9901981−08	−.6038693−01	−.8492938−03	.2942507−05	−.2894434−07	.5357130−01	.1762480−02	−.8877232−05	.1139071−06
170.000	.6093679+00	.7504471−03	−.1302620−05	.8294469−08	−.6077549−01	−.7957347−03	.2604048−05	−.2422777−07	.5476449−01	.1650134−02	−.7849428−05	.9528101−07
180.000	.6058846+00	.7063311−03	−.1162023−05	.7019466−08	−.6109841−01	−.7483962−03	.2321002−05	−.2049004−07	.5580357−01	.1550951−02	−.6990838−05	.8053227−07
190.000	.6025738+00	.6670177−03	−.1043115−05	.5994910−08	−.6136719−01	−.7062619−03	.2081885−05	−.1748887−07	.5671384−01	.1462764−02	−.6266222−05	.6869851−07
200.000	.5994202+00	.6317681−03	−.9416468−06	.5161951−08	−.6159093−01	−.6685246−03	.1878043−05	−.1505067−07	.5751545−01	.1383854−02	−.5649061−05	.5909097−07
210.000	.5964105+00	.5999872−03	−.8543609−06	.4477627−08	−.6177691−01	−.6345349−03	.1702853−05	−.1304886−07	.5822464−01	.1312843−02	−.5119091−05	.5120775−07
220.000	.5935330+00	.5711903−03	−.7787274−06	.3910066−08	−.6193101−01	−.6037650−03	.1551180−05	−.1138961−07	.5885467−01	.1248611−02	−.4660608−05	.4467718−07
240.000	.5881337+00	.5210219−03	−.6548672−06	.3034979−08	−.6216191−01	−.5502250−03	.1303071−05	−.8833322−08	.5991893−01	.1136964−02	−.3911376−05	.3462338−07
260.000	.5831517+00	.4788068−03	−.5584893−06	.2404455−08	−.6231283−01	−.5052389−03	.1110274−05	−.6993215−08	.6077525−01	.1043274−02	−.3329883−05	.2739274−07
280.000	.5785301+00	.4428033−03	−.4820120−06	.1938379−08	−.6240410−01	−.4669210−03	.9574665−06	−.5634163−08	.6147106−01	.9635603−03	−.2869492−05	.2205653−07
300.000	.5742229+00	.4117423−03	−.4203010−06	.1586246−08	−.6245020−01	−.4339003−03	.8342906−06	−.4608115−08	.6204081−01	.8949331−03	−.2498724−05	.1803057−07

(m = 36)

T^*	$B^{*(0)}$	$B^{*(1)}$	$B^{*(2)}$	$B^{*(3)}$	$T^*\frac{\partial B^{*(0)}}{\partial T^*}$	$T^*\frac{\partial B^{*(1)}}{\partial T^*}$	$T^*\frac{\partial B^{*(2)}}{\partial T^*}$	$T^*\frac{\partial B^{*(3)}}{\partial T^*}$	$T^{*2}\frac{\partial^2 B^{*(0)}}{\partial T^{*2}}$	$T^{*2}\frac{\partial^2 B^{*(1)}}{\partial T^{*2}}$	$T^{*2}\frac{\partial^2 B^{*(2)}}{\partial T^{*2}}$	$T^{*2}\frac{\partial^2 B^{*(3)}}{\partial T^{*2}}$
.300	−.1465943+02	.4555752+02	−.2487489+03	.2020919+04	.4028437+02	−.2163288+03	.1576807+04	−.1550987+05	−.1847960+03	.1400035+04	−.1247695+05	.1423912+06
.400	−.7189372+01	.1323856+02	−.4612313+02	.2577075+03	.1624736+02	−.5138936+02	.2497712+03	−.1722306+04	−.6132110+02	.2856811+03	−.1732523+04	.1401791+05
.500	−.4444152+01	.5918915+01	−.1471505+02	.6229556+02	.9223124+01	−.1983524+02	.7125826+02	−.3776697+03	−.3065272+02	.9899528+02	−.4506032+03	.2825119+04
.600	−.3062228+01	.3323108+01	−.6313966+01	.2146971+02	.6199639+01	−.9939588+01	.2809095+02	−.1209487+03	−.1888310+02	.4570279+02	−.1656777+03	.8491768+03
.700	−.2238775+01	.2139180+01	−.3253358+01	.9236215+01	.4589943+01	−.5839908+01	.1353433+02	−.4910982+02	−.1313352+02	.2515650+02	−.7555459+02	.3280311+03
.750	−.1941354+01	.1778463+01	−.2451678+01	.6428836+01	.4046719+01	−.4667631+01	.9910369+01	−.3335124+02	−.1129532+02	.1955099+02	−.5404033+02	.2180897+03
.775	−.1812463+01	.1633099+01	−.2149234+01	.5428481+01	.3817835+01	−.4208021+01	.8572389+01	−.2784138+02	−.1053831+02	.1739696+02	−.4623680+02	.1802724+03
.800	−.1694559+01	.1505898+01	−.1895129+01	.4616862+01	.3611973+01	−.3812570+01	.7462902+01	−.2342179+02	−.9866837+01	.1556618+02	−.3983499+02	.1502347+03
.825	−.1586307+01	.1393944+01	−.1680093+01	.3952786+01	.3425944+01	−.3470122+01	.6535725+01	−.1984489+02	−.9268002+01	.1399930+02	−.3453977+02	.1261515+03
.850	−.1486580+01	.1294882+01	−.1496900+01	.3405157+01	.3257108+01	−.3171800+01	.5755310+01	−.1692588+02	−.8731284+01	.1264962+02	−.3012637+02	.1066737+03
.875	−.1394417+01	.1206790+01	−.1339866+01	.2950254+01	.3103262+01	−.2910477+01	.5094024+01	−.1452531+02	−.8248018+01	.1148005+02	−.2642181+02	.9079276+02
.900	−.1308997+01	.1128093+01	−.1204474+01	.2569802+01	.2962556+01	−.2680381+01	.4530187+01	−.1253686+02	−.7811020+01	.1046092+02	−.2329168+02	.7774649+02
.925	−.1229612+01	.1057485+01	−.1087112+01	.2249593+01	.2833423+01	−.2476808+01	.4046637+01	−.1087867+02	−.7414291+01	.9568268+01	−.2063057+02	.6695318+02
.950	−.1155649+01	.9938812+00	−.9848654+00	.1978482+01	.2714532+01	−.2295892+01	.3629686+01	−.9487164+01	−.7052787+01	.8782594+01	−.1835516+02	.5796472+02
.975	−.1086576+01	.9363712+00	−.8953654+00	.1747661+01	.2604743+01	−.2134434+01	.3268327+01	−.8312554+01	−.6722243+01	.8087938+01	−.1639901+02	.5043290+02
1.000	−.1021928+01	.8841885+00	−.8166755+00	.1550113+01	.2503075+01	−.1989775+01	.2953648+01	−.7315522+01	−.6419034+01	.7471141+01	−.1470879+02	.4408493+02
1.020	−.9731183+00	.8458378+00	−.7604257+00	.1412208+01	.2427016+01	−.1884634+01	.2730587+01	−.6624521+01	−.6194049+01	.7026362+01	−.1351883+02	.3971261+02
1.040	−.9266917+00	.8101914+00	−.7093812+00	.1289602+01	.2355228+01	−.1787836+01	.2529624+01	−.6013966+01	−.5983183+01	.6619649+01	−.1245302+02	.3586981+02
1.060	−.8824791+00	.7769955+00	−.6629488+00	.1180287+01	.2287371+01	−.1698529+01	.2348098+01	−.5472861+01	−.5785206+01	.6246886+01	−.1149577+02	.3248169+02
1.080	−.8403271+00	.7460256+00	−.6206144+00	.1082555+01	.2223138+01	−.1615966+01	.2183722+01	−.4991923+01	−.5599024+01	.5904487+01	−.1063376+02	.2948541+02
1.100	−.8000963+00	.7170823+00	−.5819314+00	.9949530+00	.2162251+01	−.1539489+01	.2034523+01	−.4563281+01	−.5423659+01	.5589317+01	−.9855555+01	.2682800+02
1.120	−.7616593+00	.6899884+00	−.5465106+00	.9162339+00	.2104462+01	−.1468518+01	.1898792+01	−.4180240+01	−.5258234+01	.5298626+01	−.9151324+01	.2446460+02
1.140	−.7248998+00	.6645854+00	−.5140114+00	.8453284+00	.2049545+01	−.1402539+01	.1775043+01	−.3837080+01	−.5101962+01	.5029996+01	−.8512563+01	.2235710+02
1.160	−.6897114+00	.6407318+00	−.4841352+00	.7813145+00	.1997295+01	−.1341096+01	.1661985+01	−.3528904+01	−.4954135+01	.4781296+01	−.7931904+01	.2047301+02
1.180	−.6559964+00	.6183006+00	−.4566195+00	.7233952+00	.1947526+01	−.1283784+01	.1558487+01	−.3251500+01	−.4814112+01	.4550640+01	−.7402942+01	.1878454+02
1.200	−.6236649+00	.5971777+00	−.4312327+00	.6708798+00	.1900068+01	−.1230241+01	.1463559+01	−.3001237+01	−.4681316+01	.4336356+01	−.6920096+01	.1726782+02
1.220	−.5926344+00	.5772601+00	−.4077700+00	.6231674+00	.1854768+01	−.1180145+01	.1376331+01	−.2774974+01	−.4555221+01	.4136957+01	−.6478482+01	.1590232+02
1.240	−.5628285+00	.5584550+00	−.3860502+00	.5797341+00	.1811484+01	−.1133205+01	.1296036+01	−.2569987+01	−.4435353+01	.3951120+01	−.6073820+01	.1467030+02
1.260	−.5341768+00	.5406784+00	−.3659118+00	.5401219+00	.1770086+01	−.1089162+01	.1221997+01	−.2383905+01	−.4321276+01	.3777662+01	−.5702349+01	.1355639+02
1.280	−.5066144+00	.5238542+00	−.3472115+00	.5039293+00	.1730456+01	−.1047782+01	.1153614+01	−.2214661+01	−.4212596+01	.3615523+01	−.5360753+01	.1254724+02
1.300	−.4800807+00	.5079133+00	−.3298210+00	.4708035+00	.1692484+01	−.1008853+01	.1090357+01	−.2060448+01	−.4108953+01	.3463755+01	−.5046103+01	.1163124+02
1.320	−.4545200+00	.4927926+00	−.3136259+00	.4404337+00	.1656071+01	−.9721861+00	.1031750+01	−.1919681+01	−.4010015+01	.3321503+01	−.4755806+01	.1079824+02
1.340	−.4298801+00	.4784348+00	−.2985235+00	.4125455+00	.1621123+01	−.9376073+00	.9773738+00	−.1790966+01	−.3915479+01	.3187998+01	−.4487558+01	.1003934+02
1.360	−.4061127+00	.4647876+00	−.2844215+00	.3868959+00	.1587555+01	−.9049606+00	.9268501+00	−.1673077+01	−.3825069+01	.3062547+01	−.4239314+01	.9346770+01
1.380	−.3831728+00	.4518031+00	−.2712370+00	.3632697+00	.1555288+01	−.8741037+00	.8798421+00	−.1564930+01	−.3738527+01	.2944521+01	−.4009247+01	.8713660+01
1.400	−.3610184+00	.4394373+00	−.2588951+00	.3414755+00	.1524249+01	−.8449074+00	.8360473+00	−.1465567+01	−.3655619+01	.2833352+01	−.3795729+01	.8133970+01
1.420	−.3396102+00	.4276500+00	−.2473285+00	.3213428+00	.1494370+01	−.8172535+00	.7951939+00	−.1374138+01	−.3576126+01	.2728525+01	−.3597300+01	.7602361+01
1.440	−.3189116+00	.4164043+00	−.2364760+00	.3027195+00	.1465588+01	−.7910344+00	.7570373+00	−.1289887+01	−.3499850+01	.2629570+01	−.3412653+01	.7114106+01
1.460	−.2988883+00	.4056660+00	−.2262821+00	.2854698+00	.1437844+01	−.7661517+00	.7213570+00	−.1212143+01	−.3426603+01	.2536060+01	−.3240613+01	.6665012+01
1.480	−.2795082+00	.3954038+00	−.2166968+00	.2694717+00	.1411084+01	−.7425150+00	.6879535+00	−.1140305+01	−.3356214+01	.2447607+01	−.3080122+01	.6251351+01
1.500	−.2607412+00	.3855887+00	−.2076743+00	.2546162+00	.1385257+01	−.7200417+00	.6566466+00	−.1073837+01	−.3288524+01	.2363854+01	−.2930228+01	.5869804+01
1.540	−.2249348+00	.3671951+00	−.1911550+00	.2279498+00	.1336214+01	−.6782872+00	.5996838+00	−.9551452+00	−.3160657+01	.2209178+01	−.2658867+01	.5191515+01
1.580	−.1912628+00	.3502941+00	−.1764336+00	.2047962+00	.1290374+01	−.6403500+00	.5493326+00	−.8527877+00	−.3041937+01	.2069741+01	−.2420579+01	.4609999+01
1.620	−.1595421+00	.3347216+00	−.1632667+00	.1846054+00	.1247434+01	−.6057724+00	.5046516+00	−.7641118+00	−.2931440+01	.1943613+01	−.2210467+01	.4109052+01
1.660	−.1296100+00	.3203355+00	−.1514501+00	.1669262+00	.1207130+01	−.5741633+00	.4648562+00	−.6869560+00	−.2828358+01	.1829156+01	−.2024473+01	.3675554+01
1.700	−.1013214+00	.3070128+00	−.1408111+00	.1513864+00	.1169229+01	−.5451871+00	.4292889+00	−.6195491+00	−.2731986+01	.1724976+01	−.1859225+01	.3298817+01
1.740	−.7454647−01	.2946463+00	−.1312033+00	.1376773+00	.1133524+01	−.5185543+00	.3973958+00	−.5604315+00	−.2641704+01	.1629877+01	−.1711894+01	.2970083+01
1.780	−.4916856−01	.2831420+00	−.1225016+00	.1255412+00	.1099830+01	−.4940141+00	.3687086+00	−.5083940+00	−.2556962+01	.1542833+01	−.1580107+01	.2682135+01
1.820	−.2508273−01	.2724177+00	−.1145991+00	.1147623+00	.1067983+01	−.4713486+00	.3428286+00	−.4624293+00	−.2477276+01	.1462957+01	−.1461853+01	.2428996+01
1.860	−.2194258−02	.2624007+00	−.1074038+00	.1051591+00	.1037836+01	−.4503677+00	.3194160+00	−.4216948+00	−.2402215+01	.1389481+01	−.1355429+01	.2205688+01

(m = 36)

T^*	$B^{*(0)}$	$B^{*(1)}$	$B^{*(2)}$	$B^{*(3)}$	$T^*\frac{\partial B^{*(0)}}{\partial T^*}$	$T^*\frac{\partial B^{*(1)}}{\partial T^*}$	$T^*\frac{\partial B^{*(2)}}{\partial T^*}$	$T^*\frac{\partial B^{*(3)}}{\partial T^*}$	$T^{*2}\frac{\partial^2 B^{*(0)}}{\partial T^{*2}}$	$T^{*2}\frac{\partial^2 B^{*(1)}}{\partial T^{*2}}$	$T^{*2}\frac{\partial^2 B^{*(2)}}{\partial T^{*2}}$	$T^{*2}\frac{\partial^2 B^{*(3)}}{\partial T^{*2}}$
1.900	.1958257−01	.2530269+00	−.1008362+00	.9657785−01	.1009258+01	−.4309047+00	.2981790+00	−.3854820+00	−.2331394+01	.1321735+01	−.1259381+01	.2008050+01
1.940	.4032551−01	.2442395+00	−.9482753−01	.8888822−01	.9821300+00	−.4128133+00	.2788667+00	−.3531931+00	−.2264471+01	.1259135+01	−.1172465+01	.1832584+01
1.980	.6010525−01	.2359878+00	−.8931794−01	.8197900−01	.9563444+00	−.3959644+00	.2612624+00	−.3243207+00	−.2201137+01	.1201170+01	−.1093612+01	.1676339+01
2.020	.7898618−01	.2282267+00	−.8425522−01	.7575504−01	.9318047+00	−.3802440+00	.2451781+00	−.2984334+00	−.2141117+01	.1147390+01	−.1021900+01	.1536815+01
2.060	.9702714−01	.2209159+00	−.7959367−01	.7013463−01	.9084230+00	−.3655507+00	.2304504+00	−.2751623+00	−.2084160+01	.1097396+01	−.9565298+00	.1411884+01
2.100	.1142819+00	.2140191+00	−.7529316−01	.6504734−01	.8861196+00	−.3517945+00	.2169365+00	−.2541913+00	−.2030041+01	.1050840+01	−.8968091+00	.1299730+01
2.140	.1307998+00	.2075039+00	−.7131837−01	.6043228−01	.8648219+00	−.3388951+00	.2045115+00	−.2352482+00	−.1978556+01	.1007409+01	−.8421338+00	.1198797+01
2.180	.1466262+00	.2013409+00	−.6763810−01	.5623662−01	.8444636+00	−.3267806+00	.1930659+00	−.2180981+00	−.1929520+01	.9668266+00	−.7919758+00	.1107746+01
2.220	.1618026+00	.1955036+00	−.6422473−01	.5241440−01	.8249840+00	−.3153868+00	.1825030+00	−.2025375+00	−.1882765+01	.9288456+00	−.7458725+00	.1025424+01
2.260	.1763676+00	.1899680+00	−.6105372−01	.4892549−01	.8063277+00	−.3046557+00	.1727376+00	−.1883896+00	−.1838137+01	.8932452+00	−.7034171+00	.9508317+00
2.300	.1903566+00	.1847124+00	−.5810326−01	.4573480−01	.7884435+00	−.2945353+00	.1636942+00	−.1755005+00	−.1795496+01	.8598279+00	−.6642509+00	.8831011+00
2.340	.2038022+00	.1797170+00	−.5535388−01	.4281151−01	.7712848+00	−.2849785+00	.1553059+00	−.1637355+00	−.1754714+01	.8284158+00	−.6280572+00	.8214778+00
2.380	.2167350+00	.1749638+00	−.5278817−01	.4012853−01	.7548082+00	−.2759428+00	.1475130+00	−.1529768+00	−.1715673+01	.7988491+00	−.5945551+00	.7653028+00
2.420	.2291830+00	.1704364+00	−.5039054−01	.3766195−01	.7389740+00	−.2673896+00	.1402625+00	−.1431208+00	−.1678265+01	.7709835+00	−.5634952+00	.7139992+00
2.460	.2411723+00	.1661197+00	−.4814697−01	.3539064−01	.7237455+00	−.2592839+00	.1335069+00	−.1340762+00	−.1642391+01	.7446886+00	−.5346556+00	.6670608+00
2.500	.2527272+00	.1620000+00	−.4604487−01	.3329588−01	.7090885+00	−.2515939+00	.1272036+00	−.1257627+00	−.1607959+01	.7198462+00	−.5078381+00	.6240422+00
2.600	.2798588+00	.1524822+00	−.4133660−01	.2872660−01	.6747451+00	−.2340032+00	.1131834+00	−.1077292+00	−.1527652+01	.6634155+00	−.4485241+00	.5311778+00
2.700	.3047265+00	.1439485+00	−.3729449−01	.2494738−01	.6433483+00	−.2184464+00	.1012625+00	−.9292866−01	−.1454692+01	.6139912+00	−.3984854+00	.4554740+00
2.800	.3275955+00	.1362590+00	−.3380102−01	.2179608−01	.6145347+00	−.2046100+00	.9105326−01	−.8067691−01	−.1388124+01	.5704360+00	−.3559486+00	.3932048+00
2.900	.3486912+00	.1292987+00	−.3076310−01	.1914862−01	.5879982+00	−.1922396+00	.8225183−01	−.7045473−01	−.1327149+01	.5318353+00	−.3195349+00	.3415629+00
3.000	.3682066+00	.1229720+00	−.2810631−01	.1690903−01	.5634791+00	−.1811267+00	.7461761−01	−.6186361−01	−.1271094+01	.4974471+00	−.2881611+00	.2984081+00
3.100	.3863078+00	.1171992+00	−.2577063−01	.1500232−01	.5407556+00	−.1710994+00	.6795835−01	−.5459451−01	−.1219390+01	.4666643+00	−.2609679+00	.2620914+00
3.200	.4031386+00	.1119128+00	−.2370723−01	.1336932−01	.5196374+00	−.1620145+00	.6211904−01	−.4840543−01	−.1171551+01	.4389861+00	−.2372675+00	.2313295+00
3.300	.4188240+00	.1070558+00	−.2187613−01	.1196301−01	.4999601+00	−.1537521+00	.5697376−01	−.4310518−01	−.1127163+01	.4139964+00	−.2165049+00	.2051143+00
3.400	.4334733+00	.1025795+00	−.2024429−01	.1074564−01	.4815808+00	−.1462112+00	.5241942−01	−.3854143−01	−.1085866+01	.3913474+00	−.1982286+00	.1826472+00
3.500	.4471822+00	.9844222−01	−.1878430−01	.9686740−02	.4643751+00	−.1393061+00	.4837105−01	−.3459188−01	−.1047349+01	.3707463+00	−.1820688+00	.1632904+00
3.600	.4600354+00	.9460801−01	−.1747325−01	.8761510−02	.4482340+00	−.1329636+00	.4475816−01	−.3115761−01	−.1011341+01	.3519450+00	−.1677205+00	.1465308+00
3.700	.4721076+00	.9104570−01	−.1629185−01	.7949640−02	.4330614+00	−.1271211+00	.4152190−01	−.2815805−01	−.9776062+00	.3347325+00	−.1549306+00	.1319524+00
3.800	.4834650+00	.8772817−01	−.1522383−01	.7234393−02	.4187726+00	−.1217246+00	.3861288−01	−.2552720−01	−.9459359+00	.3189283+00	−.1434878+00	.1192159+00
3.900	.4941668+00	.8463175−01	−.1425535−01	.6601897−02	.4052924+00	−.1167275+00	.3598940−01	−.2321061−01	−.9161467+00	.3043769+00	−.1332147+00	.1080429+00
4.000	.5042659+00	.8173566−01	−.1337458−01	.6040590−02	.3925539+00	−.1120890+00	.3361611−01	−.2116314−01	−.8880761+00	.2909442+00	−.1239615+00	.9820338−01
4.100	.5138094+00	.7902158−01	−.1257142−01	.5540787−02	.3804975+00	−.1077737+00	.3146286−01	−.1934715−01	−.8615799+00	.2785138+00	−.1156012+00	.8950656−01
4.200	.5228402+00	.7647334−01	−.1183711−01	.5094335−02	.3690696+00	−.1037505+00	.2950384−01	−.1773111−01	−.8365292+00	.2669842+00	−.1080257+00	.8179306−01
4.300	.5313963+00	.7407658−01	−.1116413−01	.4694336−02	.3582223+00	−.9999207−01	.2771687−01	−.1628846−01	−.8128090+00	.2562668+00	−.1011423+00	.7492927−01
4.400	.5395126+00	.7181853−01	−.1054592−01	.4334933−02	.3479124+00	−.9647432−01	.2608277−01	−.1499675−01	−.7903163+00	.2462835+00	−.9487145−01	.6880257−01
4.500	.5472205+00	.6968779−01	−.9976776−02	.4011128−02	.3381007+00	−.9317586−01	.2458496−01	−.1383689−01	−.7689580+00	.2369660+00	−.8914437−01	.6331764−01
4.600	.5545484+00	.6767416−01	−.9451702−02	.3718641−02	.3287519+00	−.9007769−01	.2320898−01	−.1279260−01	−.7486506+00	.2282535+00	−.8390157−01	.5839346−01
4.700	.5615223+00	.6576848−01	−.8966323−02	.3453791−02	.3198340+00	−.8716289−01	.2194223−01	−.1184994−01	−.7293184+00	.2200923+00	−.7909133−01	.5396087−01
4.800	.5681659+00	.6396249−01	−.8516786−02	.3213405−02	.3113178+00	−.8441635−01	.2077366−01	−.1099694−01	−.7108926+00	.2124346+00	−.7466851−01	.4996062−01
4.900	.5745008+00	.6224877−01	−.8099689−02	.2994733−02	.3031766+00	−.8182452−01	.1969358−01	−.1022326−01	−.6933111+00	.2052377+00	−.7059360−01	.4634176−01
5.000	.5805468+00	.6062058−01	−.7712022−02	.2795388−02	.2953862+00	−.7937523−01	.1869343−01	−.9519945−02	−.6765171+00	.1984636+00	−.6683192−01	.4306032−01
5.100	.5863220+00	.5907183−01	−.7351113−02	.2613288−02	.2879243+00	−.7705752−01	.1776567−01	−.8879232−02	−.6604587+00	.1920781+00	−.6335293−01	.4007823−01
5.200	.5918432+00	.5759696−01	−.7014582−02	.2446616−02	.2807705+00	−.7486149−01	.1690360−01	−.8294350−02	−.6450886+00	.1860505+00	−.6012965−01	.3736242−01
5.300	.5971258+00	.5619093−01	−.6700306−02	.2293778−02	.2739061+00	−.7277818−01	.1610126−01	−.7759387−02	−.6303635+00	.1803531+00	−.5713820−01	.3488408−01
5.400	.6021839+00	.5484915−01	−.6406388−02	.2153371−02	.2673137+00	−.7079948−01	.1535337−01	−.7269161−02	−.6162436+00	.1749609+00	−.5435738−01	.3261802−01
5.500	.6070305+00	.5356739−01	−.6131126−02	.2024163−02	.2609776+00	−.6891801−01	.1465518−01	−.6819118−02	−.6026922+00	.1698513+00	−.5176830−01	.3054219−01
5.600	.6116778+00	.5234181−01	−.5872990−02	.1905062−02	.2548831+00	−.6712704−01	.1400246−01	−.6405249−02	−.5896756+00	.1650038+00	−.4935412−01	.2863720−01
5.800	.6204186+00	.5004532−01	−.5402722−02	.1693424−02	.2433651+00	−.6379265−01	.1281863−01	−.5672268−02	−.5651250+00	.1560222+00	−.4499177−01	.2527341−01
6.000	.6284865+00	.4793465−01	−.4986093−02	.1511947−02	.2326627+00	−.6075328−01	.1177582−01	−.5046441−02	−.5423699+00	.1478859+00	−.4116745−01	.2241240−01
6.200	.6359510+00	.4598856−01	−.4615318−02	.1355458−02	.2226920+00	−.5797275−01	.1085281−01	−.4508972−02	−.5212201+00	.1404863+00	−.3779785−01	.1996425−01

(m = 36)

T^*	$B^{*(0)}$	$B^{*(1)}$	$B^{*(2)}$	$B^{*(3)}$	$T^*\frac{\partial B^{*(0)}}{\partial T^*}$	$T^*\frac{\partial B^{*(1)}}{\partial T^*}$	$T^*\frac{\partial B^{*(2)}}{\partial T^*}$	$T^*\frac{\partial B^{*(3)}}{\partial T^*}$	$T^{*2}\frac{\partial^2 B^{*(0)}}{\partial T^{*2}}$	$T^{*2}\frac{\partial^2 B^{*(1)}}{\partial T^{*2}}$	$T^{*2}\frac{\partial^2 B^{*(2)}}{\partial T^{*2}}$	$T^{*2}\frac{\partial^2 B^{*(3)}}{\partial T^{*2}}$
6.400	.6428725+00	.4418887−01	−.4283964−02	.1219809−02	.2133803+00	−.5542043−01	.1003218−01	−.4044868−02	−.5015111+00	.1337322+00	−.3481495−01	.1785757−01
6.600	.6493037+00	.4251996−01	−.3986681−02	.1101651−02	.2046641+00	−.5307024−01	.9299527−02	−.3642080−02	−.4831002+00	.1275462+00	−.3216283−01	.1603519−01
6.800	.6552908+00	.4096831−01	−.3718991−02	.9982588−03	.1964880+00	−.5089985−01	.8642883−02	−.3290845−02	−.4658630+00	.1218626+00	−.2979517−01	.1445102−01
7.000	.6608745+00	.3952221−01	−.3477123−02	.9073995−03	.1888033+00	−.4889001−01	.8052218−02	−.2983205−02	−.4496905+00	.1166252+00	−.2767341−01	.1306758−01
7.200	.6660908+00	.3817141−01	−.3257886−02	.8272336−03	.1815667+00	−.4702411−01	.7519091−02	−.2712623−02	−.4344867+00	.1117856+00	−.2576520−01	.1185424−01
7.400	.6709716+00	.3690696−01	−.3058561−02	.7562355−03	.1747402+00	−.4528766−01	.7036354−02	−.2473703−02	−.4201668+00	.1073020+00	−.2404329−01	.1078577−01
7.600	.6755451+00	.3572096−01	−.2876826−02	.6931329−03	.1682897+00	−.4366805−01	.6597928−02	−.2261961−02	−.4066559+00	.1031380+00	−.2248458−01	.9841289−02
7.800	.6798369+00	.3460646−01	−.2710685−02	.6368596−03	.1621850+00	−.4215421−01	.6198613−02	−.2073651−02	−.3938870+00	.9926195−01	−.2106941−01	.9003404−02
8.000	.6838695+00	.3355727−01	−.2558415−02	.5865172−03	.1563990+00	−.4073640−01	.5833944−02	−.1905629−02	−.3818004+00	.9564622−01	−.1978094−01	.8257564−02
8.200	.6876633+00	.3256791−01	−.2418525−02	.5413451−03	.1509073+00	−.3940602−01	.5500071−02	−.1755243−02	−.3703428+00	.9226641−01	−.1860472−01	.7591522−02
8.400	.6912366+00	.3163348−01	−.2289716−02	.5006970−03	.1456879+00	−.3815545−01	.5193659−02	−.1620243−02	−.3594661+00	.8910103−01	−.1752828−01	.6994933−02
8.600	.6946060+00	.3074960−01	−.2170855−02	.4640208−03	.1407211+00	−.3697791−01	.4911808−02	−.1498717−02	−.3491271+00	.8613105−01	−.1654079−01	.6459010−02
8.800	.6977865+00	.2991234−01	−.2060950−02	.4308433−03	.1359889+00	−.3586736−01	.4651988−02	−.1389028−02	−.3392868+00	.8333959−01	−.1563287−01	.5976266−02
9.000	.7007917+00	.2911815−01	−.1959129−02	.4007573−03	.1314751+00	−.3481838−01	.4411986−02	−.1289773−02	−.3299099+00	.8071159−01	−.1479630−01	.5540290−02
9.200	.7036338+00	.2836385−01	−.1864621−02	.3734111−03	.1271649+00	−.3382613−01	.4189855−02	−.1199742−02	−.3209643+00	.7823363−01	−.1402391−01	.5145572−02
9.400	.7063241+00	.2764653−01	−.1776748−02	.3485000−03	.1230447+00	−.3288624−01	.3983882−02	−.1117891−02	−.3124207+00	.7589365−01	−.1330938−01	.4787362−02
9.600	.7088730+00	.2696360−01	−.1694905−02	.3257589−03	.1191024+00	−.3199478−01	.3792551−02	−.1043313−02	−.3042526+00	.7368085−01	−.1264714−01	.4461550−02
9.800	.7112897+00	.2631266−01	−.1618556−02	.3049567−03	.1153266+00	−.3114819−01	.3614520−02	−.9752196−03	−.2964357+00	.7158549−01	−.1203229−01	.4164566−02
10.000	.7135829+00	.2569156−01	−.1547223−02	.2858910−03	.1117069+00	−.3034326−01	.3448594−02	−.9129216−03	−.2889478+00	.6959877−01	−.1146046−01	.3893301−02
10.200	.7157605+00	.2509830−01	−.1480477−02	.2683844−03	.1082339+00	−.2957704−01	.3293710−02	−.8558165−03	−.2817684+00	.6771273−01	−.1092778−01	.3645038−02
10.400	.7178297+00	.2453110−01	−.1417937−02	.2522808−03	.1048988+00	−.2884689−01	.3148919−02	−.8033751−03	−.2748788+00	.6592017−01	−.1043080−01	.3417396−02
10.600	.7197972+00	.2398828−01	−.1359256−02	.2374423−03	.1016936+00	−.2815038−01	.3013370−02	−.7551316−03	−.2682618+00	.6421452−01	−.9966439−02	.3208284−02
10.800	.7216692+00	.2346833−01	−.1304127−02	.2237471−03	.9861085−01	−.2748527−01	.2886298−02	−.7106746−03	−.2619014+00	.6258983−01	−.9531936−02	.3015860−02
11.000	.7234513+00	.2296986−01	−.1252268−02	.2110871−03	.9564362−01	−.2684956−01	.2767018−02	−.6696403−03	−.2557829+00	.6104064−01	−.9124816−02	.2838496−02
11.400	.7267667+00	.2203229−01	−.1157377−02	.1884993−03	.9003075−01	−.2565899−01	.2549414−02	−.5965843−03	−.2442185+00	.5814925−01	−.8384030−02	.2523341−02
11.800	.7297809+00	.2116641−01	−.1072834−02	.1690288−03	.8480930−01	−.2456551−01	.2356285−02	−.5337842−03	−.2334712+00	.5550532−01	−.7728754−02	.2253114−02
12.200	.7325265+00	.2036441−01	−.9971913−03	.1521556−03	.7993972−01	−.2355795−01	.2184118−02	−.4795031−03	−.2234571+00	.5307926−01	−.7146442−02	.2020098−02
12.600	.7350316+00	.1961955−01	−.9292474−03	.1374606−03	.7538763−01	−.2262675−01	.2030006−02	−.4323449−03	−.2141036+00	.5084592−01	−.6626752−02	.1818115−02
13.000	.7373206+00	.1892599−01	−.8679951−03	.1246029−03	.7112300−01	−.2176372−01	.1891525−02	−.3911789−03	−.2053471+00	.4878384−01	−.6161097−02	.1642173−02
13.400	.7394150+00	.1827867−01	−.8125866−03	.1133041−03	.6711946−01	−.2096178−01	.1766643−02	−.3550833−03	−.1971321+00	.4687454−01	−.5742305−02	.1488213−02
13.800	.7413336+00	.1767316−01	−.7623037−03	.1033346−03	.6335378−01	−.2021478−01	.1653647−02	−.3233009−03	−.1894097+00	.4510209−01	−.5364345−02	.1352910−02
14.200	.7430929+00	.1710558−01	−.7165350−03	.9450436−04	.5980542−01	−.1951737−01	.1551084−02	−.2952064−03	−.1821369+00	.4345265−01	−.5022121−02	.1233526−02
14.600	.7447075+00	.1657252−01	−.6747574−03	.8665508−04	.5645614−01	−.1886485−01	.1457715−02	−.2702800−03	−.1752753+00	.4191417−01	−.4711302−02	.1127788−02
15.000	.7461904+00	.1607095−01	−.6365213−03	.7965405−04	.5328967−01	−.1825310−01	.1372478−02	−.2480874−03	−.1687910+00	.4047607−01	−.4428189−02	.1033803−02
16.000	.7493945+00	.1493789−01	−.5540021−03	.6517126−04	.4608162−01	−.1687923−01	.1189276−02	−.2023096−03	−.1540392+00	.3726177−01	−.3821865−02	.8404473−03
17.000	.7519939+00	.1395107−01	−.4865235−03	.5400645−04	.3973981−01	−.1569194−01	.1040287−02	−.1671554−03	−.1410690+00	.3450171−01	−.3331142−02	.6924909−03
18.000	.7541031+00	.1308411−01	−.4306471−03	.4526028−04	.3411748−01	−.1465617−01	.9175236−03	−.1397120−03	−.1295754+00	.3210777−01	−.2928562−02	.5773581−03
19.000	.7558108+00	.1231661−01	−.3838619−03	.3831092−04	.2909927−01	−.1374503−01	.8151953−03	−.1179750−03	−.1193196+00	.3001295−01	−.2594324−02	.4864295−03
20.000	.7571868+00	.1163252−01	−.3443005−03	.3271902−04	.2459324−01	−.1293760−01	.7290207−03	−.1005338−03	−.1101116+00	.2816548−01	−.2313869−02	.4136642−03
21.000	.7582866+00	.1101905−01	−.3105507−03	.2816820−04	.2052522−01	−.1221734−01	.6557807−03	−.8637679−04	−.1017985+00	.2652475−01	−.2076301−02	.3547431−03
22.000	.7591549+00	.1046588−01	−.2815290−03	.2442664−04	.1683471−01	−.1157104−01	.5930178−03	−.7476511−04	−.9425571−01	.2505848−01	−.1873342−02	.3065230−03
23.000	.7598279+00	.9964601−02	−.2563925−03	.2132186−04	.1347186−01	−.1098800−01	.5388303−03	−.6515086−04	−.8738098−01	.2374070−01	−.1698609−02	.2666796−03
24.000	.7603353+00	.9508303−02	−.2344781−03	.1872372−04	.1039523−01	−.1045948−01	.4917281−03	−.5712187−04	−.8108929−01	.2255030−01	−.1547123−02	.2334689−03
25.000	.7607016+00	.9091232−02	−.2152583−03	.1653276−04	.7570088−02	−.9978249−02	.4505306−03	−.5036398−04	−.7530952−01	.2146996−01	−.1414952−02	.2055652−03
26.000	.7609471+00	.8708575−02	−.1983091−03	.1467209−04	.4967091−02	−.9538313−02	.4142927−03	−.4463494−04	−.6998168−01	.2048532−01	−.1298958−02	.1819484−03
27.000	.7610889+00	.8356272−02	−.1832865−03	.1308162−04	.2561297−02	−.9134633−02	.3822507−03	−.3974589−04	−.6505480−01	.1958439−01	−.1196613−02	.1618252−03
28.000	.7611412+00	.8030876−02	−.1699095−03	.1171392−04	.3313594−03	−.8762953−02	.3537823−03	−.3554810−04	−.6048533−01	.1875709−01	−.1105865−02	.1445719−03
29.000	.7611162+00	.7729439−02	−.1579462−03	.1053125−04	−.1741099−02	−.8419654−02	.3283761−03	−.3192339−04	−.5623581−01	.1799487−01	−.1025031−02	.1296941−03
30.000	.7610243+00	.7449427−02	−.1472045−03	.9503260−05	−.3671981−02	−.8101638−02	.3056088−03	−.2877705−04	−.5227384−01	.1729046−01	−.9527222−03	.1167961−03
32.000	.7606734+00	.6945208−02	−.1287678−03	.7817724−05	−.7162613−02	−.7531158−02	.2666376−03	−.2362761−04	−.4510349−01	.1603093−01	−.8292492−03	.9572288−04

(m = 36)

T^*	$B^{*(0)}$	$B^{*(1)}$	$B^{*(2)}$	$B^{*(3)}$	$T^*\frac{\partial B^{*(0)}}{\partial T^*}$	$T^*\frac{\partial B^{*(1)}}{\partial T^*}$	$T^*\frac{\partial B^{*(2)}}{\partial T^*}$	$T^*\frac{\partial B^{*(3)}}{\partial T^*}$	$T^{*2}\frac{\partial^2 B^{*(0)}}{\partial T^{*2}}$	$T^{*2}\frac{\partial^2 B^{*(1)}}{\partial T^{*2}}$	$T^{*2}\frac{\partial^2 B^{*(2)}}{\partial T^{*2}}$	$T^{*2}\frac{\partial^2 B^{*(3)}}{\partial T^{*2}}$
34.000	.7601451+00	.6503881−02	−.1135932−03	.6509908−05	−.1023184−01	−.7034165−02	.2346685−03	−.1964124−04	−.3878860−01	.1493804−01	−.7282659−03	.7944414−04
36.000	.7594818+00	.6114442−02	−.1009542−03	.5479452−05	−.1295055−01	−.6597442−02	.2081211−03	−.1650671−04	−.3318521−01	.1398115−01	−.6446356−03	.6666851−04
38.000	.7587155+00	.5768302−02	−.9031570−04	.4656404−05	−.1537457−01	−.6210746−02	.1858363−03	−.1400772−04	−.2817998−01	.1313663−01	−.5746060−03	.5650083−04
40.000	.7578706+00	.5458663−02	−.8127678−04	.3990984−05	−.1754853−01	−.5866018−02	.1669489−03	−.1199072−04	−.2368243−01	.1238601−01	−.5153853−03	.4830714−04
42.000	.7569662+00	.5180073−02	−.7353204−04	.3447109−05	−.1950848−01	−.5556834−02	.1508021−03	−.1034466−04	−.1961949−01	.1171462−01	−.4648615−03	.4162992−04
44.000	.7560170+00	.4928113−02	−.6684563−04	.2998180−05	−.2128388−01	−.5278010−02	.1368907−03	−.8987861−05	−.1593147−01	.1111067−01	−.4214140−03	.3613336−04
46.000	.7550347+00	.4699161−02	−.6103307−04	.2624302−05	−.2289906−01	−.5025320−02	.1248204−03	−.7859344−05	−.1256912−01	.1056459−01	−.3837819−03	.3156714−04
48.000	.7540285+00	.4490221−02	−.5594842−04	.2310385−05	−.2437423−01	−.4795282−02	.1142803−03	−.6912943−05	−.9491460−02	.1006853−01	−.3509732−03	.2774208−04
50.000	.7530057+00	.4298793−02	−.5147495−04	.2044845−05	−.2572638−01	−.4585004−02	.1050222−03	−.6113269−05	−.6664126−02	.9615975−02	−.3221983−03	.2451341−04
52.000	.7519721+00	.4122778−02	−.4751843−04	.1818685−05	−.2696987−01	−.4392065−02	.9684645−04	−.5432889−05	−.4058054−02	.9201507−02	−.2968225−03	.2176903−04
54.000	.7509325+00	.3960397−02	−.4400214−04	.1624849−05	−.2811690−01	−.4214421−02	.8959067−04	−.4850309−05	−.1648514−02	.8820553−02	−.2743313−03	.1942125−04
56.000	.7498905+00	.3810132−02	−.4086306−04	.1457746−05	−.2917794−01	−.4050337−02	.8312184−04	−.4348525−05	.5856724−03	.8469245−02	−.2543038−03	.1740079−04
58.000	.7488492+00	.3670686−02	−.3804907−04	.1312910−05	−.3016199−01	−.3898327−02	.7733014−04	−.3913967−05	.2662748−02	.8144285−02	−.2363931−03	.1565239−04
60.000	.7478111+00	.3540935−02	−.3551675−04	.1186741−05	−.3107686−01	−.3757118−02	.7212424−04	−.3535716−05	.4598513−02	.7842841−02	−.2203112−03	.1413167−04
64.000	.7457516+00	.3306762−02	−.3115717−04	.9792535−06	−.3272533−01	−.3502828−02	.6317619−04	−.2914331−05	.8099392−02	.7301064−02	−.1927095−03	.1163595−04
68.000	.7437234+00	.3101228−02	−.2755548−04	.8176680−06	−.3416816−01	−.3280247−02	.5579822−04	−.2431053−05	.1117914−01	.6827981−02	−.1699920−03	.9697344−05
72.000	.7417336+00	.2919408−02	−.2454552−04	.6899307−06	−.3544014−01	−.3083827−02	.4964326−04	−.2049462−05	.1390834−01	.6411405−02	−.1510711−03	.8168351−05
76.000	.7397867+00	.2757441−02	−.2200432−04	.5876004−06	−.3656870−01	−.2909241−02	.4445513−04	−.1744095−05	.1634265−01	.6041856−02	−.1351456−03	.6946017−05
80.000	.7378848+00	.2612260−02	−.1983927−04	.5046453−06	−.3757573−01	−.2753061−02	.4004133−04	−.1496785−05	.1852657−01	.5711856−02	−.1216151−03	.5956980−05
84.000	.7360293+00	.2481397−02	−.1797956−04	.4366761−06	−.3847892−01	−.2612541−02	.3625501−04	−.1294331−05	.2049610−01	.5415422−02	−.1100222−03	.5148001−05
88.000	.7342201+00	.2362843−02	−.1637031−04	.3804467−06	−.3929273−01	−.2485451−02	.3298258−04	−.1126980−05	.2228066−01	.5147720−02	−.1000140−03	.4479804−05
92.000	.7324570+00	.2254948−02	−.1496843−04	.3335209−06	−.4002908−01	−.2369965−02	.3013501−04	−.9874217−06	.2390456−01	.4904792−02	−.9131396−04	.3922968−05
96.000	.7307390+00	.2156343−02	−.1373972−04	.2940461−06	−.4069787−01	−.2264573−02	.2764175−04	−.8701032−06	.2538803−01	.4683377−02	−.8370372−04	.3455171−05
100.000	.7290651+00	.2065884−02	−.1265676−04	.2605957−06	−.4130743−01	−.2168015−02	.2544633−04	−.7707524−06	.2674806−01	.4480757−02	−.7700848−04	.3059257−05
105.000	.7270327+00	.1962811−02	−.1147461−04	.2255870−06	−.4199667−01	−.2058140−02	.2305218−04	−.6668407−06	.2829618−01	.4250475−02	−.6971378−04	.2645424−05
110.000	.7250645+00	.1869399−02	−.1045115−04	.1966109−06	−.4261569−01	−.1958704−02	.2098151−04	−.5808929−06	.2969718−01	.4042329−02	−.6341063−04	.2303352−05
115.000	.7231576+00	.1784356−02	−.9559164−05	.1724183−06	−.4317394−01	−.1868294−02	.1917852−04	−.5091780−06	.3097045−01	.3853295−02	−.5792703−04	.2018094−05
120.000	.7213093+00	.1706613−02	−.8777033−05	.1520585−06	−.4367925−01	−.1785741−02	.1759894−04	−.4488593−06	.3213212−01	.3680872−02	−.5312673−04	.1778297−05
125.000	.7195168+00	.1635271−02	−.8087408−05	.1347994−06	−.4413820−01	−.1710069−02	.1620728−04	−.3977538−06	.3319574−01	.3522976−02	−.4890066−04	.1575228−05
130.000	.7177774+00	.1569576−02	−.7476237−05	.1200706−06	−.4455635−01	−.1640457−02	.1497486−04	−.3541623−06	.3417275−01	.3377858−02	−.4516070−04	.1402098−05
135.000	.7160885+00	.1508885−02	−.6932038−05	.1074236−06	−.4493839−01	−.1576209−02	.1387825−04	−.3167490−06	.3507291−01	.3244036−02	−.4183499−04	.1253569−05
140.000	.7144478+00	.1452651−02	−.6445360−05	.9650200−07	−.4528836−01	−.1516731−02	.1289817−04	−.2844537−06	.3590457−01	.3120249−02	−.3886448−04	.1125410−05
145.000	.7128529+00	.1400402−02	−.6008361−05	.8702041−07	−.4560973−01	−.1461515−02	.1201867−04	−.2564278−06	.3667491−01	.3005415−02	−.3620030−04	.1014236−05
150.000	.7113016+00	.1351731−02	−.5614492−05	.7874835−07	−.4590548−01	−.1410119−02	.1122642−04	−.2319862−06	.3739017−01	.2898604−02	−.3380168−04	.9173152−06
160.000	.7083217+00	.1263753−02	−.4934987−05	.6511676−07	−.4643022−01	−.1317316−02	.9860673−05	−.1917290−06	.3867643−01	.2705922−02	−.2966970−04	.7577556−06
170.000	.7054931+00	.1186388−02	−.4372146−05	.5447388−07	−.4687969−01	−.1235815−02	.8730485−05	−.1603179−06	.3979914−01	.2536904−02	−.2625341−04	.6333322−06
180.000	.7028023+00	.1117834−02	−.3900679−05	.4604127−07	−.4726710−01	−.1163679−02	.7784580−05	−.1354441−06	.4078608−01	.2387467−02	−.2339643−04	.5348566−06
190.000	.7002375+00	.1056672−02	−.3501799−05	.3927206−07	−.4760286−01	−.1099390−02	.6984921−05	−.1154871−06	.4165913−01	.2254410−02	−.2098289−04	.4558843−06
200.000	.6977882+00	.1001772−02	−.3161315−05	.3377434−07	−.4789521−01	−.1041739−02	.6302805−05	−.9928605−07	.4243578−01	.2135196−02	−.1892545−04	.3918034−06
210.000	.6954450+00	.9522249−03	−.2868344−05	.2926219−07	−.4815079−01	−.9897533−03	.5716245−05	−.8599488−07	.4313016−01	.2027781−02	−.1715728−04	.3392526−06
220.000	.6931998+00	.9072864−03	−.2614426−05	.2552361−07	−.4837499−01	−.9426410−03	.5208170−05	−.7498665−07	.4375377−01	.1930505−02	−.1562653−04	.2957441−06
240.000	.6889740+00	.8288928−03	−.2198491−05	.1976744−07	−.4874620−01	−.8605416−03	.4376540−05	−.5804601−07	.4482515−01	.1761152−02	−.1312273−04	.2288204−06
260.000	.6850603+00	.7628178−03	−.1874756−05	.1562772−07	−.4903598−01	−.7914299−03	.3729847−05	−.4587004−07	.4570857−01	.1618751−02	−.1117739−04	.1807472−06
280.000	.6814177+00	.7063800−03	−.1617818−05	.1257321−07	−.4926345−01	−.7324624−03	.3216994−05	−.3689059−07	.4644573−01	.1497370−02	−.9635797−05	.1453120−06
300.000	.6780125+00	.6576224−03	−.1410465−05	.1026944−07	−.4944242−01	−.6815674−03	.2803397−05	−.3012122−07	.4706704−01	.1392697−02	−.8393361−05	.1186100−06

References

[1] Wigner, E., Phys. Rev. **40,** 749 (1932); Uhlenbeck, G. E., and Gropper, L., Phys. Rev. **41,** 79 (1932); Kirkwood, J. G., Phys. Rev. **44,** 31 (1933).

[2] Kihara, T., Midzuno, Y., and Shizume, T., J. Phys. Soc. Japan **10,** 249 (1955); Kihara, T., Revs. Mod. Phys. **27,** 412 (1955).

[3] Boyd, M. E., Larsen, S. Y., and Kilpatrick, J. E., J. Chem. Phys. **50,** 4034 (1969).

[4] Lennard-Jones, J. E., Proc. Roy. Soc. (London), **A106,** 463 (1924).

[5] Epstein, L. F., and Hibbert, C. J., J. Chem. Phys. **20,** 752 (1952).

[6] Hirshfelder, J. O., Curtiss, C. F., and Bird, R. B., Molecular Theory of Gases and Liquids, (John Wiley and Sons, Inc., New York, 1954.) Appendix I–B, p. 1114.

[7] Michels, H. H., Phys. of Fluids **9,** 1352 (1966).

[8] Saxena, S. C., and Joshi, K. M., Ind. J. Phys. **36,** 422 (1962).

[9] Sze, M., and Hsu, H., J. Chem. and Engr. Data **11,** 77 (1966). An errata to this paper is to be published in the same journal in the near future.

[10] Sherwood, A. E., and Prausnitz, J. M., J. Chem. Phys. **41,** 429 (1964).

(Paper 75A1–650)

JOURNAL OF RESEARCH of the National Bureau of Standards—A. Physics and Chemistry
Vol. 75A, No. 1, January–February 1971

Publications of the National Bureau of Standards*

Selected Abstracts

Blaine, R. L., Tomes, L. A., **Exploratory studies of early strength development in portland cement pastes and mortars,** *Nat. Bur. Stand. (U.S.), Bldg. Sci. Ser. 28, 14 pages (July 1970) 25 cents, SD Catalog No. C13.29/2:28.*

Key words: Cement; cement mortar; cement paste; early strength; false set; hardening of cement; hydration; shear resistance; theory of cement hardening; time of set; vane-shear apparatus.

A modified vane-shear apparatus was used to measure the shear resistance of neat cement pastes of normal consistency and 1:2.75 (cement to sand) mortars of standard consistency, and to measure the increase in shear resistance with time as the cements hardened. The hardening process appeared to occur in three stages. The rate of increase of shear resistance as well as the duration of the different phases differed with the different cements. The results were analyzed in terms of the various theories proposed to explain the hardening of cements.

Brauer, G. M., **Pyrolysis-gas chromatographic techniques for polymer identification, Chapter 2. Thermal Characteristics Techniques in Techniques and Methods of Polymer Evaluations,** P. Slade, Ed., **II,** *41–105 (Marcel Dekker Publ. New York, N.Y., 1970).*

Key words: Chromatographic analysis of degradation products; Polymer characterization; polymer identification; pyrolysis-gas chromatography of polymers; pyrolytic techniques.

Pyrolytic techniques used in conjunction with gas chromatography are very useful for elucidating the structure of macromolecules. These methods are a powerful tool in the qualitative characterization of the gross structure, the study of the thermal stability of polymers and the identification of their pyrolysis products, but have also found an increasing number of applications for the quantitative analysis of copolymeric systems and in studies of the kinetics of polymer degradation. The shape of the pyrograms is dependent on the structural characteristics such as the degree of branching or crosslinking, stereoregularity, crystallinity and monomer sequence length distribution in block and graft copolymers. Thus the pyrolysis-gas chromatographic technique opens up new avenues in studying the ultimate arrangement of monomeric units within the polymer chain.

Bryson, J. O., Carpenter, E. F., **Flexural behavior of prestressed concrete composite Tee-beams,** *Nat. Bur. Stand. (U.S.), Bldg. Sci. Ser. 31, 14 pages (July 1970) 25 cents, SD Catalog No. C13.29/2:31. Catalog of standard reference materials, Nat. Bur. Stand. (U.S.), Spec. Pub. 260–1970 ed., 84 pages (July 1970) 75 cents, SD Catalog No. C13.10:260–1970 ed.*

Key words: Composite concrete construction; prestressed concrete beams; Tee-beams.

Prestressed Tee-beams constructed by the split-beam method were tested to failure in flexure to study the behavior and ultimate strength of these beams and to compare their flexural characteristics with with those of prestressed beams of conventional construction. The compressive portion of the cross section of the split-beam is cast after the web of the beam has been formed and prestressed. The variables in the study included the percentage of prestressing steel, strength of concrete in the compressive element of the composite split-beams, manner of prestressing and web reinforcement. Results showed that the composite split-beams behaved similarly to the monolithically constructed beams on the basis of flexural response and ultimate load. The strength of the concrete for the compressive element can be reduced within limits from that required for the prestressed element without sacrificing ultimate load capacity. The required percentage of reinforcing steel is less for the split-beam compared with conventional beams.

Diller, D. E., Roder, H. M., **Thermal conductivity measurements on fluid hydrogen at 17 to 200 °K and pressures to 10 MN m^{-2}** *(Proc. 1969 Cryogenic Engineering Conf., June 16–18, 1969, Univ. of California, Los Angeles, Calif.), Chapter in Advances in Cryogenic Engineering 15, Paper No. C–1, 58–64 (Plenum Press, Inc., New York, N.Y., 1970).*

Key words: Critical region; parahydrogen; thermal conductivity.

New absolute thermal conductivity measurements on fluid normal and parahydrogen are reported. A nominal accuracy of 2% has been achieved using a parallel plate apparatus in the temperature range 17 to 200 K at pressures to 100 atm and densities to 2.6 times critical. A graphical presentation of the data is given along isotherms, isochores, and isobars in the following regions: 1) the dilute gas, 2) the moderately dense gas, 3) the saturated and compressed liquid, 4) the critical region. Several interesting features of the behavior of the thermal conductivity of this fluid are pointed out: 1) the thermal conductivity of saturated liquid hydrogen increases with temperature between the triple point and the normal boiling point in contrast to the temperature dependence for most liquids other than helium, 2) a large anomalous increase in the thermal conductivity of hydrogen was found in the vicinity of the critical point.

Gonano, R., Adams, E. D., **In Situ vapor pressure measurement for low temperature thermometry,** *Rev. Sci. Instr.* **41,** *No. 5, 716–719 (May 1970).*

Key words: Capacitance manometer; cryogenic thermometry; manometry; pressure measurement; thermomolecular pressure difference; vapor pressure.

By use of a capacitance diaphragm manometer operated at cryogenic temperature, it is possible to measure the vapor pressure of cryogenic liquids without the uncertainties introduced by thermomolecular pressure gradients (thermal transpiration). Since the zero of this manometer is more stable at low temperature than at room temperature, useful sensitivity is also increased. Because of the increased accuracy at low pressure as well as great convenience and simplicity, this technique appears to have wide application in precise vapor pressure thermometry and similar work.

Hamilton, W. C., Edmonds, J. W., Tippe, A., Rush, J. J., **Methyl group rotation and the low temperature transition in hexamethylbenzene. A neutron diffraction study,** *Discussions Faraday Soc., No. 48, 192–204 (1969).*

Key words: Barrier to rotation; crystal; crystal structure; hexamethylbenzene; hindered rotation; phase transition; point methyl group; torsional oscillation.

Neutron diffraction studies of single crystals of hexamethylbenzene at 298° K and at 130° K indicate that the molecule in Phase II has approximate $D3_d$ symmetry. The amplitudes of libration of the methyl

group and of rigid body motions of the molecule are consistent with earlier data, except that the barrier to methyl group rotation appears to be somewhat lower—in the neighborhood of 2000 J/mol.
Consideration of intra- and inter-molecular hydrogen atom contact distances and calculated potential energy curves using a 6-exp potential function suggest that intermolecular forces are important in determining the barrier to rotation of the methyl groups and that substantial changes in the intermolecular packing must be responsible for the lambda-point transition at 116° K and the consequent profound change in the potential barrier to internal rotation which has been previously observed.

Heinrich, K. F. J., **Present state of the classical theory of quantitative electron probe microanalysis,** *Nat. Bur. Stand. (U.S.), Tech. Note 521, 17 pages (Aug. 1970) 30 cents, SD Catalog No C13.46:521.*

Key words: Corrections; electron probe microanalysis; quantitative analysis; x-ray spectroscopy.

Although the foundations for a procedure of data reduction in quantitative electron probe analysis have not been changed for several years, there has been progress in the choice of expressions, parameters, and constants. A brief account of recommended expressions and procedures is given. Reference is made to the Standard Reference Materials of Au-Ag and Au-Cu alloys issued for electron probe microanalysis. These are especially useful for investigating the application of correction procedures.

Madey, T. E., Yates, J. T., Jr., **Chemisorption on single crystals: H_2 on (100) tungsten,** *Proc. Colloque Intern. sur la Structure et les Proprietes des Surfaces des Solides, Paris, France, July 7–11, 1969, No. 187, pp. 155–162 (Centre National de la Recherche Scientifique, Paris, France, 1970).*

Key words: Binding state; chemisorption; hydrogen; isotopes; single crystal; tungsten; work function.

An ultrahigh vacuum apparatus has been constructed to study flash desorption of gaseous molecules from macroscopic single crystals. The crystals are in the form of thin discs, polished on both faces, whose total surface area is 95 percent of one orientation. A focussed light source external to the vacuum system is used to heat the nearly adiabatically suspended sample to $T > 1200$ K; temperature inhomogeneities and end effects which complicate kinetic measurements on resistively heated samples are not present here. The sample is cleaned by electron bombardment prior to making adsorption measurements. Work function changes upon adsorption are monitored using an electron gun; a quadrupole mass spectrometer is used as the detector of desorbed species.
The chemisorption of H_2 and D_2 on a (100) oriented tungsten disc has been examined with this apparatus. The hydrogen desorption spectra reveal that *two* binding states exist on the (100) surface. The first order β_1 state desorbs with an activation energy of ~ 25 kcal/mole and at saturation coverage, is twice as densely populated as the β_2 state. The coadsorption of an equimolar mixture of H_2 and D_2 shows that *both* states are isotopically mixed upon desorption. The work function-coverage relation is linear over the entire coverage range; the dipole moment per atom is 0.15 Debye, independent of binding state. Several models of H_2 chemisorption are discussed.

Pfeiffer, E. R., Schooley, J. F., **Effect of stress on the superconducting transition temperature of $SrTiO_3$,** *J. Low Temp. Phys.* **2,** *No. 3/4, 333–352 (August 7, 1970).*

Key words: Anisotropic stress effect; hydrostatic pressure Nb-doped $SrTiO_3$; 0–1.8 kbars; reduced $SrTiO_3$; superconductivity; transition temperatures; uniaxial compression.

The superconducting transition temperatures of several specimens of reduced $SrTiO_3$ and of Nb-doped $SrTiO_3$ have been investigated as functions of hydrostatic and uniaxial compressive stresses up to 1.8 kbars. Large decreases in T_c were observed in each specimen under hydrostatic pressure. Because of the low T_c and small compressibility of $SrTiO_3$, $\Delta(\ln T_c)/\Delta P$ and $\Delta(\ln T_c)/\Delta(\ln V)$ are orders of magnitude greater than the corresponding effects in the elemental superconductors. An anisotropic uniaxial stress effect was observed. [111] compression caused large decreases in T_c, while both small increases and small decreases in T_c were observed for specimens under [100] compression. It is believed that the present results reveal a sensitive volume dependence of one or more of the parameters important to superconductivity in $SrTiO_3$, and that no significant electron-transfer effects occurred in the range of stresses of this experiment.

Rockett, J. A., **Objectives and pitfalls in the simulation of building fires with a computer,** *Fire Tech.* **5,** *No. 4, 311–322 (November 1969).*

Key words: Building; computer; fire; simulation.

The complex interactions between a building and a fire are being studied using the NBS computer facility. A description of the building in a form suitable for use with the computer has been developed. Obtaining sufficient detail in the description to allow a good representation of the building, with an easily manageable amount of input data, has been a major problem. In describing the fire, it is necessary to determine the air movements induced by the fire, since these establish both the severity and extent of the fire, and the movement of smoke and toxic products. The technical problem is twofold; not enough is known about convective air movements and how to calculate them, and those calculations which can be carried out are excessively time consuming. Concurrently, information is lacking on the precise configuration of the building at the time of the fire; which doors are open or closed and where critical items are located. By highlighting the information needs for a successful calculation, the fire simulation study provides a guide to future research. Insofar as the study is able to represent correctly actual building fires, it provides a useful tool to the fire protection engineer.

Searles, S. K., Sieck, L. W., **High pressure photoionization mass spectrometry, III. Reactions of $NO^+(X'\Sigma^+)$ with C_3–C_7 hydrocarbons at thermal kinetic energies,** *J. Chem. Phys.* **53,** *No. 2, 794–797 (July 15, 1970).*

Key words: Alkanes; excited states; ion-molecule reactions; mass spectrometry; photoionization; rate constants.

The vapor phase reaction of $NO^+(X'\Sigma^+)$ with C_3 through C_6 normal, branched, or cyclic alkanes was found to proceed exclusively via an H^- transfer mechanism:

$$NO^+(X^1\Sigma^+) + RH_2 - RH^+ + HNO \qquad (I)$$

In addition to (I), $C_4H_9^+$ was also formed by a second order process in the reaction with 3-methylhexane. Absolute rate constants were determined for all systems at thermal kinetic energies. Isomers containing tertiary H atoms were found to be the most reactive, exhibiting rate constants on the order of 10^{-9} cm³/molecule-second. Isotopic labeling has verified that only the tertiary site is involved in the H^- transfer reaction in those molecules having both secondary and tertiary H atoms. The rate constants found for *n*-alkanes and non-substituted cycloalkanes fall in the range 10^{-12} to 10^{-10} cm³/molecule-second. The bimolecular reaction cyclo-$C_6H^+_{11} + NO - C_6H_{11}NO^+$ was also noted at higher pressures. No further reaction of the RH^+ species generated in (I) was found in any other RH_2–NO combination at pressures up to 0.5 torr.

Shinyayev, A. Y., Butrymowicz, D. B., **Interdiffusion in and the phase diagram for vanadium-rich alloys of the V–Al system at pressures 0 to 47 kbar,** *Met. Trans.* **1,** *No. 7, 1905–1907 (July 1970)* Simson, B. G., Mandel, J., Brenner, F. C., Research for a uniform quality grading system for tires. III, Breaking energy Rubber Chem. and Tech. 43, No. 2, 356–369 (March 1970).

Key words: Alloys; aluminum; diffusion; high-pressure; phase-diagram; vanadium.

The V–Al system between 16 and 39 at. pct. Al was studied at 1400 °C under pressures of 0, 30, and 47 kbar. Electron microprobe analysis, x-ray diffraction, microhardness readings, and metallographic examination revealed only a single solid solution.

Interdiffusion coefficients were determined as a function of composition and pressure. Concentration gradients were measured with an electron microprobe analyzer and the diffusion coefficients were calculated by the Matano analysis. At 1400 °C, the value of the interdiffusion coefficient varies from 1 to 12×10^{-9} cm^2/s, increasing with aluminum content and decreasing with increasing pressure.

Straty, G. D., Prydz, R., **The vapor pressure of liquid fluorine,** (*Proc. 1969 Cryogenic Engineering Conf., June 16–18, 1969, Univ. of California, Los Angeles, Calif.*), *Chapter in Advances in Cryogenic Engineering 15, Paper No. B–1, 36–41 (Plenum Press, Inc., New York, N.Y., 1970).*

Key words: Critical point pressure; fluorine; normal boiling point; vapor pressure data; vapor pressure equation.

This paper reports new vapor pressure measurements on liquid fluorine from the triple point to the critical point at 1 K intervals. Accuracies in both temperature and pressure approach a few hundredths of a percent. The data were fitted to a newly developed, non-analytic vapor pressure equation and compared graphically to earlier, inconsistent measurements available in the literature. Of this earlier data, the estimated P–T values above the normal boiling point and the value given for the critical pressure are in error by as much as 10 to 15 percent.

Sugar, J., **Spectrum of doubly ionized thulium (Tm II),** *J. Opt. Soc. Am.* **69,** *No. 4, 454–466 (April 1970).*

Key words: Doubly ionized thulium; energy levels of Tm III; radial energy integrals of Tm III; spectrum of Tm III.

A list of 848 low excitation spectral lines of Tm III has been obtained by utilizing the sliding spark light source at a peak current of 6 A. An analysis of these lines yielded 108 energy levels belonging to the configurations $4f^{13}$, $4f^{12}5d$, $4f^{12}6s$, and $4f^{12}6p$. The classified lines and level values are presented as well as a theoretical interpretation of these configurations.

Tighe, N. J., Hockey, B. J., **Ion thinning of electron microscope specimens** (*Proc. 10th Symp. Electron, Ion and Laser Beam Tech., May 21–23, 1969, National Bureau of Standards, Gaithersburg, Md.*), *Record of 10th Symposium on Electron, Ion, and Laser Beam Technology, L. Marton, Ed., pp. 375–380 (San Francisco Press Inc., San Francisco, Calif., 1970).*

Key words: Al_2O_3; argon ion bombardment; ceramics; electron microscopy; hardness; ion thinning; SiO_2.

In recent years, it has been possible to prepare ceramic specimens for transmission electron microscopy using ion bombardment for thinning bulk samples to less than ~ 0.5μm thickness. Chemical inertness and electrical insulating properties of many ceramic materials make chemical and electrochemical methods, such as those used for metals, difficult to apply. Even when suitable chemical polishes are found they often are useful only for certain crystallographic orientations and not at all useful for polycrystalline bodies. In this laboratory, the ion-thinning technique has been applied to polycrystalline and single-crystalline ceramics including alumina, magnesia, silica and zirconia.

Prior to ion thinning, disk specimens 2.3 or 3 mm in diameter are cut from thin slices (40 to 150 μm) of the selected samples. When a specimen is particularly fragile because of large deformation, fractures, or porosity, a supporting rim is cemented to it. Specimens are thinned simultaneously from both sides and are rotated during thinning to eliminate or reduce directional grooving. They are thinned with argon ion beams using accelerating voltages of 4 to 8 kV and beam currents of 50 to 150μA. Thinning rates vary from 1/2 to 4μm/hr depending on the specimen material and on the operating conditions.

The ion-thinned specimens have electron transparent regions which usually are more extensive than those in the best chemically thinned single crystal specimens. Studies of the microstructure of hot-pressed alumina, periclase brick, quartz and magnetite rocks and a number of sintered ceramics have been undertaken. The dislocation substructure, impurity precipitates, second phase grains, and voids have been revealed by transmission electron microscopy; and, in some cases, the defects have been related to the deformation sustained by specimens during forming or during mechanical testing. Because specimens can be thinned from only one side, it has been possible to study the damage in single and polycrystalline alumina specimens which is produced by hardness indents and by mechanical polishing with diamond abrasives.

Torrance, K. E., Orloff, L., Rockett, J. A., **Numerical study of natural convection in an enclosure with localized heating from below – creeping flow to the onset of laminar instability,** *J. Fluid Mech.* **36,** *Part I, 33–54 (June 1969).*

Key words: Circular cylinder; enclosures; natural convection; numerical.

An analytical study was made of the natural convection induced in an enclosure by a small hot spot centrally located on the floor. The enclosure was a circular cylinder, vertically oriented, with height equal to radius. A Prandtl number of 0.7 (air) was assumed; the Grashof number (Gr) was based on cylinder height and hot spot temperature. The equations of fluid flow in axisymmetric cylindrical coordinates were simplified with the Boussinesq approximation. The equations were solved numerically with a computationally stable, explicit method. The computation, starting from quiescent conditions, proceeded through the initial transient to the fully developed flow. Solutions were obtained for Gr from 4×10^4 to 4×10^{10}. The calculated flows were compared with the experimental flows presented in a companion paper, Torrance, Orloff and Rockett (1968). The experimental flows were laminar for $Gr \lesssim 1.2 \times 10^9$; turbulence was observed above this value. In the laminar flow region ($Gr \lesssim 1.2 \times 10^9$) agreement between the theoretical and experimental flow patterns was excellent. When extended into the experimentally observed turbulent range ($Gr = 4 \times 10^{10}$) the theoretical flow developed a periodic vortex shedding, suggestive of the onset of transition.

Verdier, P. H., **Relaxation behavior of the freely jointed chain,** *J. Chem. Phys.* **52,** *No. 11, 5512–5517 (June 1, 1970).*

Key words: Chain dynamics; polymers; random walk; relaxation; stochastic process.

A method is presented for treating the relaxation behavior of the freely jointed chain model of a random coil polymer. Exact results are exhibited for the relaxation of quantities linear in chain coordinates. For the treatment of quantities quadratic in chain coordinates, a numerical approach is employed and exemplified by obtaining the autocorrelation in the square of end-to-end length for chains of up to 16 beads. In both cases, the rapid approach of the behavior of the freely jointed chain of N beads to that of the Rouse model of N statistical segments is demonstrated.

Winogradoff, N. N., Neill, A. H., Jr., **Temperature dependence of the power output of the spontaneous emission from GaAs laser diodes,** *Intern. J. Electron.* **28,** *No. 5, 401–406 (1970).*

Key words: Band tailing; GaAs lasers; non-radiative recombination centers; radiative recombination; temperature dependence; valence band.

The spectra of the spontaneous emission from GaAs laser diodes fabricated by vapor phase epitaxy and containing a high degree of compensation in the p-type side of the junction are, in many respects, similar to those previously reported for the cathodoluminescence of homogeneous p-type material. The temperature dependence of the spectra of these diodes supports a model where the emission is attributed to radiative transitions between a narrow band of states near the conduction band edge and an exponential distribution of states extending the valence band into the forbidden gap.

An increase in temperature then results in an *increase* or a decrease in the radiative power output depending on the position of the quasi Fermi level for electrons relative to the above narrow band of states and a distribution of non-radiative levels below it.

Younglove, B. A., **Measurements of the dielectric constant of saturated liquid oxygen** (*Proc. 1969 Cryogenic Engineering Conf., June 16–18, 1969, Univ. of California, Los Angeles, Calif.), Chapter in Advances in Cryogenic Engineering 15, Paper No. C–3, 70–75 (Plenum Press, Inc., New York, N.Y., 1970).*

Key words: Clausius-Mossotti function; dielectric constant; oxygen; polarizability; saturated liquid.

Dielectric constant measurements of saturated liquid oxygen show a variation of 1.22 near the critical point to 1.57 near the triple point. The calculation "polarizability" (Clausius-Mossotti function) shows a variation of 1.3%, with the maximum occurring at about 150K. The decrease in polarizability near critical is attributed to inaccuracies in the densities in this region. The uncertainty in dielectric constant is about 0.01%.

Other NBS Publications

J. Res. Nat. Bur. Stand. (U.S.), 74B (Math. Sci.), No. 4 (October–December 1970), SD Catalog No. C13.22/sec.B:74/4. $1.25.

A property of the triangle groups. J. Lehner.
Some theorems on tensor composite graphs. M. F. Capobianco.
The diophantine approximation of roots of positive integers. C. F. Osgood.
The minimum number of problems to cover all subproblems. H. J. Greenberg.
Error estimates for the solution of linear algebraic systems. Brother K. E. Fitzgerald, F.S.C.
On the singular values of a product matrices. W. Watkins.
Contractifiable semigroups. P. R. Meyers.
Publications of the National Bureau of Standards.

J. Res. Nat. Bur. Stand. (U.S.), 74C (Engr. and Instr.) Nos. 3 & 4 (July–Dec. 1970), SD Catalog Number C13.22/sec. C:74/3 & 4. $1.25.

Techniques for comparing four-terminal-pair admittance standards. R. D. Cutkosky.
Some applications for series impedance elements in radio frequency immittance measurements. L. E. Huntley.
A pulse heating method for the measurement of melting point of electrical conductors (thin wires) above 2000 K. A. Cezairliyan.
A time-shared computer system for diffractometer control. H. A. Alperin and E. Prince.
Tensile deformation of vapor-deposited copper reinforced with tungsten wires. W. D. Jenkins, W. A. Willard, and D. A. Harne.
"Connector-pair" techniques for the accurate measurement of two-terminal low-value capacitances. A. Millea.
The use of dew-point temperature in humidity calculations. L. A. Wood.
Bolovac application for HF and microwave power measurement and standardization. M. C. Selby.

Arp, V., Heat transport through helium II, Cryogenics **10,** No. 2, 96–105 (April 1970).

Bridges, J. M., Wiese, W. L., The oscillator-strength scale for Fe I, Astrophys. J. **161,** L71–L75 (July 1970).

Brower, W. S., Jr., Fang, P. H., Dielectric constants of scheelite structure crystals, J. Appl. Phys. **40,** No. 12, 4988–4989 (November 1969).

Brower, W. S., Jr., Fang, P. H., Dielectric constants of zinc tungstate, J. Appl. Phys. **41,** No. 5, 2266 (April 1970).

Brower, W. S., Jr., Farabaugh, E. N., Dislocation etchant for single crystal Y_2O_3, J. Am. Ceram. Soc. **53,** No. 4, 225 (April 1970).

Cezairliyan, A., High-speed methods of measuring specific heat of electrical conductors at high temperatures (A review), High Temperatures – High Pressures **1,** 517–529 (1969).

Childs, G. E., Diller, D. E., Refractive index of liquid deuterium, (Proc. 1969 Cryogenic Engineering Conf., June 16–18, 1969, Univ. of California, Los Angeles, Calif.), Chapter in Advances in Cryogenic Engineering 15, Paper No. C–2, 65–69 (Plenum Press, Inc., New York, N.Y., 1970).

Clark, A. F., Childs, G. E., Wallace, G. H., Low-temperature electrical resistivity of some engineering alloys (Proc. 1969 Cryogenic Engineering Conf., June 16–18, 1969, Univ. of California, Los Angeles, Calif.), Chapter in Advances in Cryogenic Engineering 15, Paper No. C–5, 85–90 (Plenum Press, Inc., New York, N.Y., 1970).

Daney, D. E., Rapial, A. S., Preparation and characterization of slush hydrogen and nitrogen gels (Proc. 1969 Cryogenic Engineering Conf., June 16–18, 1969, Univ. of California, Los Angeles, Calif.), Chapter in Advances in Cryogenic Engineering 15, Paper No. L–4, 467–475 (Plenum Press, Inc., New York, N.Y., 1970).

Duncan, A. G., Hiza, M. J., A multipurpose phase equilibrium apparatus to study mixtures of cryogenic fluids: application to argon-methane (Proc. 1969 Cryogenic Engineering Conf., June 16–18, 1969, Univ. of California, Los Angeles, Calif.), Chapter in Advances in Cryogenic Engineering 15, Paper No. B–2, 42–45 (Plenum Press, Inc., New York, N.Y., 1970).

Geil, G. W., Feinberg, I. J., Temperature changes in specimens in microplasticity tests, Met. Trans. **1,** No. 7, 1845–1851 (July 1970).

Giacchetti, A., Stanley, R. W., Zalubas, R., Proposed secondary-standard wavelengths in the spectrum of thorium, J. Opt. Soc. Am. **69,** No. 4, 474–489 (April 1970).

Hanson, D. W., Quasi-optical components using total reflection in dielectrics, IEEE Trans. Microwave Theory Tech. **MTT–18,** No. 4, 233–234 (April 1970).

Hendricks, R. C., Simoneau, R. J., Smith, R. V., Survey of heat transfer to near-critical fluids (Proc. 1969 Cryogenic Engineering Conf., June 16–18, 1969, Univ. of California, Los Angeles, Calif.), Chapter in Advances in Cryogenic Engineering 15, Paper No. G–1, 197–237 (Plenum Press, Inc., New York, N.Y., 1970).

Heydemann, P. L., Ultrasonic measurements at pressures up to 50 kbar, Proc. Intern. Collog. Solids at High Pressures, Grenoble, France, Sept. 8, 1969, No. 188, pp. 461–467 (Centre National de la Recherche Scientifique, Paris, France, 1970).

Hiza, M. J., Solid-vapour equilibria research on systems of interest in cryogenics, Cryogenics **10,** No. 2, 106–115 (April 1970).

Kidnay, A. J., Hiza, M. J., Dickson, P. F., Adsorption kinetics in a ternary system containing hydrogen (Proc. 1969 Cryogenic Engineering Conf., June 16–18, 1969, Univ. of California, Los Angeles, Calif.), Chapter in Advances in Cryogenic Engineering 15, Paper No. B–3, 46–49 (Plenum Press, Inc., New York, N.Y., 1970).

LaFleur, P. D., Editor, Activation analysis section: Summary of activities July 1968 to June 1969, Nat. Bur. Stand. (U.S.) Tech. Note 508, 147 pages (July 1970) $1.25, SD Catalog No. C13.46:508.

Levin, E. M., X-ray determination of the thermal expansion of silver nitrate, J. Am. Ceram. Soc. 52, No. 1, 53–54 (January 1969).

Locke, J. W., Penn, R., Rick, J., Bunten, E., Hare, G., Compilation and use of criminal court data in relation to Pre-Trial Release of defendants: pilot study, Nat. Bur. Stand. (U.S.), Tech. Note 535, 242 pages (Aug. 1970) $1.75, SD Catalog No. C13.46:535.

Lutz, G. J., Masters, L. W., Determination of carbon in high purity metals by photon activation analysis, Anal. Chem. **42,** No. 8, 948–950 (July 1970).

Marvin, R. S., Rheological Models and measurements (Proc. 5th. Intern. Congress on Rheology, Kyoto, Japan, Oct. 7–11, 1968), Chapter in Fifth International Congress on Rheology, S. Onogi, Ed., 1, 85–96, University of Tokyo Press and University Park Press, Tokyo, Japan, 1969).

Mauvais, C. J., Latanision, R. M., Ruff, A. W., Jr., On the anisotropy observed during the passivation of nickel monocrystals, J. Electrochem. Soc. 117, No. 7, 902–903 (July 1970).

McNish, A. G., Progress on the Metric Study Program, Proc. Conf. 18th Annual Meeting of Standards Engineers Society, Washington, D.C., Sept. 17–19, 1969, pp. 53–56 (Standards Engineers Society, Philadelphia, Pa., 1969).

McNish, A. G., The impact of increasing metric usage, Proc. Conf. Industrial Heating Equipment Association, Spring (77th Consecutive) Meeting, Hot Springs, Virginia, May 19–21, 1969, Exhibit E (Industrial Heating Equipment Assoc., Washington, D.C., 1969).

Melmed, A. J., Carroll, J. J., Ellipsometry, LEED, and FEM study of evaporated epitaxial films of iron on (011) tungsten, Surface Sci. Letters to the Editor 19, No. 1, 243–248 (January 1970).

Mighell, A. D., Reimann, C. W., Santoro, A., The crystal structure of the 2:1 dimer [(pyridine *N*-oxide)$_2$CuBr$_2$]$_2$, Chem. Commun, 4, 204 (1970).

Molino, J. A., Noise the growing hazard, Dialog **1**, No. 4, 26–28 (1970).

Negas, T., Roth, R. S., The system $SrMnO_{3-x}$, J. Solid State Che **1**, 409–418 (1970).

Page, C. H., Relations among systems of electromagnetic equations, Am. J. Phys. **38**, No. 4, 421–424 (April 1970).

Page, C. H., The trolley problem, Am. J. Phys. **38**, No. 5, 608–610 (May 1970).

Phillips, S. L., Johnson, C. E., Effect of atmospheric exposure on the contact resistance of selected tin alloys, J. Electrochem. Soc. **117**, No. 6, 827–830 (June 1970).

Reed, R. P., Durcholz, R. L., Cryostat and strain measurement for tensile tests to 1.5 °K (Proc. 1969 Cryogenic Engineering Conf., June 16–18, 1969, Univ. of California, Los Angeles, Calif.), Chapter in Advances in Cryogenic Engineering 15, Paper No. D–3, 109–116 (Plenum Press, Inc., New York, N.Y., 1970).

Robertson, A. F., Gross, D., Fire load, fire severity, and fire endurance, Am. Soc. Testing Mater. ASTM Spec. Tech. Publ. **464**, Fire Test Performance, pp. 3–29 (January 1970).

Searles, S. K., Sieck, L. W., Ausloos, P., Reactions of $C_2H_6^+$. Formation of the $(C_2H_6)_2^+$ ion, J. Chem. Phys. **53**, No. 2, 849–850 (July 15, 1970).

Sher, A. H., Nomographs for use in the fabrication and testing of Ge(Li) detectors, Nat. Bur. Stand. (U.S.), Tech. Note 537, 18 pages (Aug. 1970) 30 cents, SD Catalog No. C13.46:537.

Sindt, C. F., Ludtke, P. R., Slush hydrogen flow characteristics and solid fraction upgrading (Proc. 1969 Cryogenic Engineering Conf., June 16–18, 1969, Univ. of California, Los Angeles, Calif.), Chapter in Advances in Cryogenic Engineering 15, Paper No. I–6, 382–390 (Plenum Press, Inc., New York, N.Y., 1970).

Snyder, N. S., Heat transport through helium II: Kapitza conductance Cryogenics **10**, No. 2, 89–95 (April 1970).

Stevenson, D. R., Technical Standards Coordinator, Heavy-duty alpha-cellulose-filled melamine tableware, Nat. Bur. Stand. (U.S.), Voluntary Prod. Stand. 25–70, 8 pages (Aug. 1970) 10 cents, SD Catalog No. C13.20/2:25–70. Supersedes Commercial Standard CS 173–50.

Stevenson, D. R., Technical Standards Coordinator, Melamine dinnerware (alpha-cellulose-filled) for household use, Nat. Bur. Stand. (U.S.), Voluntary Prod. Stand. 24–70, 9 pages (Aug. 1970) 10 cents, SD Catalog No. C13.20/2:24–70. Supersedes Commercial Standard CS 210–57.

Steward, W. G., Smith, R. V., Brennan, J. A., Cooldown transients in cryogenic transfer lines (Proc. 1969 Cryogenic Engineering Conf., June 16–18, 1969, Univ. of California, Los Angeles, Calif.), Chapter in Advances in Cryogenic Engineering 15, Paper No. I–2, 354–363 (Plenum Press, Inc., New York, N.Y., 1970).

Stief, L. J., Payne, W. A., DeCarlo, V. J., Gorden, R., Jr., Ausloos, P., Comment on "Xenon sensitized photolysis of carbon dioxide", J. Chem. Phys. **53**, No. 1, 475–476 (July 1, 1970).

Straty, G. C., Prydz, R., Melting curve and triple-point properties of fluorine, Physics Letters **31A**, No. 6, 301–302 (March 23, 1970).

Sugar, J., Configuration $4f^{13}5d$ of doubly ionized ytterbium, J. Opt. Soc. Am. 60, No. 4, 571–572 (April 1970).

Swartzendruber, L. J., Bennett, L. H., Clustering, cold work, and the Mössbauer effect doublet structure in Cu-Ni-Fe alloys, Physics Letters **31A**, No. 10, 581–582 (May 18, 1970).

Torrance, K. E., Orloff, L., Rockett, J. A., Experiments on natural convection in enclosures with localized heating from below, J. Fluid Mech. 36, Part I, 21–31 (1969).

Weber, L. A., The P-V-T surface of oxygen in the critical region; densities of saturated liquid and vapor (Proc. 1969 Cryogenic Engineering Conf., June 16–18, 1969, Univ. of California, Los Angeles, Calif.), Chapter in Advances in Cryogenic Engineering 15, Paper No. B–4, 50–57 (Plenum Press, Inc., New York, N.Y., 1970).

Wegstein, J. H., Automated fingerprint identification, Nat. Bur. Stand. (U.S.), Tech. Note 538, 33 pages (Aug. 1970) 40 cents, SD Catalog No. C13.46:538.

White, H. J., Jr., Counties and county equivalents of the states of the United States, Nat. Bur. Stand. (U.S.), Fed. Info. Process. Stand. Publ. (FIPS Pub) 6–1, 34 pages (1970) 45 cents, SD Catalog No. C13.52:6–1. Supersedes FIPS PUB 6, Nov. 1, 1968.

White, H. J., Jr., States and outlying areas of the United States, Nat. Bur. Stand. (U.S.), Fed. Info. Process. Stand. Publ. (FIPS Pub) 5–1, 4 pages, (1970) 20 cents, SD Catalog No. C13.52:5–1. Supersedes FIPS PUB 5, Nov. 1, 1968.

Winogradoff, N. N., Neill, A. H., Petrescu-Prahova, J. B., Band tailing and the spontaneous spectra of compensated epitaxial GaAs laser junctions, IEEE J. Quantum Electron. Q.E. **6**, No. 6, 305–310 (June 1970).

**Publications for which a price is indicated are available by purchase from the Superintendent of Documents, U.S. Government Printing Office, Washington, D.C. 20402 (foreign postage, one-fourth additional). The NBS non-periodical series are also available from the National Technical Information Service, Springfield, Va. 22151. Reprints from outside journals and the NBS Journal of Research may often be obtained directly from the authors.*

U.S. GOVERNMENT PRINTING OFFICE : 1971 OL - 408-434

UNITED STATES
GOVERNMENT PRINTING OFFICE
PUBLIC DOCUMENTS DEPARTMENT
WASHINGTON, D.C. 20402

OFFICIAL BUSINESS
PENALTY FOR PRIVATE USE, $300

POSTAGE AND FEES PAID
U.S. GOVERNMENT PRINTING OFFICE

JOURNAL OF RESEARCH of the National Bureau of Standards
A. Physics and Chemistry

Vol. 75A, No. 1 Jan.–Feb. 1971

Contents

	Page
High-speed (subsecond) measurement of heat capacity, electrical resistivity, and thermal radiation properties of tantalum in the range 1900 to 3200 K. A. Cezairliyan, J. L. McClure, and C. W. Beckett.	1
Thermophysical properties of methane: orthobaric densities and some thermal properties. Robert D. Goodwin.	15
The infrared spectrum of matrix isolated BaO_2. S. Abramowitz and N. Acquista.	23
Refinement of the crystal structure of the aragonite phase of $CaCO_3$. B. Dickens and J. S. Bowen.	27
Simple shearing flows in polyisobutylene solutions. L. J. Zapas and J. C. Phillips.	33
Synthesis of fluorodienes. James E. Fearn.	41
Quantum corrections to the second virial coefficient for the Lennard-Jones (m–6) potential. Marjorie E. Boyd.	57
Publications of the National Bureau of Standards.	91

Library of Congress Catalog Card Number: 62–37059

For sale by the Superintendent of Documents, U.S. Government Printing Office, Washington, D.C. 20402. (Order by SD Catalog No. C 13.22/sec.A:75/1). Single copy price varies. This issue $1.25. Subscription price: $9.50 a year; $2.25 additional for foreign mailing.

UNITED STATES GOVERNMENT PRINTING OFFICE, WASHINGTON : 1971